eman ta zabal zazu

Universidad del País Vasco

Euskal Herriko Unibertsitatea

Stock structure of tropical tuna in the Indian Ocean: an otolith microchemistry approach

Iraide Artetxe Arrate

PhD Thesis 2021

PhD Thesis

Stock structure of tropical tuna in the Indian Ocean: an otolith microchemistry approach

Presented by

Iraide Artetxe Arrate

Thesis supervisors

Igaratza Fraile Ugalde

Hilario Murua Aurizenea

Department

Zoology and Animal Cell Biology

PhD Program

Marine Environment and Resources

April 2021

AZTI
MEMBER OF
BASQUE RESEARCH
& TECHNOLOGY ALLIANCE

eman ta zabal zazu
Universidad del País Vasco
Euskal Herriko Unibertsitatea

The research carried out in this Dr.Philos thesis has been developed in AZTI -BRTA (Pasaia, Spain) and it has been financed by the Population Structure of Tunas, Billfish and Sharks of interest of the Indian Ocean (PSTBS-IO) project [GCP/INT/233/EC] within the framework of a collaborative project between FAO/IOTC and CSIRO Oceans and Atmosphere, AZTI, Institut de Recherche pour le Développement (IRD), and Indonesia's Center for Fisheries Research (CFR). The views expressed herein can in no way be taken to reflect the official opinion of the European Union. Iraide Artetxe Arrate was funded by a Doctoral Fellowship (Convocatoria ayudas de formación a jóvenes investigadores y tecnólogos 2017) from the Department of Agriculture, Fisheries and Food Policy from the Basque Government.

Recommended citation:

Artetxe-Arrate, I. (2021). Stock structure of tropical tuna in the Indian Ocean: an otolith microchemistry approach. PhD Thesis. Department of Zoology and Animal Cell Biology, University of the Basque Country, 257 pp,

A las tres mujeres de mi vida,

Isabel, Amama Amelia y Amama Josune

(y a aita y ama, siempre)

“So, should we race to see how quickly we can consume the last tuna, swordfish, and grouper? Or race to see what can be done to protect what remains? For now, there is still a choice.”

Sylvia Earle

CONTENTS

ACKNOWLEDGEMENTS

Eskerrik asko era batean edo bestean bidai hau nirekin egin duzuen guztioi.

A todas las personas que han hecho de este viaje, un gran viaje. Gracias.

Thanks to everyone who sailed this journey by my side.

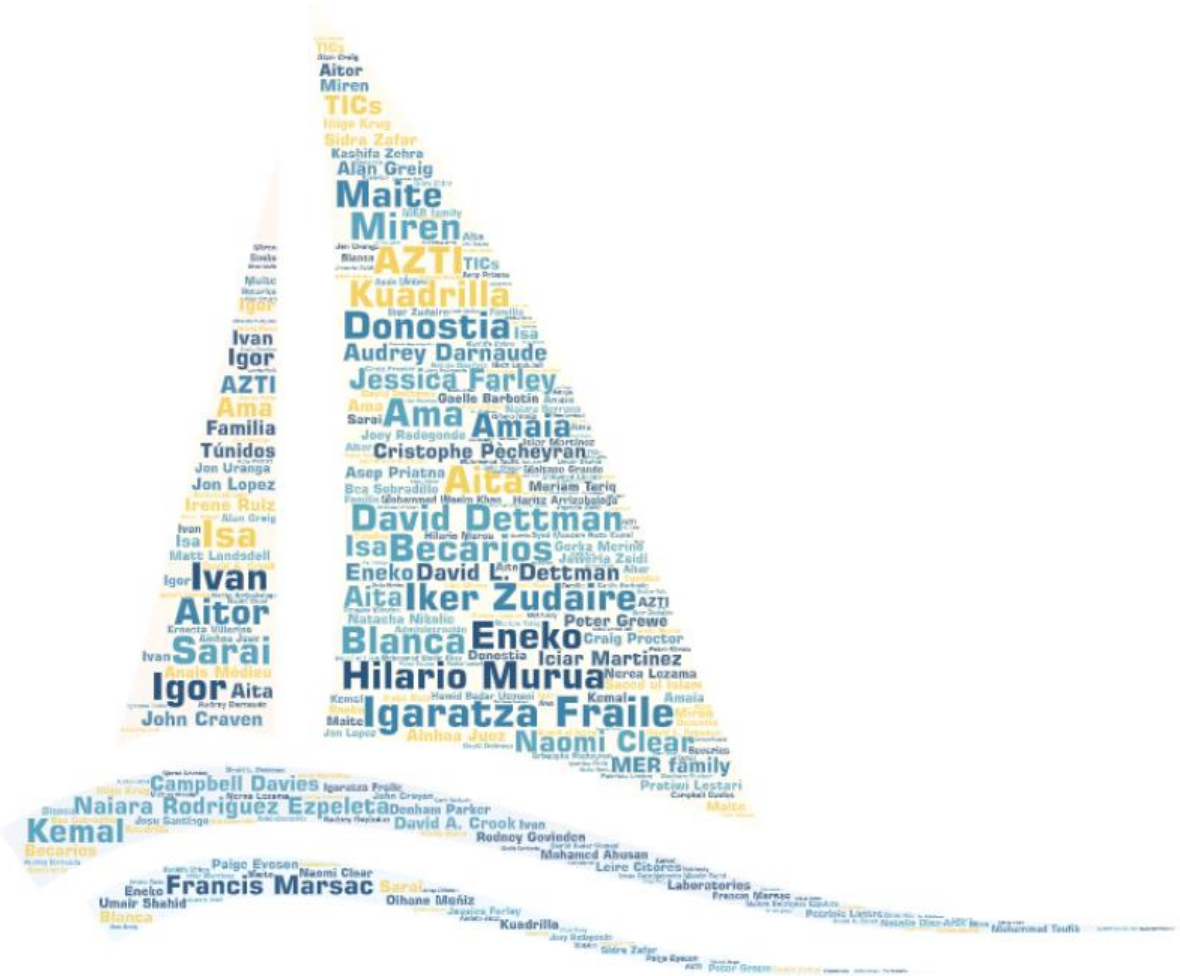

LIST OF ACRONYMS

ANN	Artificial Neural Network
Ba	Barium
BET	Bigeye tuna (*Thunnus obesus*)
C	Carbon
Ca	Calcium
CAP	Analysis of Principal Coordinates
CCSBT	Convention on the Conservation of Southern Bluefin Tuna
CHL	Chlorophyll
Cu	Cupper
DO	Disolved Oxygen
EEZ	Exclusive Economic Zone
EFI	Elemental Fingerprinting Index
EU	European Union
FAO	Food and Agricultural Organization
Fe	Iron
FL	Fork Length
IATTC	Inter-American Tropical Tuna Commission
ICCAT	International Commission for the Conservation of Atlantic Tunas
IHO	International Hydrographic Organization
IOTC	Indian Ocean Tuna Commission
IOTTP	The Indian Ocean Tuna Tagging Programme
IP	Inflection Point
IRMS	Isotope Ratio Mass Spectrometry
IS	Internal Standard
ISSF	International Seafood Sustainability Foundation
IUPAC	International Union of Pure and Applied Chemistry
LDA	Linear Discriminant Function
Li	Lithium
MDA	Mean Decrease in Accuracy
Mg	Magnesium

MLD	Mixed Layer Depth
Mn	Manganese
MSY	Maximum Sustainable Yield
NBS	National Bureau of Standards
NGS	Next Generation Sequencing
NIST	National Institute of Standards and Technology
NW	North West
O	Oxygen
OTO	Otolith
QDA	Quadratic Discriminant Function
RF	Random Forest
RMFO	Regional Fisheries Management Organization
RSD	Relative Standard Deviation
RTTP-IO	Regional Tuna Tagging Project of the Indian Ocean
SDGs	Sustainable Development Goals
SIMS	Secondary Ion Mass Spectometer
SKJ	Skipjack tuna (*Katsuwonus pelamis*)
SNP	Single nucleotide polymorphism
Sr	Strontium
SSS	Sea Surface Salinity
SST	Sea Surface Temperature
tRMFO	tuna Regional Fisheries Management Organization
UNCLOS	United Nations Convention on the Law of the Sea
UNFSA	United Nations Fish Stocks Agreement
USD	United States Dollars
USGS	United States Geological Survey
VSMOW	Vienna Standard Mean Ocean Water
VPDB	Vienna Pee Dee Belemnite
WCPF	Western and Central Pacific Fisheries Comission
YFT	Yellowfin tuna (*Thunnus albacares*)
YOY	Young of the year
Zn	Zink

SCIENTIFIC PRODUCTION

The scientific and technical material produced and communicated during the period of this Dr. Philos Thesis (February 2017 – April 2021) are detailed bellow:

Peer reviewed publications

Artetxe-Arrate, I., Fraile, I., Farley, J., Darnaude, A.M., Clear, N., Rodríguez-Ezpeleta, N., Dettman, D.L., Pécheyran, C., Krug, I., Médieu, A., Ahusan, M., Proctor, C., Priatna, A., Lestari, P., Davies, C., Marsac, F., and Murua, H. (2021) Otolith chemical fingerprints of skipjack tuna (*Katsuwonus pelamis*) in the Indian Ocean: first insights into stock structure delineation. *PLOS ONE*, 16(3), e0249327, doi: 10.1371/journal.pone.0249327.

Artetxe-Arrate, I., Fraile, I., Marsac, F., Farley, J.H., Rodríguez-Ezpeleta, N., Davies, C., Clear, N., Grewe, P., Murua, H. (2020) A review of the fisheries, life history and stock structure of tropical tuna (skipjack *Katsuwonus pelamis*, yellowfin *Thunnus albacares* and bigeye *Thunnus obesus*) in the Indian Ocean. *Advances in Marine Biology*, 88, In press. doi.org/ 10.1016/bs.amb.2020.09.002

Artetxe-Arrate, I., Fraile, I., Crook, D.A., Zudaire, I., Arrizabalaga, H., Greig, A., Murua, H. (2019). Otolith microchemistry: a useful tool for investigating stock structure of yellowfin tuna (*Thunnus albacares*) in the Indian Ocean. *Marine and Freshwater Research*, 70 (12), 1708-1721, doi.org/10.1071/MF19067

Scientific reports and working documents

Artetxe-Arrate, I., Fraile, I., Rodriguez-Ezpeleta, N., Farley, J., Darnaude, A.M., Clear, N., Dettman, D., Pécheyran, C., Krug, I., Nicolic, N., Médieu, A., Lasdell, M., Ahusan, M., Proctor, C., Priatna, A., Lestrari, P., Taufik, M.,Usmani, H., Zehra, K., Khan, M., Shahid, U., Kazmi, S.M.R., Islan, S., Tariq, M., Zafar, S., Zaidi, J., Marsac, F., Davies, C., and Murua, H. Investigating early stages of skipjack tuna (*Katsuwonus pelamis*) in the Indian Ocean using otolith chemistry. Working paper submitted to the 22nd Working Party on Tropical Tunas: Stock Assessment meeting, 19-23 October 2020, Virtual [IOTC-2020-WPTT22AS-05_Rev1] available at https://www.iotc.org/documents/WPTT/2202/05

Artetxe-Arrate, I., Fraile, I., Farley, J., Clear, N., Darnaude, A.M., Dettman, D., Krug, I., Nicolic, N., Médieu, A., Lasdell, M., Ahusan, M., Proctor, C., Priatna, A., Lestrari, P., Taufik, M.,Usmani, H., Zehra, K., Khan, M., Shahid, U., Kazmi, S.M.R., Islan, S., Tariq, M., Zafar, S., Zaidi, J., Davies, C., Marsac, F., and Murua, H. Otolith $\delta^{18}O$ as a tracer of yellowfin tuna (*Thunnus albacares*) nursery origin in the Indian Ocean.

Working paper submitted to the 22nd Working Party on Tropical Tunas: Stock Assessment meeting, 19-23 October 2020, Virtual [IOTC-2020-WPTT22AS-06_Rev1] available at https://www.iotc.org/documents/WPTT/2202/06

Davies, C., Marsac, F., Murua, H., Fraile, I., Fahmi, Z., Farley, J., Grewe, P., Proctor, C., Clear, N., Landsdell, M., Aulich, J., Feutry, P., Cooper, S., Foster, S., Rodríguez-Ezpeleta, N., **Artetxe-Arrate, I.,** Nikolic, N., Krug, I., Mendibidil, I., Leone, A., Labonne, M., Darnaude, A.M., Arnaud-Haond, S., Devloo-Delva, F., Rougeuc, C., Parker, D., Diaz-Arce, N., Wudianto, Ruchimat, T., Satria, F., Lestari, P., Taufik, M., Priatna, A., Zamroni, A. (2020) Study of population structure of IOTC species and sharks of interest in the Indian Ocean using genetics and microchemistry: 2020 Final Report to IOTC.

Rodriguez-Ezpeleta, N., **Artetxe-Arrate, I.,** Mendibil, I., Diaz-Arce, N., Krug, I., Ruiz, J., Nicolic, N., Médieu, A., Pernak, M., Farley, J., Grewe, P., Lansdell, M., Aulich, J., Clear, N., Proctor, C., Wudianto, Ruchimat, T., Fahmi, Z., Satria, F., Lestari, P., Taufik,M., Priatna, A., Zamroni, A., Davies, C., Marsac, F., Fraile, I., and Murua, H. Co-occurrence of genetically isolated groups of skipjack tuna (*Katsuwonus pelamis*) within the Indian Ocean. Working paper submitted to the 22nd Working Party on Tropical Tunas: Stock Assessment meeting, 19-23 October 2020, Virtual [IOTC-2020-WPTT22AS-07] available at https://www.iotc.org/documents/WPTT/2202/07

Clear N., Eveson P., Darnaude, A.M., Labonne, M., **Artetxe-Arrate, I.,** Fraile, I., Farley, J., Grewe, P., Lestari, P., Taufik,M., Priatna, A., Zamroni, A., Aulich, J., Landsdell, M., Lozano-Montes, H., Danyushevsky, L., Fahmi, Z., Wudianto, Murua, H., Marsac, F., and Davies, C. Investigating population structure of bigeye tuna in the Indian Ocean using otolith microchemistry. Working paper submitted to the 22nd Working Party on Tropical Tunas: Stock Assessment meeting, 19-23 October 2020, Virtual [IOTC-2020-WPTT22AS-11] available at https://www.iotc.org/documents/WPTT/2202/11

Grewe, P., Feutry, P., Foster, S., Auluch, J., Lansdell, M., Cooper, S., Clear, N., Nicolik, N., Krug, I., Medibil, I., Parker, D., Wudianto, Ruchimat, T., Satria, F., Lestari, P., Fernando, D., Priatna, A., Zamroni, A., Rodriguez-Ezpeleta, N., **Artetxe-Arrate, I.,** Fahmi, Z., Murua, H., Marsac, F., and Davies, C. Genetic population connectivity of yellowfin tuna in the Indian Ocean from the PSTBS-IO project. Working paper submitted to the 22nd Working Party on Tropical Tunas: Stock Assessment meeting, 19-23 October 2020, Virtual [IOTC-2020-WPTT22AS-12] available at https://www.iotc.org/documents/WPTT/2202/12

Darnaude A.M., Labonne M., Petit C., Médieu A., Pernak M., Nikolic N., **Artetxe-Arrate I.,** Clear N., Farley J., Eveson P., Lozano-Montes H., Davies C., and

Marsac F. Otolith microchemistry suggests probable population structuring in the Indian Ocean for the brodabill swordfish Xiphias gladius. Working paper submitted to the 18th Working Party on Billfish, 2-4 September, Virtual [IOTC-2020-WPB18-10_Rev1] available at https://iotc.org/documents/WPB/18/10

Davies, C.R., Marsac, F, Murua, H., Fraile, I., Fahmi, Z., Farley, J., Grewe, P., Proctor, C., Clear, N., Lansdell, M., Aulich, J., Feutry, P., Cooper, S., Foster, S., Rodríguez-Ezpeleta, N., **Artetxe-Arrate, I.**, Krug, Mendibil, I., Agostino, L., Labonne, M., Nikolic, N., Darnaude, A., Arnaud-Haond, S., Wudianto, Ruchimat, T., Satria, F., Lestari, P., Taufik, M., Priatna, A., and Zamroni, A. Population Structure of IOTC species and sharks of interest in the Indian Ocean: Estimation with Next Generation Sequencing Technologies and Otolith Micro-chemistry. Working paper submitted to the IOTC 22nd Scientific Committee Meeting, 2-6 December 2019, Karachi, Pakistan [IOTC-2019-SC22-INF05] available at https://iotc.org/documents/SC/22/INF05

Conference contributions: Oral communications

Artetxe-Arrate, I., Fraile, I., and Murua, H. (2020). "Chemical composition of fish hard parts as a natural marker for tropical tuna stocks". *International Postgraduate Course Research in Marine Environment & Resources RiMER-2020*, Donostia-San Sebastián (Spain), 3-7th February 2020.

Artetxe-Arrate, I., Fraile, I., Pecheyran, C. and Murua, H. (2019). Natal signatures in otoliths of young-of-the-year yellowfin (*Thunnus albacares*) and skipjack (*Katsuwonus pelamis*) tuna from the Indian Ocean. Front. Mar. Sci. Conference Abstract: *XVI European Congress of Ichthyology*. Lausanne (Switzerland), 2-6th September 2019. doi: 10.3389/conf.fmars.2019.07.00086

Artetxe-Arrate, I., Fraile, I., Crook, D., Greig, A., Zudaire, I., and Murua, H. (2018). "Investigating the origin of yellowfin tuna (*Thunnus albacares*) in the western Indian Ocean using an otolith chemistry approach". *6th International Otolith Symposium*, Keelung (Taiwan), 15-20th April 2018.

Artetxe-Arrate, I., Fraile, I., and Murua, H. (2018). Stock structure and connectivity of tropical tuna in the Indian Ocean. 12th International *Postgraduate Course Research in Marine Environment & Resources RiMER-2018*, Donostia-San Sebastián (Spain) 29th March -2nd February 2018.

Conference contributions: Posters

Artetxe-Arrate, I., Fraile, I., Crook, D., Greig, A., Zudaire, I., and Murua, H. (2018). Investigating the origin of yellowfin tuna (*Thunnus albacares*) in the

western Indian Ocean using an otolith chemistry approach. *Student Conference in Conservation Science*, Cambridge (UK), 26th-29th March 2018.

Contribution to workshops and working groups

22nd Working Party on Tropical Tuna (WPTT22): Stock Assessment Meeting. Online, 19-23rd October 2020.

Synthesis workshop on Population Structure of Tuna, Billfish and Sharks of Interest in the Indian Ocean. CSIRO Marine Laboratories, Hobart (Tasmania), 26th Feb-3rd Mar 2020.

Sampling campaigns

Project: Monitoreo Científico de la Flota Atunera Vasca en el Océano Índico
Reference: 33-2016-00089
Dates: 27 Mar-11 Apr 2019
Location: Mahé, Seychelles
Centres involved: AZTI Foundation and Seychelles Fishing Authority (SFA)

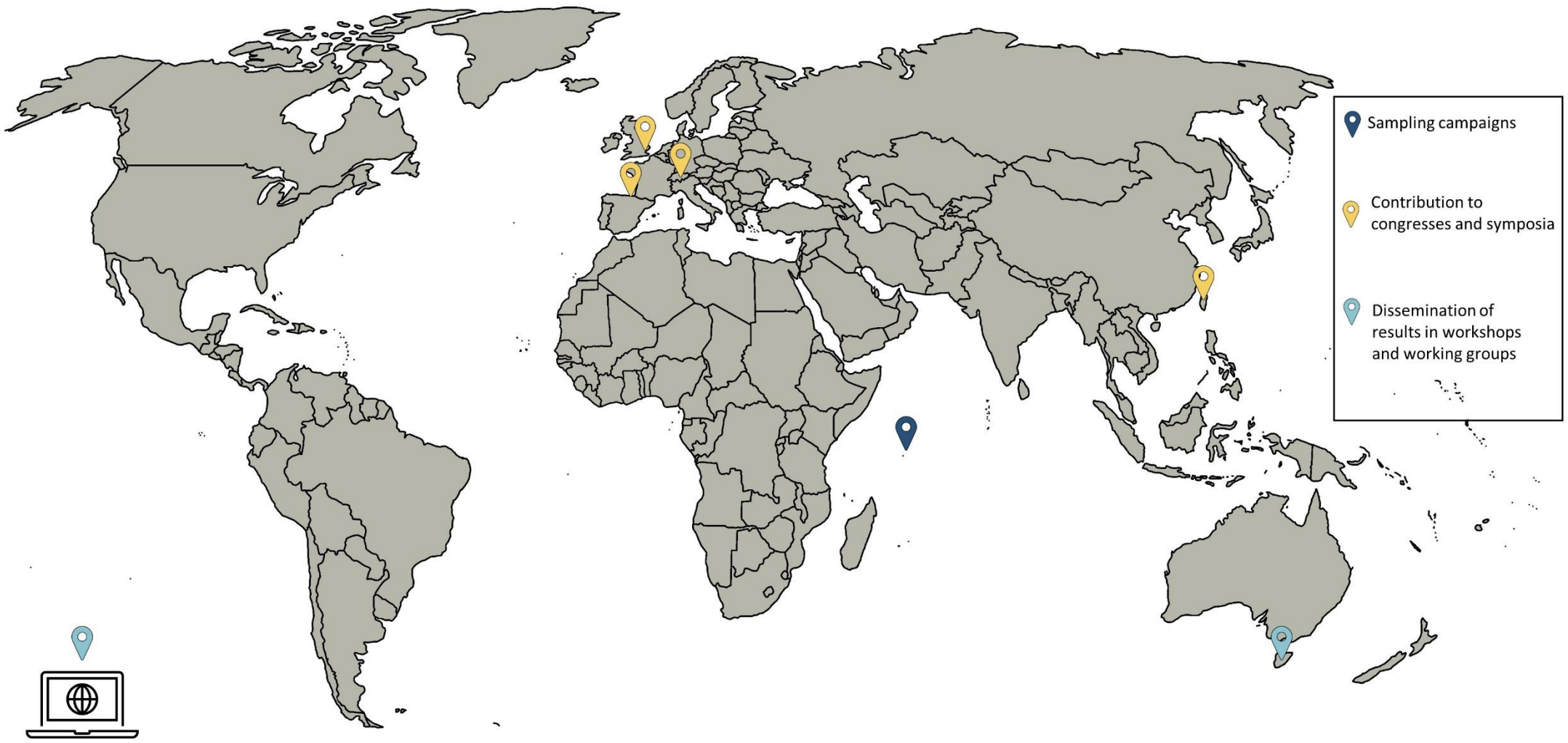
Sampling campaigns
Contribution to congresses and symposia
Dissemination of results in workshops and working groups

LABURPENA

Itsas arrainak munduko elikadura-sistemaren funtsezko atal bat dira, arrantza munduan zehar milioika pertsonen proteina iturri eta bizimodu izanik. Munduko populazioak hurrengo hamarkadetan zehar gora egitea espero da, eta, beraz, munduko arrain kontsumoa ere handitzea espero da. Gehiegizko arrantza saihesteko, ezinbestekoa izango da itsas baliabideen kudeaketa eraginkor bat burutzea, elikagaien segurtasuna eta ekosistemen osotasuna bermatuko dituenak. Erronka honetan, zientziak funtsezko zeregina du; ozeanoen erabilera eraginkorra eta jasangarria bermatuko duten kudeaketa-ekintzak garatzea ahalbidetzen baitu. Izan ere, plangintza-prozesuaren funtsezko zati bat arrantzak eta ingurumenak arrain-populazioetan duten eragina balioesteko erabiltzen diren stock ebaluazio ereduak sortzean datza. Hala ere, eredu matematiko horietatik lortutako emaitzak ahalik eta fidagarrienak izan daitezen, stock-aren ezaugarri diren parametroek eta distribuzio mugek ondo deskribatuta egon behar dute. Gaur egun aplikatzen diren stock ebaluazio gehienek onartzen dute aztertutako taldeko norbanakoek bizi-tasa homogeneoak dituztela eta bizi-ziklo itxia dutela stock-aren distribuzio mugen barnean. Horregatik, stock ebaluazioak populazio estruktura eta nahaste-tasei dagokienez baliozkoak ez diren kasuetan oinarritzen direnean, aztertutako baliabidearen kontserbazioarekin eta errendimendu ekonomiko optimoarekin lotutako helburuak ez betetzeko arriskua dago.

Elikadura segurtasunean paper garrantzitsua betetzen duten espezieen artean, atun espezie tropikalak daude; lanpo sabelmarraduna *Katsuwonus pelamis*, atun hegats-horia *Thunnus albacares* eta atun moja *Thunnus obesus*. Espezie hauek migratzaile handiak dira eta hiru ozeano nagusietako (Atlantikoa, Indiako Ozeanoa eta Ozeano Barea) ur tropikal eta subtropikaletan bizi dira. Bere banaketa geografikoaren barnean, Indiako Ozeanoa, hiru espezie hauen harrapaketetarako berebiziko garrantzia duen arrantzaleku bat da, hala ere, gutxien aztertu izan dena. Egun, hiru espezieetako bakoitza Indiako Ozeanoan stock bakar gisa kudeatzen den arren, stock hauen konektibitate eta dinamika espazialari buruzko zalantzak daude. Testuinguru honetan, tesi honen **helburu nagusia**, Indiako lanpo sabelmarradun eta atun hegats-horiaren stock estruktura ikertzea da, otolitoen (arrainen barne

belarrian dauden kaltzio kabonatozko estruktura pareak) analisi kimikoen bidez. Helburu orokor hori lortzeko, tesia bost kapitulutan banatu da.

Indiako Ozeanoan atun tropikalen kudeaketa iraunkorra bermatzeko lehentasunez landu beharreko ezagutza-arrakala espezifikoak identifikatzeko, **1. kapituluan** espezie horien biologiari, ekologiari eta populazio-egiturari buruzko berrikuspen bibliografiko sakona egin da. Kapitulu honetan, Indiako Ozeanoko atun tropikalen arrantzalekuen dinamika deskribatzen da, eta espezie hauen bizi-zikloaren funtsezko ezaugarriak laburbiltzen dira, hala nola biogeografia, ekologia trofikoa, hazkuntza eta ugalketa-biologia. Ikerketa gutxi topatu dira arlo hauen inguruan, eta eskuragarri dauden gutxi horiek adin-tarte desberdinetako eta/edo azterketa-metodo desberdinak erabiltzen dituzten indibiduoetan oinarritzen dira. Hau dela eta, zaila egiten da ikusitako desberdintasunak leku desberdinen arteko diferentzia biologikoen edo laginketa-estrategia desberdinen ondorio diren zehaztea. Honez gain, lanpo sabelmarradun, atun hegats-hori eta atun mojaren buruzko populazio egiturari buruzko bibliografia ere berrikusten da, hainbat ikuspegitatik abiatuta: arrantza-datuak, espezieen ezaugarri morfometrikoak eta meristikoak, konposizio parasitikoa, genetika, otolitoen konposaketa kimikoa eta markatze-datuak. Ikerketak oso mugatuak diren arren, emaitzek adierazten dute lanpo sabelmarradunaren eta atun hegats-horiaren dinamika espazialak eta populazioa egiturak gaur egun kudeatzeko kontuan izandakoa baino konplexuagoak izan daitezkeela.

Otolitoen konposaketa kimikoaren analisia bizi-historia desberdinak dituzten arrain-taldeak bereizteko balio duen markatzaile natural gisa erabiltzen da. Analisi genetikoekin alderatuz, desberdintasun nagusia da lehenengoek eboluzio-mailan garrantzitsua den informazioa ematen duten bitartean, otolitoen analisi kimikoek indibiduoaren informazio ekologikoa ematen dutela. Adibidez, otolitoaren bizitzako lehen etapetan pilatutako materialaren konposizio kimikoa "aztarna kimiko" bat izan daiteke, errute eremu ezberdinetako arrain taldeak identifikatzeko. Indiako Ozeanoko atun hegats-horiaren populazio-egitura ikertzeko otolitoen konposaketa kimikoaren erabilgarritasuna ebaluatzen du **2. kapituluak**. Zehazki, karbonoaren ($\delta^{13}C$) eta oxigenoaren ($\delta^{18}O$) isotopo egonkorren balioak neurtu ziren Mozambikeko kanalean eta Indiako Ozeanoaren ipar-mendebaldean jasotako atun

arrainkumeen, 0-urte, eta gazteen, urte-1, otolitoetan, baita traza-elementuen proportzioak ere (Ba: Ca, Sr:Ca, Mn:Ca eta Mg: Ca). Emaitzek arrainaren bizitzako lehen asteetan traza-elementuen kontzentrazioen denbora-profilak oso aldakorrak izan daitezkeela erakutsi zuten, ziur asko ingurunearen propietate fisiko-kimikoekin zerikusi gutxi duten berezko faktoreengatik. Horregatik, otolitoaren nukleoan metatutako lehen materiala baztertzea eta, horren ordez, eklosioa gertatu eta aste gutxira dagoen seinale kimikoa, bizi-ziklo goiztiarraren adierazle gisa erabiltzea berme hobea izan daiteke. Ba, Mg eta Mn elementuak, otolitoaren zati honetan, bi eskualdeetako arrainkumeak bereizteko ahalbidetzeko bezain ezberdinak izan ziren. Aldiz, $\delta^{13}C$ eta $\delta^{18}O$ sinadurak ez ziren aldatu Mozambikeko kanaleko eta Indiako Ozeanoko ipar-mendebaldeko arrainen artean, ziur aski, mendebaldeko Indiako Ozeanoan karbonoaren eta oxigenoaren konposizio isotopikoan aldaketarik ez zegoelako. Atun hegats-horiaren arrainkumeak bere harrapaketa lekuei esleitzeko sailkapen-metodo desberdinen erabilgarritasuna ere ebaluatu zen, eta frogatu zen sailkapenaren zehaztasuna hobetu egiten zela Random Forest (RF) ikasteko teknika automatikoa erabiltzen zenean. Azkenik, mendebaldeko Indiako Ozeanoan harrapatutako atun hegats-hori gazteen balizko jatorria ebaluatu zen RF kluster analisi baten bidez, eta larba-iturri bakarra hauteman zen aztertutako arrainen artean. Arrain hauen aztarna kimikoak Indiako Ozeanoko ipar-mendebaldeko arrainkumeen seinalearen antz handiagoa zuten. Oro har, ikerketak, otolitoen kimikaren erabilera babestu zuen, Indiako Ozeanoko atun hegats-horiaren stock estruktura aztertzeko etorkizun handiko tresna bezala.

Halaber, **3. kapituluan**, otolitoen mikrokimikaren egokitasuna aztertzen da, Indiako Ozeanoko lanpo sabelmarradunaren dinamika espaziala hobeto ulertzeko tresna gisa. Horretarako, Indiako Ozeano ekuatorialean hiru errute eremu nagusietan (Mendebaldea, Erdialdea eta Ekialdea) harrapatutako arrainkumeen (4-6 hilabete) konposizio kimikoa alderatu zen. Zehazki, bi urtetan jarraian harrapatutako indibiduoen aztarna kimikoak (Li:Ca, Sr:Ca Ba:Ca, Mg:Ca eta Mn:Ca) eta isotopikoak ($\delta^{13}C$, $\delta^{18}O$) aztertu ziren. Ikusi zenez, nahiz eta markatzaile kimiko batzuk errute eremu desberdinetako arrainen artean nabarmen ezberdinak izan, desberdintasunak ez ziren izan beren jatorrizko eremuari indibiduo nagusiak esleitzeko erreferentzia datu base bat sortzeko bezain indartsuak. Era berean, otolitoen konposaketa kimikoaren aldagai anitzeko analisiek Erdialdeko eta

Ekialdeko zonaldeen arteko banaketa geografiko eskasa erakutsi zuten. Gainera, denbora efektu bat antzeman zen otolitoen traza-elementuen sinaduretan, jaiotza-urte eta urtaro desberdinetako arrainen artean. Lanpo sabelmarraduna urtean zehar ugalketa denboraldi bat baino gehiago dituen espeziea denez, ondorioztatzen dugu, otolitoen konposaketa kimikoaren analisiak eragingarriagoa izateko, kontuan hartu behar direla urteen arteko baldintza ozeanografikoen aldaketei lotutako sinadura kimikoen aldaketak Indiako Ozeanoan. Etorkizuneko ikerketak lan honetan aintzat hartutakoak baino indibiduo gazteagoetan oinarritu beharko lirateke (<4 hilabete) ere, otolitoen seinale kimikoan behatutako homogeneotasuna laginketaren aurreko indibiduoen errute eremuen arteko mugimenduen ondorio izateko aukera murrizteko. Aldi berean, laginketaren denbora-banaketa kontuan hartu beharko litzateke, urteen eta urtaroen arteko ozeanografian kondizioak errute eremuen arteko desberdintasun posibleetatik bereizi ahal izateko. Gainera, beste teknika batzuk (adibidez, genetika, partikulen jarraipena) otolitoen kimikarekin batera aztertu beharko liratezke, ikuspegi holistakoagoa emateko. Honek kudeaketa-unitateak hobeto definitzea ahalbidetuko luke; izan ere, baliteke ikuspegi tekniko bakarra nahikoa ez izatea stock estruktura konplexu bat argitzeko.

Arrain helduak beren jatorrizko eremuari esleitu ahal izan baino lehen, zehaztu behar da errute eremu bakoitzerako denboran zehar egonkorrak diren aztarna kimiko desberdinak dauden ala ez. Hori dela eta, **4. kapituluaren** helburua da Indiako Ozeanoan atun hegats-horiaren errute eremu nagusien aztarna kimikoen erreferentzia datu base bat sortzea, ondoren indibiduo helduen jatorria iragartzeko erabili ahal izateko. Horretarako, bi urtez jarraian Indiako Ozeanoan lau errute zonaldetan (Madagascar, Seychelles-Somalia, Maldivas eta Sumatra) harrapatutako arrainkumeen otolitoetan (< 4 hilabete) traza-elementuen (Li:Ca, Sr:Ca, Ba:Ca, Mg:Ca eta Mn:Ca) eta isotopo egonkorren ($\delta^{13}C$, $\delta^{18}O$) konposizioa neurtu zen. Lehenik eta behin, arrainaren adinaren eta neurriaren arteko erlazioa aztertu zen, otolitoaren eraztunen zenbaketan oinarrituta. Estimazioen arabera, primordioko (otolitoaren nukleoa) 65 mikratarako distantzia 10.2 ± 1.3 eguni dagozkie, eta, beraz, larba-faseari dagokion otolitoaren zati gisa identifikatu zen. Traza-elementuen kontzentrazioen bi dimentsiotako mapak egin ziren, otolitoaren barruko elementuen banaketa espaziala aztertzeko. Aztertutako elementuen artean banaketa-patroi ezberdinak ikusi ziren; Li, Sr eta Ba, bizitza goiztiarra irudikatzen

zuen otolitoaren zatian aberastuak zeuden, Mn eta Mg kontzentrazioak, hazkuntza banden barnean heterogeneoak ziren bitartean. Banaketa hau ez da lehenago kontuan hartu atun espezieen otolitoen azterketa kimiko bakar batean ere, baina garrantzitsua da, adibidez, elementuen analisiak egiteko otolitoen barruko kokalekuak hautatzeko orduan. Otolitoan nahierara jarritako transektu edo puntuetako konposizio mikrokimikoa laginen artean alda daiteke, soilik otolitoaren hazkunde-bandan duten kokapenaren arabera, emaitzen interpretazio okerra eraginez. Gainera, larba-faseari dagokion otolitoen konposizio kimikoaren urte arteko eta errute eremuen arteko aldaketa ebaluatu zen. Otolitoen aztarna kimikoetan aldaketa nabarmena hauteman zen errute eremu guztien artean, Madagaskar eta Seychelles-Somalia alboz-alboko eremuen artean izan ezik. Otolitoen $\delta^{13}C$ eta $\delta^{18}O$ balioak mendebaldeko (Madagaskar + Seychelles-Somalia) eta Maldivetako eta Sumatrako errute eremuak desberdintzeko garrantzisuak izan ziren, traza-elementuen konposaketa urtero aldatzen zen bitartean.

Atun hegats-hori gazteen (<2 urte) eta helduen (>2 urte) laginak ez zetozenez bat erreferentziazko datu basea deskribatzeko erabilitako arrainkumeen jaiotza-urtearekin, **5. kapituluan** oxigenoaren sinadura isotopikoa baino ez zen erabili. Arrazoia, atun hegats-hori hauen jatorriaren iragarpenetan, urte arteko aldakortasunaren ondorioz sortutako edozein efektu ezabatzea izan zen. Lehenik eta behin, Reunion uharteetan eta Pakistan aldean harrapatutako atun hegats-hori gazteak aurreko kapituluan deskribatutako $\delta^{18}O$ erreferentzia-balioekin alderatu ziren. Reunion aldeko indibiduoen otolitoen $\delta^{18}O$ balioak mendebaldeko errute-eremukoen antzekoak ziren (Madagaskar + Seychelles-Somalia). Hala ere, Pakistango arrainen otolitoen $\delta^{18}O$ balioak lagindutako edozein errute eremuetakoen desberdinak ziren. Beraz, Pakistango zonaldeko laginen otolitoen $\delta^{18}O$ balioak erreferentzia-iturri gehigarri gisa hartu ziren atun hegats-hori helduen jatorria esleitzeko, erregresio logistiko multinomial sailkapen metodo batetik abiatuta aurreikusi zena. Mendebaldeko Indiako Ozeanoa atun hegats-hori ekoizpenerako eremu kritikoa zela ikusi zen, errute eremu hau, Indiako Ozeanoan lagindutako hiru arrantza-eremu subtropikaletako errekluten iturri nagusia baitzen. Pakistango gazteen antzeko jatorria zuten arrainen ekarpen txikiago bat ere antzeman zen, eta lagin bakar bat ere ez zen esleitu Maldivak eta Sumatra erruteko eremuetara. Gainera, heldu baten otolito bat aztertu zen bigarren mailako ioien

masen espektrometriaren (SIMS) analisi bidez, otolitoaren hazkuntza transektuan zehar $\delta^{18}O$-aren estimazioen erresoluzio on bat eman zuelarik. Orain arte atun tropikaletan erabili ez den analisi metodo hau etorkizun handiko tresna izan daiteke atunen bizitza osoko mugimenduak ondorioztatzeko, baldin eta $\delta^{18}O$-aren mapa isotopikoekin konparatzen badira.

Tesi honetatik eratorritako emaitzek, atun tropikalen otolitoen konposaketa kimikoko etorkizuneko ikerketetarako metodologia hobetzen lagundu dute eta arlo honetan ikerketa berriak suspertu ditzazke. Gainera, tesi honek lehen urrats garrantzitsu bat eman du Indiako Ozeanoan lanpo sabelmarradunaren eta atun hegats-horiaren estruktura espaziala eta konektibitatea ulertzeko. Egun ustiapen-tasa handiak daudenez, Indiako Ozeanoko arrantza eremuen espezien populazio egitura eta berain arteko biomasa-fluxuak hobeto ulertzea ezinbestekoa da stock-en ebaluazioa hobetzeko. Zenbat eta antzekoagoak izan kudeaketarako erabilitako populazio unitateak eta horien berezko populazio-egitura, orduan eta eragingarriagoa izango da baliabide horien kudeaketa jasangarria lortzea.

RESUMEN

Los peces marinos son una parte esencial del sistema alimentario mundial, ya que son una fuente de proteína y sustento para millones de personas alrededor del mundo. Se espera que la población mundial aumente en las próximas décadas, y, por lo tanto, es de esperar que con ello aumente también el consumo mundial de pescado. Con el fin de evitar la sobrepesca, una gestión eficaz de los recursos marinos, que garantice tanto la seguridad alimentaria como la integridad de los ecosistemas, será indispensable. En este aspecto, la ciencia juega un papel fundamental, ya que, permite desarrollar acciones de gestión que garanticen un uso eficiente y saludable de los océanos, pudiendo así explotar los recursos marinos a su máximo rendimiento y sin perder la sostenibilidad futura. Esto es debido a que una parte clave en el proceso de planificación, consiste en la creación de modelos de evaluación de stocks que se utilizan para estimar el impacto de la pesca y factores medioambientales en las poblaciones de peces. Sin embargo, para que los resultados obtenidos a partir de estos modelos matemáticos sean lo más fiables posibles, los parámetros utilizados y los límites de distribución de los stocks deben de estar bien caracterizados. La mayoría de los modelos de evaluación de stock que se aplican hoy en día, asumen que los individuos pertenecientes al grupo analizado tienen tasas vitales homogéneas, están expuestos a la misma mortalidad por pesca, y poseen un ciclo vital cerrado dentro de los límites de distribución. Es por ello, que cuando los modelos de evaluación de stocks se basan en supuestos no válidos en cuanto a estructura poblacional y las tasas de mezcla, existe el riesgo de que no se cumplan los objetivos relacionados con la conservación y el rendimiento económico óptimo del recurso analizado.

Entre las especies que desempeñan un papel importante en la seguridad alimentaria, se encuentran las denominadas como túnidos tropicales; el listado, *Katsuwonus pelamis*, el rabil *Thunnus albacares* y el patudo *Thunnus obesus*. Estas especies son altamente migratorias y habitan las aguas tropicales y subtropicales de los tres océanos principales (Atlántico, Índico y Pacífico). Dentro de su área de distribución geográfica, el Océano Índico es un caladero de vital importancia para las capturas de estas tres especies, sin embargo, es del que menos información se

posee. Aunque en la actualidad cada una de las tres especies se gestiona como un único stock en el Océano Índico, siguen existiendo dudas sobre la conectividad y dinámica espacial de los túnidos tropicales en el Océano Indico. En este contexto, **el objetivo principal** de esta tesis es investigar la estructura poblacional del listado y del rabil en el Océano Índico, mediante el análisis microquímico de los otolitos (pares de estructuras cálcicas que se encuentran en el oído interno de los peces). Para lograr este objetivo general, la tesis se ha dividido en cinco capítulos.

Con el fin de identificar las brechas de conocimiento específicas que deben abordarse de forma prioritaria para garantizar una gestión sostenible y eficaz de los túnidos tropicales en Océano Índico, en el **capítulo 1** se ha realizado una revisión bibliográfica exhaustiva sobre la biología, la ecología y la estructura poblacional de estas especies. Este capítulo, describe la dinámica de las pesquerías de túnidos tropical del Océano Índico, y sintetiza rasgos clave de su ciclo vital como la biogeografía, la ecología trófica, el crecimiento, y la biología reproductiva. Lo que se ha encontrado es una falta de estudios, siendo los pocos disponibles, basados en ejemplares de diferentes rangos de edad y/o que utilizan diferentes métodos de análisis, lo que hace difícil, si no imposible, analizar si las diferencias observadas se deben a variaciones espaciales o a diferencias en las estrategias de muestreo. Además, se revisa la bibliografía disponible sobre la estructura poblacional del listado, rabil y patudo, a partir de diferentes enfoques: datos pesqueros, caracteres morfométricos y merísticos, composición parasítica, genética, microquímica de los otolitos, y datos de marcado. Aunque los estudios son muy limitados, los resultados indican que la dinámica espacial del listado y el rabil puede ser más compleja que la asumida actualmente para su gestión.

En relación con lo anterior, el análisis de la composición química de los otolitos es reconocido como un marcador natural útil para discriminar entre grupos de peces con historias vitales diferentes. Su principal diferencia con los análisis genéticos es, que mientras que los primeros proporcionan información relevante a escala evolutiva, el análisis microquímico de los otolitos aporta información ecológica relevante para la vida del individuo. Por ejemplo, la composición química del material acumulado durante las primeras etapas de la vida en el otolito sirve como una "huella química" que puede diferir entre grupos de peces pertenecientes

a diferentes zonas de puesta. El **capítulo 2** evalúa la viabilidad de esta técnica como herramienta potencial para investigar la estructura poblacional del rabil en el Océano Índico. En concreto, se midieron los valores de los isótopos estables carbono y oxígeno ($\delta^{13}C$ y $\delta^{18}O$) y las proporciones de elementos traza (Ba:Ca, Sr:Ca, Mn:Ca y Mg:Ca) en otolitos de atunes alevines, edad-0, y juveniles de edad-1 recogidos en el Canal de Mozambique y del noroeste del Océano Índico. Se observó que los perfiles temporales de las concentraciones de elementos traza pueden ser muy variables durante las primeras semanas de vida del pez, probablemente debido a factores intrínsecos que poco tienen que ver con las propiedades físico-químicas del entorno. Es por esto, que descartar el primer material acumulado en el núcleo del otolito, y en su lugar usar como indicador del ciclo vital temprano la señal correspondiente a pocas semanas después de la eclosión puede ser una mejor garantía. Los elementos Ba, Mg y Mn fueron lo suficientemente diferentes en esta porción del otolito como para discriminar entre los alevines de las dos regiones. En cambio, las firmas $\delta^{13}C$ y $\delta^{18}O$ no variaron entre los peces del Canal de Mozambique y el noroeste del Océano Índico, probablemente debido a la falta de variación en la composición isotópica del carbono y el oxígeno en las aguas del Índico occidental. También se evaluó la utilidad de diferentes métodos de clasificación para asignar los alevines de rabil a sus respectivos lugares de captura, y se demostró que la precisión de la clasificación mejoraba cuando se utilizaba una técnica de aprendizaje automático como Random Forest (RF). Se evaluó el posible origen de los rabiles de edad-1 del Océano Índico occidental mediante un análisis clúster de RF, y se detectó una única fuente larvaria entre los peces analizados. La señal de estos peces se asemejaba más a la de los alevines del noroeste del Océano Índico. En general, el estudio respaldó el uso de la química de los otolitos como una herramienta prometedora para analizar la estructura de las poblaciones de rabil en el Océano Índico.

Asimismo, el **capítulo 3** examina la idoneidad de la microquímica de los otolitos como herramienta para comprender mejor la dinámica espacial del listado en el Océano Índico. Para ello, se comparó la composición química de los otolitos en alevines (4 a 6 meses de edad) capturados en las tres principales zonas de puesta del Océano Índico ecuatorial (Oeste, Centro y Este). Específicamente, se analizaron las firmas elementales (Li:Ca, Sr:Ca, Ba:Ca, Mg:Ca y Mn:Ca) e isotópicas ($\delta^{13}C$, $\delta^{18}O$) de individuos capturados en dos años consecutivos. Se observó que, aunque algunos

marcadores químicos (Sr:Ca, Ba:Ca, Mg:Ca y $\delta^{18}O$) diferían significativamente entre los peces de las diferentes zonas de puesta, las diferencias no fueron lo suficientemente fuertes como para crear una base de referencia que permitiera asignar los individuos mayores a su zona de origen. Igualmente, los análisis multivariantes de la composición microquímica de los otolitos revelaron una escasa separación geográfica entre las zonas del Centro y Este. Además, se detectó un efecto temporal en las firmas de elementos traza de los otolitos entre los peces pertenecientes a cada año de nacimiento. Dado que el listado es una especie con varios picos reproductivos a lo largo del año, concluimos que, para un mejor uso de la microquímica de los otolitos como herramienta para delinear su estructura poblacional en el Océano Índico, las variaciones en las firmas químicas asociadas a los cambios estacionales en las condiciones oceanográficas han de ser tenidas en cuenta. Estudios futuros deberían basarse en individuos más jóvenes (<4 meses) que los considerados en este estudio, para reducir la posibilidad de que la homogeneidad observada en la señal microquimica de los otolitos sea debida a movimientos previos al muestreo entre las diferentes zonas de puesta. Al mismo tiempo, debería considerarse la estratificación temporal del muestreo, de modo que las diferencias estacionales en la oceanografía puedan disociarse de las posibles diferencias regionales. Además, otras técnicas (por ejemplo, la genética, el seguimiento de partículas) deberían de considerarse en conjunto con la microquímica de los otolitos, para proporcionar una visión más precisa que permita definir mejor las unidades de gestión, ya que, un único enfoque técnico puede no ser suficiente para delinear una estructura poblacional compleja.

Antes de que los individuos adultos puedan ser asignados a su zona de origen, debe determinarse si existen huellas químicas distintas y temporalmente estables para las diferentes zonas de puesta. Por ello, el **capítulo 4** tiene como objetivo crear una base de referencia de las principales zonas de puesta del rabil en el Océano Índico, de modo que pueda utilizarse posteriormente para predecir el origen de los individuos mayores. Con este fin, se midió la composición de elementos traza (Li:Ca, Sr:Ca, Ba:Ca, Mg:Ca y Mn:Ca) y de isótopos estables ($\delta^{13}C$, $\delta^{18}O$) en otolitos de alevines (<4 meses) capturados durante dos años consecutivos en cuatro zonas de puesta del Océano Índico: Madagascar, Seychelles-Somalia, Maldivas y Sumatra. En primer lugar, se examinó la relación entre la edad y la talla del pez basándonos en el

conteo de los microincrementos del otolito, se estimó que 65 micras del primordio (núcleo del otolito) correspondían a 10,2±1,3 días y por lo tanto se identificó como la porción del otolito correspondiente a la fase larvaria. Se elaboraron mapas en dos dimensiones de las concentraciones de elementos traza para examinar la distribución espacial de los elementos dentro del otolito. Se observaron diferentes patrones de distribución entre los elementos analizados; Li, Sr y Ba estaban enriquecidos en la porción del otolito que representaba la vida temprana, mientras que las concentraciones de Mn y Mg eran heterogéneas dentro de las bandas de crecimiento. Esta cuestión no se ha tenido en cuenta anteriormente en ningún estudio microquímico de los otolitos relacionados con los túnidos, pero es una cuestión importante para, por ejemplo, seleccionar las ubicaciones de los ensayos elementales. La composición microquimíca en transectos o puntos colocados arbitrariamente en el otolito, puede diferir entre las muestras sólo por su ubicación en la banda de crecimiento del otolito, dando pie a una interpretación errónea de los resultados. Además, se evaluó la variación interanual y regional de la composición química de los otolitos correspondiente a la fase larvaria. Se detectó una variación regional significativa en las firmas químicas de los otolitos entre todas las zonas de puesta, excepto entre las zonas adyacentes de Madagascar y Seychelles-Somalia. Los valores $\delta^{13}C$ y $\delta^{18}O$ de los otolitos fueron importantes para diferenciar las zonas de puesta más occidentales (Madagascar + Seychelles-Somalia), de las zonas de Maldivas y Sumatra, mientras que la composición de elementos traza variaba de forma diferente cada año.

Dado que las muestras disponibles de sub-adultos (<2 años) y adultos (>2 años) de rabil no coincidían con el año de nacimiento de los alevines utilizados para describir la base de referencia, en el **capítulo 5** se utilizó únicamente la firma isotópica del oxígeno ($\delta^{18}O$). El fin fue eliminar cualquier posible efecto de la variabilidad interanual en las predicciones del origen de estos rabiles. Primero, se compararon los rabiles sub-adultos capturados en las islas Reunión y en la zona de Pakistán con los valores de referencia de $\delta^{18}O$ descritos en el capítulo anterior. Los valores de $\delta^{18}O$ de los otolitos de los atunes de la zona de Reunión eran similares a los de la zona puesta occidental (Madagascar + Seychelles-Somalia), sin embargo, los valores de $\delta^{18}O$ de los otolitos de los peces de Pakistán eran distintos a los de cualquier zona de puesta muestreadas. Por lo tanto, los valores de $\delta^{18}O$ de los

otolitos de las muestras de la zona de Pakistán se consideraron como una fuente de referencia adicional para la asignación del origen de los rabiles adultos, que se predijo a partir de un método de clasificación de regresión logística multinomial. Se observó que el Océano Índico occidental era una zona crítica de producción de rabil, ya que esta región parecía ser el principal contribuyente de reclutas de rabil a las tres zonas de pesca sutropicales muestreadas en el Océano Índico. También se detectó una contribución menor de peces con un origen similar al de los sub-adultos de Pakistan, y ninguna muestra fue asignada a las zonas de puesta de Maldivas y Sumatra. Además, se analizó un otolito de adulto mediante un análisis de espectrometría de masas de iones secundarios (SIMS), el cual proporcionó una buena resolución de las estimaciones de $\delta^{18}O$ a lo largo del transecto de crecimiento del otolito. Este análisis, que no ha sido utilizado hasta la fecha en túnidos tropicales, puede ser una herramienta prometedora para inferir los movimientos a lo largo de la vida del rabil si son comparados con mapas isotópicos de $\delta^{18}O$ en el océano.

Los resultados derivados de esta tesis han ayudado a perfeccionar la metodología para estudios futuros en microquímica de otolitos de túnidos tropicales, y esperamos que puedan estimular nuevas investigaciones en este campo. Además, esta tesis proporciona un primer paso importante hacia la comprensión de la estructura espacial y la conectividad del listado y del rabil en el Océano Índico. Dadas las elevadas tasas de explotación que se dan en la actualidad, una mejor comprensión de los flujos de biomasa entre los distintos caladeros del Océano Índico es crucial para mejorar los modelos de evaluación de los stocks. Finalmente, cuanto más se asemejen las unidades consideradas para la gestión a la estructura poblacional de las mismas, mejor será la consecución de los objetivos para una gestión sostenible de estos recursos.

SUMMARY

Marine fish stocks are an essential part of global food system, providing nourishment and livelihood for millions of people around the world. Given the anticipated increase in the world´s population over the next decades, global fish consumption is also expected to increase. An effective management of marine resources is essential to prevent from overfishing while ensuring food security and ecosystem integrity. To enable the exploitation of marine resources at their maximum sustainable yield, science-based management advise is fundamental for developing management actions that guarantee an efficient and healthy use of the oceans. An essential part of management process involves the development of stock assessment models to understand population dynamics and the impact of fisheries and environmental factors on fish stocks. However, before carrying out stock assessment mathematical models, biological/fishery parameters used and boundaries that characterise the stock should be well understood. Most applied stock assessment models assume that the group individuals being analysed have homogeneous vital rates through its geographical distribution and have a closed life cycle. Therefore, when stock assessment models are based on invalid assumptions in terms of stock structure and mixing rates, there is the risk that stated objectives related to conservation and optimal economic use of the resource are not met.

Among the marine species that play a significant role in the food security, we can find the so-called tropical tuna species; skipjack tuna, *Katsuwonus pelamis*, yellowfin tuna *Thunnus albacares*, and bigeye tuna *Thunnus obesus*. These species are highly migratory top predators that inhabit the tropical and subtropical waters of the three major oceans (Atlantic, Indian, and Pacific). Within their distributional range, the Indian Ocean is a fishing ground of vital importance for tropical tuna catches yet is the least studied. Currently each of the tropical tuna species is managed as a single stock in the Indian Ocean, however, fundamental questions remain regarding their connectivity and spatial dynamics. In this context, the **aim** of this thesis was to investigate the stock structure of skipjack and yellowfin tunas in this ocean using otolith (i.e. hard-calcareous structure found in the inner ear of fish)

natural markers linked to ambient physicochemical conditions of the ocean. To achieve this overall aim, the thesis was divided in five chapters.

In a move towards identifying specific knowledge gaps that should be addressed with priority to ensure a sustainable and effective management of tropical tuna in the Indian Ocean, in **chapter 1** we performed a comprehensive review of available knowledge on the biology, ecology, and stock structure of these species. We described the characteristics of Indian Ocean tropical tuna fisheries, and synthesized skipjack, yellowfin, and bigeye tunas key life history attributes such as biogeography, trophic ecology, growth, and reproductive biology. The lack of oceanic scale studies together with the fact that available studies are based on fish from different size/age classes and/or using different methods, make difficult to know whether observed differences stem from regional differences, or if they are just derived from different sampling/reporting strategies. Besides, we reviewed the available literature about stock structure sourced from different stock delineation approaches; fisheries data, morphometric and meristic characters, parasites, genetics, otolith microchemistry and tagging data. Results indicated that the spatial dynamics of skipjack and yellowfin tunas may be more complex than currently assumed for management.

With regard to the foregoing, analyses of otolith chemical composition have been recognized as useful natural markers to discriminate among groups of fish with different life histories. While genetic analyses provide information over evolutionary timescales, otolith chemistry informs over ecological time frames relevant to the individual life span. The chemical composition of the otolith material accreted during early life stages, for instance, serves as a "chemical fingerprint" that may differ among groups of fish belonging to different nursery areas. We assess the feasibility of this technique as a potential tool for investigating yellowfin tuna stock structure in the Indian Ocean in **chapter 2**. Specifically, carbon and oxygen stable isotopes ($\delta^{13}C$ and $\delta^{18}O$) and trace element ratios (Ba:Ca, Sr:Ca, Mn:Ca and Mg:Ca) were measured in otoliths of young-of-the-year (YOY, age-0) and age-1 yellowfin tuna collected from the Mozambique Channel and north-west Indian Ocean regions. Elemental profiles of trace element data showed that concentrations can highly vary during the first weeks of life of the fish, probably due to factors other than ambient

physicochemical properties. The use of otolith material from the portion of the otolith corresponding to few weeks after hatch may therefore represent a better alternative for early life history comparisons than the first material accreted in the core of the otolith. Differences in YOY near-core chemistry were then used for natal-origin investigation. Ba, Mg and Mn were sufficiently different to discriminate YOY individuals from the two regions. In contrast, $\delta^{13}C$ and $\delta^{18}O$ signatures did not vary between Mozambique Channel and north-west Indian Ocean. We also evaluated the usefulness of different classification methods in assigning YOY yellowfin tuna to their respective capture locations and showed that the classification accuracy improved when using a machine learning technique such as Random Forest (RF). The origin of age-1 yellowfin tuna from the western Indian Ocean was assessed using a RF cluster analysis, and a unique larval source was detected. The signal of these fish resembled that of YOY from a north-west Indian Ocean origin, highlighting the importance of local production. Overall, the study supported the use of otolith chemistry as a promising approach to analyse yellowfin stock structure in the Indian Ocean.

Similarly, in **chapter 3** we examined the suitability of otolith microchemistry as a tool to better understand the spatial dynamics of skipjack tuna in the Indian Ocean. For that, we compared the early life otolith chemical composition of YOY (4–6 month old) skipjack tuna captured from the three main nursery areas of the equatorial Indian Ocean (West, Central and East). Elemental (Li:Ca, Sr:Ca, Ba:Ca, Mg:Ca and Mn:Ca) and stable isotopic ($\delta^{13}C$, $\delta^{18}O$) signatures from individuals captured in two consecutive years were analysed. We show that even if some chemical markers (Sr:Ca, Ba:Ca, Mg:Ca and $\delta^{18}O$) significantly differed among fish from different nurseries, differences were not strong enough to describe a reference baseline for each nursery area that allows the assignment of older individuals to their nursery origin. Moreover, multivariate analyses of otolith chemical signatures revealed low geographic separation among Central and Eastern nurseries. A cohort effect on otolith trace element signatures was also detected. As skipjack tuna is a species with several reproductive peaks throughout the year, we concluded that for the delineation of Indian Ocean skipjack tuna stock structure using otolith microchemistry, variations in chemical signatures associated with seasonal changes in oceanographic conditions must be considered. Further research on skipjack

population structure using otolith microchemistry should rely on younger (<4 months) individuals to reduce the possibility of movements between nursery areas prior to sampling, while also considering temporal stratification of sampling so that seasonal differences in oceanography can be disentangled from potential regional differences. Besides, otolith microchemistry in conjunction with other techniques (e.g., genetics, particle tracking) should be further investigated to provide a more accurate overview that allow to better define management units, as a single technical approach may not be sufficient to delineate a complex stock structure.

Before adult individuals can be assessed to their nursery of origin, it must be determined if distinct and temporally stable chemical fingerprints do exist for each nursery area. Thus, in **chapter 4** the objective was to create a baseline of chemical signatures from major nurseries of yellowfin tuna in the Indian Ocean, so that it could subsequently be used to predict the origin of older individuals. For that, we measured trace element (Li:Ca, Sr:Ca, Ba:Ca, Mg:Ca and Mn:Ca) and stable isotope ($\delta^{13}C$, $\delta^{18}O$) composition in otoliths of YOY (<4 months) captured in two consecutive years from 4 nursery areas in the Indian Ocean; Madagascar, Seychelles-Somalia, Maldives, and Sumatra. First, we examined the age-length relationship based on otolith microstructure and identified the portion of the otolith corresponding to the larval stage; 65 microns from the primordium was estimated to be 10.2±1.3 days. We also developed two dimensional maps of trace element concentrations to examine spatial distribution of elements. Different distribution patterns were observed among the elements analysed; Li, Sr and Ba were enriched in the portion of the otolith representing early life, whereas Mn and Mg concentrations were heterogeneous across growth bands. This issue has not previously been considered in tuna otolith microchemistry studies, but it is an important issue to, for example, select elemental assay locations. Arbitrarily laid transects or spots can differ in element composition among samples just because of their placement in the otolith growth band, confounding the results. We also assessed the inter-annual and regional variation in larval stage otolith chemical composition. Significant regional variation in otolith chemical signatures was detected among all nurseries, except for between Madagascar and Seychelles-Somalia. Otolith $\delta^{13}C$ and $\delta^{18}O$ were important drivers of differentiation between western (Madagascar and Seychelles-Somalia),

Maldives and Sumatra nurseries, whereas the elemental signatures were cohort specific.

The sub-adult (<2 years) and adult (>2 years) yellowfin tuna available for study did not match the cohort of those YOY described in the baseline, in **chapter 5** we used only the $\delta^{18}O$ signature described in the baseline, to remove any potential effect of interannual variability in nursery origin predictions. Sub-adult yellowfin tuna captured in Reunion and Pakistan area were first compared to $\delta^{18}O$ reference values described in the previous chapter. Otolith $\delta^{18}O$ values of tuna from Reunion area were similar to the western nursery signature, but otolith $\delta^{18}O$ values of fishes from Pakistan area were distinctive to any of the nursery areas sampled. Consequently, otolith $\delta^{18}O$ values of samples from Pakistan area were considered as an additional nursery source for adult tuna origin assignments (age>2), which was predicted from a multinomial logistic regression classification method. We found that the west Indian Ocean was a critical nursery area and production zone for yellowfin tuna, as this region appeared to be the major contributor of yellowfin tuna recruits to three south-tropical fishery grounds sampled in the Indian Ocean. Minor contribution of Pakistan-like origin was also detected among adult samples, but contribution of central and eastern nurseries to the adult population on the main fishing grounds was negligible. One adult otolith was analysed by secondary ion mass spectrometry (SIMS) analysis, which provided a good resolution of $\delta^{18}O$ estimates along the otolith growth transect. This approach may be a promising tool to infer lifetime movements of yellowfin tuna when comparing to observed values of $\delta^{18}O$ isoscapes.

The findings from this thesis can help researchers to refine the methodology for tropical tuna related otolith microchemistry studies and can stimulate new research on the field. Besides, this thesis provided an important first step towards the understanding the spatial structure and connectivity of skipjack and yellowfin tunas in the Indian Ocean. Given the high exploitation rates experience by these species nowadays, understanding the connectivity among different fishery grounds in the Indian Ocean is crucial to inform stock assessment models. Ultimately, the closer management units reflect the stock structure, the better for achieving sustainable management goals.

“Nothing in life is to be feared,

it is only to be understood.

Now is time to understand more,

So that we may fear less.”

Marie Curie

GENERAL INTRODUCTION

1. Organization

The nature of this work and the questions and methodologies addressed during this dissertation led to the presentation of different research themes separately in 5 chapters. Each chapter is therefore presented in the format of an individual scientific paper, with its own abstract, introduction, material and methods, results, discussion, and conclusions. It is therefore possible that some redundant information is included throughout different chapters. In addition to these chapters, the present thesis includes a general introduction, general methods, general discussion, overall conclusions, references, and appendices sections. Detailed information on what is found in each section as follows:

General Introduction section gives an overview of the dissertation structure, provides the necessary background information to contextualize the present dissertation and the choice of the research method, underlines the need of the performed research, and sets the working hypothesis and main objectives of the present work.

General Methods section provides a description of the overall approach followed for data collection, sample preparation and laboratory analyses. Detailed information on sample number and characteristics, machine calibration parameters and particularities and statistical analyses performed are given at each chapter.

Chapter 1 is a review of the available literature on tropical tuna in the Indian Ocean, summarizes the existing knowledge on their biology, ecology, stock structure and fisheries dynamics and identifies the specific knowledge gaps need to be addressed to ensure a sustainable and effective management of these species.

Chapter 2 assess the feasibility of otolith microchemistry as a potential tool for investigating yellowfin tuna stock structure in the Indian Ocean, by exploring the variation of otolith chemistry profiles in young-of-the-year (YOY) yellowfin tuna during the first weeks of life of the fish. It also evaluates the usefulness of different classification methods in assigning YOY yellowfin tuna origin to their respective collection regions and investigates potential origin of age-1 yellowfin tuna from the western Indian Ocean.

Chapter 3 seeks to determine whether otolith chemical signatures of YOY skipjack tuna are distinct among the 3 putative nursery areas in the Indian Ocean. Here, the importance of interannual variability in nursery specific chemical signatures is assessed.

Chapter 4 examines otolith microconstituents to estimate the age-length relationship in young-of-the-year yellowfin tuna and to identify the portion of the otolith corresponding to the larval stage. This chapter also evaluates the chemical distribution of trace elements throughout the otolith by two-dimensional mapping analysis. It also determines whether YOY yellowfin tuna from 4 putative nursery areas in the Indian Ocean have distinct early life chemical signatures in their otoliths, also assessing the effect that interannual variability may have in nursery specific chemical signatures.

Chapter 5 uses otolith $\delta^{18}O$ signatures of young-of-the-year yellowfin tuna described in chapter 4 as reference samples to identify the origin of sub-adult and adult yellowfin tuna captured from 4 regional fishery grounds of the Indian Ocean. Additionally, evidence of lifetime movements of an adult yellowfin tuna is described by exploring the variation of the chemical profile along the growth axis of the otolith and comparing it with predicted isoscapes of otolith $\delta^{18}O$ values.

General Discussion summarizes the major findings presented in chapters 1-5, providing the results in an integrated way, highlighting the major implications and limitations of the performed research for skipjack and yellowfin stock structure identification in the Indian Ocean.

Overall Conclusions lists the main contributions derived from chapters 1-5 and states the thesis to the working hypothesis posed in this dissertation.

References section provides a list of all the studies cited along this dissertation.

Appendices contains supplementary material to inform chapters 1-5 that do not fit in the main body.

2. Theoretical framework

To give a general understanding on the key components of this PhD dissertation, the theoretical framework is structured following an adapted five Ws method (**Figure I.1**), which will frame the rationale of the present work and the basis of the working hypothesis and research questions.

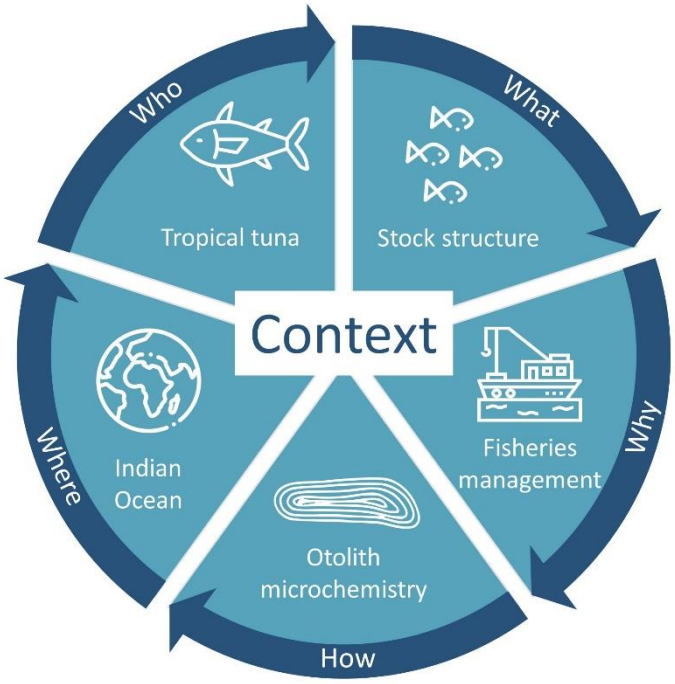

Figure I.1 The context of the study in a nutshell.

2.1 Who? The tropical tuna

Taxonomic classification

Skipjack (*Katsuwonus pelamis* Linnaeus, 1758), yellowfin (*Thunnus albacares* Bonnaterre, 1788) and bigeye (*Thunnus obesus* Lowe, 1839) tunas are highly mobile fishes that inhabit the epipelagic ecosystem of tropical and subtropical waters around de world and, therefore, are commonly named as tropical tuna. They are classified into the Scombridae family, and together with other 12 tuna species form the tribe Thunini. Among the five genera that form this tribe, yellowfin and bigeye tunas belong to the genus *Thunnus* while skipjack tuna belongs to the genus *Katsuwonus* (Collette et al., 2001) (**Figure I.2**).

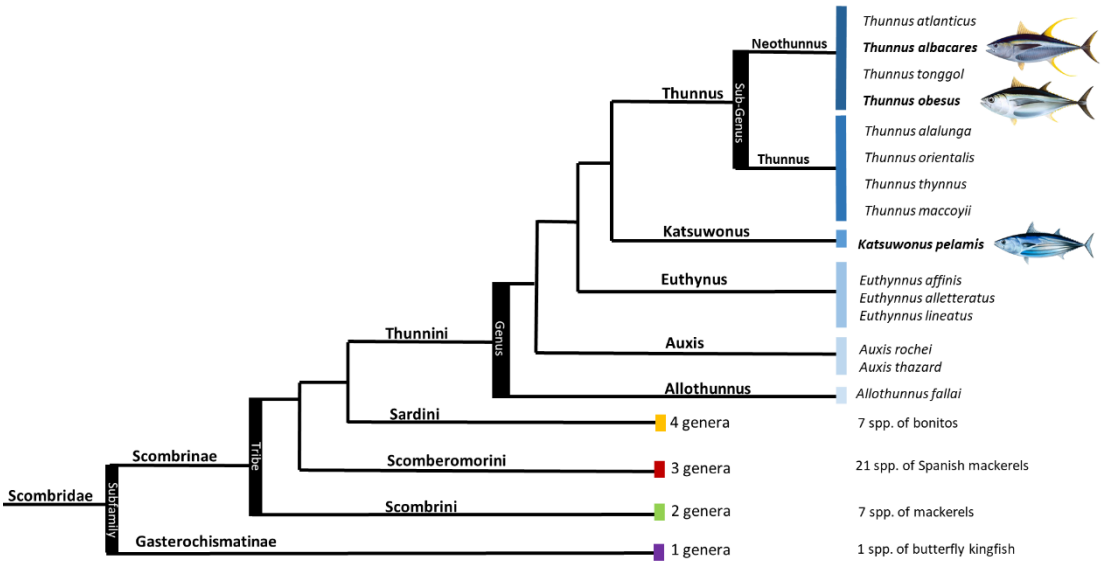

Figure I.2. Phylogenetic tree of the Scombridae family, which consist of 15 genera and 51 species, among which the three main species of tropical tuna yellowfin (*Thunnus albacares*), bigeye (*Thunnus obesus*) and skipjack tuna *(Katsuwonus pelamis*) are found (Collette et al., 2001). The sub-genus branch is based on findings from Díaz-Arce et. al. (2016).

Tunas (except *Allothunnus sp.*) are unique among bony fishes as they possess a counter-current heat exchanger system of *retia mirabilia* (i.e. a vein-arterial vascular system for heat conservation in muscles, viscera and brain) that allows them to maintain body tissue temperatures warmer than the surrounding waters (Collette et al., 2001). This regional endothermy, along with an elevated metabolic rate and frequency modulated cardiac output, support continuous, relatively fast swimming and minimize thermal barriers to habitat exploitation (Graham and Dickson, 2004). Skipjack and yellowfin tunas possess both central and lateral heat exchangers, although lateral retia mirabilia are relatively small. Bigeye tuna has no central heat exchanger but a well-developed lateral heat exchanger (Carey et al., 1971; Graham, 1975), as well as an additional retia which function is to increase the temperature of their viscera, eyes and brains. Due to this adaptation to cooler waters, bigeye tuna has traditionally been grouped with the larger temperate species into the subgenus *Thunnus*, whereas yellowfin tuna and the other tropical tuna species belong to the subgenus *Neothunnus* (Collette et al., 2001). However, a recent work aiming to study tuna (*Thunnus sp.*) phylogeny using a genome-wide

nuclear marker (RAD-seq), reported that bigeye tuna should be included within the *Neothunnus* subgenus, rather than in *Thunnus* as previously assumed (Díaz-Arce et al., 2016).

Identification

Skipjack tuna (SKJ) have the smallest body size of the three species, reaching a maximum length of 110 cm fork length (FL), and a maximum weight of 35.5 kg; common to 80 cm FL and a weight of 8 to 10 kg 2014(IOTC, 2017b; Murua et al., 2017). Regarding shape morphology, skipjack tuna have a fusiform body, elongated and rounded. They have a dark back, and their most characteristic feature for visual identification is their silvery abdomen with four to six black longitudinal stripes (**Figure I.3A**) (Collette and Nauen, 1983; Matsumoto et al., 1984). The first dorsal fin has 14 to 16 spines, while the second has 7 to 9. There is a small inter space between them. The pectoral fins are short and have a triangular shape. Skipjack tuna have more vertebrae than *Thunnus sp*. (41 compared to 39) and do not have swim bladder, so the intestine is straight without folds (Collette et al., 2001; Collette and Nauen, 1983).

Yellowfin tuna (YFT) can attain maximum length around 200 cm FL and maximum weight around 240 kg, common to 150 cm FL (IOTC, 2017a; Murua et al., 2017). Their shape morphology is characterized by being deeper near the middle of the first dorsal fin base as well as having long, narrow and straight outline behind the second dorsal fin (Collette and Nauen, 1983). Additionally, large specimens present very long second and dorsal anal fins (**Figure I.3B**). Their pectoral fin is long and extends beyond the first dorsal fin. The colour of yellowfin tuna changes from dark blue at the dorsal side, followed by a blue and gold lines on the pectoral side, and changing to silvery towards the belly. The belly is also frequently crossed by about 20 broken, almost vertical, and closely spaced silvery lines, which are alternated with rows of dots. Fins are yellow to yellowish and the anal fin is sometimes tinged with silver. Finlets appear in bright yellow colour, with a slightly black border (Collette and Nauen, 1983; Itano, 2005).

Bigeye tuna (BET) can reach a maximum size of 200 cm FL and maximum weigh of 210 kg, common to 180 cm FL (IOTC, 2017b; Murua et al., 2017). Their

body is outline rounded, forming a smooth dorsal and ventral arch between snout and caudal peduncle (Roul et al., 2016). Yellowfin and bigeye tuna can be hard to distinguish, particularly when they are not yet mature (see Box 1). Bigeye tuna possess a streamlined body that is dark metallic blue on the back and white on the undersides (**Figure I.3C**). The dorsal fin is deep yellow, while the second dorsal and the anal fins are of a lighter yellow. The finlets are also yellowish but black edged. Bigeye tuna possess long pectoral fins, that reach beyond the origin of the second dorsal fin in adults. Contrary, the second dorsal and anal fins are relatively short (Collette and Nauen 1983). One of the most characteristic features of this species, is their large eyes that gives its name.

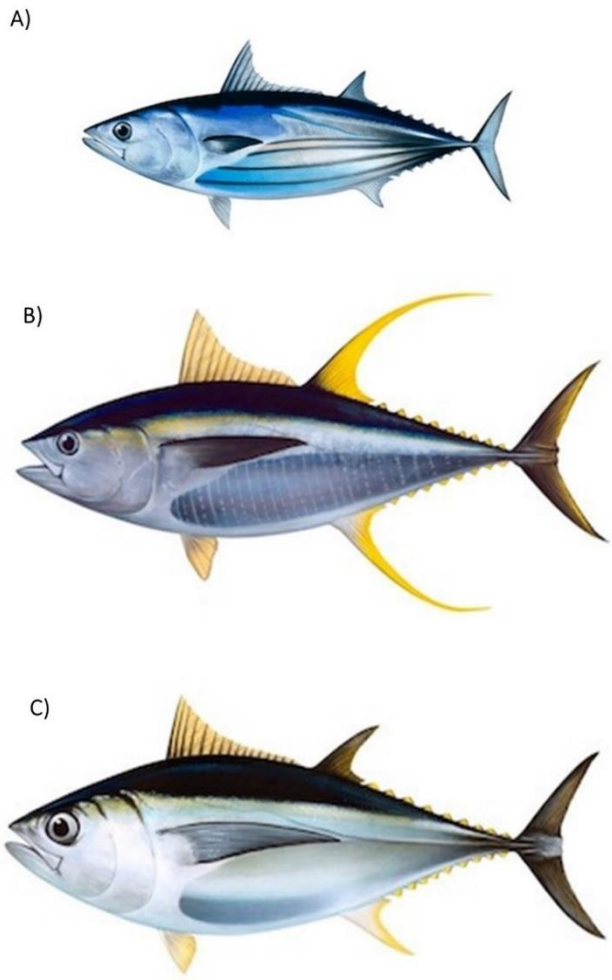

Figure I.3. Morphology of (A) skipjack, Katsuwonus pelamis, (B) yellowfin, Thunnus albacares and (C) bigeye, Thunnus obesus, tuna. Source: IOTC ©

Box 1

Tips to distinguish *in-situ* yellowfin and bigeye tunas

Yellowfin (YFT) and bigeye (BET) tunas can be hard to distinguish when fish are young or when sampled individuals are not in fresh conditions.

When that occurs, there are some comparative diagnostic features that you might consider for help (a,b):

1. Relative larger size of eyes in BET, compared to those in YFT.
2. Longer pectoral fins in BET; reaching to second dorsal fin.
3. More closely spaced vertical lines on YFT with dots in 'chevron' pattern. Broadly spaced and less regular lines in BET
4. More rounded, broader body shape in BET while in YFT narrower and torpedo-like
5. Longer head (to base of pectoral fin) in BET, relative to total body length
6. More pronounced notch at centre of caudal fork in YFT

However, when external markings have diminished through time and storage it may be necessary to open the fish and identify the species by internal characteristics, as the liver (c) or the swim bladder size (d).

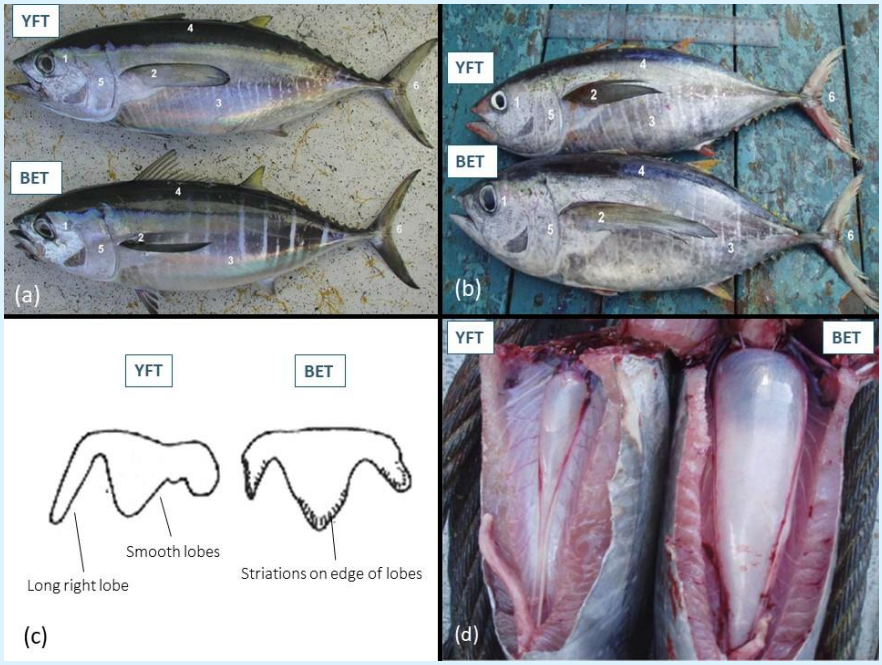

Source:

Abaunza, P., Murta, A.G., Campbell, N., Cimmaruta, R., Comesaña, A.S., Dahle, G., García Santamaría, M.T., Gordo, L.S., Iversen, S.A., MacKenzie, K., Magoulas, A., Mattiucci, S., Molloy, J., Nascetti, G., Pinto, A.L., Quinta, R., Ramos, P., Sanjuan, A., Santos, A.T., Stransky, C., Zimmermann, C., 2008. Stock identity of horse mackerel (Trachurus trachurus) in the Northeast Atlantic and Mediterranean Sea: Integrating the results from different stock identification approaches. Fish. Res. 89, 196–209. https://doi.org/10.1016/J.FISHRES.2007.09.022

Adam, S., Sibert, J.R., 2002. Population dynamics and movements of skipjack tuna (Katsuwonus pelamis) in the Maldivian fishery: analysis of tagging data from an advection-diffusion-reaction model. Aquat. Living Resour. 15, 13–23. https://doi.org/10.1016/S0990-7440(02)01155-5

2.2 What? Stock structure

Definition of stock: an evolving concept

Since the earliest days of fisheries science, the fish "stock" concept has been central to the management of marine living resources (Waldman, 2005). However, numerous definitions are available for "stock" in the literature (**Table I.1**), and there is still not a universally accepted definition. First attempts to exchange the knowledge on the stock concept and its applications led to an ambitious symposium *Stock Concept International Symposium* held in Ontario, Canada in the early 80s (Canadian Journal of Fisheries and Aquatic Sciences, 1981, vol. 33, no. 12). But further than concluding in an agreement on the definition, the presented works reflect a wide diversity of definitions (Berst and Simon, 1981; Waldman, 2005).

Table I.1. Examples of different definitions for the "stock" concept that can be found in the literature.

Definition of stock	Author
A specific portion of a population that is influenced by an anthropogenic activity that affects population productivity.	(Dahl, 1909)
Population or portion of a population, all members of which are characterized by similarities which are not heritable, but are induced by the environment, and which may include members of several different subpopulation	(Marr, 1957)
A population of organisms which, sharing a common gene pool, is sufficiently discrete to warrant consideration as a self-perpetuating system which can be managed	(Larkin, 1972)
A reproductively isolated unit, which is genetically different from other stocks	(Jamieson, 1974)
Local populations that maintain recognizable genetic differentiation by separation of their spawning place or time	(Bailey and Smith, 1981)
A species group, or population, of fish that maintains and sustains itself over time in a definable area	(Booke, 1981)
Group of randomly mating, reproductively isolated individuals with temporal or spatial integrity	(Ihssen et al., 1981)
A population of fish that behaves as a cohesive unit whose members exhibit common responses to environmental conditions within its geographic boundaries	(Casselman et al., 1981)
A reproductively isolated unit	(MacLean and Evans, 1981)
Characteristic populations or sets of subpopulations within subareas of the geographic range of a species	(Saila and Jones, 1983)
A group of fish exploited in a specific area or by a specific method	(Smith, 1990)
Any group of fish species available for exploitation in a given area	(Milton and Shaklee, 1987)

Locally accessible fish resources in which fishing pressure on one resource has no effect on the abundance of fish in another contiguous resource	(Gauldie, 1988)
A reproductively isolated unit, which is genetically different from other stocks	(Ovenden, 1990)
A species, subspecies, geographic grouping, or other category of fish capable of management as a unit	(Fox and Nammack, 1995)
Arbitrary groups of fish large enough to be essentially self-reproducing, with members of each group having similar life history characteristics	(Hilborn and Walters, 1992)
A subset of one species having the same growth and mortality parameters, and inhabiting a particular geographic area	(Sparre and Venema, 1998)
A population unit assumed homogeneous for particular management purposes	(Begg and Waldman, 1999)
A subset of a species with similar growth and mortality parameters within a given geographical area and with negligible interbreeding with other stocks of the same species in adjacent areas	(Maguire et al., 2006)

These various definitions depend on the context of the study, mainly differing in the emphasis given to the spatio-temporal integrity, the degree of homogeneity among stocks, the importance of reproductive isolation and their relevance to exploitation (Gauldie, 1991). Carvalho and Hauser (1994) argues that the stock concept in fisheries is based on a mixing of ideas influenced by biological, practical, and political considerations. As there is not a single stock definition that can accommodate all this factors, the working definitions should adapt to the aims proposed and the field of knowledge in which researchers developed their work (Carvalho and Hauser, 1994).

What is nowadays recognised is that the stock unit and biological population (discrete self-reproducing groups *sensu* Marr 1957), do not necessarily need to be the same (Secor, 2005). The reason is twofold: (1) external pressures such as fishing occur at multiple scales so that groups other than populations can be affected; and (2) the individual dynamics (e.g. movements) are not necessarily homogeneous nor exclusive for a certain population or group (Secor, 2014). Thus, although a stock is still an idealized fundamental unit, it is essential underpinning for the management of fishery resources (**Figure I.4**), because is the unit at which assessments are undertaken and management measures are applied (Begg et al., 1999; Waldman, 2005). In this work we will use the stock concept in the sense of Begg and Waldman

(1999) "… [a "stock"] describes characteristics of semi-discrete groups of fish with some definable attributes which are of interest to fishery managers" and we will refer to "population" when groups are genetically distinct.

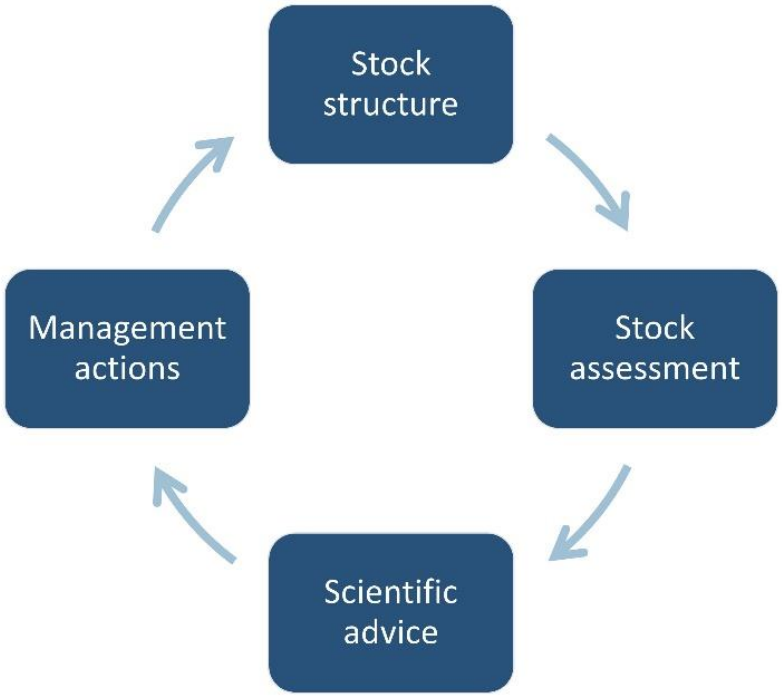

Figure I.4. Simplified schematic representation of fisheries management, understanding stock structure as an essential part of the process. Source: Arrizabalaga (2003).

Stock structure of tropical tuna

Tropical tuna species are highly mobile and can show complex spatial dynamics due to their migratory behaviour (Secor, 1999). Skipjack tuna spawns in vast warm water tropical areas (Grande, 2013; Schaefer, 2001). As those areas are often poor feeding grounds, skipjack tuna can move towards the colder and richer subtropical areas, adjacent to the spawning areas, where they can temporarily feed more and grow faster (**Figure I.5A**). Yellowfin and bigeye tunas, spawn in large but specific equatorial areas (Schaefer, 2001; Zudaire et al., 2013a), making large migrations as adults to subtropical and temperate (often deep) waters (**Figure I.5B**) (Fonteneau and Pallares-Soubrier, 1995). The complexity of tropical tuna spatial dynamics poses a significant challenge to stock structure elucidation (see Box 2). Past and ongoing studies aiming to identify stock structure of broadly distributed

fish species, have generally attempted to address one of the following three main subjects (Moore et al., 2018):

1) Drivers of spawning (timing, location, and behaviour)

2) The extent of individual movement and mixing, including origin, or where the individual is sourced from, and

3) The existence of natal homing, or the tendency of individuals to return to their natal location to spawn.

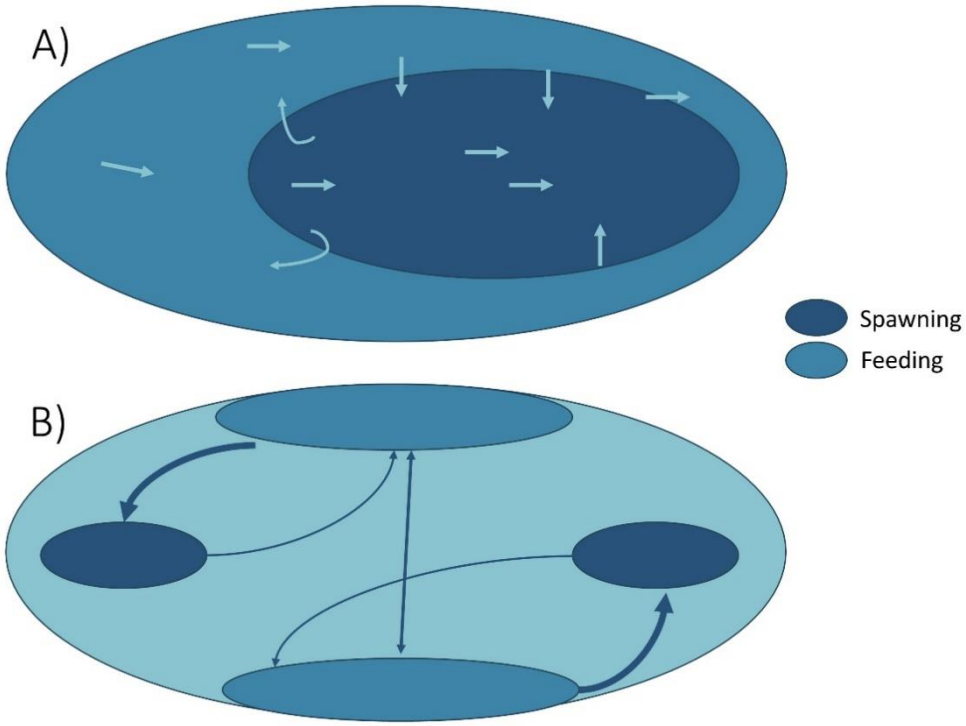

Figure I.5. A simplified ecological classification of tropical tuna according to spawning and feeding grounds distribution: (A) A large equatorial spawning area that is slightly smaller than the area of distribution and (B) large but specific equatorial spawning areas, with large migrations of adults in subtropical and temperate waters. Adapted from: Fonteneau, A., and Pallares-Soubrier, P. (1995).

Box 2

Stock structure in marine fish

Although reproductive isolation is often difficult to achieve due to large population sizes and high exchange rates among fish from different groups, marine stocks can be more structured than typically assumed due to local adaptations, oceanographic barriers and/or behavioural traits.

Panmixia:
A single ocean basin-wide stock, with no mating restrictions, neither genetic nor behavioural, where all combinations between individuals are possible (i.e., mating between two organisms is not influenced by any environmental, hereditary, or social interaction).

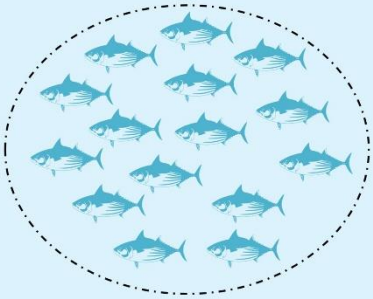

Isolation by distance:
A continuous stock with individuals mating with those from geographically close areas.

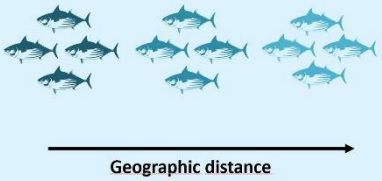

Metapopulations:
A series of small sub-stocks with small amounts of connectivity between them. This can result either through advection of eggs or larvae, or movement of post-larval life history stages (juveniles and adults).

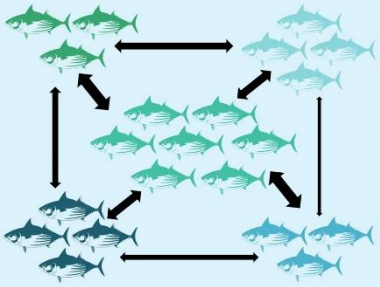

Closed populations:
The species is structured into multiple, reproductively isolated units.

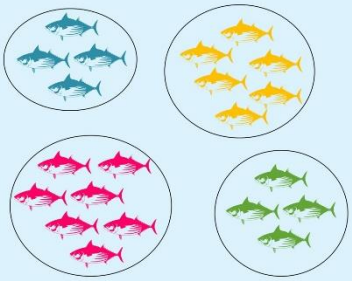

Sources:

Allendorf FW, Luikart G, Aitken SN. Conservation and the genetics of populations. second edi. Wiley-Blackwell; 2013.

Cowen RK, Lwiza KMM, Sponaugle S, Paris CB, Olson DB. Connectivity of Marine Populations: Open or Closed? Science (2000). *Science*;287: 857–859. doi:10.1126/science.287.5454.857

2.3 Why? The importance of stock structure recognition

The role of stock structure in fisheries management

Stock identification is a central theme in fisheries science, because of the need to define discrete groups of fish in which their internal dynamics could be revised against the effects of fishing (Cadrin and Secor, 2009; S.X. Cadrin et al., 2014). As such, stock structure studies seek to identify coherent groups of individuals that have complete-to-partial discreteness in space or time from their congeners (e.g. Rooker et al. 2008; Cadrin and Secor 2009; Fowler et al. 2017; Rogers et al. 2019). Stock structure understanding is needed to determine a suitable spatial scale for management, as the way a stock will respond to management decisions cannot be accurately predicted if the boundaries that characterise a stock are not correctly defined (Begg et al., 1999; Kerr et al., 2017). Different stocks may possess specific genetic, physiological and/or behavioural traits that can influence life processes such as growth rates, fecundity, abundance and disease resistance, and thus own different resilience to exploitation and environmental changes (Stepien, 1995). Prolonged exploitation of an species without a reference on the structure of the stock complexity in the region can lead to unintended consequences (Kerr et al., 2017; Petitgas et al., 2010; Stephenson, 1999). For instance, when the stock structure is more complex than recognized, management measures based on a single stock assumption can potentially lead to overexploitation and possible collapse of less productive stocks (Cardinale et al., 2012; Ying et al., 2011). Conversely, ignoring the stock structure of a species can also lead to a suboptimal utilization of the resource (Ying et al., 2011).

Attention to stock structure increased during the early 20s as management bodies became more aware of the importance of correctly identifying species' stock structure for the preservation of natural resources and ensure the resilience of marine species (Stephenson, 2002). However, the management of complex fish stocks at appropriate scales, still remains a major challenge (Bosley et al., 2019; S.X. Cadrin et al., 2014).

Shared fish stocks and high seas issues

Monitoring migratory species adds another dimension of complexity to the challenge of resolving appropriate scale units for fisheries management (Kritzer and Liu, 2014). Tropical tuna are highly mobile and capable of performing trans-oceanic migrations (Fonteneau and Hallier, 2015). These implies that these migratory species are assumed to straddle different Exclusive Economic Zones and the high seas, swimming through international waters belonging to many nations (**Figure I.6**).

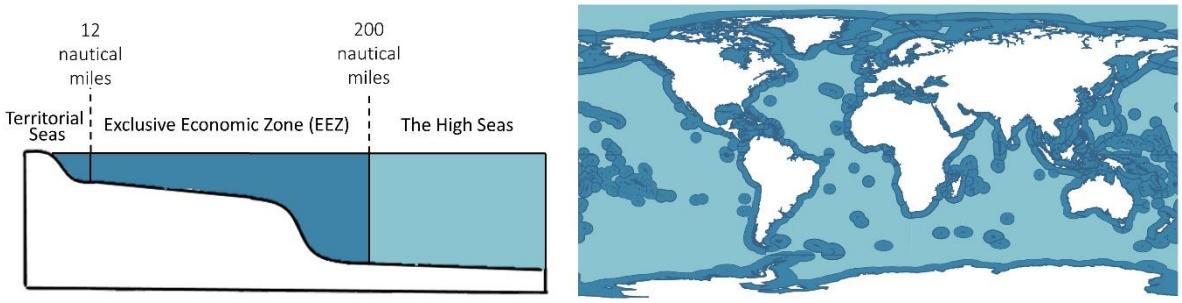

Figure I.6. Marine boundary definitions (left panel) and worlds Economic Exclusive Zones and High Seas distribution (right panel). Source of data: Flanders Marine Institute (2018). The intersect of the Exclusive Economic Zones and IHO sea areas, version 3. Available online at http://www.marineregions.org/. https://doi.org/10.14284/324

Due to this highly migratory nature, the management of tuna stocks imply the participation of many nations and require cooperative international management. To address this issue, global jurisdictional frameworks are needed, such as the United Nations Convention on the Law of the Sea (UNCLOS), and the United Nations Fish Stocks Agreement (UNFSA). Under the umbrella of the latter, countries sharing and targeting tuna and tuna like species joined to create the so-called tuna Regional Fisheries Management Organizations (tRFMOs, see Box 3). These tRFMOs provide a framework to member countries to cooperate and oversee the monitoring and management of these species. Besides, member states are obliged to apply the conservation and management measures stablished by the tRFMO. There are currently five tRFMOs (**Figure I.7**);

CCSBT - Commission for the Conservation of Southern Bluefin Tuna,

IATTC - Inter American Tropical Tuna Commission,

ICCAT - International Commission for the Conservation of Atlantic Tunas

IOTC – Indian Ocean Tuna Commission, and

WCPFC – Western and Central Pacific Fisheries Commission.

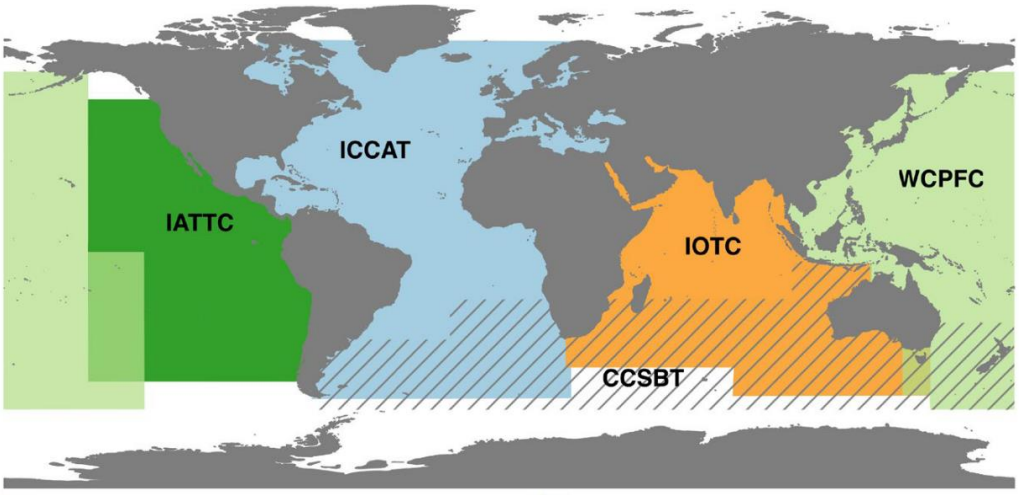

Figure I.7. tRFMOS in charge of the conservation and management of tuna and tuna-like species. Source: Juan-Jordá et al. (2017).

This cooperative management of shared fish stocks among different countries, confers many ecological and economic advantages, but also implies a complex political process (Aranda et al., 2006). The interest of different parties may be diverse and contrasting, which may generate conflicting objectives, when, for example, designing allocation schemes (Bailey et al., 2013). Several tRFMOs are currently in the process of initiating or reformulating these allocation schemes, which will have important implications for current and future access to fish (Seto et al., 2021).

Box 3

Brief history of tuna management

Timeline of major milestones for the governance in of international fisheries.

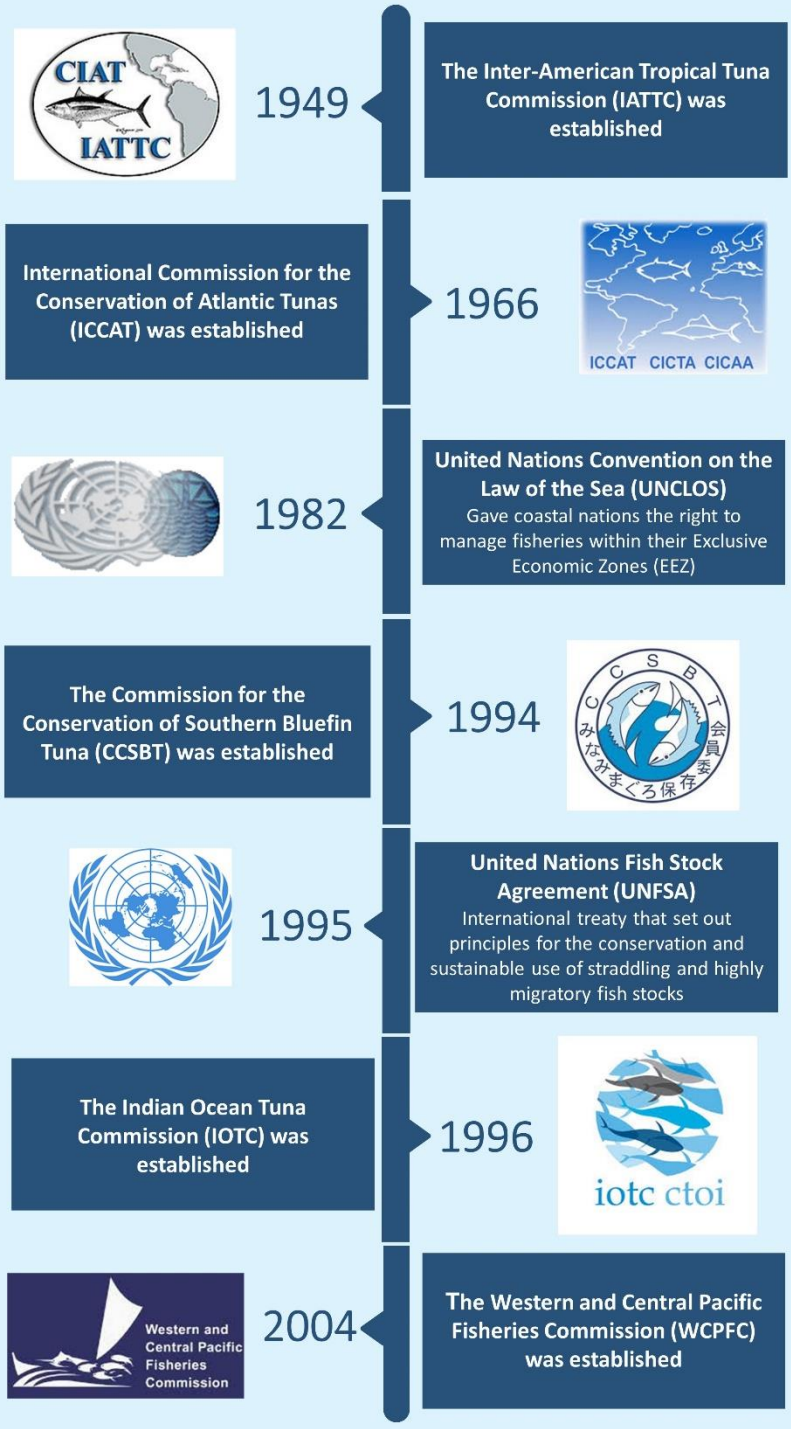

2.4 How? Otolith chemistry in stock delineation

Definition and function

Otoliths, also known as "ear stones" or "ear bones", are hard calcareous structures found in the inner ear of vertebrates (see Box 4). In teleost fishes, otoliths play important roles in two main sensory functions: the perception of the sound (i.e., acoustic function) and the perception of angular acceleration and gravity (i.e., equilibrium function). These structures are located within the optic capsule of the cranium, just behind the fish brain (**Figure I.8**). All teleost fish have three pair of otoliths, each pair associated to one otolithic organ (Fritzsch, 2000):

1. Asterisci; the smallest of the three, placed in the lagena, is involved in the detection of sound and the process of hearing.

2. Lapilli; of intermediate size, placed in the utricle, is mainly involved in the detection of the gravitation and the control of the equilibrium.

3. Sagittae; the largest of the three otolith pairs, placed in the saccule, is specialised in receiving the sound. When a sound wave arrives, the otolith acts as a transductor to the fish nervous system (Popper and Lu, 2000). Sagittal otoliths are the most used in biological studies, and hereafter we will refer to them simply as "otoliths".

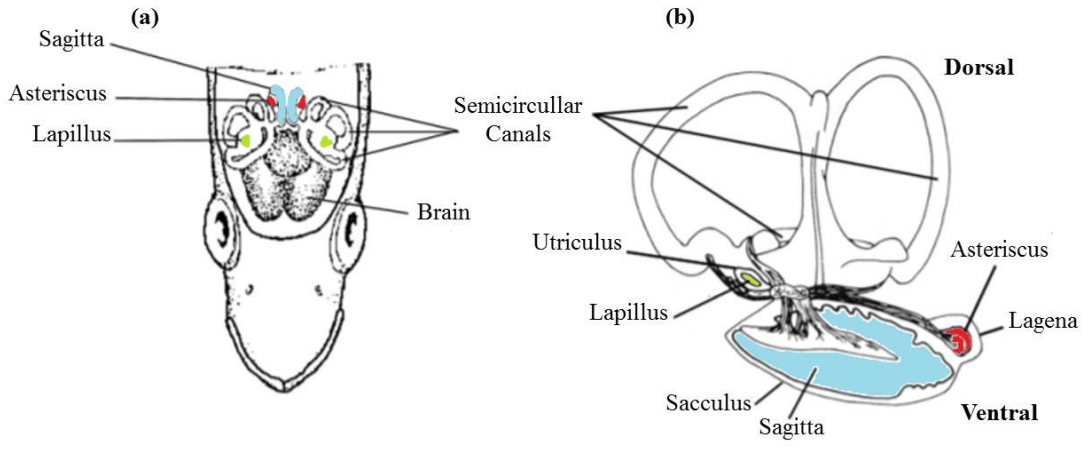

Figure I.8. Position of the saggitae (blue), asteriscus (red) and lapilli (green) in a typical teleost species viewed from a frontal section of the cranium (a) and within the inner ear otolith organs (b). This image has been modified from Panfili et al. (2002).

Box 4

Otolith morphological diversity

Examples of the diversity of otolith shapes present among teleost fish;

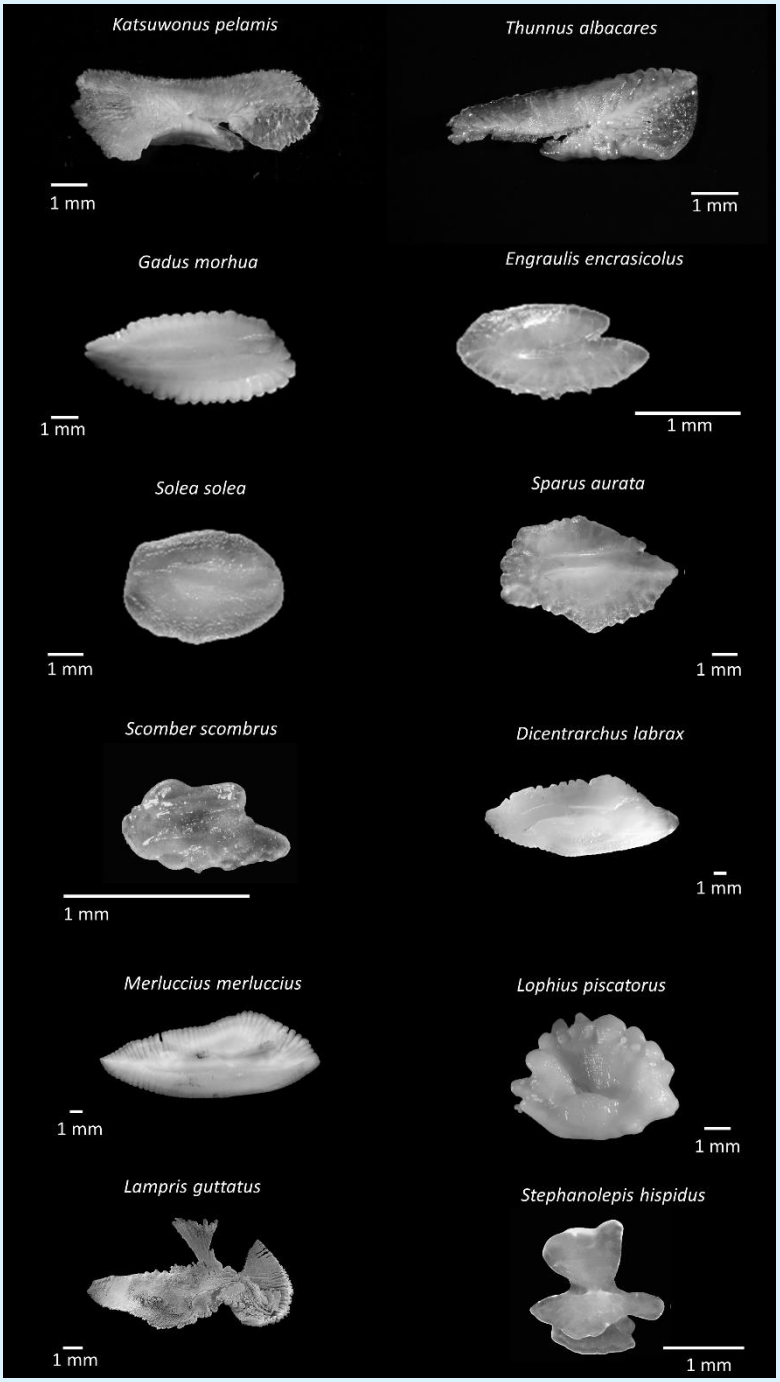

Source of non-tuna otolith pictures:
Lombarte, A., Ò. Chic, V. Parisi-Baradad, R. Olivella, J. Piera & E. García-Ladona. 2006. A web-based environment from shape analysis of fish otoliths. The AFORO database. *Scientia Marina* 70: 147-15

Composition and Pathways of Elemental Incorporation

Otolith formation results from a biomineralization process that takes place in a large acellular compartment, the endolymph (Payan et al., 2004). Fish otoliths are principally composed of calcium carbonate mineral ($CaCO_3$, 90-99% of the total weight) while the rest is composed of an organic fraction (1-10% of the total weight) (Degens et al., 1969). The mineral fraction is precipitated from the endolymphatic fluid and deposited continuously throughout the entire lifetime of the fish (Campana, 1999). Within the existing different isoforms of calcium carbonate biominerals, aragonite is most commonly deposited in sagittal otoliths (Loewen et al., 2016). An organic matrix comprises the underlaying medium upon which calcium carbonate is deposited in otoliths (Degens et al., 1969) and the organic matrix is composed approximately of 30% proteoglycans, 20% of collagen-like proteins, and the remaining 50% by other type of proteins (Allemand et al., 2007; Thomas and Swearer, 2019). This organic matrix is continuous over the entire mineral surface and is necessary for the structure and morphology of the forming mineral, as well as for elemental incorporation, nucleation, orientation inhibition, crystal nature and growth regulation of the otolith (Mann, 2001). Otolith formation involves rhythmic variations in the deposition and size of alternate $CaCO_3$-rich and protein-rich layers that result in the formation of opaque and translucent increments in the otolith that can be used for age estimation (Morales-Nin, 2000). A total of 50 elements have been detected in otoliths to date (Sturrock et al., 2012) (**Figure I.9**). The major elements that dominate the elemental composition are those forming the calcium carbonate matrix (i.e., Ca, C and O). However, the majority of elements are present at minor (i.e. >100 ppm) and trace (i.e. <100 ppm) levels (Campana, 1999; Chen and Jones, 2006).

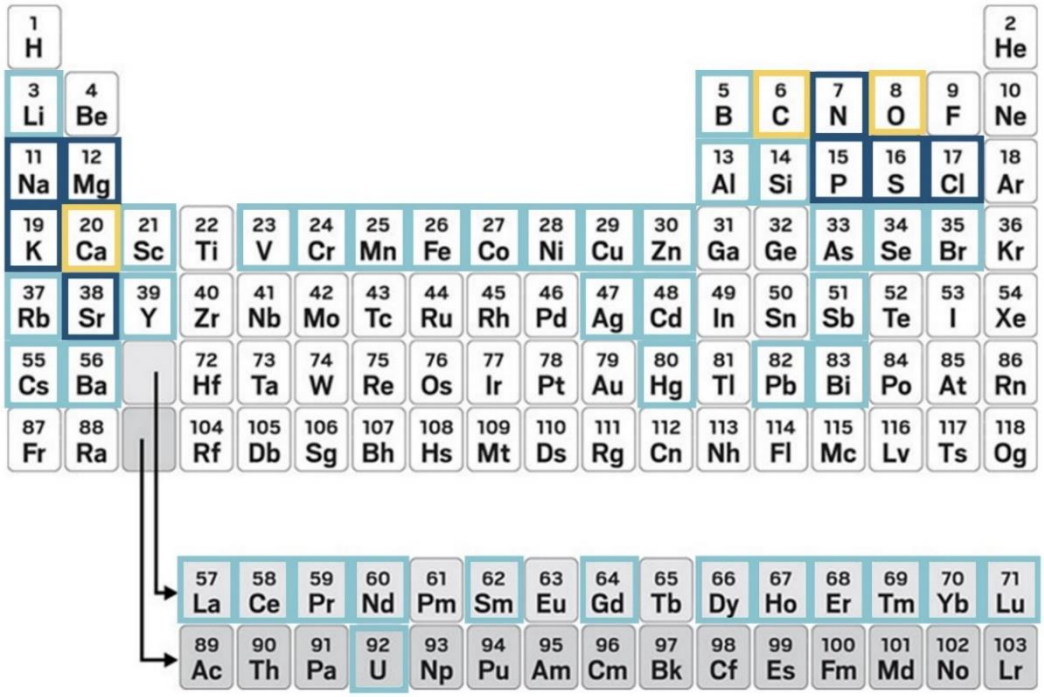

Figure I.9. The 50 elements that have been detected to be present in otoliths (bordered squares). Yellow borders indicate the major elements dominating the composition, dark-blue bordered elements are found at minor levels (>100 ppm) and light-blue bordered are trace elements (<100 ppm). Periodic table image has been adapted from Chemical and Engineering News website (https://cen.acs.org/physical-chemistry/periodic-table/periodic-table-icon-chemists-still/97/i1).

Elemental incorporation into otolith aragonite is a complex multistage process that involves the transport of dissolved ions over several membranes (**Figure I.10**). Elements are incorporated primarily from the ambient water into the blood plasma via branchial or intestinal uptake (i.e., in freshwater and marine fish, respectively). Then, ions are transported across the inner ear membranes into the endolymph fluid, to finally get into the crystallizing otolith (Campana, 1999; Sturrock et al., 2012). Therefore, elemental discrimination can potentially occur at any of the three interfaces; environment-blood, blood-endolymph and endolymph-otolith, and varies for the different elements and isotopes (Campana, 1999). Major and physiologically regulated ions will have greater discrimination, whereas trace elements with no major structural or physiological role will be less discriminated (Loewen et al., 2016). The interface of maximum discrimination is however, usually unpredictable (Campana, 1999). Apart from the fractionation across different membranes, ion availability can also be influenced by protein binding and tissue synthesis and/or breakdown rates (Hüssy et al., 2020). These, in turn, can be

influenced by distinct environmental (e.g. photoperiod, temperature), physiological (e.g. metabolic rate, gonad development) or behavioural (e.g. migration, feeding rate) factors (Hüssy et al., 2020).

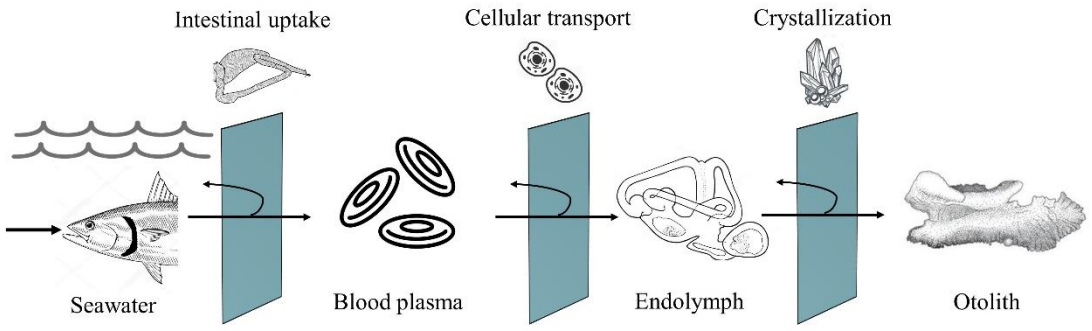

Figure I.10. Simplified overview of elemental incorporation into the otolith for a marine fish. Black arrows indicate the pathway followed by the different ions, and blue layers the main physiological barriers at which elemental discrimination can occur.

Chemical elements may pass from the blood plasma, through the endolymphatic epithelium, into the endolymph and can be then incorporated into the growing surface of the otolith. How biomineralization process affects elemental incorporation, however, is one of the issues that remains partially unsolved. Recent studies suggest that the preferential binding site of different elements will be related to the group in the periodic table the element belongs to, their atomic radii and whether the elements are essential to the fish physiology or not (Hüssy et al., 2020; Izzo et al., 2016; Thomas et al., 2017). Accordingly, elements may incorporate to different binding sites during the biomineralization process: (1) directly into the crystal lattice by substituting Ca^{2+} ions for other metal ions with similar atomic radii and identical charge (e.g. Sr^{+2} or Ba^{+2}), (2) randomly trapped within the interstitial spaces of the aragonite, as likely with elements of smaller atomic radii or univalent charge (e.g. Mg^{+2}, Li^{+1}); or (3) in association with the proteinaceous component, for those elements essential to fish physiology or adhering to biomolecules (e.g. P, Cu, Zn) (Campana, 1999).

Applications and limitations of the approach

Since the beginning of the 20s there has been a growing number of investigations using chemical tools to unravel important information about fish life histories (**Figure I.11**). There are two features that make otolith concentrations of

selected elements and isotopes (the "chemical fingerprint") suitable as natural tags to discriminate among groups of fish that have inhabited at least part of their lives in different environments: (1) Otoliths are both acellular and metabolically inert (i.e., newly deposited material is neither reabsorbed nor reworked after deposition) and (2) they grow continually throughout the life (from hatching to death) of the fish (Campana and Neilson, 1985). Hence, otoliths provide a chemical chronology over the entire life of a fish. As the ambient water chemistry and environmental conditions affect the elemental uptake into the growing otolith, variations in the concentrations of selected elements and isotopes (also known as 'chemical fingerprints') can be used as natural markers to discriminate among groups of fish that have expend parts of their lives in water masses with different physicochemical properties (Kerr and Campana, 2014).

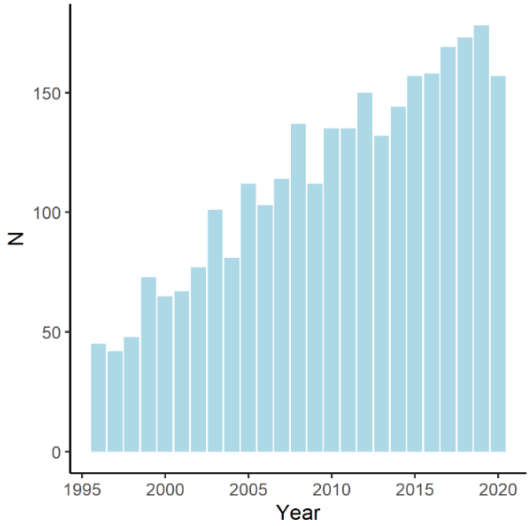

Figure I.11. Annual publications of otolith chemistry related studies from 1995 to 2020 as indexed in ISI Web of Science (http://wos.fecyt.es , accessed 15/01/2021). Search run using the following terms "otolith AND chem* OR otolith AND microchem* OR otolith AND elem* OR otolith AND isotop*)".

However, factors other than ambient chemistry have also shown to play important roles in elemental incorporation. For instance, the contribution from dietary sources to the chemical signature has also been described, although it seems to be minor for many elements (Buckel et al., 2004; Doubleday et al., 2013; Marohn et al., 2009; Ranaldi and Gagnon, 2008). There is an increasing evidence that intrinsic factors can also drive elemental uptake dynamics of otoliths (Walther et al., 2017). Otolith concentration can vary for individuals under identical environmental

conditions due to physiological biokinetic factors and processes, such as ontogeny, growth, gonad development, sex, stress etc. (Grammer et al., 2017; Loewen et al., 2016; P Reis-Santos et al., 2018; Sturrock et al., 2015). Genetics might also influence within-species differences in elemental processing (Barnes and Gillanders, 2013; Clarke et al., 2011). Therefore, the chemical composition of the otolith will reflect a combination of both the physico-chemical factors of the environment inhabited by the fish, and other intrinsic factors (Hüssy et al., 2020; Macdonald et al., 2020).

Although the understanding of factors contributing to the variability of chemical signatures can be helpful, the mere recognition of among groups differences in chemical signatures is enough for groups identification purposes (Kerr and Campana, 2014; Tanner et al., 2016), which is the focus of the present thesis. By means of otolith microchemistry we can obtain relevant information that may not be obtained by solely looking to the genetic population structure, as both techniques provide information at distinct spatio-temporal resolutions (**Table I.2**); otolith chemistry provides information over an ecological time frame (i.e., individual life span), while genetic markers inform on gene flow over evolutionary time scales (Leis et al., 2011; Tanner et al., 2016). Yet, the absence of differences in otolith chemistry does not necessarily imply that groups of fish have a common origin, but that there are insignificant differences in the properties of the environments inhabited. Therefore, otolith elemental fingerprints can be categorized as powerful discriminators of groups when differences exist, but less valuable when differences cannot be detected (Kerr and Campana, 2014).

Table I.2. General comparison of the spatio-temporal scope and usefulness between otolith microchemistry and genetics.

Approach	**Spatial scale (km)**	**Time scale**	**Able to define…**	
			Homogeneous groups	**Heterogeneous groups**
Otolith microchemistry	10-1000	Individual life span (larval history, juvenile, adult phases…)	No	Yes
Genetic inference	100-1000	Few generations (adaptative markers) to evolutionary time scale (neutral markers)	Yes	Yes

2.5 Where? Biogeochemistry of the Indian Ocean

Geography and sea surface circulation

The Indian Ocean is bounded by the Eurasian continent on the north and the 60° latitude parallel on the south, where it meets the Southern Ocean. The northernmost extent of the Indian Ocean is approximately 30°N, in the Persian Gulf. Meridionally, it borders with the Atlantic Ocean at 20°E, running south from Cape Agulhas, and with the Pacific Ocean at 146°55´E, running south from the southernmost tip of Tasmania (**Figure I.12**). The fact that the Indian Ocean is lack-locked on the north induces a wind forcing pattern over the ocean basin which is unlike the pattern observed in other oceans equatorial regions.

Figure I.12. Extent of the Indian Ocean (shaded area). Source: Word Atlas©.

The wind annual cycle is characterized by a seasonal reversal of surface winds (monsoons) north of 10°S (Ramage, 1969). The southwest monsoon, also known as summer monsoon, takes place from May to September. It is characterized by the continuation of the southern hemisphere trade winds into the Arabian Sea, generating strong northward cross-equatorial stresses and southward Ekman flow on both sides of the equator (Schott et al., 2002). Additionally, the East African Coast Current and the South Equatorial Current support the cross-equatorial northward Somali Current flow, which becomes one of the fastest open ocean currents worldwide (Shotton, 2005). During the northward flowing phase and after crossing the equator (about 4°N) the Somali Current turns offshore, generating two anticyclonic gyres along the Somalian coast; the Great Whirl and the Southern Gyre

(Schott and McCreary, 2001). This intensification of the Somali Current generates coastal upwelling throughout northeast African coast (**Figure I.13A**). The combination of these coastal upwelling events together with the horizontal advection and Ekman pumping, generate remarkable phytoplankton blooms off the coast of Oman and Somalia (Wiggert et al., 2006). By contrast, both in the Arabian Peninsula and Indian coast, the upwelling events are weaker, but there are cyclonic circulation cells located both west and east of southern India and Sri Lanka for which models suggest a contribution of open-ocean upwelling (Schott et al., 2002). Finally, the Southwest Monsoon Current flows eastwards south of Sri Lanka and enters into the Bay of Bengal. An outflow from the Southwest Monsoon Current, however, flows south-eastward and crosses the equator along the coast off Sumatra, where it meets the Indonesian throughflow (i.e. the flow of Pacific water into the Indian Ocean through the Indonesian passages), and as a result a coastal upwelling can be also observed (Miyama et al., 2003; Ningsih et al., 2013) (**Figure I.13A**).

The northeast monsoon, or the winter monsoon, takes place between November and March. During this period wind blowing is reversed, the meridional wind components of the equator are southward, and the Ekman transports are now northward on both sides of the equator, favouring the creation of equatorial upwelling (**Figure I.13B**). In addition, the upper-layer flow of the Somali Current is now directed southward, where it meets the East African Coast Current and converge to form the South Equatorial Countercurrent that flows along the equator (Schott and McCreary, 2001). At its eastern end, the South Equatorial Countercurrent meets a boundary current the South Java Current, which flows south-eastward. In the Indian coast and Sri Lanka, the winds now flow westward, generating the Northeast Monsoon Current, which branches and end up in the Arabian Sea (Schott and McCreary, 2001). This creates a mayor subduction zone in the Arabian Sea during the winter monsoon (**Figure I.13B**).

March–April and October are the intermonsoon months with weak winds when strong equatorial downwelling occurs. This is because winds turn eastward at the equator, generating an eastward annual-mean wind stress and producing Ekman transport convergence (Tomczak and Godfrey, 2003a). Thus, in this period the biological activity is generally low (Wiggert et al., 2006). Besides this seasonal

pattern on wind forcing, interannual variability also plays an important role in ocean circulation patterns (see Box 5).

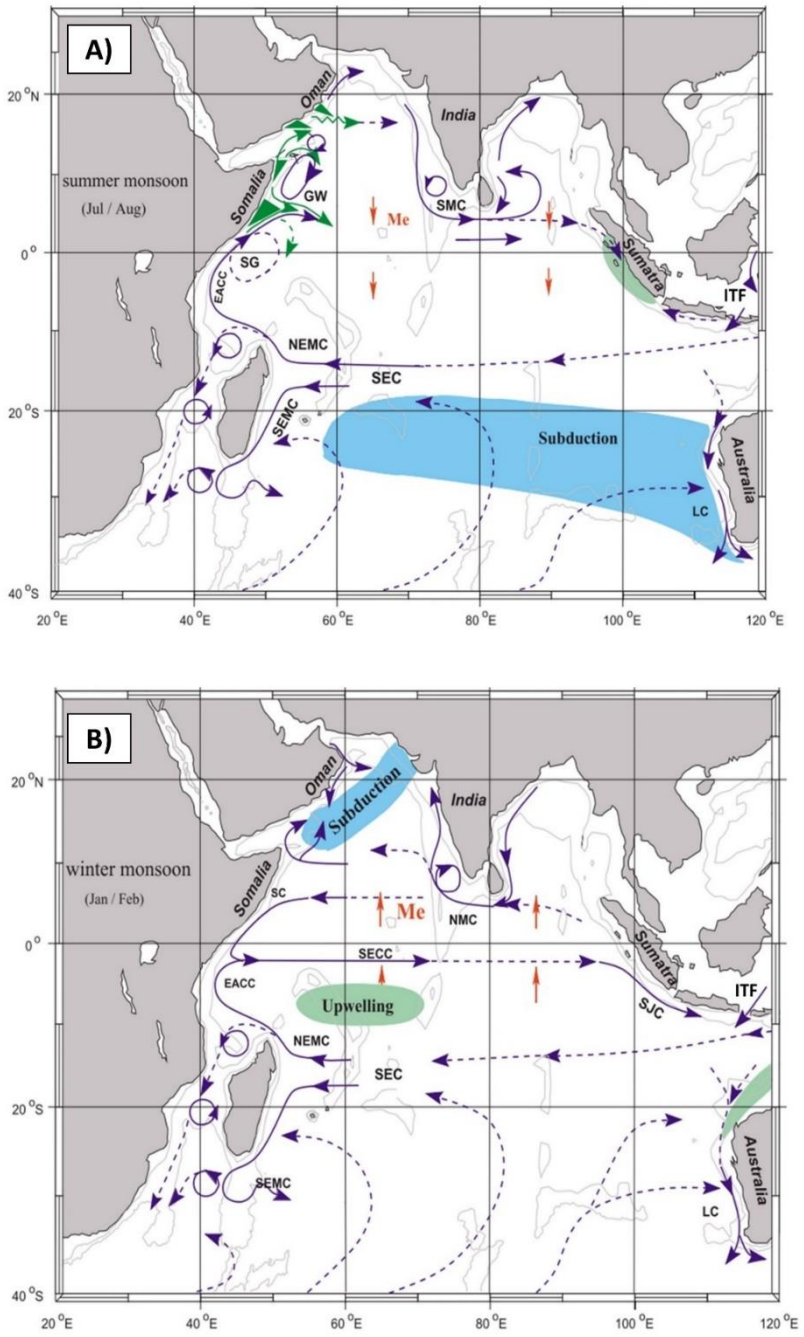

Figure I.13. A schematic representation of identified current branches during southwest (boreal summer) monsoon (A) the northeast (boreal winter) monsoon (B). Marked are subduction areas (blue), upwelling areas (green) and southward Ekman transport on both sides of the equator (red). Current branches indicated are the South Equatorial Current (SEC), Northeast and Southeast Madagascar Current (NEMC and SEMC), East African Coast Current (EACC), Somali Current (SC), Southern Gyre (SG) and Great Whirl (GW), Southwest Monsoon Current (SMC), Indonesian Throughflow (ITF) and Leeuwin Current (LC). Source: Schott et al. (2002).

Outside the direct influence of the monsoons, south of 10°S, the wind regime is constant, and southeast trade winds persist year-round. This implies that the circulation pattern remains unchanged in direction, such as the southward flowing Leeuwin Current along Australian west coast, and the westward flowing South Equatorial Current which splits into two branches along Madagascar to form the the Northeast and Southeast Madagascar Currents (**Figure I.13**). The Mozambique Channel works as a southward water mass route and is characterized by the presence of anticyclonic eddies (**Figure I.14**), which generate an upward movement of nutrient rich waters around their edge and advection of nutrient rich coastal waters when they run along the coast (Quartly and Srokosz, 2004; Schouten et al., 2003).

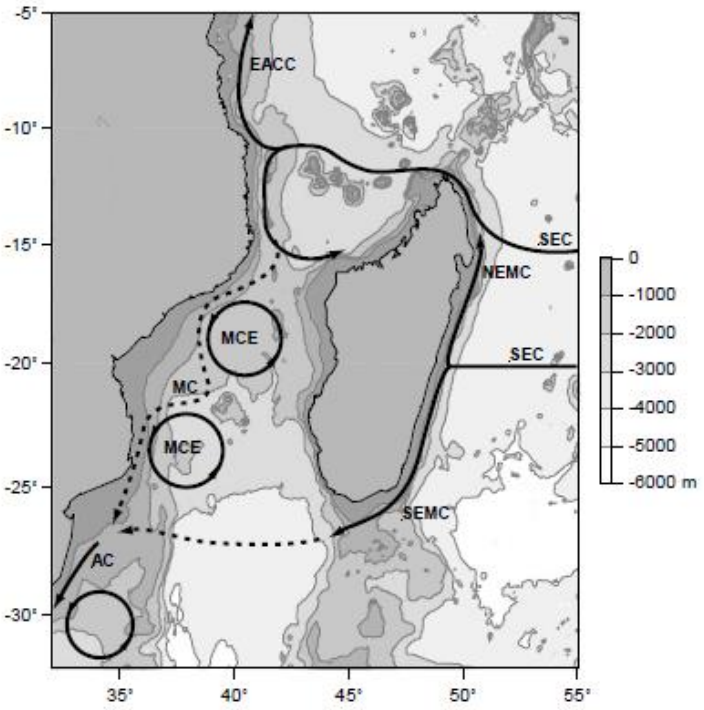

Figure I.14. Main currents and flow features of the region around Madagascar and Mozambique Channel. Arrows point out the direction of the flow. Features shown are the South Equatorial Current (SEC), the Northeast and Southeast Madagascar Currents (NEMC and SEMC), the East African Coastal Current (EACC), the Agulhas Current (AC) Mozambique Channel Eddies (MCE) and the Mozambique Current (MC). The dotted line represents an unclear nature and existence of the flow. Bathymetry of the region is also indicated with shaded isobars (0-6000 m depth). Source: Schouten et al. (2003).

Box 5

A Dipole mode in the Indian Ocean

The interaction between the ocean and the atmosphere creates a unique pattern of interannual ocean-atmosphere variability in the Indian Ocean; this is known as the Indian Ocean Dipole (IOD), or the "Indian niño". This dipole mode air-sea interaction accounts for about 12% of the SST variability in the Indian Ocean. Its evolution is controlled by equatorial ocean dynamics which are forced by the zonal winds of the region. During neutral IOD phases, westerly winds are predominant and blow along the equator. During this phase, the expected temperatures in the tropical Indian Ocean are found. Sometimes due to supressed local convection, however, these westerly winds weaken along the equator, allowing warm water to shift towards Africa. The changes in wind regime also let cool water to rise from the deep ocean in the eastern Indian Ocean, creating a temperature difference across the tropical Indian Ocean; cooler than normal water in the east and warmer than normal water in the west. This situation is known as a positive IOD phase. By contrast, in a negative IOD phase westerly winds intensify along the equator. A temperature difference is then created, with warmer than normal water in the eastern Indian Ocean and cooler than normal water in the western Indian Ocean. The greenhouse warming effect is increasing the frequency of extreme positive IOD events.

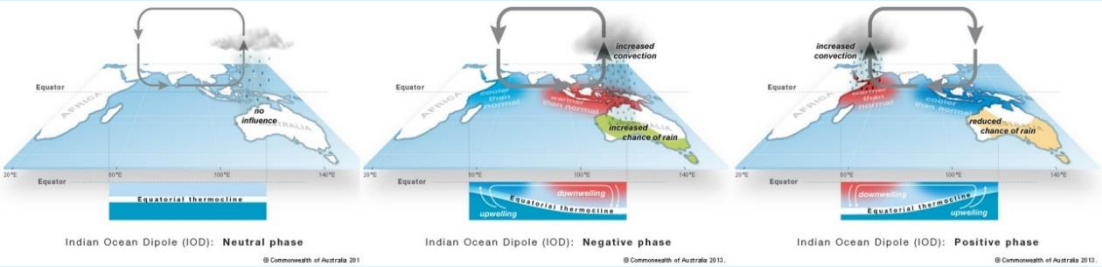

Sources:

Saji NH, Goswami BN, Vinayachandran PN, Yamagata T. A dipole mode in the tropical Indian Ocean. Nature. 1999;401: 360–363. doi:10.1038/43854

Cai W, Santoso A, Wang G, Weller E, Wu L, Ashok K, et al. Increased frequency of extreme Indian Ocean Dipole events due to greenhouse warming. Nature. 2014;510: 254–258. doi:10.1038/nature13327

Seasonal patterns of oceanographic conditions

The monsoon system governs the seasonal ocean climate in the tropics and northern subtropics region of the Indian Ocean. In January, cold and dry winter monsoon winds cool surface waters along the northwestern Arabian Sea (23.5°C) to the Somali basin (26.5°C), whereas the sea surface temperature (SST) is above 28°C over the rest of the equatorial region (**Figure I.15**). During the spring intermonsoon regime, a SST maximum occurs (>28°C) north of the equator in the western Indian Ocean, and north of 10°S in the eastern part, creating a convergence zone along the equator with an increased thickness of the mixed-layer in the east (Tomczak and Godfrey, 2003b). In July when the summer monsoon is well established, west of 60°E, SST decreases again (<26°C) due to the upwelling events off the Somalian coast. The central and eastern equatorial Indian Ocean, however, form a warm pool at all seasons (**Figure I.15**). In the southern hemisphere, SST isotherms show nearly perfect zonal orientation, with decreasing SSTs poleward. The small deviations observed along both coastlines reflect the poleward boundary currents, Agulhas in the southeast African Coast and Leeuwin in the western Australian coast (Tomczak and Godfrey, 2003b).

The precipitation patterns are remarkably similar to those for SST (**Figure I.15**). Due to the impact of the summer moonson, precipitation is high over the Indian subcontinent during this period, with an anomalous difference in rainfall intensity distribution among the eastern and western regions north of 7°N (Keshtgar et al., 2020). Annual mean precipitation can vary from 10 cm/year in the west (on the Arabian coast) to more than 300 cm/year in the east (near Sumatra and Over Andaman Sea) (Tomczak and Godfrey, 2003b). During the boreal winter two bands of maximum precipitation are formed, a stronger one in the south equator (4.5°S) and a weaker on in the north equator (3°N) (Keshtgar et al., 2020). During the boreal winter the maximum precipitation is place in the south of the equator, between 0-15°S (Schott et al., 2009).

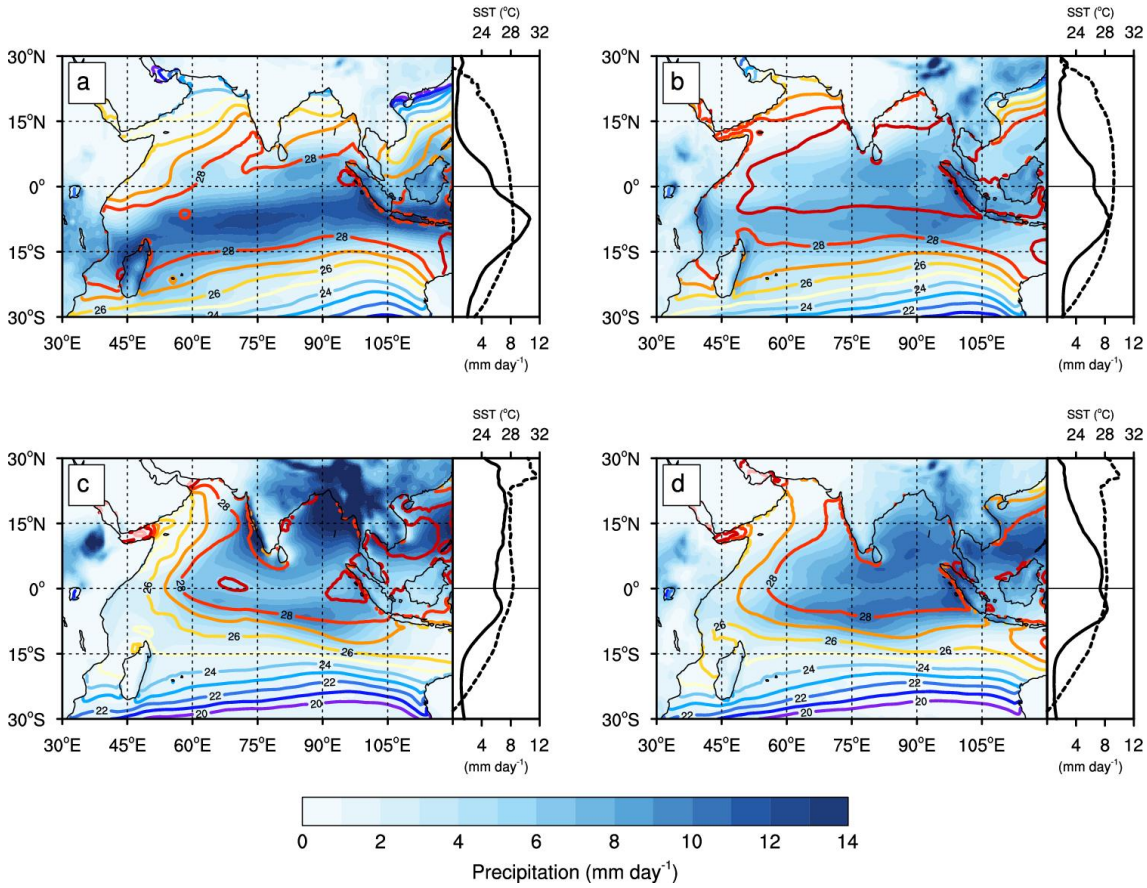

Figure I.15. Seasonal mean SST (°C) and precipitation (mm day^{-1}) in the Indian Ocean averaged for the 1980-2018 period in December, January and February (a), March, April and May (b), June, July and August (c) and September, October and November (d). The right-hand side panels show zonal means of precipitation (solid line, mm day^{-1}) and SST (dashed line, °C) in the longitudinal range of 40-110°E. Source: Keshtgar et al. (2020).

Like in other oceans, the sea surface salinity (SSS) variation in the Indian Ocean follows the precipitation-evaporation (P-E) distribution (i.e. minimum P-E, maximum SSS). Other events driving the Indian Ocean salinity distributions include the river inflow in the Bay of Bengal, the influx of saltier waters from the Red Sea and Persian Gulfs and the influx of freshwater in the Indonesian Throughflow (Han and McCreary, 2001). These events influence the large SSS contrast that can be found among the northern regions (**Figure I.16**). The Arabian Sea is under the influence of the high salinity Persian Gulf water mass, which together with the Red Sea show highest SSS in the Indian Ocean due to extreme freshwater loss from evaporation (Tomczak and Godfrey, 2003b). By contrast, the lowest SSS are found in Bay of Bengal, which is driven by large river runoff and excess precipitation (Han and McCreary, 2001). Such a contrast prevails all year round (**Figure I.16**). The freshwater influx from the Indonesian throughflow is extended under the influence

of the South Equatorial current, flowing relatively low saline waters at the 0°-20°S latitudinal range. Its maximum extension occurring during the April-May intermonsoon (**Figure I.16**). Finally, relatively high SSS is found in the core of the subtropical gyre along at 30°S, east of 70°E, decreasing southward to the Southern Ocean due to the freshwater supply from melting Antarctic ice (Tomczak and Godfrey, 2003b).

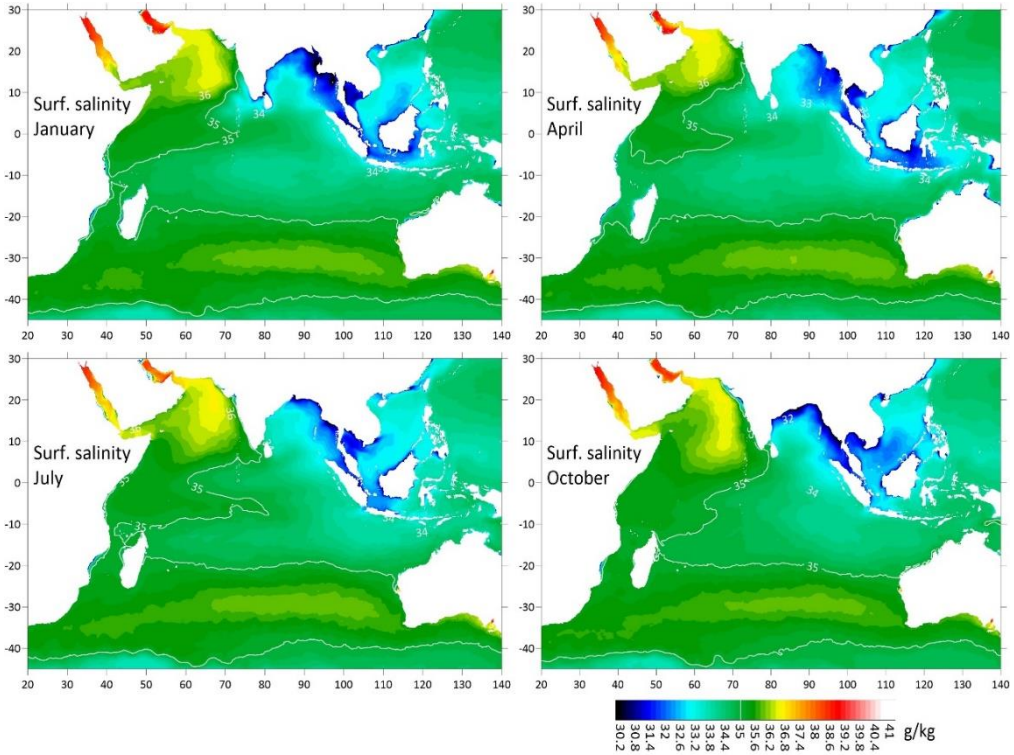

Figure I.16. Surface salinity average for January, April, July and October. The white contour denotes the isohaline 35 g.kg^{-1}. Maps generated from outputs of the Global Ocean Physical reanalysis product at 1/12° resolution, EU Copernicus Marine Environment Monitoring Service. Source: Source: Davies et al., (2020).

3. Rationale for the study

Fishing is the last remnant of major hunting and harvesting in the wild, and, as such, it supports livelihood, food security and human wellbeing all over the world (Golden et al., 2016; Kittinger et al., 2017; Smith et al., 2010). Whereas mayor concerns regarding actual fisheries are about food security in the Global South, debates on the Global North are more focused on sustainability (Belton et al., 2020). But the truth is that one cannot be achieved without the other, as a fishery to be sustainable *per se* must achieve not only environmental protection, but also economic and social development (Asche et al., 2018). This is the basis of the so-

called Blue Economy, which is defined by the United Nations as "*an ocean economy that aims at the improvement of human wellbeing and social equity, while significantly reducing environmental risks and ecological scarcities*" (United Nations, 2014). In an effort to move towards this Blue Economy, The United Nations included Life Bellow Water (Goal 14: Conserve and sustainably use the oceans, seas and marine resources for sustainable development) as one of the 17 Sustainable Development Goals (SDGs) adopted by all United Nations Member States in 2015, and has proclaimed 2021 to 2030 as the "Decade of Ocean Science for Sustainable Development" (Lee et al., 2020; UNESCO, 2019).

Against this backdrop, we have skipjack (*Katsuwonus pelamis*) and yellowfin (*Thunnus albacares*) tunas which are included in the top 10 marine species with highest landings in the world, and belong to one of the four most highly valuable commercial fish groups (FAO, 2020a). Both species, together with bigeye tuna (*Thunnus obesus*) are harvested in the tropical and subtropical waters around the world (ISSF, 2020a). As a result of increasing demand for canned tuna and beginning of the industrialized fisheries around 1950s, the catches of tropical tuna started to increase, reaching an historic maximum of 5,034,240 tonnes in 2018 (FAO, 2020b). The Pacific Ocean supports the world´s largest tropical tuna fisheries (67%), followed by the Indian (22%) and the Atlantic (11%) Oceans (FAO, 2020b). Spain, and particularly the Basque fleet, is one the ten main fishing fleets of tropical tuna in the world (Báez et al., 2020; Miyake et al., 2004). Apart from supporting the diet of millions of people in both developed and developing countries, tropical tuna also play an important role to the marine ecosystem structuring via food web dynamics (van Denderen et al., 2018). Hence, the overexploitation of these species cannot only compromise food security, but also jeopardise the stability of marine ecosystems as a whole (Heithaus et al., 2008).

At the present time, 13 stocks of tropical tuna are considered for management. Bigeye and yellowfin tunas are assessed and managed considering four stocks: the Atlantic Ocean stock, the Indian Ocean stock and the western and the eastern Pacific Ocean stocks. For skipjack tuna, five stocks are considered for management, two in the Atlantic (eastern and western), two in the Pacific (eastern and western) and one in the Indian Ocean (ISSF, 2020a). Of these, the Atlantic Ocean

bigeye tuna and the Indian Ocean yellowfin tuna are considered to be overfished and subject to overfishing (ISSF, 2020a). A prerequisite for the stock assessments is that stocks are correctly identified. Most models assume that the group of individuals being assessed have homogeneous vital rates (e.g. maturity, growth, mortality…) and a closed life cycle, in which young fish were produced by previous generations within the same group (S.X. Cadrin et al., 2014). However, the single stock assumption for stock assessments of tropical tuna species in the Indian Ocean has not yet been proved, and the true nature of the stock structure remains uncertain for skipjack, yellowfin, and bigeye tunas. If the stock assessment advice is based on invalid assumptions in terms of stock structure and connectivity, management decisions may not achieve pursued conservation objectives (Kerr et al., 2017).

To that need, a collaborative project between CSIRO (Australia), AZTI-BRTA (Spain), IRD (France) and CFR (Indonesia) on population structure of tuna, billfish and sharks of the Indian Ocean (PSTBS-IO) was developed in 2017 (Davies et al., 2020). The aim of this project was to describe the population structure and connectivity of priority tuna and tuna-like species within the Indian Ocean. For that aim, muscle tissues for genetic analyses by means of Next Generation Sequencing (NGS) methods were collected and complemented with otolith sampling. As the comparison of the chemical signature of the otolith associated with the early life stage (i.e. the core), can allow to resolve questions regarding natal origins of fish (Thorrold et al., 2001), the purpose of this dissertation was to use the otoliths collected within the PSTBS-IO project framework to gain insights into the stock structure of skipjack and yellowfin tunas in the Indian Ocean by analysing their chemical signature.

Although there is no available information on the movements of small tropical tuna in the Indian Ocean (Fonteneau and Hallier, 2015), it can be assumed that this fish are not capable to make large scale movements. Studies in other oceans for instance, highlighted that yellowfin tuna from the Atlantic do not leave their nursery areas until they attain 60-80 cm FL (Fonteneau and Pallares-Soubrier, 1995; Pecoraro et al., 2016). Besides, tropical tuna are known to spawn in habitats with mesoscale oceanographic activity, that helps to minimize long-distance dispersal (Bakun, 2006; Reglero et al., 2014). Therefore, we considered the early life chemical signature of YOY tuna otoliths reflect the environment experienced by the fish in their nursery areas. If these signatures are distinct and unique for each known nursery ground in the Indian Ocean,

this would provide a potential natural marker that can ultimately be used to elucidate the nursery of origin of older individuals, by comparing the same early life portion of their otoliths. This information will contribute to better understand the connectivity and mixing rates among different fishery areas within the Indian Ocean and, ultimately, the stock structure of the species. Evidence-based stock structure scenarios are essential to implement and enforce management strategies that ensure the long-term conservation and sustainable exploitation of the fishery.

4. Hypothesis, aim and objectives

4.1 Working hypothesis

"Otoliths of young of the year skipjack and yellowfin tunas from putative nursery grounds in the Indian Ocean differ in their chemical signatures, providing a tool to understand their connectivity and stock structure within this ocean".

4.2 Overarching aim and objectives

The overarching aim of this dissertation is to contribute to the understanding of the stock structure of skipjack and yellowfin tunas in the Indian Ocean, using otolith natural markers linked to ambient physicochemical conditions of the ocean.

To fulfil the general aim, specific research objectives have been defined as follows:

1. Undertake a review of the fisheries, life history and stock structure of tropical tuna species in the Indian Ocean (**Objective 1**), which is addressed in chapter 1.

2. To explore different methodological frameworks and factors to be considered in order to study the stock structure of skipjack and yellowfin species using otolith chemical signatures (**Objective 2**), which is addressed throughout chapters 2, 3, 4 and 5.

3. Develop a baseline of chemical signatures (stable isotopes and trace elements) in otoliths of young-of-the-year skipjack and yellowfin tunas collected from distinct nursery areas in the Indian Ocean (**Objective 3**), which is addressed in chapters 3 and 4.

4. Predict the nursery of origin of sub-adult and adult yellowfin tuna collected from regional fisheries in the Indian Ocean to evaluate their connectivity and the contribution of each nursery area to each fishery (**Objective 4**), which is addressed in chapters 2 and 5.

“The secret of getting ahead is getting started.”

Agatha Christie

GENERAL METHODS

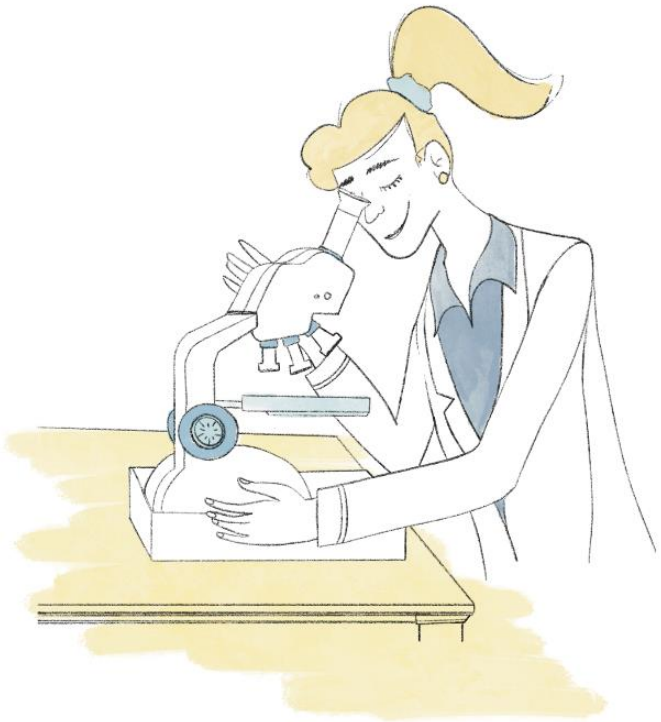

1. Sample collection

Samples used in chapter 2 were derived from otoliths collected in the western Indian Ocean by a scientific observer (Iker Zudaire) on board Spanish commercial purse seiners in 2009 and 2010, before this dissertation. The data acquisition for chapters 3-5 involved the participation of many people and partner agencies that collected samples as part of a collaborative research project on Population Structure of Tuna, Billfish and Sharks of the Indian Ocean (Davies et al., 2020). A standard operating procedure was developed to provide a standardized sample collection guidance that was used by trained observers at sea and during port sampling by project staff and participating coastal states. Otolith samples were obtained by scientists or scientific observers directly on-board purse seine vessels or at port during two consecutive years (2018 and 2019). On board observers had access to fish with detailed information on fish size, date, latitude, and longitude, among others. Fish were sampled right after the fishing operation or were immediately frozen for their posterior sampling in the lab. To achieve a good representation of each region, fish from different schools (i.e., fishing sets) were sampled, and the number of samples from a certain fishing set was limited to a maximum of 5 fish.

Yellowfin and skipjack tunas have fragile, thin, and elliptic otoliths that require particular care during extraction and posterior preparation. To extract the sagittal otoliths from the cavities they are immersed in , “lifting-the-lid” technique of otolith removal was applied (Proctor et al., 2019). A first vertical cut (dorsal-ventral) was made at a point one eye-diameter distance from the posterior edge of the eye, down to the level of an imaginary horizontal line across from the top of the eyes. For the second cut, an almost horizontal cut at the level of the top of the eyes, with a slight angle (no more than 10° from horizontal), down towards the tail was made, intersecting with the first cut (**Figure M.1A**). If necessary, successive small cuts were made until the brain tissue was exposed. Then, tissue from the posterior area of the brain region was removed with stainless tweezers (**Figure M.1B**). After removal, very carefully tweezers were inserted into the otolith cavities, and otoliths were grabbed and extracted from the fish. This is an extremely delicate process, where otoliths can often be broken if too much pressure is exerted. Otoliths were

then cleaned with ultrapure (Milli-Q) water from adhering organic tissue, and the membrane surrounding the otolith was removed. Once cleaned, otoliths were let air dried for 8-12 hours in referenced loosely capped microtubes.

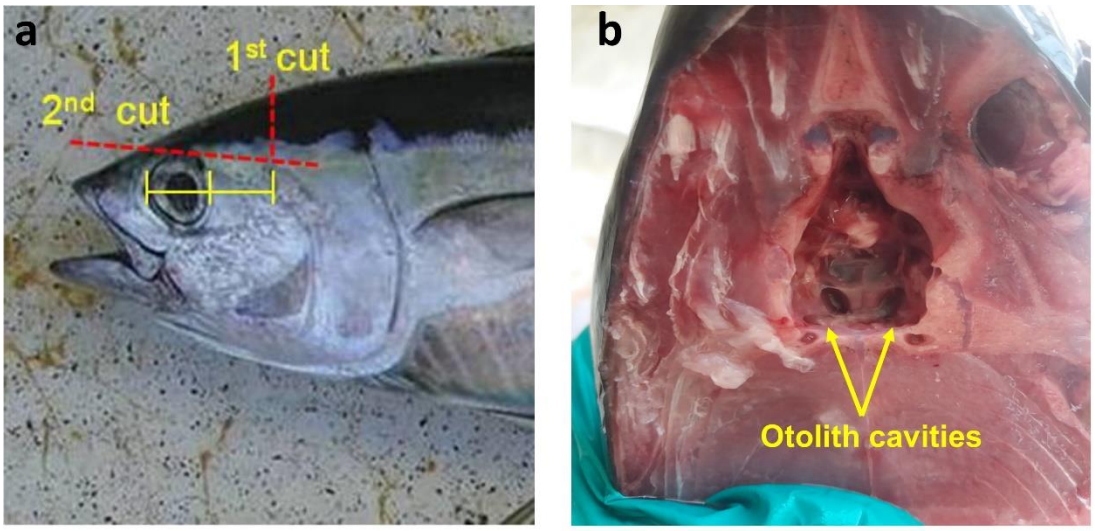

Figure M.1. (A) "Lifting-the-lid" technique. First cut is made vertical, at one eye-diameter distance from rear margin of the eye. Second cut is almost horizontal at level of top of the eye. (B) The brain tissue removed to expose the bone cavities in which the otoliths lie. Source of figure (A): Proctor et al. 2019.

2. Sample preparation

In the laboratory otoliths were embedded in two-part epoxy resin (Araldite 2020, Huntsman Advanced Materials, Switzerland). Once hardened, blocks were polished using 3M® silicon carbide sandpaper (particle size= 220 µm) and a lapping wheel with a series of decreasing grain diameter (30, 15, 9, 3 and 1 µm) 3M® silicon carbide lapping discs, moistened with ultrapure water, to obtain a transverse section where the primordium of the otolith was exposed (**Figure M.2**). Sections were then ultrasonically cleaned using ultrapure water for 10 minutes. Following sonication, otolith sections were left to air dry in loosely capped microtubes for 24 h. Then, sections of similar heigth were glued together in sample plates using Crystalbond thermoplastic glue (Crystalbond 509; Buehler).

Prepared otolith samples were analysed differently at each chapter depending on the specific objectives of each chapter (**Figure M.3**).

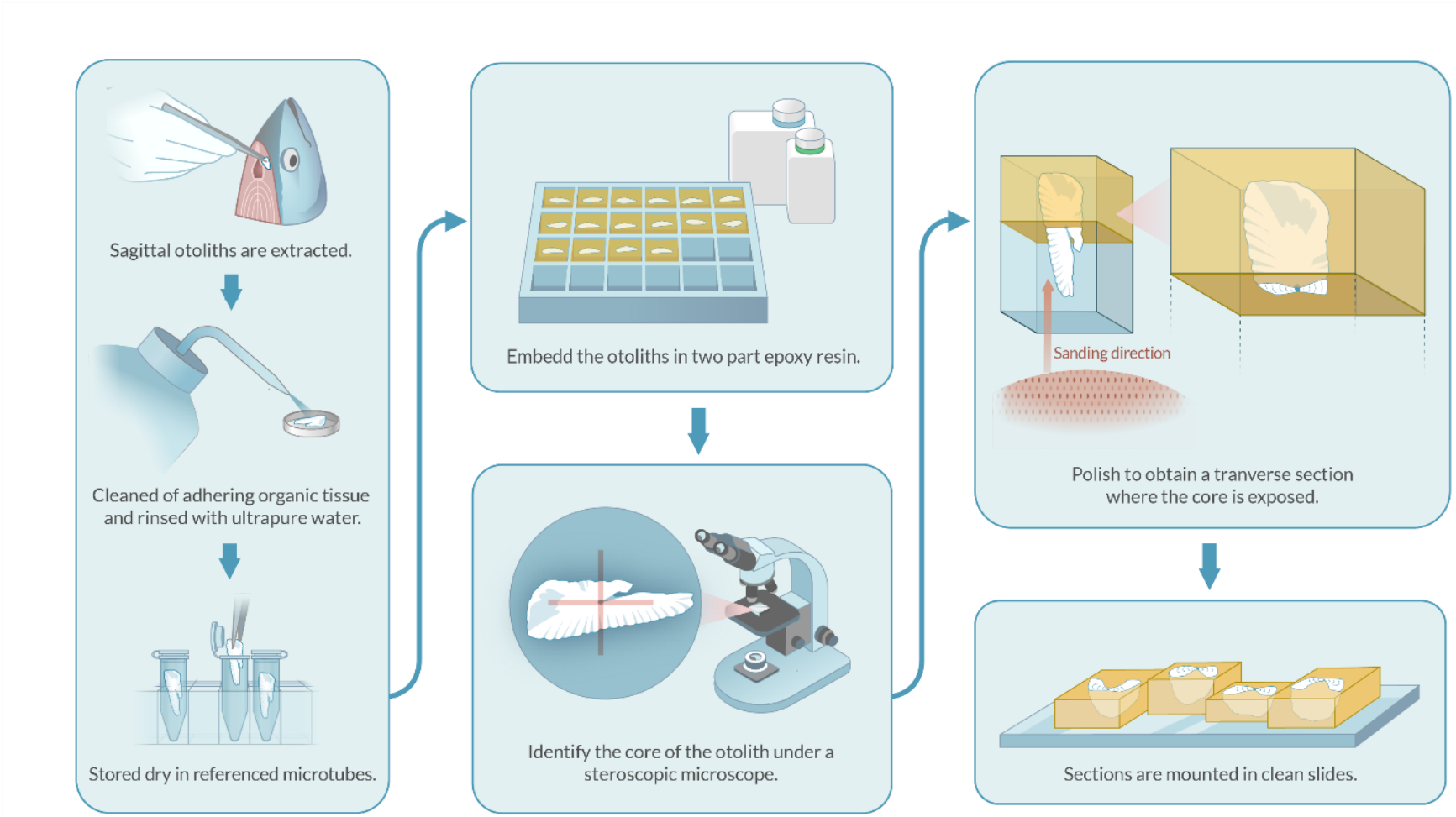

Figure M.2. Illustration of otolith preparation processes for posterior microchemical analyses. NorArte Studio©.

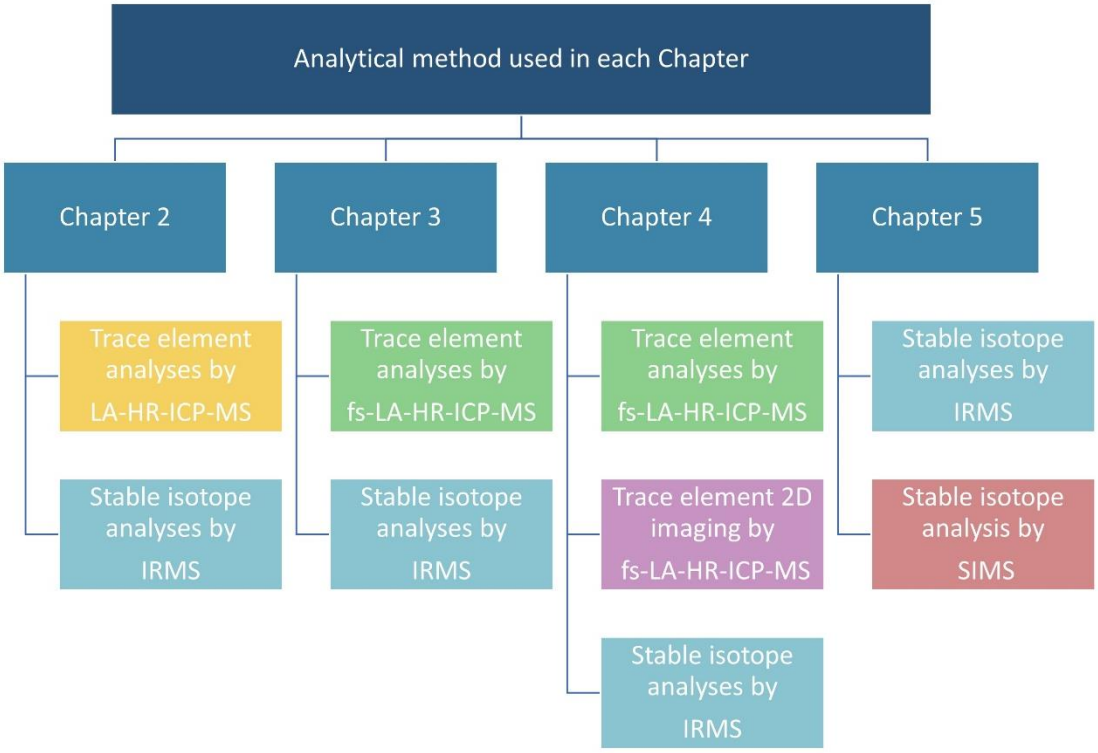

Figure M.3. List of different analytical methods used in each chapter of the PhD.

3. Trace element analyses

Analyses of trace element data available for Chapter 2 were performed using a 7700X quadrupole inductively coupled plasma mass spectrometer (ICP-MS, Agilent Technologies, Santa Clara, CA, USA) coupled to a laser ablation system with a Laurin Technic 2 volume cell (RESOlution LA system, Resonetics, Nashua, NH, USA) available at the School of Earth Sciences, The University of Melbourne (Melbourne, Vic., Australia). For Chapters 3 and 4 otoliths trace element chemistry was analysed using a high resolution inductively coupled plasma mass spectrometer (HR-ICP-MS, Element Element XR, Thermo Scientific, Bremen, Germany), coupled to a high repetition rate 1030 nm femtosecond laser (fs-LA) system (Alfamet, Neseya, Canejan, France) available at the Institut des Sciences Analytiques et de Physico-Chimie pour l'Environnement et les Matériaux, Université de Pau et des Pays de l'Adour/CNRS (Pau, France). Imaging of spatial distribution of trace elements analyses in Chapter 4, was performed using the same fs-LA-HR-ICP-MS. Quantification of trace element data was done by external calibration NIST 610 and 612 glass standards with known chemical composition and internal standard (IS). We used ^{43}Ca, as the internal standard, which concentration in the otolith was

assumed to be constant at 38.3% (Sturgeon et al., 2005). Trace element concentrations (ppm) were converted to element:Ca ratios (µmol mol^{-1}) using a normalized calibration curve (white corrected) (**Figure M.4**).

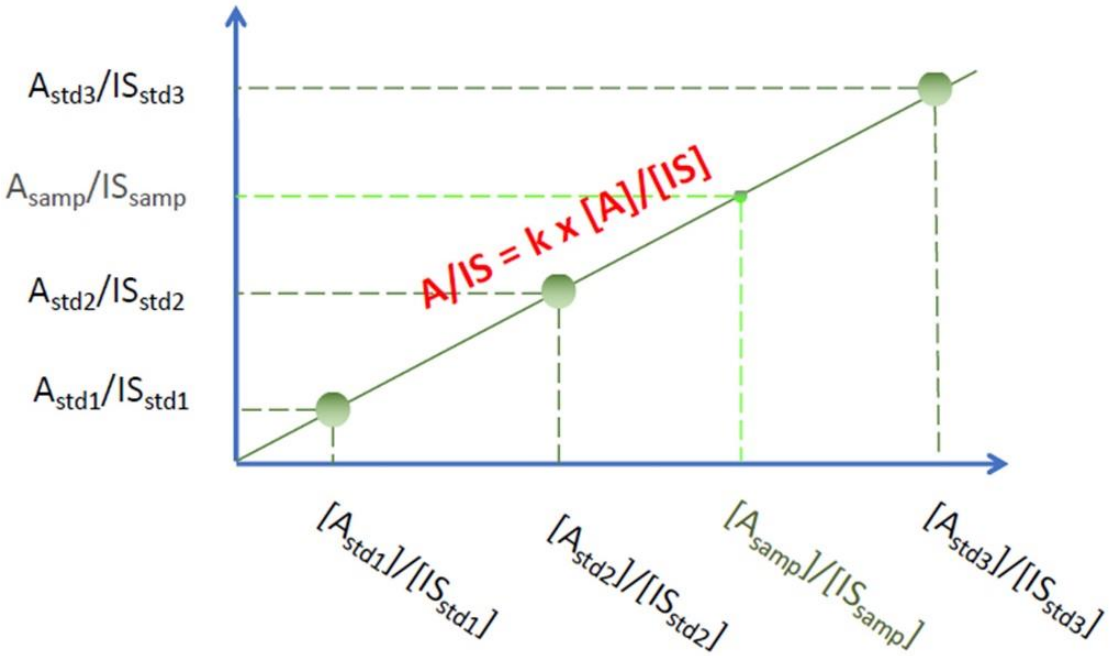

Figure M.4. Calibration curve with normalization by internal standard (IS), where; A_{stdi}= Net intesity of the analyte for the standard i, IS_{stdi}= Net intensity of the internal standard for standard i, A_{samp}=Net intensity of the analyte for the sample, IS_{samp}= Net intensity of the internal standard for the sample, k= slope and [ ]= concentration. Image by Cristophe Péycharan.

Thus, knowing the IS concentration in the standard sample, that of the analyte (A) is expressed by:

$$[A]_{samp} = \frac{\frac{A_{samp}}{IS_{samp}} \times [IS]_{samp}}{K}$$

Specific laser ablation conditions, elements analysed, and calibration parameters are given at each chapter.

4. Stable isotope analyses

Microsampling of otolith powder for carbon ($\delta^{13}C$) and oxygen ($\delta^{18}O$) stable isotope analyses for Chapter 2, 3, 4 and 5 was performed using a high-resolution computerised micromill (New Wave MicroMill System, NewWave Research G. C. Co., Ltd, Cambs,UK) on the transverse sections including the core. The otoliths of the

smallest individuals were used to create standard templates for each species. These templates were used for the remaining otoliths, to ensure that the same portion of the otolith was milled in every fish. The properties of the microsampling (portion of the otolith powdered, the number and depth of the drill passes, and the diameter of the carbide bit) are specified at each chapter. Powdered material was then analysed for $\delta^{13}C$ and $\delta^{18}O$ Isotope-Ratio Mass Spectometry (IRMS) on an automated carbonate preparation device (KIEL-III, Thermo- Fisher Scientific, Waltham, MA, USA) coupled to a gas-ratio mass spectrometer (Finnigan MAT 252, ThermoFisher Scientific) at the Environmental Isotope Laboratory of the University of Arizona. The isotope ratio measurement was calibrated based on repeated measurements of NBS-19 and NBS-18 (International Atomic Energy Agency standards). All isotope values were reported according to standards of the International Atomic Energy Agency in Vienna. Otolith $\delta^{13}C$ and $\delta^{18}O$ values (‰) were expressed in standard delta (δ) notation as $^{13/12}C$ and $^{18/16}O$ ratios (R) in the sample in the sample relative to the Vienna Pee Dee Belemnite (VPDB) scale:

$$\delta^{18}O = \left(\frac{R_{sample}}{R_{standard}}\right) \times 1000\ (‰)$$

The otolith $\delta^{18}O$ signature of a single yellowfin tuna was also measured using Secondary Ion Mass Spectrometry (SIMS). Otolith $\delta^{18}O$ values were acquired at the NERC Ion Microprobe Facility (SIMS) from the University of Edinburgh with a Cameca IMS 1270, using a ~5 nA primary $^{133}Cs^{+}$ beam. Specific laser ablation conditions and calibration parameters are given at Chapter 5.

"The aim of science is to discover and illuminate truth. And that, I take it, is the aim of literature, whether biography or history or fiction. It seems to me, then, that there can be no separate literature of science."

Rachel Carson

CHAPTER 1

A review of the fisheries, life history and stock structure of tropical tuna in the Indian Ocean

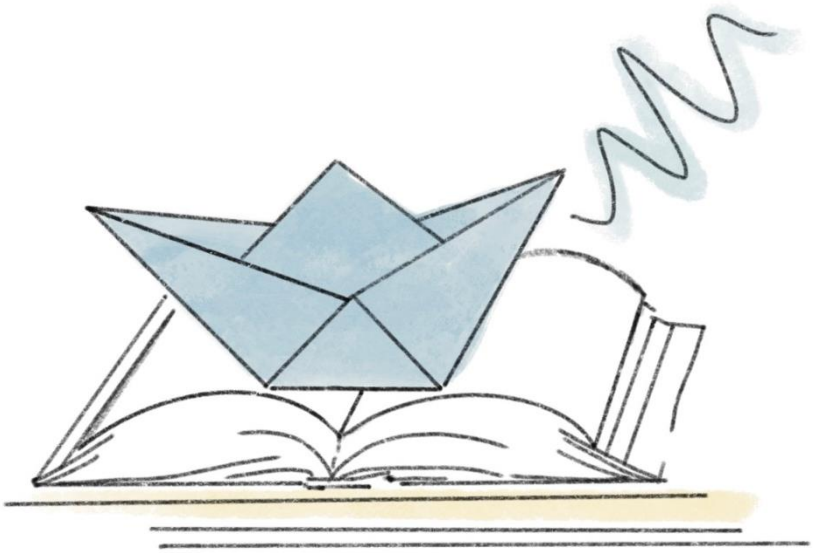

Abstract

Skipjack (*Katsuwonus pelamis*), yellowfin (*Thunnus albacares)* and bigeye (*Thunnus obesus*) tunas are the target species of tropical tuna fisheries in the Indian Ocean, with high commercial value in the international market. High fishing pressure over the past three decades has raised concerns about their sustainability. Understanding life history strategies and stock structure is essential to determine species resilience and how they might respond to exploitation. Here we provide a comprehensive review of available knowledge on the biology, ecology, and stock structure of tropical tuna species in the Indian Ocean. We describe the characteristics of Indian Ocean tropical tuna fisheries and synthesize skipjack, yellowfin, and bigeye tunas key life history attributes such as biogeography, trophic ecology, growth, and reproductive biology. In addition, we evaluate the available literature about their stock structure using different approaches such as analysis of fisheries data, genetic markers, otolith microchemistry and tagging, among others. Based on this review, we conclude that there is a clear lack of ocean basin scale studies on skipjack, yellowfin and bigeye tunas life history, and that regional stock structure studies indicate that the panmictic population assumption of these stocks should be investigated further. Finally, we identify specific knowledge gaps that should be addressed with priority to ensure a sustainable and effective management of these species.

Published as:

Artetxe-Arrate, I., Fraile, I., Marsac, F., Farley, J.H., Rodriguez-Ezpeleta, N., Davies, C.R., Clear, N.P., Grewe, P., and Murua, H. (2020). A review of the fisheries, life history and stock structure of tropical tuna (skipjack *Katsuwonus pelamis*, yellowfin *Thunnus albacares* and bigeye *Thunnus obesus*) in the Indian Ocean. *Advances in Marine Biology*, 101, pp 1-51, doi:10.1016/bs.amb.2020.09.002

1. Introduction

Skipjack (*Katsuwonus pelamis*), yellowfin (*Thunnus albacares*) and bigeye (*Thunnus obesus*) tunas are members of the Scombridae family. They are commonly referred to as tropical tuna because they inhabit tropical and subtropical waters of the three major oceans (Atlantic, Indian, and Pacific). These species represent a vital source of food, employment and livelihood for numerous coastal communities and nations (FAO, 2016). Two main markets drive tuna production; traditional canned tuna, dominated by light meat species such as skipjack and yellowfin, and sashimi/sushi products, where red meat species such as bluefin and bigeye tunas are preferred (FAO, 2018). Market demand for tuna has increased over the last few decades, which has led to increased exploitation. Global catch of tuna species in 2018 was 5.1 million tonnes, of which tropical tuna species accounted for 95% (ISSF, 2020b). In addition to being a major component of the global fishing industry, tropical tuna are also amongst the world´s most valuable fish (Galland et al., 2016), Tropical tuna contribute considerably to the global economy ($29.17 billion market value), and account for the 88.5% of the global tuna sales value in 2014 (Macfadyen, 2016). The Pacific Ocean supports the world´s largest tuna fisheries, followed by the Indian Ocean, which accounts for 21% of worldwide tropical tuna catches (Galland et al., 2016). Tropical tuna are an important source of food for millions of people around the world, and support the livelihoods and employment of local communities and fishermen who depend on them (FAO, 2016). These species are top predators that play a significant role in the open ocean ecosystems, due to their influence in marine food webs structure and dynamics (Estes et al., 2016; van Denderen et al., 2018), hence their decline can initiate trophic cascades (Heithaus et al., 2008), and jeopardise the resilience and stability of marine resources (Kerr et al., 2017).

Despite their inherent importance to the marine ecosystem, the global economy and human wellbeing, the complex and diverse range of countries participating in tuna Regional Fisheries Management Organizations (tRFMOs), organizations responsible for managing tuna and tuna-like species, hinder the implementation of effective conservation strategies to ensure the sustainability of tuna and related ecosystems (Collette, 2017; Cullis-Suzuki and Pauly, 2010; Juan-

Jordá et al., 2017). This is particularly true in the Indian Ocean, where the co-existence of artisanal and industrial fisheries (total catches are divided about equally between them), poses a major challenge for the assessment and management of Indian Ocean tropical tuna stocks by the Indian Ocean Tuna Commission (IOTC) (McCluney et al., 2019; Murua et al., 2015). Overall, data collection is less coordinated and naturally more difficult when it comes to small vessels, and management and enforcement outcomes harder to implement (Pons et al., 2017). Many developing countries experience serious capacity and infrastructure constraints, which can impede adequate data collection and reporting (Ceo et al., 2012). And this is particularly the case of the Indian Ocean, where for many tuna species artisanal fisheries, and in some case semi-industrial, tuna catches are estimated by IOTC using several sources of information (see for more details IOTC, 2019c). The difficulty of monitoring the fisheries within the Indian Ocean not only affects the stock assessment process, but also the implementation of the agreed management measures in the IOTC area. For instance, although catch limitations of yellowfin tuna in the Indian Ocean were agreed due to the overfished status of the stock (IOTC Resolution 19/01), the measure failed to achieve its goal as catches has increased by around 9% in 2018 from 2014/2015 levels despite limitations (IOTC, 2019b). Similarly, a Harvest Control Rule was agreed in 2016 for skipjack tuna (IOTC Resolution 16/01), but the resultant catch limit for 2018-2020 has been exceeded in 2018 (IOTC, 2019b). As mis-assessment and mis-management of a species can lead to stock depletion (Hutchings, 2000; Pauly et al., 2003), efforts must focus on improving the capacity of monitoring the fishery to collect fishery statistics and statistical methods needed for improved assessment as well as improving the capacity to implement the agreed management measures of the three tropical tuna stocks (i.e., skipjack, yellowfin and bigeye) under the IOTC mandate.

Understanding life history strategies and stock structure is essential in determining how a species might respond to fishing pressure (Begg et al., 1999; Jennings et al., 1998; Juan-Jordá et al., 2013). Life history information such as age and growth, reproduction, maturity and mortality is required to determine population productivity and, hence, resilience to fisheries (King and McFarlane, 2003; Morgan et al., 2009), while the knowledge on habitat utilization and niche exploitation at different life stages can be useful for evaluations of species-specific

vulnerability to different fisheries. Besides, the understanding of stock structure helps determine the appropriate units for stock assessment and suitable spatial scale for management (Kerr et al., 2017). Different stocks (i.e. semi-discrete groups of fish with some definable attributes that are of interest to fishery managers *sensu* Begg and Waldman 1999) may possess specific genetic, physiological or/and behavioral traits, that can influence life history processes (Stepien, 1995). As such, when the stock structure is more complex than recognized, management measures based on a single stock assumption can potentially lead to overexploitation and possible collapse of less productive subpopulations, and under-exploitation of more productive populations (Stephenson, 1999; Ying et al., 2011). Each tropical tuna species is considered to form a single stock in the Indian Ocean for management purposes (IOTC, 2017b, 2017a, 2017c) although spatial structure is recognized in current stock assessments, which need to determine relative abundances among regions (Hoyle, 2018; Hoyle and Langley, 2020). Since 2008, Indian Ocean yellowfin tuna assessments used a spatial stratification (Fu et al., 2018; Langley et al., 2008), and so did recent bigeye assessments (Fu, 2019; Langley, 2016). These models consider spatial differences in catches but assume a single-stock recruitment relationship (i.e., a unique spawning population with no reproductively isolated units). However, scientific evidence on how tropical tuna are structured in the Indian Ocean is required to validate the adequacy of the divisions used in this approach and to resolve the single stock hypothesis assumption, as different scenarios may lead to different management strategies and implications (**Figure 1.1**).

The aim of this review is to (i) describe the particularities of Indian Ocean tropical tuna fisheries (ii) synthesize the existing information on Indian Ocean skipjack, yellowfin and bigeye tunas life history strategies, (iii) compile the available information on stock structure sourced from studies using a range of different approaches, and (iv) identify major knowledge gaps and highlight future research priorities needed for the implementation of an effective conservation strategy for the tropical tuna in the Indian Ocean.

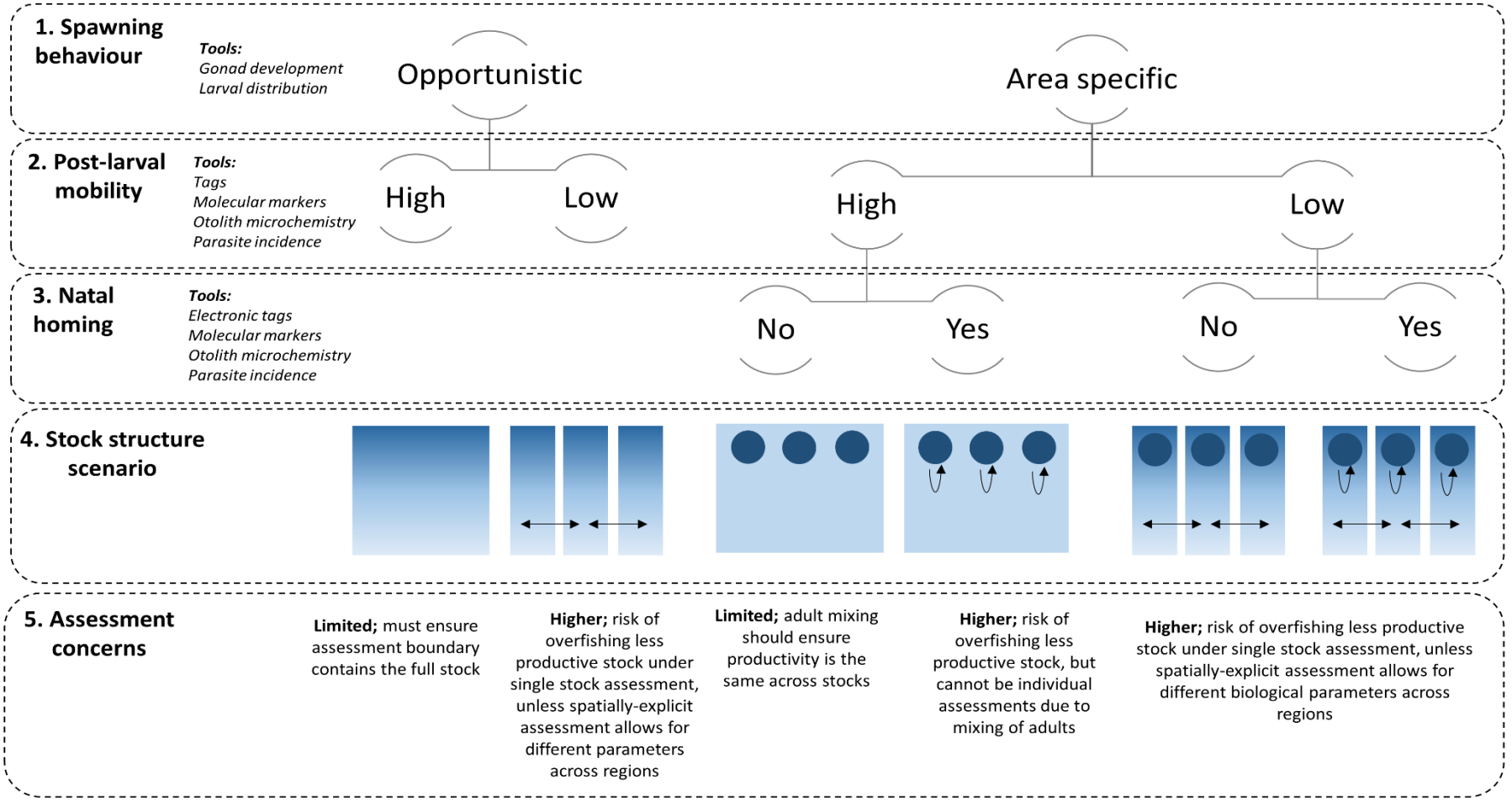

Figure 1.1. Conceptual summary of key research themes necessary to clarify the stock structure of tropical tuna species in the Indian Ocean; (1) spawning conditions (opportunistic vs. discrete), (2) post-larval mobility (low vs high) and (3) natal homing (yes vs no). Different combinations lead to different scenarios of stock structures (4), associated with potential stock assessment concerns (5). Stock structure diagrams indicate spawning areas (dark blue) within the overall distribution range (ligth blue) of the species. Main tools to study each research theme are also indicated. This figure is an adaptation from Moore et al. (2018).

2. Tropical tuna fisheries in the Indian Ocean

Tropical tuna are the main target species of many industrial and artisanal fisheries in the Indian Ocean, representing 53% of the total IOTC catches in 2018. Of the tropical tuna, skipjack tuna contributes the most to catches (~53%), followed by yellowfin (~38%) and bigeye (~9%) tunas (IOTC, 2019c). Tuna fishing operations increased rapidly during the 1980s (Majkowski et al., 2011; Marsac et al., 2014), with tropical tuna catches growing from 146,483 tonnes (t) in 1980 to 560,308 t in 1990. At the beginning of the 20th century, catches reached record levels, with 1,204,041 t reported in 2005. Over the last decade, total catches have fluctuated between ~0.8-1.0 million tonnes, with evidence of an increasing trend since 2015 with 1,130,359 t landed in 2018 (IOTC, 2019c) (**Figure 1.2A**). Until the late 1960s catches of tropical tuna were dominated by Japan, but the large increase of catches during the 1980s was mainly driven by Taiwan, European Union, Maldives and Indonesia (Fonteneau, 2010).

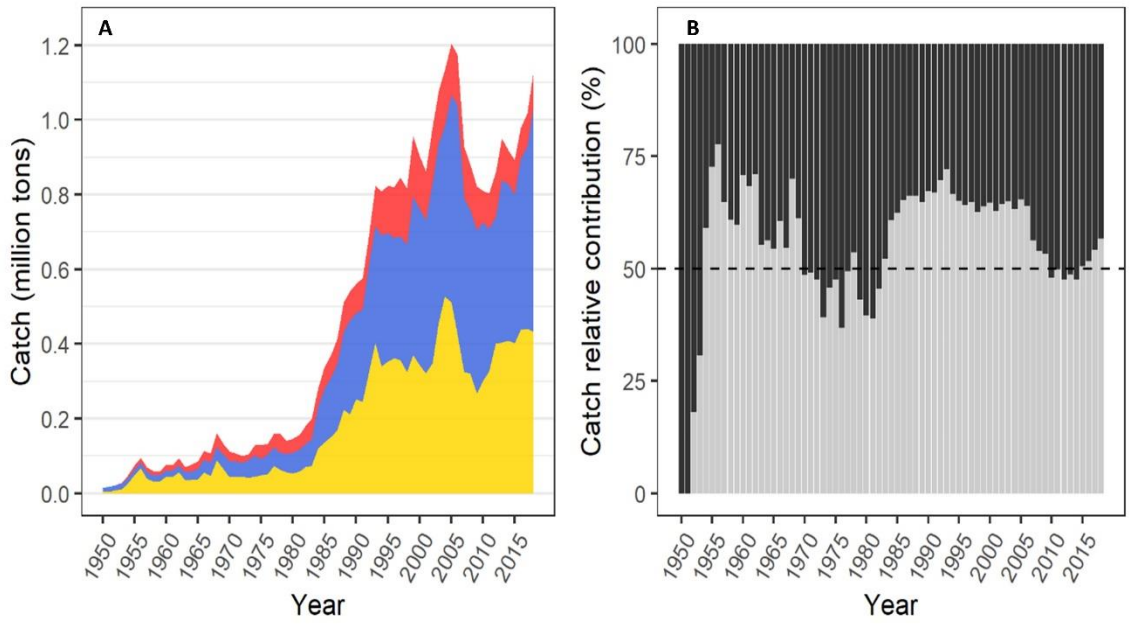

Figure 1.2. Evolution of tropical tuna catches in the Indian Ocean over the 1950-2018 period; (a) Catch trends of, bigeye *Thunnus obesus* (red), skipjack *Katsuwonus pelamis* (blue) and yellowfin *Thunnus albacares* (yellow) in the Indian Ocean, (b) Relative contribution (% of total catches for each year) from the artisanal (light grey) vs industrial fisheries (dark grey). Data source: Indian Ocean Tuna Comission (IOTC) (avaible at: https://www.iotc.org/data/datasets/latest/NC).

A characteristic of the Indian Ocean tropical tuna fishery is the relatively high contribution by the artisanal sector (e.g., handline, gillnet, and pole-and-line) with around of 50% of total Indian Ocean tuna catches. Domestic fisheries represent the main livelihood for millions of people in developing countries of the eastern African coastal countries (van der Elst et al., 2005; Walmsley et al., 2006), and are of crucial importance for food and employment security (Christ et al., 2020). At the beginning of the 2000s, these fisheries accounted for ~35% of the total catch, exceeding 50% in the 2010-2014 period, after which it steadily decreased down to ~43% in 2018 (**Figure 1.2B**). The remaining catch is landed by industrial purse seiners and longliners (IOTC, 2019c; Murua et al., 2015). The contribution of each fishing gear to the catch varies among species. During the 2014-2018 period, skipjack tuna was mostly caught by industrial purse seiners (~40%), pole-and-line (~20%), and gillnet (~20%) whereas yellowfin was mostly caught by purse seiners (~36%), handline (~29%,) gillnet (~21%) and longline (~10%) (IOTC, 2019b). This indicates, that for these two species, catches are relatively evenly split between industrial and artisanal fisheries. By contrast, industrial fisheries account for the majority of bigeye tuna catches in the Indian Ocean; deep-freezing and fresh longline (~42%) and purse seiners (~31%) for the 2014-2018 period (IOTC, 2019c).

The majority of tropical tuna catches in the Indian Ocean are taken from the western region, with ~80% of total catches occurring west of 80°E (i.e. FAO fishing area 51) in 2018 (IOTC, 2019c). However, location of catches can vary seasonally, interannually and between gear types (Kaplan et al., 2014). Longline fisheries operate throughout the entire Indian Ocean but catches of tropical tuna (primarily bigeye and yellowfin tunas) are predominantly taken between latitudes 30°S-20°N, and peak from November to June (**Figure 1.3**). From November to February (**Figure 1.3A**), high catches are widespread from west to east whilst they become concentrated in the Somali basin, north of 5°S, from March to June (**Figure 1.3B**). Although catches in July to October are generally lower than other months, they are again spread across the whole ocean basin (**Figure 1.3C**). An interesting characteristic of the fishery is the dominance of yellowfin tuna in catches in the Mozambique Channel and the Bay of Bengal, in all seasons, whereas bigeye is the primary target species in the equatorial region of the fishery. To a lesser extent, longline fisheries also operate in the southern Indian Ocean along a zonal region

between South Africa and Australia, where bigeye (and albacore – not shown here) is caught as a bycatch of the southern bluefin fishery.

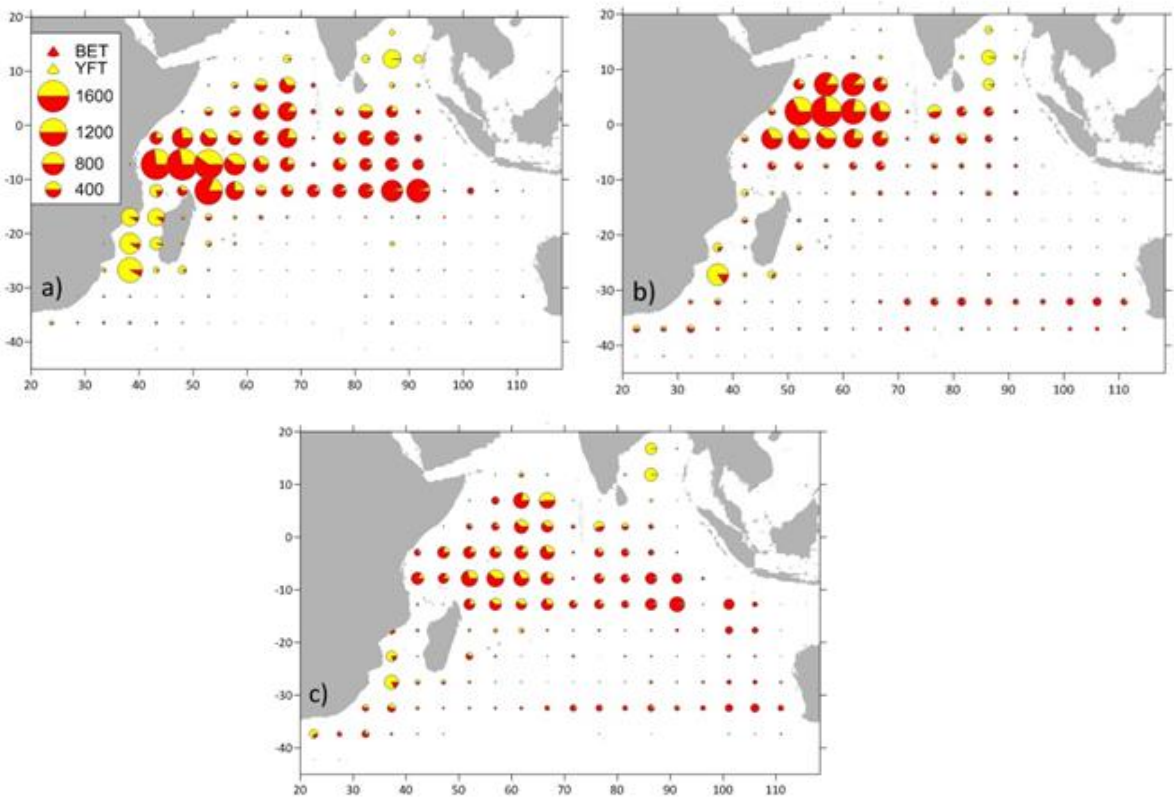

Figure 1.3. Average spatial distribution of longline catches over 2010-2017 for the months November-February (a), March-June (b) and July-October (c). Circles are plotted on a 5°x5° grid and pies are proportional to the catch by species (yellow: yellowfin; red: bigeye). The spatialized data originate from the Indian Ocean Tuna Comission, IOTC (avaiable at: http://www.iotc.org/documents/all-ce-files) but as they are incomplete, they have been raised to the nominal catches by applying raising factors established by fleet, year and species. A few data were available by 1°x1° and they have been aggregated on a 5°x5° grid to enhance visibility.

Purse seiners fishing activity is mainly concentrated in the western and central Indian Ocean, between latitudes 20°S-15°N (**Figure 1.4)**. Skipjack tuna, and to lesser extent juveniles of yellowfin and bigeye tunas, are the predominant species caught by purse seiners fishing around fish aggregating devices (FADs) (**Figure 1.4A, B and E**), while yellowfin tuna dominate catches by purse seiners fishing on free-swimming schools (**Figure 1.4B, D and F**). From November to February, purse-seine catches on FADs are mainly in the western-equatorial Indian Ocean (**Figure 1.4A**), whereas purse seine catches on free-swimming schools increase around the Seychelles and Chagos archipelagos (**Figure 1.4B)**. From March to June, the purse

seine fishery operates in the western-equatorial area but extends as far south as the Mozambique Channel, which is a mixture of FAD and free school fishing (**Figure 1.4C and D**). During this period, tropical tuna catches by purse seiners are also higher off the East African continent relative to central Indian Ocean. During the southwest monsoon (July-October, **Figure 1.4E and F**), catches shift northward 5°S again, being highest off Somalian coast up to the Seychelles archipelago.

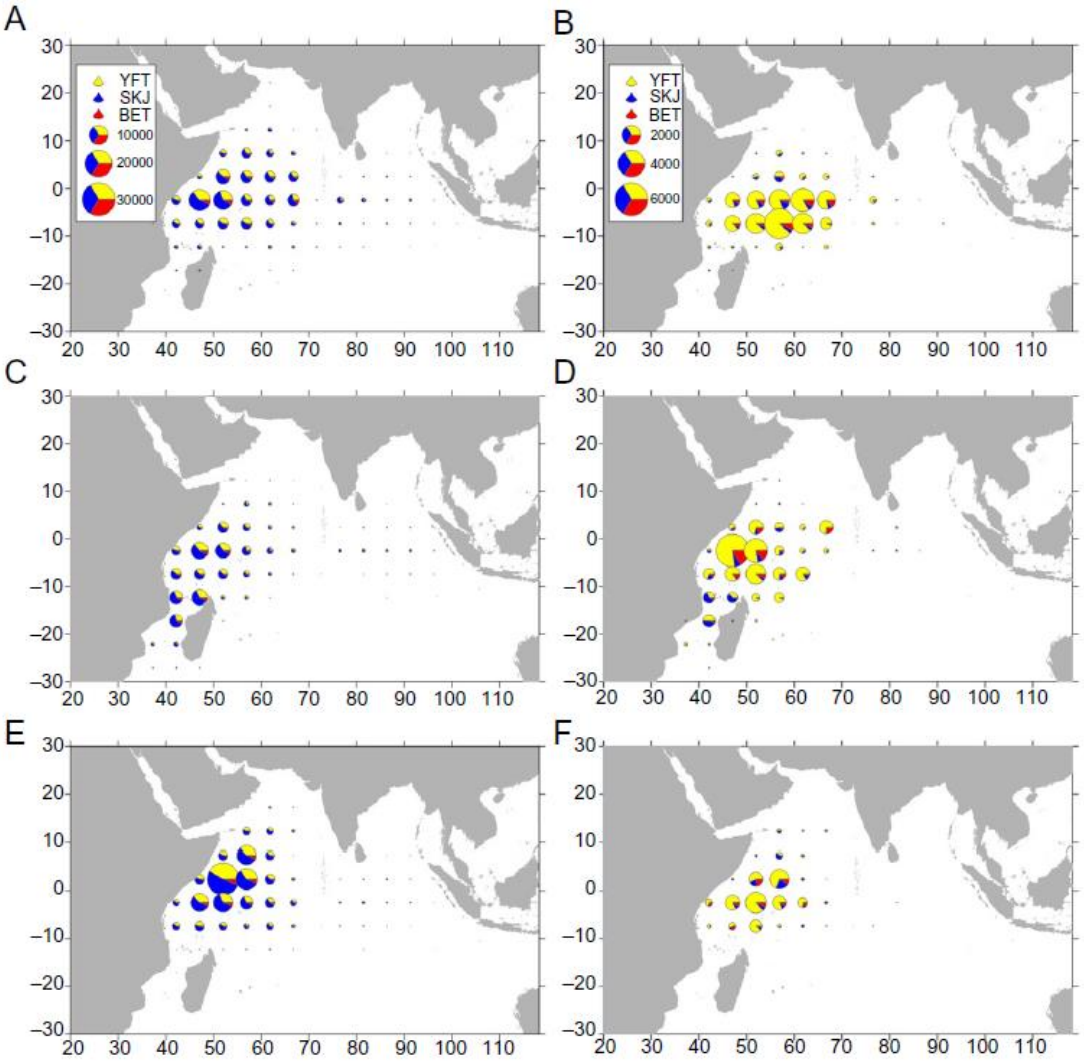

Figure 1.4. Average spatial distribution of purse seine catches over 2010-2017 for the months November-February (a,b), March-June (c,d) and July-October (e,f). Left column (a,c,e) show catches on floating objects, while right column (b,d,f) represent catches on free-swimming schools. Circles are plotted on a 5°x5° grid and pies are proportional to the catch by species (yellow: yellowfin; blue: skipjack; red: bigeye). Note the different scales and maximum between floating objects and free-swimming schools. The spatialized data originate the Indian Ocean Tuna Comission, IOTC (avaiable at: http://www.iotc.org/documents/all-ce-files) but as they are incomplete, they have been raised to the nominal catches by applying raising factors established by fleet, year and

species. Purse seine data are mostly available by 1°x1° and they have been aggregated on a 5°x5° grid to enhance visibility.

Spatio-temporal patterns of activity of artisanal and semi-commercial fisheries cannot be described accurately because spatialized catch and effort data are not usually provided by the fleets. Within the Indian Ocean, the major pole-and-line fishery occurs in Maldives. This fishery is active all year round, targeting mainly skipjack tuna, and to less extent yellowfin tuna (Kolody and Adam, 2011; Miller et al., 2017). Maldivian hand-line also operates year around catching large yellowfin (Ahusan et al., 2016). The gillnet fishery of yellowfin tuna is also important in Sri Lanka, Pakistan and Iran, catching yellowfin and skipjack (IOTC, 2019b).

Since 2001 a significant progress has been made to reduce illegal, unreported, and unregulated fishing (IUU) within the Indian Ocean (Agnew et al., 2009; Anganuzzi, 2004), but the true extent of this problem may be underestimated due to paucity of information on non-industrial fisheries (Pauly and Zeller, 2016). Considering all fisheries in the region (not only tuna), reconstructed catch trajectories of the Indian Ocean differ considerably from the national landings data submitted to the FAO, especially in the western region (Pauly and Zeller, 2016). Inconsistencies between reported landings and reconstructed catch data for all taxa have been described for the south-western Indian Ocean (Temple et al., 2018), the Seychelles (Christ et al., 2020), Madagascar (Le Manach et al., 2016) and Somalia (Glaser et al., 2019).

3. Life history

Skipjack, yellowfin, and bigeye tunas are classified into the Scombridae family, and together with the other 12 tuna species, form the tribe Thunnini. Among the five genera that form this tribe, yellowfin and bigeye tunas belong to the genus *Thunnus* while skipjack tuna belongs to the genus *Katsuwonus* (Collette et al., 2001) (**Figure 1.5**). Tunas (except Allothunnus sp.) are unique among bony fishes as they possess a counter-current heat exchanger system of retia mirabilia (i.e., a vein-arterial vascular system for heat conservation in muscles, viscera and brain tissue) that allows them to maintain the temperature of body tissue warmer than the surrounding waters (Collette et al., 2001). This endothermy, along with an elevated metabolic rate and frequency modulated cardiac output, support continuous,

relatively fast swimming and reduce thermal barriers to habitat exploitation (Graham and Dickson, 2004). Skipjack and yellowfin tunas possess both central and lateral heat exchangers, although lateral retia mirabilia are relatively small. Bigeye tuna have no central heat exchanger, but a well-developed lateral heat exchanger (Carey et al., 1971; Graham, 1975), as well as an additional retia, the function of which is to increase the temperature of their viscera, eyes and brain. This allows bigeye to explore deeper and cooler waters than yellowfin or skipjack. These adaptations imply different life history traits and behaviours among the three species of tropical tuna (Díaz-Arce et al., 2016).

3.1 Biogeography and habitat utilization

Tropical tuna are circumtropical species that inhabit marine pelagic regions of the world's oceans between 45°N and 45°S (**Figure 1.6**) (Sharp, 2001). Whereas adult yellowfin and bigeye tunas inhabit mid-ocean waters, juveniles of these species and skipjack tuna can be found both in coastal and offshore waters (Goujon and Majkowski, 2010). In the Indian Ocean, the three species are more abundant between the 15°S-15°N longitudinal band, the Arabian Sea and the Mozambique Channel, although they can also be found in other regions (Kaplan et al., 2014; Lee et al., 2005; Stéquert and Marsac, 1989). North of 10°S, the Indian Ocean is characterized by a marked seasonality, due to the monsoonal system that determines the ocean circulation and climate (Schott and McCreary, 2001). Two monsoon periods occur annually, the southwest monsoon (June-September) and the northeast monsoon (December-March), with two inter-monsoon periods in between, one from April to May and the second from October to November (Han et al., 2014; Schott et al., 2009). In addition, there is a non-periodical mode of natural climate variability in the Indian Ocean, known as the Indian Ocean Dipole (IOD). This phenomenon is the result of sustained changes in the differences between sea surface temperatures (SST) of the western and eastern Indian Ocean (Saji et al., 1999). Both processes have an impact on the biological production and ecological processes of the area (Jury et al., 2010; Wiggert et al., 2006), and thus may affect the seasonal distribution and behaviour of tropical tuna in the Indian Ocean (Marsac., 2017; Marsac and Le Blanc, 1999, 1998; F. Ménard et al., 2007).

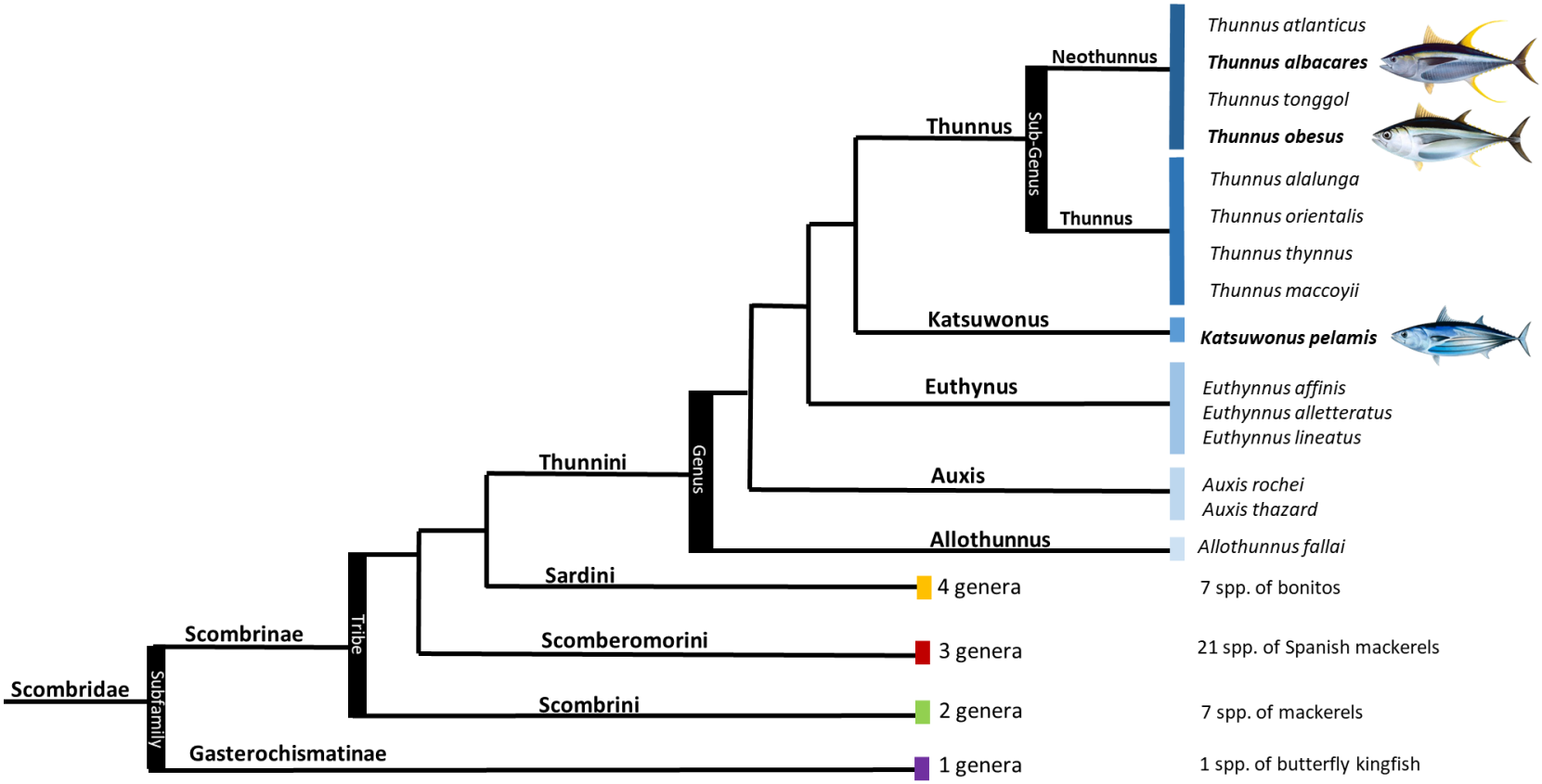

Figure 1.5. Phylogenetic tree of the Scombridae family, which consists of 15 genera and 51 species, among which the three main species of tropical tuna, yellowfin (*Thunnus albacares)*, bigeye (*Thunnus obesus)* and skipjack (*Katsuwonus pemalis) tunas* are found (Collette et al., 2001). The sub-genus branch is based on findings from Díaz-Arce et al. (2016).

Although investigations of Indian Ocean tuna habitat preferences are scarce, experimental studies (Dizon et al., 1977; Sharp, 2001; Sharp and Dizon, 1978) have defined the main environmental preferences and physiological adaptation characterizing tuna habitats. As confirmed by other authors (e.g. Reygondeau et al., 2012; Arrizabalaga et al., 2015; Druon et al., 2017), tropical tuna prefer relatively warm and stratified waters. Skipjack, yellowfin and juvenile bigeye tunas inhabit the epipelagic zone, preferentially occupying the surface mixed layer above the thermocline and waters with sea surface temperatures (SSTs) ranging from 18 to 31°C (Barkley et al., 1978; Pecoraro et al., 2016; Stéquert and Marsac, 1989). Particularly in the Indian Ocean, adult yellowfin tuna preferred habitat has been described to be at depths between 100 and 180m and water temperatures between 15.0-17.9°C (Song et al., 2008). By contrast, adult bigeye tuna inhabit mesopelagic waters, and prefer depth and water temperatures between 240 and 280 m and 12 to 13.9°C, respectively (Song et al., 2009).

Tropical tuna larvae require warmer water (Conand and Richards, 1982; Kim et al., 2015; Wexler et al., 2011), being confined to narrower habitat ranges than juveniles and adults (Reglero et al., 2014) (**Figure 1.6**). The isothermal boundary of tropical tuna spawning areas is >24°C (Schaefer, 2001), although Reglero et al., (2014) suggested that this assumption should be revisited as they found a lower tolerance for tropical tuna larvae of 20°C. Larval occurrence seems to increase at intermediate values (0.01-0.06 $m^2 s^{-2}$) of eddy kinetic energy (Kimura et al., 2004; Reglero et al., 2014).

Despite temperature preferences restricting tropical tuna spatial distribution, electronic tagging has shown that these species are able to perform deep dives into colder waters (e.g. Schaefer et al., 2009). Depth preference is known to change according to body size (Barkley et al., 1978; Graham and Dickson, 2004) and time of the day (Evans et al., 2008). In the Indian Ocean, deep diving behaviour has only been studied in yellowfin tuna; archival tagging of adults showed that large individuals can dive to depths in excess of 1000 m (Dagorn et al., 2006). Oxygen availability also limits the bathymetric range of tropical tuna species. Skipjack and yellowfin tuna have limited tolerance to low levels of dissolved oxygen (Barkley et al., 1978; Graham and Dickson, 2004), while bigeye tuna can tolerate, and even

favour, less oxygenated (e.g. <0.2 mmol/L) waters (Arrizabalaga et al., 2015; Graham and Dickson, 2004; Sharp and Dizon, 1978; Song et al., 2009). These species-specific physiological abilities and tolerances to environmental characteristics of their vertical habitat, result in exploitation of distinct ecological niches at different stages of their life-histories.

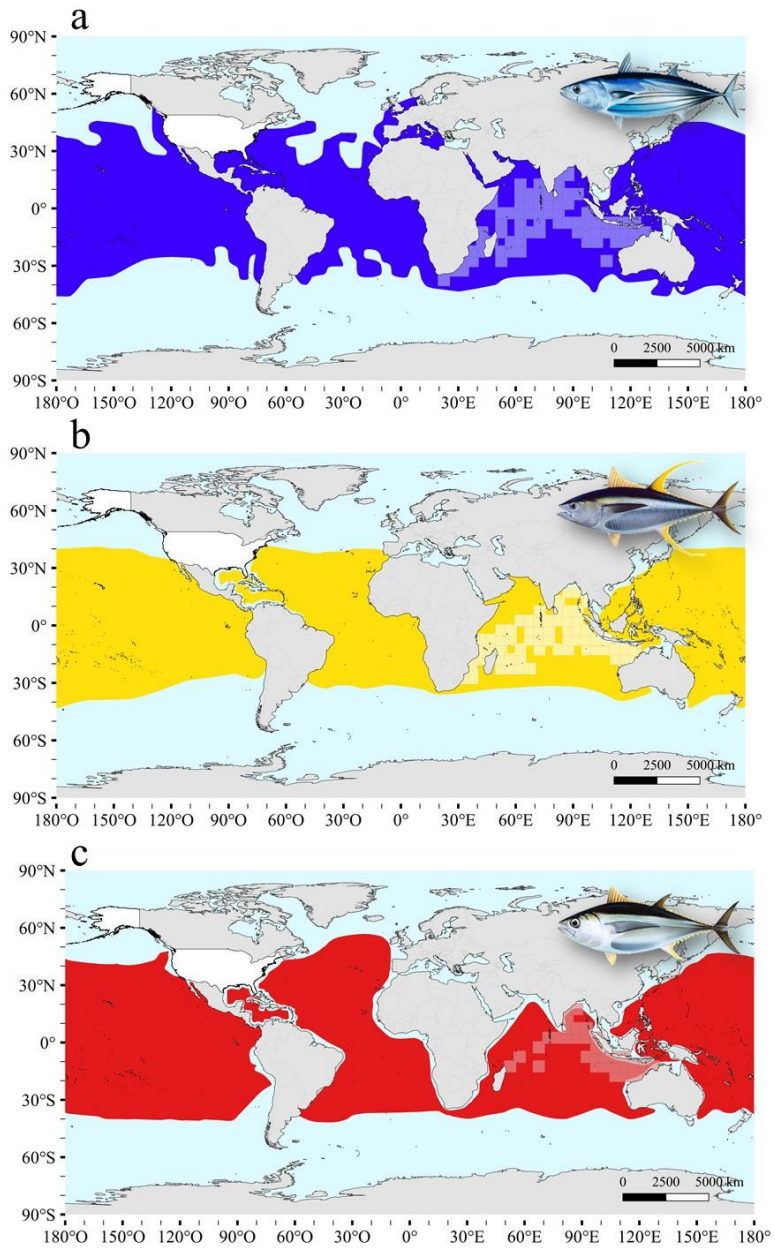

Figure 1.6. Potential habitat distribution range of (a) skipjack tuna Katsuwonus pelamis, (b) yellowfin tuna, Thunnus albacares, and (c) bigeye tuna, Thunnus obesus. Lighter squares represent the presence of larvae (based on Reglero et al. 2014). Distribution range was obtained from the IUCN Red List Spatial Data of tunas and billfishes version 5.2 (available at: https://www.iucnredlist.org/resources/spatial-data-download). Tuna images: IOTC © 2020.

3.2 Trophic Ecology

Tropical tuna have been described as energy speculators, meaning that high rates of energy expenditure are invested to obtain even higher rates of energy (Korsmeyer and Dewar, 2001). Thus, their lifestyle implies the necessity for searching large areas of their habitat in search of food (Dickson, 1995). As such, tropical tuna are visual opportunistic predators that feed on a wide variety of prey (Duffy et al., 2017; Olson et al., 2016); the particular composition will be mainly determined by body size, location, period and feeding depth of each species (Ménard et al., 2006; Olson et al., 2016). In the Indian Ocean, studies analyzing the composition and size of the prey in stomachs of skipjack, yellowfin and bigeye tunas, are limited to the western region.

As larvae and small juveniles, tropical tuna diet consists of planktonic organisms inhabiting the shallow mixed layer (Graham et al., 2007; Young and Davis, 1990). Tuna larvae are precocious feeders; skipjack larvae start feeding two days after hatching (Matsumoto et al., 1984), while rotifers have been found in digestive tracks of 4-day old yellowfin tuna larvae (Kaji et al., 1999). With the development of thermal capability, a progressive diet shift occurs (Graham et al., 2007; Kaji et al., 1999). Maldeniya (1996) found a gradual increase in fish consumption in yellowfin tuna > 40 cm fork length (FL) from Sri Lanka. This ontogenetic shift in diet has also been reported for bigeye tuna of the Indian Ocean: the diet of juvenile bigeye tuna consists mainly on stomatopod crustaceans, while piscivory increases in larger specimens (Duffy et al., 2017). Juveniles of skipjack, yellowfin and bigeye tunas can be found in mixed schools feeding at the surface, generally near the continental shelf, islands or around floating objects (IOTC, 2017b, 2017a, 2017c). Trophic markers revealed high potential of resource overlap between smaller individuals of these species (Sardenne et al., 2016).

In contrast, adults consume a larger range of prey sizes (mainly small fish, cephalopods and crustaceans) (Jaquemet et al., 2011; Frédéric Ménard et al., 2007; Olson et al., 2016), and exhibit predation plasticity depending on prey availability between times and locations (Duffy et al., 2017; Olson et al., 2016). Changes in diet composition with distance from the coast have been reported for skipjack and yellowfin tunas (Smale, 1986). Small pelagic fish (*Cubiceps pauciradiatus, Sardinella*

ocellata and *Engraulis capensis*) dominate by volume for skipjack and yellowfin tunas diets near the shore (Potier et al., 2008; Smale, 1986), whereas in open-ocean waters the ommastrephid cephalopod *Lycotheuthis diadema* also forms part of the diet (Smale, 1986). For yellowfin tuna feeding in offshore waters, the pelagic crab *Charybdis smithii* was found to be the dominant prey item (Potier et al., 2007; Romanov et al., 2009). Long-term dietary changes have been observed for open-water surface swimming skipjack and yellowfin tunas in the western-equatorial Indian Ocean, shifting from fishes to crustacea. During the 1980´s, the main prey item was the small cupleid *Engraulis japonicus* (Roger, 1994), whereas in the 2000s the stomatopod *Natosquilla investigatoris* was by far the dominant prey item (Potier et al., 2004, 2002) for yellowfin and skipjack tunas captured in the Seychelles archipelago.

Foraging depth also influences the type of prey consumed by tropical tuna species (Kornilova, 1980). The stomach content of surface swimming yellowfin and bigeye tunas was dominated by the stomatopod *N. investigatoris*. Additionally, surface caught yellowfin tuna showed preference for fish (scombrids) and bigeye tuna for squids (ommaestrephids) (Potier et al., 2004). Deep swimming bigeye tuna showed a generalized feeding behavior with no dominant prey species found in their stomach. For yellowfin tuna swimming in deep waters both types of feeding strategies were found (i.e. generalized and specialized), with specialized feeders favoring crustaceans such as crab larvae or the swimming crab *Charybdis edwardsi* (Potier et al., 2004). Specialized feeding behaviors have also been reported in reproductive females of yellowfin tuna from Atlantic, Pacific and Indian Oceans (Bard et al., 2002; Flynn and Paxton, 2013; Zudaire et al., 2015). During the spawning period, the latter seem to feed more intensively on lipid-rich fish, particularly on cigarfish, *Cubiceps pauciradiatus* (Zudaire et al., 2015).

Stomach content analyses also indicate differential diel feeding behavior among species (**Figure 1.7**). Skipjack tuna feed during the day on prey that remain in shallower depths (0 to 200 m according to Roger, 1994), with a bimodal peak of feeding activity around crepuscular periods (Olson et al., 2016). Peak feeding of yellowfin and bigeye tunas occurs between 8 a.m. and 12 noon, although stomach fulness indices show that yellowfin tuna feed throughout the day, while bigeye tuna

is, in general, a daytime feeder (Olson et al., 2016). Carbon and nitrogen isotopic signatures measured in muscles of the three species of tropical tuna in the western Indian Ocean, suggested that bigeye tuna have a higher trophic position than skipjack and yellowfin tunas (Olson et al., 2016; Sardenne et al., 2016). Due to their relative tolerance to lower temperature and oxygen levels, bigeye tuna are able to prey at greater depths and lower light intensity (Stobberup et al., 1998). Finally, skipjack tuna possess greater daily ratios of ingestion (3.5-4.2%, percentage of body weight per day), than yellowfin (1.1-2.0%) and bigeye (0.6-3.6%) tunas (Olson et al., 2016) .Research on the trophic ecology of tropical tuna of the western Indian Ocean indicate some degree of resource portioning both intra- and interspecifically, which allows the exploitation of different trophic niches and effectively reduces the potential for food competition.

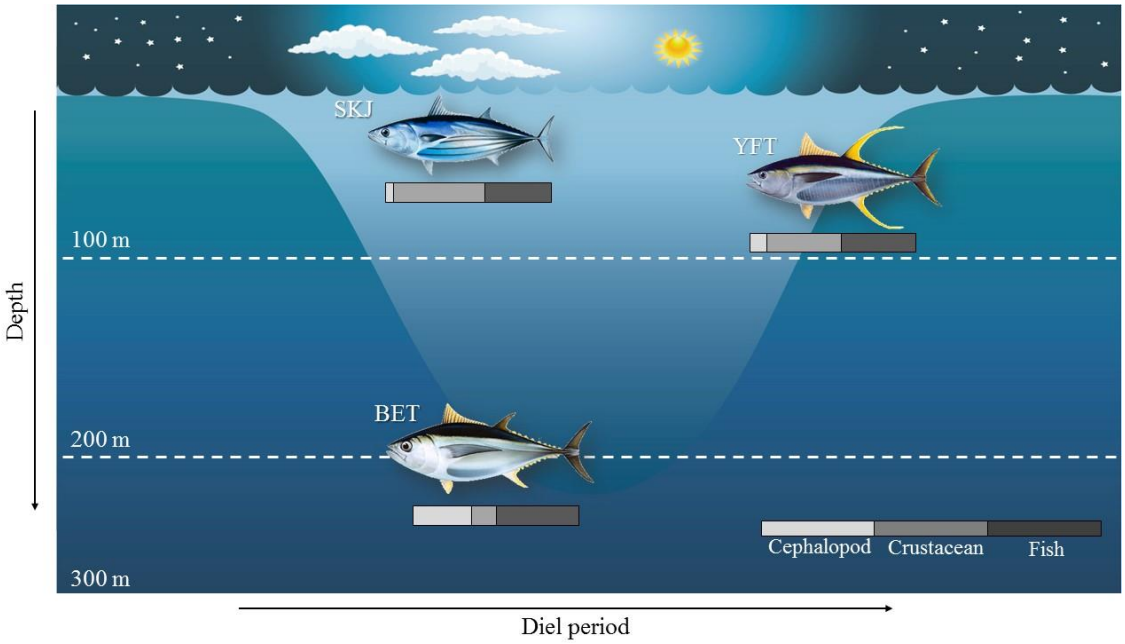

Figure 1.7. Trophic niche partitioning of adult tropical tuna in the western Indian Ocean: SKJ, skipjack tuna, *Katsuwonus pelamis*; YFT, yellowfin tuna, *Thunnus albacares*; BET, bigeye tuna, *Thunnus obesus*. Bars represent the importance of the main prey categories, squid (light grey), crustacean (mid grey) or fish (dark grey), in the diet of each predator (percent of the reconstituted weight). Adapted from Olson et al. (2016). Tuna images: IOTC © 2020.

3.3 Age and Growth

Several approaches have been used to estimate growth of tropical tuna, including modal analyses of length frequencies, the examination of daily and annual rings in calcified structures (e.g. otoliths, spines, vertebrae) and information obtained from tag and recapture data (for an exhaustive review see Murua et al.,

2017). In addition, some growth models have combined the methods described above in an integrated model, with the aim of reducing the biases associated with any single approach (Dortel et al., 2015; Eveson et al., 2015).

Tropical tuna possesses a relatively high growth performance, characterized by having both high growth rate coefficients (k) and, in the case of yellowfin and bigeye tuna, high asymptotic fork lengths (L_∞). Skipjack tuna is considered the fastest growing species of all tunas (Murua et al., 2017). In the Indian Ocean, estimated k values range between 0.23 and 1.41 $year^{-1}$ and L_∞ values from 60.6 to 94.8 cm FL, but most growth curves reported k values >0.4 and L_∞ <82.5 cm FL (**Figure 1.8**). Yellowfin tuna is the second fastest growing tuna species but has a higher growth performance than skipjack tuna. Reported k and L_∞ values in the Indian Ocean range from 0.18 to 1.54 and from 123.6 to 272.7, respectively (Murua et al., 2017). Mean reported k value was 0.34 and most L_∞ values were ~160 cm FL (**Figure 1.8**). Fewer studies have reported growth parameters of bigeye tuna in the Indian Ocean. They have slower growth rates than the other two tropical tuna species, reported k values ranging from 0.06 to 0.45, with a mean k of 0.22 ($year^{-1}$) (Murua et al., 2017). Reported asymptotic lengths range from 150.9 to 423.0 cm FL (**Figure 1.8**), although mean reported L_∞ values were ~190 cm FL. The large variations in growth parameter estimates among studies are probably due to the different techniques used (i.e. disagreements between otoliths and spines), size of analysed fish (i.e. different ages can produce different parameters), lack of inter-laboratory calibrations (i.e. different readers might produce different results), sampling strategy and/or sampling coverage (i.e. spatio-temporal variability in growth). All these factors caution against extrapolating the growth model outside the range of the data used for parameter estimation.

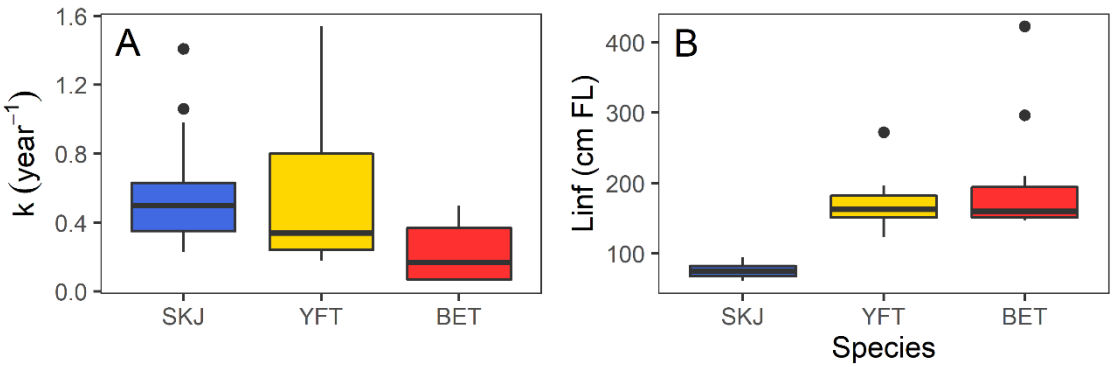

Figure 1.8. Growth parameters of tropical tuna. (A) Comparison of reported growth rate coefficients (k) and (B) asymptotic fork lengths (L_∞) for skipjack (blue), yellowfin (yellow) and bigeye (red) tunas in the Indian Ocean. Growth parameters have been obtained from Murua et al., 2017 supplementary material tables 10S, 13S and 16S.

Previous studies have indicated that tropical tuna may pass through different stanzas of growth rates during their life (Bard, 1984; Fonteneau, 1980; Marsac, 1991). This hypothesis was revisited and supported by Dortel et al., (2015) and Eveson et al., (2015) for the three tropical species in the Indian Ocean. In the case of skipjack tuna, the two-stanza growth model is characterized by a rapid growth in the first stage, followed by a slower growth in the second stage (Eveson et al., 2015, 2012) (**Figure 1.9A**). Due to the initial high growth rates, skipjack tuna can reach ~45 cm FL in the first year of life, and between 50- 65 cm FL in the second year, from which the growth rates diminish (Tanabe et al., 2003). Similar results were obtained by Kayama et al., (2004) for skipjack in the eastern Indian Ocean (45 cm FL), although reported sizes for the second year were smaller (50-55 cm FL). By contrast, yellowfin and bigeye tunas have a phase of slower growth rate as juveniles, followed by a stanza of a higher growth rate. The first slow-growth phase in yellowfin tuna (around 2.1 cm month-1) lasts until they reach 56-70 cm FL. After a quick transition, yellowfin tuna then grow at a faster rate (4.1 cm month-1) until they reach approximately 145 cm FL, with a progressive decrease in the growth rate with size thereafter (0.01 cm month-1) (**Figure 1.9B**) (Dortel et al., 2015; Eveson et al., 2015; Olivier, 2002). In bigeye tuna, the transition between slow- and fast-growth phases occurs at a similar length (around 60 cm FL), however this transition is more gradual (**Figure 1.9C**) (Eveson et al., 2015). There is evidence for sexual-dimorphism in growth in Indian Ocean yellowfin and bigeye tunas (Nootmorn, 2004; Nootmorn et al., 2005; Stéquert et al., 1996; Zudaire et al., 2013a), with male

individuals attaining larger maximum sizes compared to females (Eveson et al., 2015; Farley et al., 2006; Shih et al., 2014).

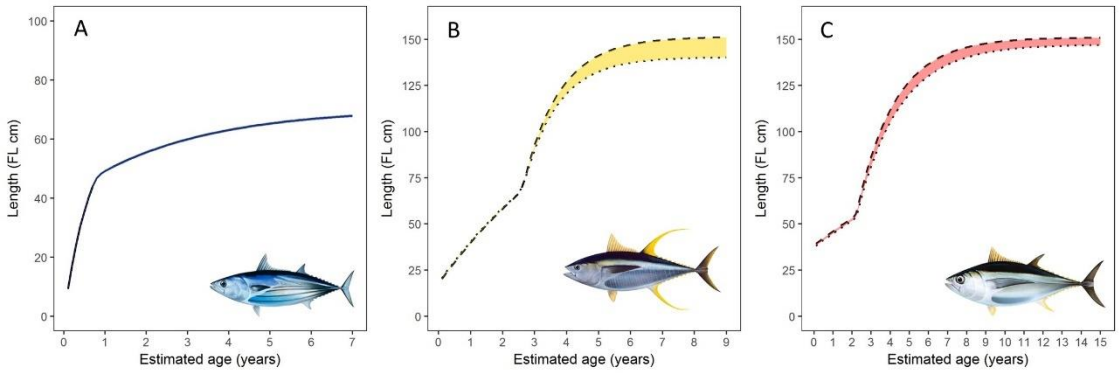

Figure 1.9. VB log K growth curves for (a) skipjack *Katsuwonus pelamis,* (b) yellowfin, *Thunnus albacares,* and (c) bigeye *Thunnus obesus* tunas in the Indian Ocean after following (Eveson et al., 2015). In the case of yellowfin and bigeye tunas, growth is sex-specific, represented with a longdashed lines in males and with dotted lines in females. Tuna images: IOTC © 2020

Bigeye tuna possess the greatest life expectancy among tropical tuna. Based on otolith interpretation and tagging studies, Farley et al. (2006) proposed a maximum age of at least 16 years for bigeye tuna caught in the eastern Indian Ocean, based on validated annual bands. Maximum age for skipjack however is ~6-7 years, whereas reported longevity for yellowfin tuna is in the order of 9 years in the Indian Ocean (Murua et al., 2017; Shih et al., 2014). However, bomb radiocarbon dating has recently validated age estimates of 16-18 years for yellowfin tuna in the Atlantic Ocean (Andrews et al., 2020). After this, our understanding on maximum ages of yellowfin tuna in the Indian Ocean should be revisited.

3.4 Reproductive biology

Tropical tuna are oviparous, have an asynchronous oocyte development and spawn multiple batches of oocytes each spawning season (Hunter et al., 1986; Joseph, 1963; Schaefer, 2001; Stéquert and Ramcharrun, 1995). In terms of reproductive strategy, female skipjack tuna follow what has been described as an income breeder strategy, that is, required energy is obtained directly from food intake rather than from accumulated energy reserves (Grande et al., 2016). Female yellowfin tuna however, are considered to be mixed income-capital breeders (Zudaire et al., 2014). Analyzing lipid allocation of yellowfin tuna from the western Indian Ocean, Zudaire et al., (2014), found that required energy for gonad

development depended mainly on the energy provided by feeding during the prolonged spawning period and, to a lesser extent, on stored lipids. For bigeye tuna, there are no studies addressing the breeding strategy and energy allocation to reproduction in the Indian Ocean. However, Sardenne et al., 2017 suggested an income-capital breeding strategy for bigeye tuna after concluding that liver neutral fatty acids levels were similar to those from yellowfin.

Mean size at maturity, i.e., length at which 50% of female skipjack tuna are classed as mature (L_{50}), has been estimated at between 39.9 cm and 42.0 cm FL in the western Indian Ocean (Grande et al., 2014; Stéquert, 1976). In the case of yellowfin tuna, L_{50} values range between 75 and 114 cm FL. In the western Indian Ocean, L_{50} of yellowfin tuna was estimated at 75.0 cm to 102.0 cm FL, depending on the threshold oocyte development stage considered to indicate maturity (i.e., cortical alveolar vs. vitellogenic) (Zudaire et al., 2013a). In the eastern and west-central Indian Ocean, L_{50} for females has been estimated at 109.6 cm and 114.0 cm respectively, whereas L_{50} reported for males was at 104.9 cm and 120.0 cm FL (Nootmorn et al., 2005; Zhu et al., 2008). Similarly, different L_{50} estimations have been reported for bigeye tuna in the Indian Ocean. Mean size at maturity estimates range from 88.1 cm FL (females) and 86.8 cm FL (males) in the eastern Indian Ocean (Nootmorn, 2004) to 102.0 (females) and 119.3 (males) cm FL in the western Indian Ocean (Zhu et al. 2011; Zudaire et al. 2016).

Tropical tuna show an indeterminate fecundity type (i.e., oocyte maturation is continuous during their extended spawning periods) (Grande et al., 2012; Zudaire et al., 2013b). Studies carried out in the western Indian Ocean show that skipjack tuna has a higher mean relative batch fecundity, 140.0±64.0 oocyte g^{-1} of gonad-free weight (Grande et al., 2014), than yellowfin, 74.4 oocyte g^{-1} of gonad-free weight (Zudaire et al., 2013a), and bigeye tuna, 11.5±7.1 oocyte g^{-1} of gonad-free fish (Zudaire et al., 2016). Reported individual fecundity for skipjack tuna range from 80,000 oocytes for a 44 cm FL female to 1.25 million oocytes for a large (75 cm FL) female in the western Indian Ocean (Stéquert and Ramcharrun, 1995). Grande et al. (2010) estimated batch fecundity from 100,828 oocytes to 627,325 oocytes in female skipjack ranging from 32 to 68 cm FL. In the case of yellowfin tuna, estimated batch fecundity varied from 0.3 to 5.3 million oocytes in females from the eastern

Indian Ocean (Nootmorn et al., 2005). In the western Indian Ocean mean batch fecundity for female yellowfin tuna 79-147 cm FL was estimated at 3.1 million oocytes (Zudaire et al., 2013a). Finally, mean batch fecundity of bigeye tuna in the western Indian Ocean has been estimated at 0.75±0.52 million oocytes (Zudaire et al., 2016). Spawning frequency of tropical tuna species in the Indian Ocean has not been reported yet, but in the Pacific Ocean the mean spawning interval has been determined as 1.18 , 1.53 and 1.09 days for skipjack, yellowfin and bigeye tunas respectively (Schaefer, 2001).

Timing of spawning varies in relation to the geographical distribution of the three species of tropical tuna (**Table 1.1**). In the western Indian Ocean, spawning of skipjack tuna occurs throughout the year, with peaks of intensity between November-March and June-July, coinciding with the north-eastern and south-western monsoon period respectively (Grande et al., 2014; Stéquert et al., 2001b). Koya et al., (2012) also observed year-round spawning in Indian waters but reported a peak in activity between December-March and a smaller peak from June to August. Spawning period seems to shorten as the distance from equator increases (Matsumoto et al., 1984). Yellowfin tuna predominantly spawn from November to February in equatorial waters, primarily on spawning grounds west of 75°E (Hassani and Stéquert, 1991; Shung, 1973; Zudaire et al., 2013a). A shorter spawning period (i.e., from December to February) has been reported for females smaller than 100 cm FL (Zudaire et al., 2013a). The offshore waters of Mozambique Channel and the eastern Indian Ocean are also known as secondary spawning grounds. In the east, spawning is prolonged from November until April (John, 1995; John et al., 1998; Nootmorn et al., 2005). Secondary spawning peaks have also been described; in June for the western Indian Ocean, between April and June around Sri Lanka, and from October to December off northern Australia and Madagascar (Stéquert et al., 2001b; Stéquert and Marsac, 1989; Zudaire et al., 2013a). Bigeye tuna from different areas of the Indian Ocean possess differences in spawning seasonality. In equatorial waters of the Indian Ocean, bigeye tuna are able to spawn year round (Kume et al., 1971; Stobberup et al., 1998). In the eastern Indian Ocean, the spawning season is reported from December to January, with another peak in June (Nootmorn, 2004), whereas in the western Indian Ocean, high reproductive activity has been observed from January to March (Zudaire et al., 2016).

Table 1.1. Summary of studies on Indian Ocean tropical tuna spawning seasonality. SKJ; skipjack tuna, *Katsuwonus pelamis*, YFT; yellowfin tuna, *Thunnus albacares,* and BET; bigeye tuna, *Thunnus obesus*. When two spawning seasons have been described in the same study 1; Main spawning season and 2; Secondary spawning season.

Species	Region	Spawning season	Source
SKJ	Western Indian Ocean	Year- round, but peaks of activity between November-March and June-July	(Stéquert et al., 2001a)
SKJ	Western Indian Ocean	Year-round, but peaks of activity between November-March and June-July	(Grande et al. 2014)
SKJ	Indian waters	Year-round, peak of activity between December-March and a minor one from June to August	(Koya et al. 2012)
YFT	Central Indian Ocean, south Seychelles, west Sumatra Sri Lanka North Madagascar, north Australia	January to March 1: January to March 2: April to June 2: October to December	(Stéquert and Marsac, 1989)
YFT	Western Indian Ocean	November to April	(Hassani and Stéquert, 1991)
YFT	Seychelles EEZ	November to February	(Majid and Ahmed, 1991)
YFT	Pooled data for the Indian EEZ	January to April/May	(John and Sudarsan, 1993)
YFT	Andaman Sea	November to April	(John, 1995)
YFT	Bay of Bengal	November to April	(John et al., 1998)
YFT	North Arabian Sea	December to June	(Govindraj et al., 2000)
YFT	Western Indian Ocean	1: November to March 2: June to August	(Stéquert et al., 2001a)
YFT	Eastern Indian Ocean	November to April	(Nootmorn et al., 2005)
YFT	West Central Indian Ocean	January to June	(Zhu et al., 2008)
YFT	Western Indian Ocean	1: November to February, 2: June	(Zudaire et al., 2013a)

YFT	Equatorial Area (0-10°S)	December to March	(IOTC, 2017c)
BET	Indian Ocean	January to March	(Solovieff, 1970)
BET	Eastern Indian Ocean	October to January	(Ye et al., 2003)
BET	Southern Central Indian Ocean	October to January	(Li et al., 2010)
BET	Indian Ocean Eastern Indian Ocean	1: December to January 2: June	(IOTC, 2017b)
BET	Western Indian Ocean	January to March	(Zudaire et al. 2016)

4. Stock structure

There is little information available to determine whether the tropical tuna of the Indian Ocean constitute single or several stocks. Current stock assessments are conducted assuming that there are single, Indian-wide stocks of skipjack, yellowfin, and bigeye tunas; and that there is no exchange of fish among Atlantic, Indian and Pacific Oceans. This assumption is based on the results obtained from the Indian Ocean Regional Tuna Tagging Program (RTTP-IO) that suggest rapid and large-scale movements of the three tropical species in the Indian Ocean (Fonteneau and Hallier, 2015). However, findings obtained from other approaches (e.g. fishery data and genetic markers) show a more fragmented population structure than typically assumed in the assessment and management of these species. The aim of this section is therefore to compile and evaluate the scientific evidence available on Indian Ocean skipjack, yellowfin, and bigeye stock structure.

4.1 Fisheries Data

Spatial and temporal distribution of catch and effort data from the commercial fishery can be used as a crude indicator of stock structure if, for example, strong geographic differences in age composition, relative abundance and/or distribution are reported. Early studies used catch data distribution and fishery length data of skipjack, yellowfin, and bigeye tunas to describe the stock structure in the Indian Ocean. A study based on size composition of skipjack caught by longline vessels in the Indian Ocean during 1972-1975, reported relatively smaller specimens in the central and eastern Indian Ocean (Pillai and Silas, 1979).

Similarly, analysing Japanese longline fishery data (1961-1965), Morita and Koto, (1970) suggested a two-stock structure for the Indian Ocean yellowfin tuna; the western and eastern stocks separated approximately at 100°E and possibly mixing in adjacent waters. Later, Nishida (1992) concluded that there were two major and two minor stocks of yellowfin tuna in the Indian Ocean, using catch-per-unit-effort (CPUE), age-specific CPUE and size variations obtained from longline fishery data. The two major stocks (named western and eastern) were defined at 40°-80°E and 80°-120°E respectively. The two minor stocks were defined westward 40°E and eastward of 120°E, and named far western and far eastern respectively, with the latter possibly being part of the Pacific stock. In the case of the bigeye tuna, a single stock was suggested for the Indian Ocean, based on the distribution, size composition and sexual maturity of the fish, although some differences between eastern and western bigeye tuna were reported (Kume et al., 1971).

4.2 Morphometric and meristic characters

Phenotypic variation in anatomical characters have historically been used for stock identification purposes. Morphometrics analyse quantitatively the size and shape of the body, whereas meristic analyses refer to countable traits (e.g. fin rays, scales in rows, gill-rakers and myomeres). By comparing different body characters of yellowfin tuna collected from six grounds in the Indian Ocean, Kurogane and Hiyama (1958) suggested a 3-stock structure, one stock in the western Indian Ocean and two in the eastern Indian Ocean, with a strong intermingling between 80-100°E. Although a preliminary study demonstrated the potential utility of otolith shape variation for skipjack tuna stock structure identification in the Indian Ocean (Wujdi et al., 2017), this marker has not yet been used for tropical tuna stock structure analyses in this ocean.

4.3 Parasites

Geographical variation in species composition and abundance of parasites has been used as a natural tag for fish stock structure analyses. This is because parasite occurrence depends on biogeography, distinct environmental tolerances of parasites, differential availability of intermediate hosts, and basically different life history characteristics of the fish stocks *per se* (Catalano et al., 2014). Lestari et al.

(2017) found 7 potential parasites that might be useful to discriminate juvenile yellowfin and bigeye tunas from Indonesian waters. More recently parasite data from juvenile yellowfin and bigeye tunas from the Maldives proved to be significantly different from those belonging to Indonesian waters (Moore et al., 2019). Therefore, authors have suggested movements of yellowfin and bigeye from the Maldives archipelago into the eastern Indian Ocean were limited.

4.4 Genetics

With the development of new molecular techniques, the use of molecular markers such as allozymes, mitochondrial or nuclear DNA polymorphisms have increased in stock identification studies. Each of these markers presents a series of advantages and limitations, but all have been used in Indian Ocean tropical tuna stock structure studies. Often, the use of different techniques and sampling designs provide contradictory results, especially when the organism being studied has a widespread distribution and/or complex natural history, as is the case of skipjack, yellowfin and bigeye tunas (Kumar and Kocour, 2015).

For example, Menezes et al. (2006) found high levels of genetic differentiation between skipjack tuna collected from the east coast of India and the coast of Japan (Pacific Ocean) after using PCR-RFLP analysis of the mitochondrial D-loop region. However, when using nuclear microsatellite markers, there was no differentiation between samples from the two aforementioned regions (Menezes et al., 2008). Also at the inter-oceanic scale, Fujino et al. (1981) found significant differences in allozyme allele frequencies in skipjack from the Indian Ocean compared to those collected both from the Atlantic and western Pacific Oceans. Additional studies comparing Atlantic and Pacific Ocean skipjack tuna revealed a high degree of genetic similarity among these two oceans (e.g. Graves et al., 1984; Ely et al., 2005). Few genetic studies have been conducted on skipjack tuna population structure within the Indian Ocean to date. Although limited to a regional scale, these studies reported the presence of heterogeneous groups of skipjack in the north-central and eastern Indian Ocean. In adjacent waters of Sri Lanka, Maldives and Laccadive islands, two differentiated stocks have been described after analysing patterns of genetic variation with both a mitochondrial gene and six microsatellite loci (Dammannagoda et al., 2011). Additionally, sequence data of the

mitochondrial D-loop region revealed the presence of four clades of skipjack tuna in the east and west coasts of India (Menezes et al., 2012). Although both studies failed to find a clear spatial pattern among samples, Dammannagoda et al. (2011) proposed different hypotheses for the physical mixture of these two distinct skipjack tuna clades around Sri Lanka: (i) different stocks may spawn in distant areas of the Indian Ocean, and juveniles subsequently separately migrate towards Sri Lanka, which is a highly productive foraging ground and (ii) the monsoonal currents in the Indian Ocean could drive the larvae towards this area by passive transport. Menezes et al. (2012) suggested that the absence of a symmetrical pattern of haplotype distribution in the analysed clades could be due to secondary contact and interbreeding of populations after being geographically isolated for a prolonged period. In the eastern Indian Ocean, the results from three microsatellite loci suggest the presence of two stocks of skipjack tuna in Indonesian waters, with genetic differentiation between skipjack from west of Sumatra and south of Java (Jatmiko et al., 2019).

In the case of yellowfin tuna, the use of different genetic markers has also lead to discordances both at intra- and inter-oceanic patterns of differentiation (Pecoraro et al., 2016). Using allozyme markers, Smith et al. (1988) described genetic heterogeneity between yellowfin tuna from the Pacific and Indian Oceans. However, Wu et al. (2010) did not detect any genetic differentiation between yellowfin tuna from the western Pacific and western Indian Oceans using mitochondrial markers. A global genetic study of yellowfin tuna combining both allozymes and mitochondrial DNA, suggested differentiation between the Atlantic, Indian, west-central Pacific and east Pacific oceans (Ward et al., 1997). Recently, the use of next generation sequencing has shed new light on the global population structure of yellowfin tuna. Using genomic wide single nucleotide polymorphisms (SNPs), Pecoraro et al. (2018) identified genetic differentiation of yellowfin tuna between Indian, Atlantic and Pacific Oceans. Moreover, genomic analyses have revealed asymmetrical dispersal from the Indian Ocean yellowfin tuna into the Atlantic and highlighted that yellowfin tuna found along all the South African coast are derived from the Indian population (Barth et al., 2017; Mullins et al., 2018). This connection was also noticed during the RTTP-IO with a few yellowfin tuna tagged in Tanzania that were recovered in the southern Agulhas current, along the South

African coasts. In light of this evidence, Mullins et al. (2018) proposed that the current operational boundary for management between the Atlantic and Indian stocks should be revisited. Using genome wide SNPs, Barth et al. (2017) found genetic differentiation of yellowfin tuna from the Arabian Sea with respect to those from the Atlantic and Indo-Pacific. Results from genome wide SNPs also indicate a marked genetic difference between samples from the central Indian Ocean (Maldives) and the western Pacific Ocean, but not between samples from eastern Indian Ocean (Indonesia) and the western Pacific Ocean (Proctor et al., 2019). Proctor et al. (2019) proposed that the observed pattern of differentiation may indicate limited gene flow between the central and eastern Indian Ocean, with more pronounced gene flow among Indonesian and Western Pacific regions. At intra-oceanic scale, the comparison between samples from the westernmost and easternmost parts of the Indian Ocean, did not reveal any genetic differentiation (Chow et al., 2000a; Nishida et al., 2001). In contrast, mitochondrial and nuclear microsatellite loci variations of yellowfin tuna collected from six fishing grounds around Sri Lanka and one in Maldives, suggested the existence of discrete yellowfin tuna populations in the northwest Indian Ocean (Dammannagoda et al., 2008). Additionally, a study using the mitochondrial D-loop region supported the presence of three genetically different stocks of yellowfin tuna in the north Indian Ocean (Kunal et al., 2013).

Global genetic studies have also reported an inter-oceanic division between Atlantic and Indo-Pacific bigeye tuna both by analysing nuclear (Durand et al., 2005) or mitochondrial (Alvarado-Bremer et al., 1998; Chow et al., 2000b; Martinez et al., 2006) markers. Indo-Pacific bigeye tuna intermingle off southern Africa with Atlantic bigeye tuna (Chow et al., 2000b; Durand et al., 2005). However, Gonzalez et al., 2008 found discordant results when analysing genetic structuring and migration patterns of Atlantic bigeye tuna. Microsatellite loci supported a single worldwide panmictic bigeye tuna population, whereas mitochondrial markers show genetic differentiation between Atlantic and Indo-Pacific bigeye tuna populations, as previous studies did. However, a recent study using SNP data proved restricted connectivity between Indian Ocean (central and eastern) and the western Pacific Ocean bigeye tuna, with samples from central Indonesia having limited connectivity also with the previous areas (Proctor et al., 2019). Few studies have been carried

out to describe the structure of bigeye tuna in the Indian Ocean. Most of them did not observe signs of heterogeneity, supporting the existence of a single panmictic population in this ocean. After analysing variations in mitochondrial DNA polymorphisms and seven microsatellite loci of bigeye tuna distributed in the eastern, central and western Indian Ocean, minimal and generally non-significant genetic differentiation was reported (Appleyard et al., 2002). Likewise, a study using mitochondrial DNA data from bigeye tuna sampled among 4 regions (Cocos Islands, south-eastern Indian Ocean, south-western Indian Ocean and Seychelles) failed to detect any differences between areas (Chiang et al., 2008). A local study carried out in distinct locations off Indonesia however, reported the existence of two genetically distinct groups of bigeye tuna in the eastern Indian Ocean, based on genetic distances and RFLPs mitochondrial D-loop region (Nugraha et al., 2010). Similarly, SNP analyses indicated a gradient in geneflow between the Indonesian archipelago, the eastern Indian Ocean, and the Maldives, consistent with an isolation by distance model (Proctor et al., 2019).

Overall, it seems that results obtained from the application of a single type of molecular marker should be interpreted with caution. For the three species of tropical tuna, different population structure was suggested depending on the analyses. In general, results relying on mitochondrial DNA showed higher heterogeneity than those based on nuclear DNA. Qiu et al. (2013) hypothesized that this mito-nuclear discordance found in tuna species, may be a result of behavioural differences between sexes rather than a misuse of the chosen marker; mitochondrial DNA is inherited from females which may present greater philopatric behaviour. If so, female philopatry would have enhanced mitochondrial DNA diversity, while male-biased dispersal would have homogenized group differences that could be revealed in the nuclear genome (Qiu et al., 2013). The current rise of next generation sequencing (NGS) based genotyping methods, presents a cost-effective alternative to increase the precision in detecting small genetic differences (Rodríguez-Ezpeleta et al., 2019). At local scale, NGS techniques have been already used to discriminate among yellowfin tuna populations of the Pacific Ocean (Grewe et al., 2015). To date no studies of that kind have been published in the Indian Ocean. It is recognised that this technique, combined with a structured basin-wide sampling design, would

provide a powerful tool to finally reveal a clear picture of the population structure of tropical tuna in this ocean.

4.5 Otolith microchemistry

Chemical composition of fish otoliths and other calcified structures (e.g. scales, fin-rays and spines), have been recognised as useful natural markers to discriminate among groups of fish that have inhabited different environments. While genetic analyses provide information over evolutionary timescales, otolith chemistry inform over ecological time frames (i.e., larval history, individual life span…) (Campana, 1999, 2005; Tanner et al., 2016). Thus, this technique is useful to identify differences in natal origin or migration patterns, revealing complex population structures and biologically meaningful units. Despite their importance to delineate fish stocks, otolith microchemistry has barely been used in tropical tuna structure analyses. Natal origin studies have been conducted for bigeye tuna of the Pacific Ocean (Rooker et al., 2016), and for yellowfin tuna both in the Pacific (Rooker et al., 2016; Wells et al., 2012) and the Atlantic Oceans (Kitchens, 2017; Shuford et al., 2007). Arai et al. (2005) described movements and life history patterns of skipjack tuna in the Pacific Ocean based on otolith Sr:Ca ratios. In the Indian Ocean, initial investigations of otolith trace element data proved useful for yellowfin tuna stock delineation (Artetxe-Arrate et al., 2019). Moreover, the study detected some level of separation between two potential nursery regions (Seychelles-Somalia and Mozambique Channel) using young-of-the-year (YOY) yellowfin tuna from the western Indian Ocean. Similarly, otolith microchemistry analyses showed restricted movements of yellowfin and bigeye tunas of the eastern Indian Ocean during their first 4-6 months of life (Proctor et al., 2019). Otolith isotopic analyses, and particularly oxygen isotope $\delta_{18}O$ composition, might also be useful in discriminating among fish of different origins in the Indian Ocean **(Figure 1.10**). Both techniques need now to be expanded at ocean basin scale, to help clarify unresolved population structure of the three species of tropical tuna in this ocean.

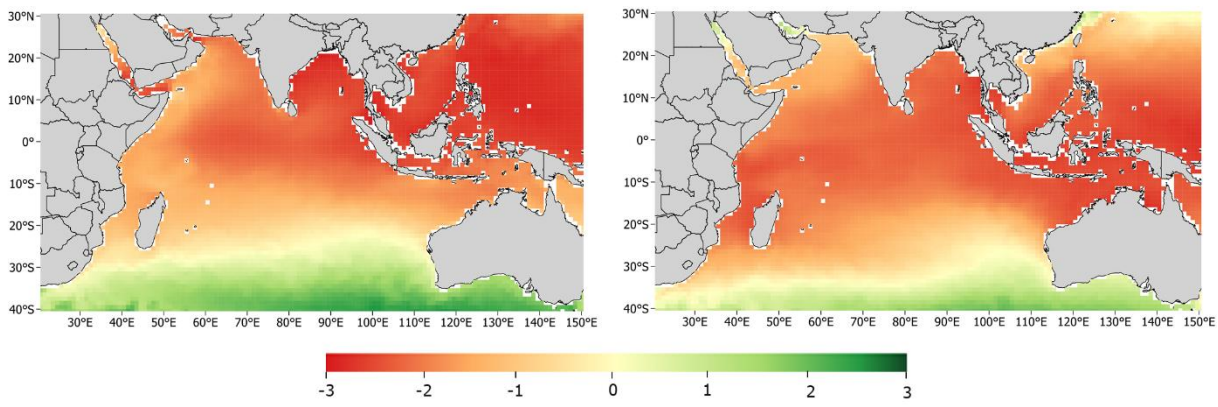

Figure 1.10. Predicted spatial variations in isotopic composition of oxygen in otoliths ($\delta^{18}O_{oto}$) following Trueman and MacKenzie (2012) and based on global surface water (0-50 m) measured $\delta^{18}O_w$ values (LeGrande and Schmidt, 2006), and parameters γ and β from Kitagawa et al., (2013). Maps are differentiated for summer monsoon (Jun-Sept 2017) and winter monsoon (Dec-Apr 2016-2017). Monthly data of Sea Surface Temperature (SST, °C) was obtained from the "global-reanalysis-phy-001-031-grepv2-montlhy" dataset available in the EU Copernicus Marine Service Information (avaible at: https://marine.copernicus.eu/). Note that this simplistic model assumes constant parameters for the otolith fractionation equation and is based on coupled measurements of $\delta^{18}O_w$ values and SST at a spatial resolution of 1×1° grid.

4.6 Tagging

Artificial tags have commonly been used as an indirect approach to identify stock structure. Tagging provides information of fish dynamics (e.g. movement range and pattern), and hence can be a useful tool to infer the degree of mixing among potential stocks. There is an extensive tagging data collection in the Indian Ocean, as tagging programs were initiated in the Maldives in 1990-1994 and continued 15 years later (2005) when the IOTC started a large-scale Indian Ocean Regional Tuna Tagging Program (RTTP-IO) (Murua et al., 2015).

Results obtained from these programs describe fast and large-scale skipjack movements, with an average monthly distance of 1066 miles between tagging and recovery positions in the first year (Fonteneau and Hallier, 2015). Skipjack tagged in Tanzania showed the larger and fastest migrations (e.g. average distances of 1129 miles after one month at liberty), followed by skipjack tagged in Mozambique Channel (an average of 894 miles travelled). Despite the rapid movements described for skipjack tuna tagged in the Mozambique Channel, most tagged tuna returned to this area within one year, coinciding with the March-May fishing season, a pattern that was recurrent over the studied years (Fonteneau and Hallier, 2015). Authors

suggested that rather than a random movement, this return may correspond to a fidelity behavior towards a feeding area. Average distances travelled were shorter in the Seychelles tagging (698 miles) and the lowest for skipjack tuna tagged in the Maldives (358 miles) (Fonteneau, 2014). This result is very similar to the results of the early Maldivian tagging program carried out between 1990 and 1995 (Adam and Sibert, 2002). Although the heterogeneity of skipjack movement patterns was high, Adam and Sibert (2002) found evidences of low emigration rates from Maldives to the rest of the Indian Ocean. This could be because skipjack tuna travel longer distances in the open ocean than in archipelagic waters (Fonteneau, 2014). This is the case for the Maldives, which comprises a network of nearly 1200 islands. In addition, the presence of numerous anchored FADs in this region, under which skipjack aggregate, may be reinforcing the "island effect", reducing the distance travelled by this species. Conversely, drifting FADs may increase the mobility of skipjack in other areas (Hallier and Gaertner, 2008; Marsac et al., 2000). Thus, based on these results, Fonteneau (2014) proposed that future stock assessment of the skipjack population should consider at least 4 different regions with differential mixing rates in the Indian Ocean: southwest Indian Ocean, northwest Indian Ocean, central Indian Ocean and eastern Indian Ocean.

The evidence of fast and large movements of yellowfin tuna reported by the RTTP-IO supports the assumption of a single well-mixed yellowfin tuna population within the Indian Ocean (IOTC, 2017c). For instance, short-term recoveries were associated with relatively long distances (249 miles on average), about 5 times longer than the distances of short-term recoveries in other oceans (Fonteneau and Hallier, 2015). Past tagging studies showed that there was exchange of yellowfin tuna between the central and the western Indian Ocean (Yano, 1991) and movements of yellowfin from Maldives to Sri Lanka (Nishida et al., 1998). However, Kolody and Hoyle (2013) found that tag releases from the Maldives area were sometimes retained there, without mixing into the rest of the population. It is also noteworthy that most tagging events occurred in the western part of the Indian Ocean and few recoveries have been reported from the eastern part. Langley and Million (2012) suggested that the 28-29°C SST isotherm may limit the eastward dispersal of the tagged fish. Thus, there may be some degree of separation between the yellowfin tuna populations of the west and east Indian Ocean.

Results obtained from the RTTP-IO also describe fast and large-scale bigeye movements. The average monthly distance between tagging and recovery positions is 918 miles in the first year, with distances increasing slowly in subsequent years (Fonteneau and Hallier, 2015). For instance, bigeye released off Tanzania were subsequently recovered as far away as the subtropical Indian Ocean, eastern Indian Ocean and the southern and western coasts of South Africa (Hallier and Million, 2012). The reported fast and extensive movements of bigeye tuna in the Indian Ocean led to the assumption that its population is highly mobile, supporting the current assumption of a single stock for the Indian Ocean (IOTC, 2017b).

Conventional tagging studies, however, depend on tag-recapture efforts, and can be sensitive to the distribution of releases and assumptions related to the tagged population (e.g. random selection, independence and complete mixing) (Berger et al., 2014; Pollock and Pine, 2007). This may lead to biased results and data misinterpretation. Fonteneau and Hallier (2015) advised that current tagging programs targeting tropical tuna, may still not be adequate to estimate the potential stock mixing rates. For instance very few tags have been returned from the eastern Indian Ocean (Murua et al., 2015), which may reflect a lack movement from west to east, but more certainly, this is a consequence of poor reporting rates by longliners operating in the east Indian Ocean. Therefore, movement dynamics within the eastern Indian Ocean have not yet been adequately evaluated. Electronic tags may present a complementary platform to elucidate tropical tuna real movements. This technique proved to be useful in identifying population structure in other tuna species (Block et al., 2005). Finally, an accurate knowledge of tropical tuna movements in the Indian Ocean will be essential to establish management boundaries if different stocks are revealed.

5. Conclusions and future research directions

Since tropical tuna fisheries of the Indian Ocean play an important role in the three sustainability pillars (i.e., social, environmental and economic) of the region, there is an urgent need to advance our understanding of the resource and the fisheries to ensure a proper and sustainable management of these species (Asche et al., 2018). Scientific advice on tropical tuna of the Indian Ocean is based, among

others, on the results of the stock assessment models. However, more accurate and comprehensive fishery data statistics, which cover all fisheries components, are needed to improve the monitoring and stock evaluation of these species which will, in turn, reduce the uncertainty of the assessment and improve the scientific advice for management. IOTC should, therefore, prioritize the capacity of the countries in the region to implement monitoring systems. This will allow to collect fishery statistics that contribute to the provision of the scientific advice for management of IOTC species. Strong monitoring systems, once implemented, will also ensure a better control mechanism to enforce any agreed management measure by IOTC (e.g., yellowfin catch limits and skipjack annual quota). Here, available information regarding Indian Ocean yellowfin, skipjack and bigeye tuna fisheries, life history and stock structure has been reviewed. This will help identify gaps in our knowledge that need to be filled to improve the assessment and management advice for these resources.

Firstly, there is, in general, a lack of information regarding life-history traits of skipjack, yellowfin and bigeye tunas at an oceanic scale in the Indian Ocean. Most studies are regionally limited, which impedes a global overview of the complex interaction between the environment and these species and makes it difficult to incorporate life-history parameters at the appropriate scale into stock assessment models. Studies that characterize fundamental life-history characteristics (e.g., growth and reproductive parameters) at ocean scale are needed to understand if differences stem from regional differences or just from different sampling strategies. Growth, mortality and reproduction are determinant factors for population productivity and, thus, key variables for stock assessment and management advice (Maunder et al., 2015). However, there are discrepancies regarding the growth and reproduction parameters of these key species in the Indian Ocean, which increases uncertainties in assessments of their status and advice for their management. Moreover, the fact that different studies calculate growth models based on fish from different size/age classes, caution the extrapolation of the results outside the range of the data. Therefore, future studies should ensure that sampling covers the full length-range of fish in the population to better inform stock assessment. Despite strong evidence of sexual-dimorphism in yellowfin and bigeye tunas growth (Eveson et al., 2015), which can lead to elevated

sex-biased fishing mortality rates, this is not currently being considered in stock assessments due to a lack of the necessary data. Similarly, there is still not a consensus on spawning time and location of tropical tuna in the Indian Ocean, which is important to inform assumptions about total reproductive output. In order to move towards ecosystem-based fisheries management (EBFM), a better understanding of the habitat utilization and trophic relationships of the three tropical tuna in the Indian Ocean is also needed. Expanding the knowledge of vertical movements of these species would be useful to evaluate the species-specific and/or age class vulnerability to different fishing gears (e.g., purse-seine and longline) in the Indian Ocean and evaluate the impacts of FADs and potential utility of alternative management measures. Besides, a comprehensive approach that combines stomach content data, trophic markers (e.g., stable isotopes, mercury, lipid classes and fatty acids), and fish condition indices will allow delineation of trophic pathways for skipjack, yellowfin, and bigeye tunas from the Indian Ocean. This information will be essential in understanding the effect of human induced pressures, such as fishing, climate change or the impact of the deployment of FADs, on these species. For example, skipjack tuna have fast growth rates and reach sexual maturity the fastest among three tropical tuna species (Murua et al., 2017) and, hence, it is considered more resilient and less susceptible to overfishing than yellowfin and bigeye tunas. However, Worm and Tittensor (2011) reported that skipjack tuna has undergone distribution range reduction in the Indian Ocean, contrary to what occurred in the Pacific Ocean. Although is very difficult to establish the scale and ultimate cause of the observed range change in skipjack tuna, an understanding of habitat preferences, species interactions, climate change and variability and other factors can contribute to a better understanding of their population dynamics and resilience to fishing pressure.

Secondly, the current assumptions of single stocks for yellowfin, skipjack and bigeye tunas in the Indian Ocean, are based on the latest result of tag-recoveries from the RTTP-IO, which provide evidence of rapid and large-scale movements for these tuna species. However, tagging events do not represent the whole Indian Ocean. Moreover, the distances between tag release and recovery positions do not provide a full picture of the real movements of tagged tunas, which can, more effectively, be tracked by electronic tagging. Indeed, other methods should also be

considered for realistic stock structure determination. With the advent of NGS methods, a comprehensive study of these tropical tuna genetic structures using genome-wide highly informative SNP markers should be an important additional source of information to establish the underlying population structure. Natural markers, such as parasite tags or otolith microchemistry, can inform about the degree of connectivity over an ecological time scale (i.e., individual life span) and hence provide information on the environmental history experienced by individuals throughout different life stages. Therefore, they can contribute valuable insights of population structuring and highlight migration behaviours or population dynamics that might be sufficiently independent to guarantee spatially structured management. As each method provides information about stock structure at different spatial and/or temporal scales, the combination of different approaches has proved to be a powerful and reliable way to clarify unresolved questions related to stock structure (Izzo et al., 2017; Pita et al., 2016; Proctor et al., 2019; D. Welch et al., 2015) Thus, a holistic study that integrates results gained from several methods including different spatial and temporal scales, will be beneficial in defining appropriate units for the management of tropical tuna species in the Indian Ocean.

In summary, a broad-ranging collaborative program of research and data collection covering the complete distribution and life-history of the skipjack, yellowfin, and bigeye tunas in the Indian Ocean, should be carried out to improve stock assessment. These studies should be done together with the implementation of different and complementary stock delineation methods to establish the most realistic stock structure of the three tropical tuna species in the Indian Ocean, because species response to management decisions cannot be accurately predicted if the boundaries that characterise the stock are not correctly defined. Ultimately, an incorrect characterization of both life history parameters and stock structure perspectives may mislead the productivity and management of these globally important species. For example, if distinct stocks do exist, management measures based on the single stock assumption may lead to overexploitation and eventual collapse of less productive stocks. Therefore, an increased knowledge of these species' life-history characteristics and an accurate validation of stock structure of tropical tuna fisheries in the Indian Ocean will be essential to implement and enforce management strategies that ensure long-term sustainable fisheries.

“Be curious and make mistakes,

be patient and don’t give up”

Jane Goodall

CHAPTER 2

Otolith microchemistry as a tool to study stock structure of Indian Ocean yellowfin tuna

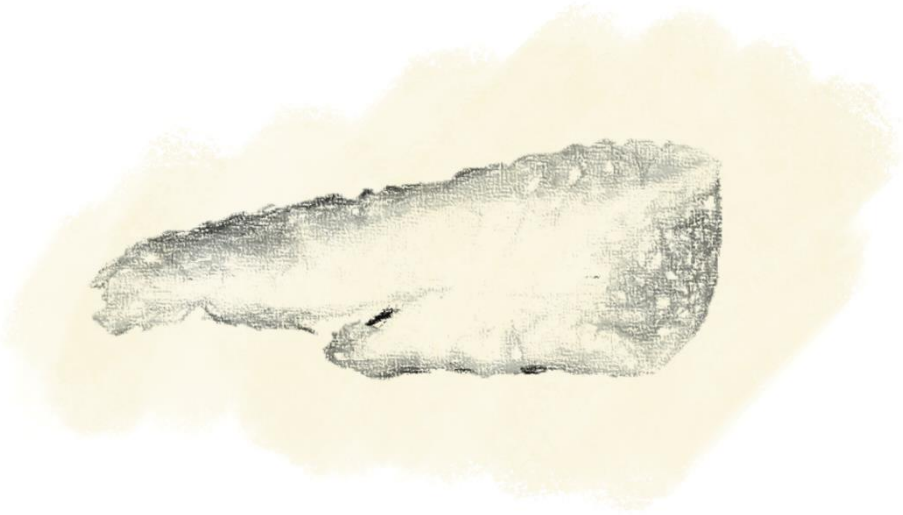

Abstract

A better understanding of the stock structure of yellowfin tuna (*Thunnus albacares*) in the Indian Ocean is needed to assure the sustainable management of the fishery. Carbon and oxygen stable isotopes ($\delta^{13}C$ and $\delta^{18}O$) and trace elements (^{138}Ba, ^{55}Mn, ^{25}Mg, and ^{88}Sr) were measured in otoliths of young-of-the-year (YOY) and age-1 yellowfin tuna collected from Mozambique Channel and northwest Indian Ocean regions. Elemental profiles showed variation in Ba, Mg and Mn in YOY otolith composition, but only Mn profiles differed between regions. Differences in YOY near-core chemistry were used for natal origin investigation. Ba, Mg and Mn were sufficiently different to discriminate individuals from the two regions, contrary to carbon and oxygen stable isotopes. A linear discriminant analysis resulted in 80% correct classification of yellowfin tuna to their natal origin. Classification success increased to 91% using a random forest algorithm. Finally, a unique larval source was detected among age-1 yellowfin tuna. The signal of these fish resembled to that of YOY from NW Indian Ocean origin, highlighting the importance of local production. The present study supports the use of otolith chemistry as a promising approach to analyse yellowfin stock structure in the Indian Ocean.

Published as:

Artetxe-Arrate, I., Fraile, I., Crook, A., Zudaire, I., Arrizabalaga, H., Greig, A., and Murua, H. (2019). Otolith microchemistry: a useful tool for investigating stock structure of yellowfin tuna (*Thunnus albacares*) in the Indian Ocean. *Marine and Freshwater Research*, 70(12), 1708-1721, doi: 10.1071/MF19067

1. Introduction

Stock identification is an essential component of modern fisheries management (Pita et al., 2016). Although several definitions of "stock" have been used in the fisheries literature, the stock concept essentially describes demographically discrete units of fish assumed to be homogeneous for particular management purposes (Begg et al., 1999). A fundamental requirement for sustainable fisheries management is the match between management action units and biologically relevant processes (Reiss et al., 2009). Different stocks may possess specific genetic, physiological and/or behavioral traits that can influence life processes such as growth rates, fecundity, abundance and disease resistance (Stepien, 1995) and, thus, different resilience to exploitation and/or environmental changes. As such, when stock structure is more complex than recognized, the sustainability of the resource and the profitability of the fishery can be jeopardized (Kerr et al., 2017; Taillebois et al., 2017).

Among the existing methods for fish stock structure assessment (e.g. genetic markers, tagging, life history parameters, parasites, etc.), otolith microchemistry has been recognized as a useful stock discriminant (Kerr and Campana, 2014; Tanner et al., 2016). These hard calcareous structures are found in the inner ear of vertebrates and are used for balance and hearing in teleost fish. Otoliths are acellular and metabolically inert (i.e. newly deposited material is neither reabsorbed nor reworked after deposition) and grow continually throughout the life of the fish (Campana and Neilson, 1985). Ambient water chemistry and environmental conditions influence elemental incorporation into the otolith (Elsdon and Gillanders, 2004; Walther and Thorrold, 2006) and variations in the concentrations of selected elements and isotopes (also known as "chemical fingerprints") can, therefore, be used as natural markers to discriminate among groups of fish for stock identification purposes (Kerr and Campana, 2014). However, factors that influence the elemental incorporation into otoliths are not yet completely understood as various factors other than ambient water chemistry, including dietary sources, physiological processes and genetic variation may also play important roles in elemental incorporation (Ranaldi and Gagnon, 2008; Clarke *et al.*, 2011; Sturrock *et al.*, 2015; Izzo *et al.,* 2018).

The potential of otolith chemistry to improve our understanding of population structure (e.g. Wells *et al.*, 2015), natal origin (e.g. Rooker *et al.*, 2003; Shiao *et al.*, 2010; Wells *et al.*, 2012) and movement patterns (e.g. Arai *et al.*, 2005; Macdonald *et al.*, 2013; Fraile *et al.*, 2016) of different tuna species has been demonstrated. However, few studies have used otolith microchemistry to assess the stock structure of yellowfin tuna, *Thunnus albacares* (Bonnaterre, 1788), and these studies are limited to the Pacific (Rooker et al., 2016; Wells et al., 2012) and Atlantic (Kitchens et al., 2018; Shuford et al., 2007) Oceans.

Yellowfin tuna, is a highly migratory species that inhabits the epipelagic zone of tropical and subtropical marine waters around the world (Froese and Pauly, 1999). It is a significant component of the global fishing industry and economy (Galland et al., 2016), and constitutes the second largest tuna fishery worldwide (FAO, 2016). The high levels of exploitation of yellowfin tuna render the species vulnerable to unsustainable harvest. In the Indian Ocean, in particular, increased harvest in recent years has led to overexploitation of the stock (ISSF, 2017). The most recent stock assessment model by the Indian Ocean Tuna Commission (IOTC), which takes into account both stock abundance and fishing mortality, confirmed that the yellowfin tuna stock in the IOTC area is overfished (IOTC, 2017d).

The current stock assessment model for yellowfin tuna in the Indian Ocean assumes a single stock (IOTC, 2017d). This assumption is based on the tag-recoveries from the Regional Tuna Tagging Program of the Indian Ocean (RTTP-IO), which showed large and rapid movements of the species around the Indian Ocean (Fonteneau and Hallier, 2015). However, uncertainties remain regarding the stock structure of yellowfin tuna in this region, as tag-recapture studies may not reveal important aspects of the movement dynamics of wide-ranging species (see Rooker *et al.*, 2008). Indeed, genetic studies using mtDNA suggest that a more complex stock structure may exist within yellowfin tuna populations. For example, genetically discrete groups of this species have been reported in the north Indian Ocean (Dammannagoda et al., 2008) and within Indian Ocean waters (Kunal et al., 2013).

In the present study, we analysed stable isotopes and trace elements in otoliths of young-of-the-year (YOY) and age-1 yellowfin tuna, which are both considered immature (Zudaire et al., 2013a). During the YOY period, it is assumed

that movements are restricted to a small area around their natal site, whereas for age-1 individuals large-scale movements can be expected (Fonteneau and Hallier, 2015). Fish were collected in two regions of the western Indian Ocean, the northwest (NW) Indian Ocean and Mozambique Channel, as major yellowfin tuna spawning grounds have been identified westward of 75°E (Zudaire et al., 2013a). In particular, the equatorial area (0-10°S) and Mozambique Channel have been identified as primary and secondary spawning areas (IOTC, 2017c; Reglero et al., 2014). The western region accounted for the 80% of the Indian Ocean catches in 2017 (IOTC, 2018a), being the most important area for the Indian Ocean yellowfin tuna fishery. Our aim was to assess the feasibility of otolith microchemistry as a potential tool for investigating yellowfin tuna stock structure in the Indian Ocean. Specifically, our objectives were to: (i) explore otolith chemistry profiles of YOY yellowfin tuna, (ii) seek the best methodology for fish origin analyses and test region-specific differences on chemical composition of YOY yellowfin tuna otoliths, (iii) evaluate the usefulness of different classification methods in assigning YOY yellowfin tuna origin to their respective collection regions, and (iv) investigate potential natal origin differences in age-1 yellowfin tuna.

2. Material and methods

2.1 Study area

Samples were collected across two regions of the western Indian Ocean: (1) offshore western Madagascar (15°53′S-13°30′S, 43°33′E-47°05′E), hereafter "Mozambique Channel" and (2) offshore Somalia and Seychelles regions (7°77′S-7°22′N, 48°57′E-58°37′E), hereafter "NW Indian Ocean" (**Figure 2.1**). These two regions belong to two distinct provinces according to the Longhurst biogeographical classification of the pelagic ecosystem (Longhurst, 2007): Mozambique Channel belongs to the East African Coastal Province (EAFR) and NW Indian Ocean is part of the Indian Monsoonal Gyre Province (MONS). These two regions are defined by different oceanographic characteristics that affect the biological production of the area (for further information see Appendix A, Figures A1-A5). North of 10°S the Indian Ocean is characterized by two seasons with distinct wind regimes driving the ocean climate and circulation; the Monsoon system (Schott and McCreary, 2001).

The southwest (summer) monsoon drives upwelling events that lead to high primary productivity off the coast of Somalia. In contrast, during the northeast (winter) monsoon, conditions are not favourable for upwelling and primary productivity is generally lower (Wiggert et al., 2006). The Mozambique Channel is characterized by the presence of anticyclonic eddies that generate an upward movement of nutrient rich waters around their edge, and advection of nutrient rich coastal waters when they run along the coast (Quartly and Srokosz, 2004; Tew Kai and Marsac, 2010).

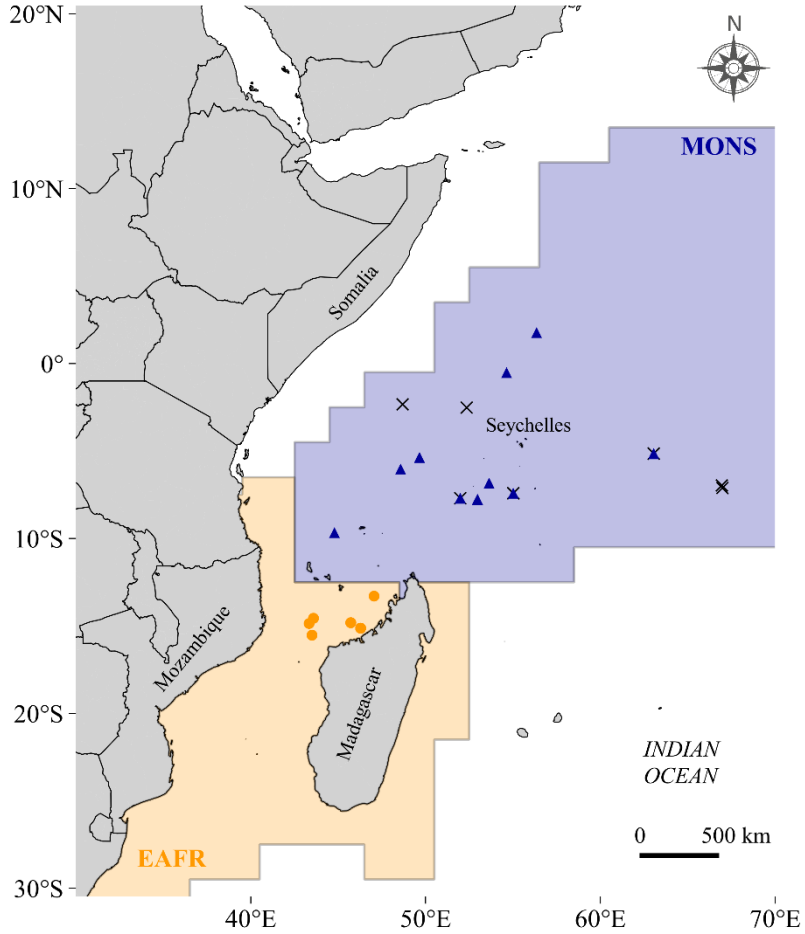

Figure 2.1. Study area in the western Indian Ocean, where two Longhurst provinces, the Eastern Africa Coastal Province (EAFR) and the Indian Monsoon Gyres Province (MONS) are represented. Sampling locations of the different groups of yellowfin tuna (*Thunnus albacares*) used in this study are indicated as circles in the Mozambique Channel and triangles in the north-west Indian Ocean for young-of-the-year, and as crosses for age-1 fish of unknown origin.

2.2 Fish sampling

Yellowfin tuna (n=106) were collected in the western Indian Ocean by scientific observers on board Spanish commercial purse seiners between February 2009 and July 2010. Fish were measured (fork length - FL- to the nearest cm) and weighed (to the nearest 0.1 kg) on board. Sagittal otoliths were extracted, cleaned of adhering organic tissue, rinsed with ultrapure water and stored dry in plastic vials. The otolith collection available for this study was comprised of fish from different collection dates, age-classes and cohorts. Following the growth curve described by Sardenne *et al.*, (2015), fish were classified as YOY(<43 cm FL) or age-1 (43-75 cm FL). Birth year was then back-calculated from the catch date using the age-length relation of Sardenne *et al.*, (2015). In order to reduce potential variability due to temporal variation among samples, only fish born in the same monsoonal regime (i.e. summer monsoon) were selected for analysis. In addition, to minimize the possibility that YOY tuna had migrated outside of their origin areas prior to sampling, only fish smaller than 40 cm were considered in the study. To date, no tagging experiments have considered fish of that size in movement range studies of yellowfin tuna (see Hallier and Fonteneau, 2015). Nevertheless, our threshold size is even more conservative than those already considered in Atlantic Ocean yellowfin tuna stock structure analyses (Kitchens et al., 2018; Pecoraro et al., 2018). Thus, the final dataset consisted of 52 YOY and 15 age-1 fish (**Table 2.1**).

Table 2.1. Summary of young-of-the-year (YOY) and age-1 yellowfin tuna (Thunnus albacares) used for otolith chemistry analyses from two regions of the western Indian Ocean: the Mozambique Channel and the north-west (NW) Indian Ocean. Size is fork length (FL). The cohort was calculated by back-calculation after age estimation following the growth curve described by Sardenne et al. (2015).

Analytical method	Capture location	FL range (cm)	Age group	Collection dates	Cohort	Number of fish collected
Trace elements	Mozambique Channel	31–39	YOY	February–April 2010	2009	14
	NW Indian Ocean	29–35	YOY	February 2009	2008	27
	NW Indian Ocean	52–64	Age-1	February–July 2009	2007	15
Stable isotopes	Mozambique Channel	31–40	YOY	April–May 2010	2009	20
	NW Indian Ocean	29–39	YOY	February–May 2009	2008	32

2.3 Otolith chemistry analysis

Whole otoliths were briefly soaked in nitric acid (1%) and cleaned with ultrapure (Milli-Q) water, to eliminate any remaining biological material (Rooker et al., 2001). Left and right otoliths were embedded in two-part resin (EpoFix; Struers, Ballerup, Denmark) and sectioned using a Buehler low-speed Isomet saw (Buehler Ltd, Lake Bluff, IL, USA) fitted with a diamond-edged blade to obtain a transverse section that included the core. When both otoliths from the same fish were available, one otolith was randomly selected for stable carbon and oxygen isotope analysis and the other was used for trace element analysis. When only one otolith was available, stable isotope analyses were carried out.

Transverse sections were polished with a series of grinding and polishing films moistened with ultrapure water, and then with a micro cloth and 0.3 mm alumina powder to ensure a smooth surface. Sections were glued in a sample plate using Crystalbond™ thermoplastic glue (Crystalbond™ 509, Buehler Ltd, Lake Bluff, IL, USA). For YOY, 41 otoliths were used for trace element chemistry and 52 for stable isotope analyses (**Table 2.1**). For age-1 fish, trace element composition of 15 yellowfin tuna was analysed (**Table 2.1**).

Trace element analysis. Trace element analysis was performed using an Agilent 7700X quadrupole inductively coupled plasma mass spectrometer (ICP-MS) coupled to a Resonetics laser ablation system (LA) with a Laurin Technic 2 volume cell (School of Earth Sciences, University of Melbourne, Australia). The laser was operated using a spot size of 26 μm diameter with laser energy at 2.4 J/cm^2 and a repetition rate of 10 Hz. Otoliths were placed in the sealed chamber and ablated continuously across the growth axis from the primordium to proximal edge at a scan speed of 6 μm/s (**Figure 2.2A**). Ablation occurred in an atmosphere of pure He to minimize condensation of ablated material. The ablated material was transported to the ICP-MS mixed with argon carrier gas. A pre-ablation step was implemented to minimize potential surface contamination. NIST 612 (National Institute of Standards and Technology) glass standard with known chemical composition was used for calibration. Standards were analysed twice at the beginning and at the end of each session, and once after 1/3rd and 2/3rds of the duration of the run. In addition, measurement precision was determined based on the analyses of NIST610

and MACS-3 carbonate standard (United States Geological Survey, Reston, VA, USA; (Limburg et al., 2011; Wolf and Wilson, 2007). The variation in ablation yields between standards and unknown samples was corrected with the use of calcium as an internal standard (Craig et al., 2000). Relative abundances of 10 isotopes (^{7}Li, ^{25}Mg, ^{55}Mn, ^{57}Fe, ^{59}Co, ^{60}Ni, ^{63}Cu, ^{66}Zn, ^{88}Sr and ^{138}Ba) were measured along the whole transect using the LA-ICPMS system, and elemental concentrations (ppm) were then calculated. Data reduction and processing were performed with the software package Iolite version 2.2 (School of Earth Sciences, University of Melbourne, Australia), which operates within IGOR Pro version 6.2 (WaveMetrics, Inc., Lake Oswego, OR, USA, Paton et al., 2011; Paul et al., 2012). Minimum Detection Limits (LOD) were calculated based on the ablation yield equivalent to three times the standard deviation of the blank signal. Averaged LOD values (ppm) of each element across all samples were as follows: Li, 0.049; Mg, 0.423; Mn, 0.079; Fe 0.920; Co, 0.020; Ni, 0.030; Cu, 0.023; Zn, 0.120; Sr, 0.0145; and Ba, 0.004. Five elements (Ba, Mg, Mn, Fe and Sr) were consistently present at concentrations above minimum detections limits within the whole transects. However, low measurement precision and accuracy was reported for Fe in MACS3 and NIST610 (Appendix A, Table A1), due to time-dependant increases in apparent concentrations. This is likely due to decreasing oxide/hydroxide interferences (eg. ^{40}Ca-^{16}O-H) with time affecting the low Fe/Ca NIST612 calibration standard proportionally more than the higher Fe/Ca NIST610 and MACS3 standards. Thus, Fe was discarded for analyses. Additionally, an ablation transect was performed on a test sample composed only of resin and thermoplastic glue. This analysis showed that resin was enriched in Zn whereas high levels of Cu were found on the thermoplastic glue. Therefore, unusually high concentrations of Cu and Zn throughout the transect were used as indicators of potential sample contamination. Aragonitic calcium carbonate stoichiometry (400 000 mg Ca g^{-1} otolith) was used for calcium concentration calculation, and hereafter the concentrations of the rest of the elements are expressed as element:Ca ratios (Ludsin et al., 2006).

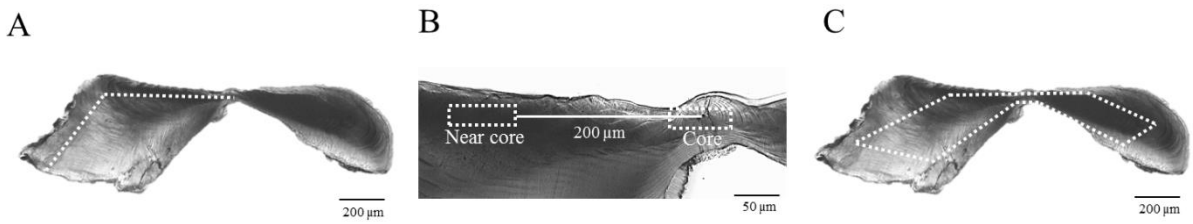

Figure 2.2. Transverse section of a young-of-the-year yellowfin tuna (*Thunnus albacares*) sagittal otolith showing (*A*) the transect of the laser ablation spots performed along the growth axis, (*B*) the position of the data slices represented as the core and near-core and (*C*) pattern of the portion milled for stable isotope analysis.

In addition to whole transects, two data slices of 78 µm in length were isolated from the primordium (hereafter "core") and 200 µm beyond the primordium (hereafter "near-core"), by averaging all trace element concentration estimates across each data slice (**Figure 2.2B**). Daily increment formations were counted along the first 550 µm of the transect in a sub-set of YOY otoliths (n=8) under a light microscope (Appendix A, Figure A6). It was determined that the 78 µm slices represent the otolith material accreted during the first ~10 days and the first ~2-3 weeks post-hatch respectively, when the fish are still in larval phase (Kaji et al., 1999).

Stable isotope analysis. Microsampling of otolith powder for carbon ($\delta^{13}C$) and oxygen ($\delta^{18}O$) stable isotope analysis was performed using a high resolution computerized micromill (New Wave MicroMill System) only in YOY yellowfin tuna. The portion of the smallest fish (29 cm FL) in our sample was used to create a standard template that was then used with the remaining otoliths (**Figure 2.2C**), to ensure that the same portion of the otolith was analysed in each individual. This is approximately related to the first 5-6 months of life according to the age-length relationship described by Sardenne *et al.*, (2015).

Fourteen drill passes were run at 50 µm depth per pass over a pre-programmed drill path using a 200 µm diameter carbide bit (Komet dentral, Gebr. Basseler, GMbH & Co, KG). Powdered material was then analysed for $\delta^{13}C$ and $\delta^{18}O$ on an automated carbonate preparation device (KIEL-III) coupled to a gas-ratio mass spectrometer (Finnigan MAT 252) from the Environmental Isotope Laboratory of the University of Arizona. All isotope values were reported according

to standards of the International Atomic Energy Agency in Vienna. $\delta^{13}C$ and $\delta^{18}O$ represent the ratio between the $^{13/12}$ C and $^{18/16}$O in the sample, relative to the Pee Dee Belemnite (PDB) scale.

2.4 Statistical analysis

All statistical analyses were performed using open access R software (R Core Team, 2019). Prior to all multivariate analyses, trace element data were scaled to give the same weight to all elements. We used an alpha level of .05 for all statistical tests.

Elemental profile analysis. Whole transects of YOY yellowfin tuna were transformed into equally spaced observations, generating a regular time series of elemental concentration from 0 to approximately 550 μm (i.e. ~first month post-hatch). Data transformation and ordination were performed using *zoo* (Zeileis and Grothendieck, 2005) and *vegan* (Oksanen et al., 2017) packages. To examine leading patterns and temporal variations for the elements, regular time series data were simplified by averaging concentrations every 25 μm. Estimates of standard deviation (sd) were also calculated. Mean estimates of concentrations and profiles of element:Ca ratios were obtained for each region. In addition, a principal component analysis (PCA) was applied to each element in the time series data. To determine whether differences existed between regions, a permutational multivariate analysis of variance (PERMANOVA) test on the scores of the first two axes was performed.

Natal origin microchemistry of YOY. Young of the year yellowfin tuna were used to determine whether the fish collected at Mozambique Channel and NW Indian Ocean origin could be differentiated based on otolith stable isotope and trace element concentrations measured in the otolith core and near-core. Normality and homoscedasticity were tested using Shapiro-Wilks and Fligner-Killeen tests respectively. Stable isotope data did meet these assumptions, so a Student´s t-test was used for inter-region comparisons. Trace element data violated parametric assumptions, consequently a robust statistical method was used for their study; bootstrapped yuen t-test (trimmed level for the mean = 0.2, number of bootstrap samples=599). Robust statistics are not unduly affected by outliers and violations of

parametric assumptions, reducing the probability of making a Type-I error and improving test power when data are not normal or homogeneous (Daszykowski et al., 2007; Erceg-Hurn and Mirosevich, 2008; Wilcox, 2012). Accordingly, Hotelling T^2 test was used to test for differences in $\delta^{13}C$ and $\delta^{18}O$ values among regions and PERMANOVA for differences in element:Ca ratios. Finally, core and near-core trace element data were examined using non-metric multidimensional scaling (NMDS) to obtain a reduced two-dimension graphical representation of the relationships between samples (Hout et al., 2013). The dissimilarity matrix construction was based on Euclidean distances. The otolith portion showing greatest variation among regions was used as the origin indicator in subsequent analyses.

Comparison of classification methods. Discrimination capacity between fish collected in these two regions was assessed using YOY otolith near-core microchemistry data using different classification methods. Four different methodologies were applied: 2 classical methods (Linear Discriminant Analysis -LDA- and Quadratic Discriminant Analysis -QDA-) and 2 data-mining methods (Random Forest -RF- and Artificial Neural Network -ANN-). LDA and QDA were completed using *lda* and *qda* functions from the MASS library. RF was implemented using *randomForest* function from the *randomForest* library, using default settings (Liaw and Wiener, 2002). ANN was performed using *nnet* function from *nnet* library, using default settings and 30 hidden neurons at the intermediate layer (Venables and Ripley, 2002). A detailed description of each technique and their assumptions can be found in Jones *et al.,* (2017) and Mercier *et al.,* (2011). In all cases, data were randomly split into a training data set (75%) and a testing data set (25%) to perform a cross-validation procedure and measure prediction quality. To avoid sampling effects, the training subset was resampled 10 times and mean prediction accuracy (i.e. percentage of correct assignment of the fish to their known region) was obtained. Additionally, kappa index was also calculated as a measure of classification success. Kappa values are always less than or equal to 1, the last implying perfect agreement. Kappa index is unbiased when the number of samples differ between groups, and can present more reliable results, as it considers the possibility of the agreement occurring by chance (Fielding and Bell, 1997; Jones et al., 2017). Following Mercier *et al.*, (2011) the elemental combination maximising habitat discrimination was selected by performing a stepwise forward variable

selection procedure using the Wilk´s lambda criterion for LDA and QDA. In the case of RF, the best elemental combination was obtained by stepwise procedure using Gini Index (Cutler et al., 2007), and in the case of ANN, following Olden *et al.,* 2004.

Natal sources of age-1 fish. Random Forest clustering analysis of the near-core trace element data was performed in age-1 fish to determine the number of larval sources contributing to the sample. This approach proved to be useful for natal origin related investigations when there is no previous baseline of potential larval sources (Gibb et al., 2017; Régnier et al., 2017; Wright et al., 2018). Moreover, the RF clustering approach does not require continuous multivariate data with normal distribution (Shi and Horvath, 2006), an assumption which is often violated when working with otolith microchemistry data. The Random Forest classification process was applied following Shi and Horvath, (2006). First, a synthetic dataset was created by random sampling from the product of empirical marginal distributions of the elements. Then, unsupervised RF was used to separate the synthetic data (used as a class factor) from the observed data, and a dissimilarity matrix was created. Secondly, the dissimilarity matrix was used as input for partitioning around the medoid (PAM) clustering. Finally, the appropriate number of clusters was determined using the gap statistic (Tibshirani et al., 2001), with the *fviz_nbclust* function from the *factoextra* library (bootstrap number=100). Canonical variable coefficients of YOY and age-1 yellowfin tuna trace element composition were plotted to visualize relationships (Hamer et al., 2005).

3. Results

3.1 Elemental profile analysis

Patterns of element:Ca variation in YOY along the analysed transect were very similar between the two regions, except for Mn:Ca (**Figure 2.3 and Figure 2.4**). Ba:Ca concentrations declined with increasing time post-hatch, with NW Indian Ocean presenting higher mean Ba values than Mozambique Channel along most of the transect. As of the 3rd week post hatch, the decreasing trend smoothed and became more similar between regions (**Figure 2.3A**). Mg:Ca concentrations of both regions declined almost linearly within the first month of life. However, Mozambique Channel showed higher mean concentrations than NW Indian Ocean

along the whole transect (**Figure 2.3B**). Mean Mn:Ca concentrations showed different trends between regions. For Mozambique Channel, they were relatively constant during the first month post-hatch However, for NW Indian Ocean YOY Mn:Ca increased sharply in the first ~2.5 weeks post-hatch, with a progressive decrease thereafter (**Figure 2.3C**). Sr:Ca showed little variation both among regions and along the transect, although slightly decreasing trends of concentrations were observed (**Figure 2.3D**).

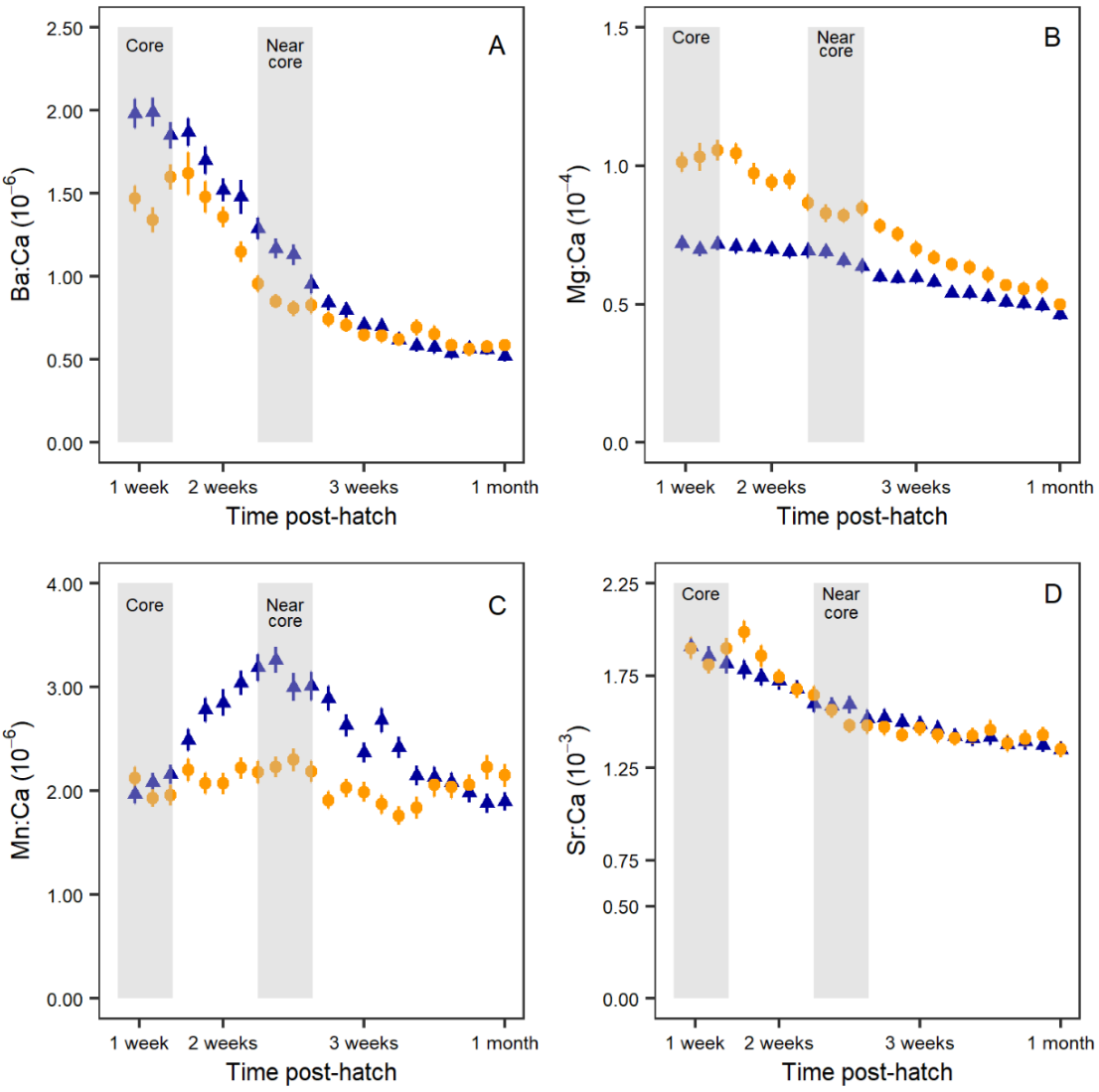

Figure 2. 3. Mean (s.d.) element : Ca concentrations across the first month of life of young-of-the-year yellowfin tuna (*Thunnus albacares*) collected in the Mozambique Channel (circles) and north-west Indian Ocean (triangles). Shaded areas represent the signatures that will correspond to the core and near-core portions of the otolith.

The PCA showed that all element:Ca time series were related among regions with the exception of Mn:Ca (**Figure 2.4**). For this element, the scores of the first

two axes of the PCA varied significantly between fish from the two regions (PERMANOVA, F(1,39)=14.96, p=0.01). The first two axes explained 39% of the total variation.

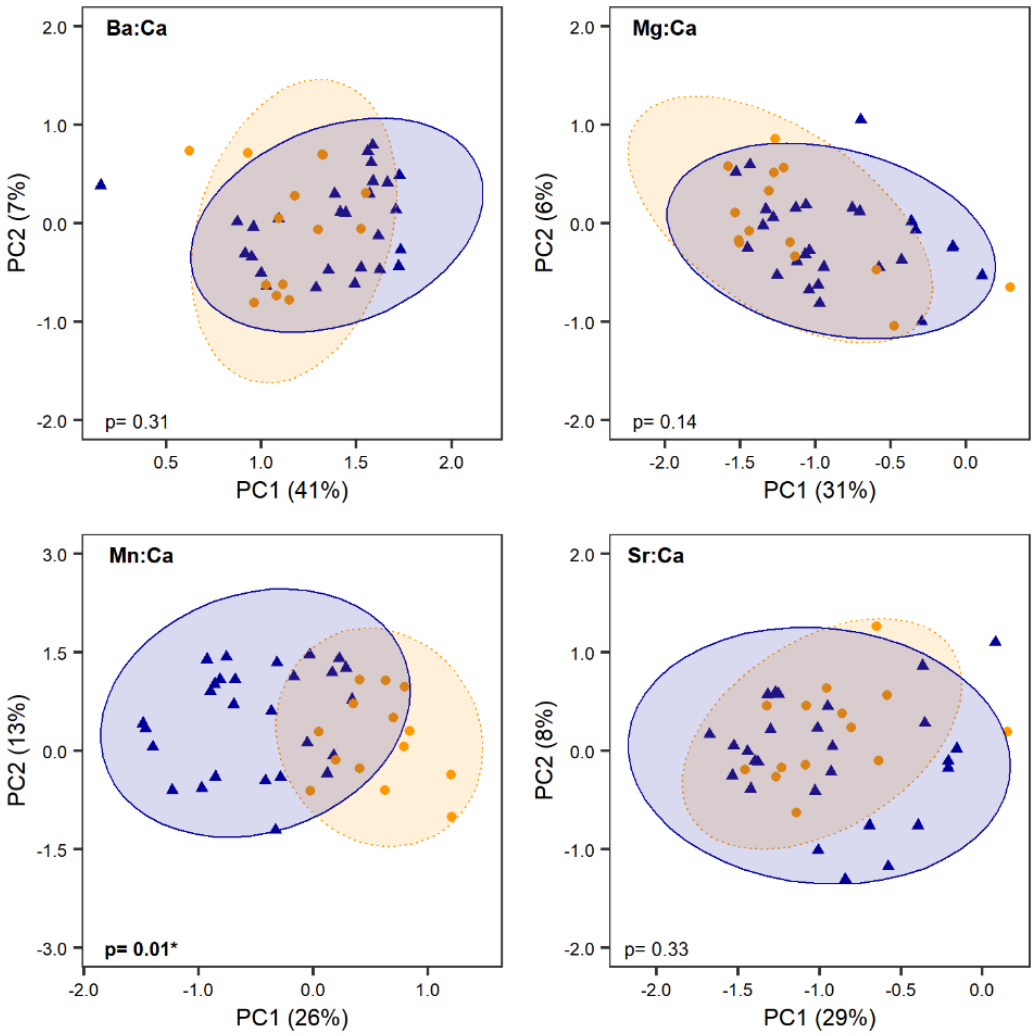

Figure 2.4. Principal component (PC) analysis correlation biplot on element : Ca time series data of the first month of life in young-of-the-year yellowfin tuna (*Thunnus albacares*) collected in the Mozambique Channel (circles) and north-west Indian Ocean (triangles). Ellipses represent the 95% confidence intervals for each region (dotted ellipse, Mozambique Channel; solid ellipse, north-west Indian Ocean). *P*-values are for differences in PC1 and PC2 scores according to permutational multivariate analysis of variance (PERMANOVA).

3.2 Natal origin microchemistry of YOY

Significant differences in multi-elemental trace signatures (i.e. Ba:Ca, Mg:Ca, Mn:Ca and Sr:Ca) were found between Mozambique Channel and NW Indian Ocean in the near-core portion of the otolith (PERMANOVA, F(1,39)=4.09, p=0.010) but not in the core (PERMANOVA, F(1,39)=2.32, p=0.050). Similarly, differences in trace element composition were more marked in the two-dimension NMDS plot of the otolith near-core than in the core (**Figure 2.5**).

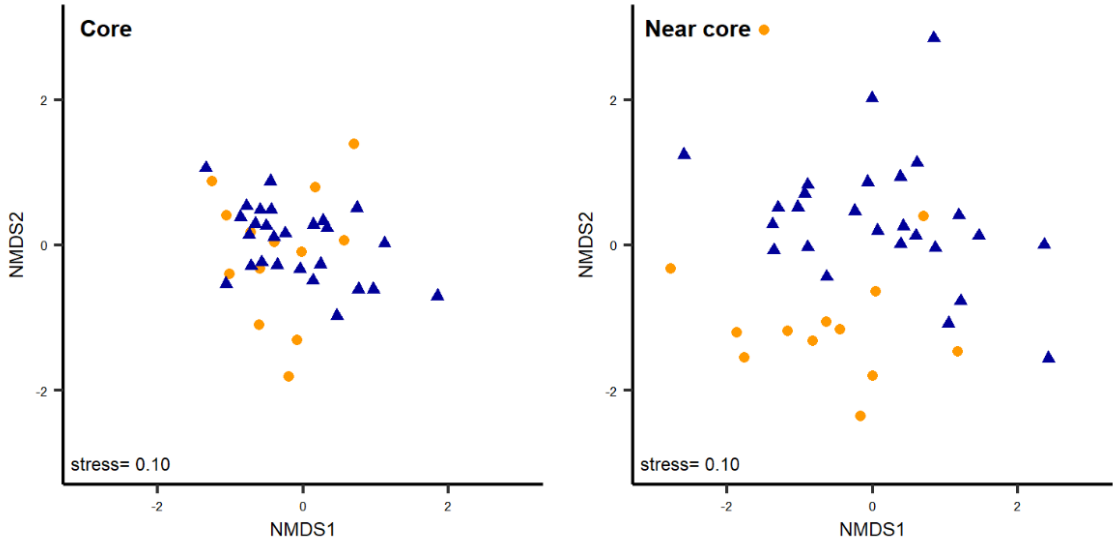

Figure 2.5. Non-metric multidimensional scaling (nMDS) of young-of-the-year yellowfin tuna (*Thunnus albacares*) otolith core and near-core trace elements (Ba : Ca, Mg : Ca, Mn : Ca and Sr : Ca). Each point represents an individual fish belonging to the Mozambique Channel (circles) and north-west Indian Ocean (triangles) regions.

Indeed, only Mg:Ca ratios were significantly different in the otolith core (yuen test, Y(11.36)=2.22, p=0.046), with Mozambique Channel showing higher values than NW Indian Ocean (**Figure 2.6B**). Mozambique Channel also had higher Mg concentrations than NW Indian Ocean in the near-core portion (**Figure 2.6B;** yuen test, Y(12.06)=4.05, p=0.001). Ba and Mn also varied significantly in the otolith near-core among regions (yuen test, Y(24.89)=2.11, p=0.045 and Y(16.60)=2.36, p=0.030 respectively), but in this case NW Indian Ocean had higher values of both elements **(Figure2.6A and Figure 2.6C**). There were no significant variations in Sr concentrations between regions in near-core signatures (**Figure 2.6D**, Y(16.08)=1.18, p=0.256).

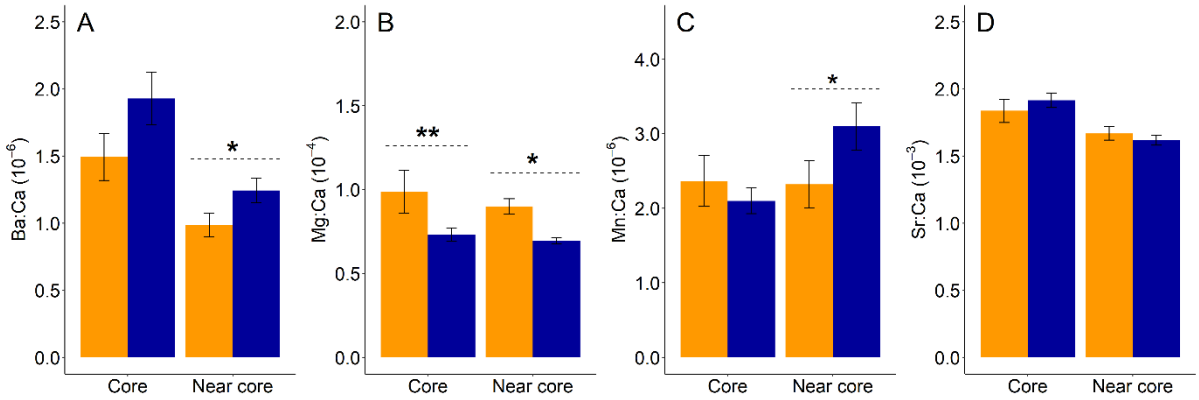

Figure 2.6. Mean (s.d.) element : Ca ratios in otolith cores and near-cores ofyoung-of-the-year yellowfin tuna (*Thunnus albacares*) collected at two different regions, Mozambique Channel (left bars) and NW Indian Ocean (right bars). Asterisks indicate the significance of differences among regions according to bootstrapped Yuen *t*-tests (*, *P* , 0.05; **, *P* , 0.01).

Stable isotope composition of YOY yellowfin tuna did not vary between fish collected in Mozambique Channel and the NW Indian Ocean (**Figure 2.7**; Hotelling T-square test, T(2,41)=0.76, p=0.474). Mean otolith $\delta^{13}C$ values were -10.27±0.43 ‰ and -10.13±0.35 ‰ for Mozambique Channel and NW Indian Ocean, respectively (student t-test, t(26.84)=-1.15, p=0.259). Mean otolith $\delta^{18}O$ value for fish collected in Mozambique Channel was -2.32±0.14 ‰, whereas for fish collected in NW Indian Ocean it was -2.29±0.23 ‰ (student t-test, t(41,72)=-0.53, p=0.600).

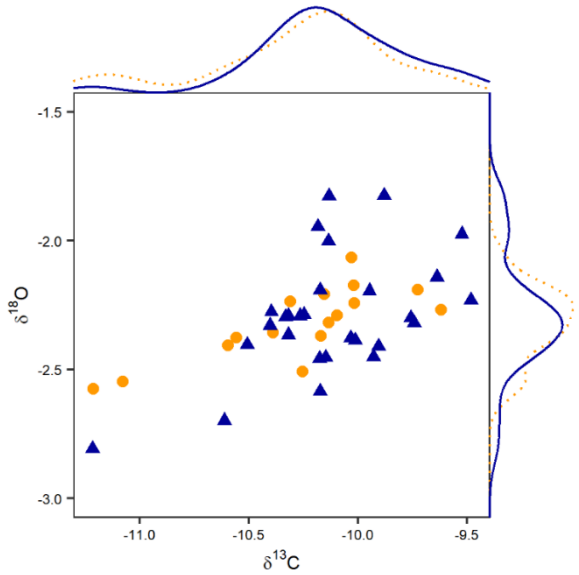

Figure 2.7. Scatter plot of otolith $\delta^{13}C$ and $\delta^{18}O$ of young-of-the-year yellow- fin tuna (*Thunnus albacares*) captured in the Mozambique Channel (circles) and north-west Indian Ocean (triangles) regions. Marginal distribution curves $\delta^{13}C$ and $\delta^{18}O$ are also presented for the Mozambique Channel (dotted lines) and north-west Indian Ocean (solid lines).

3.3 Comparison of classification methods

Cross-validated classification success based on YOY yellowfin tuna near-core trace element data ranged from 80 to 91% depending on the statistical method selected. However, results were more conservative according to kappa index (k=0.53-0.72). LDA had the lowest differentiation capacity (**Table 2.2**). QDA and ANN showed similar results, with ANN presenting slightly higher accuracy and kappa value than QDA (**Table 2.2**). RF outperformed the other methods and produced the highest classification success (91%, k=0.72). Regardless of the method used for prediction, the best elemental combination always included Mg:Ca and Mn:Ca.

Table 2.2. Comparison of classification methods for assigning young-of-the-year (YOY) yellowfin tuna (*Thunnus albacares*) collected in the Mozambique Channel and north-west (NW) Indian Ocean to their origin location based on near-core otolith microchemistry. Best elemental combination and performance, as a measure of maximal accuracy and the kappa index, are shown for each method. LDA, linear discriminant analysis; QDA, quadratic discriminant analysis; ANN, artificial neural network; RF, random forest

Classification method	Element combination	Maximal accuracy (%)	Kappa index
LDA	Mg, Mn	80	0.53
QDA	Mg, Mn	81	0.60
RF	Ba, Mg, Mn, Sr	91	0.72
ANN	Ba, Mg, Mn, Sr	83	0.63

3.4 Natal sources of age-1 fish

RF clustering of age-1 fish from unknown origin suggested a common larval source among the analysed samples. The canonical variate plot displaying spatial differences of the multi-elemental data showed that age-1 yellowfin near-core elemental composition was more similar to YOY of NW Indian Ocean than to YOY of Mozambique Channel, although there was considerable overlap among the regions (**Figure 2.8**).

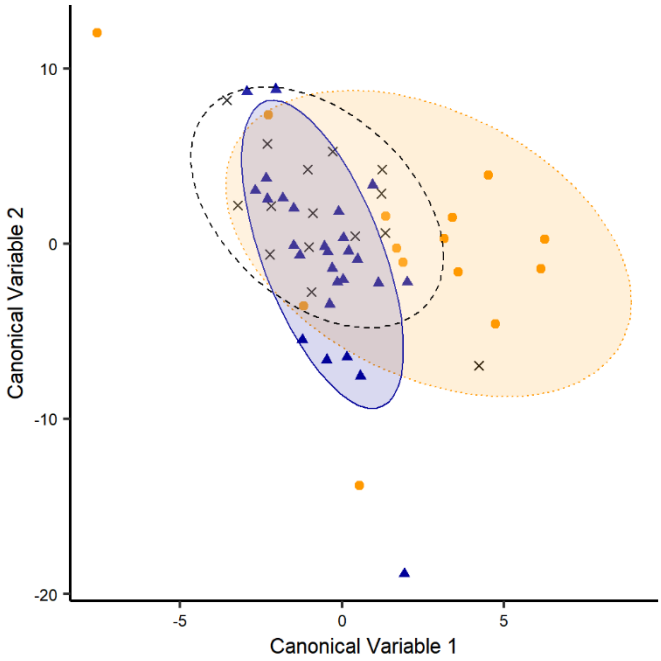

Figure 2.8. Canonical variable plots comparing trace element tags (Ba : Ca, Mg : Ca, Mn : Ca and Sr : Ca) of age-1 yellowfin tuna (Thunnus albacares) from unknown origin (crosses) with those of young-of-the-year (YOY) yellowfin tuna captured in the Mozambique Channel (circles) and north- west Indian Ocean (triangles) regions. Confidence ellipses cover the 95% of each group (dashed ellipse, age-1 tuna; dotted ellipse, Mozambique Channel YOY; solid ellipse, north-west Indian Ocean YOY).

4. Discussion

Improving the understanding of stock structure of exploited species is essential for defining appropriate management units and optimising the use of fishery resources. In this context, this study used for the first time an otolith microchemistry approach for yellowfin tuna in the Indian Ocean, revealing the potential of this technique to provide valuable information about its stock structure.

The main limitation of the study was that the YOY yellowfin tuna collected in the two regions were sampled from different cohorts. Therefore, observed differences between regions could result from the interannual variability in the oceanic system rather than variability among regions. However, this hypothesis seems unlikely, as interannual variability in environmental conditions was negligible for the observed periods (Appendix A, Table A2).

4.1 Elemental profile analysis

Almost all elements followed a similar pattern of variation within the first month post-hatch in both regions. Element profile analyses of natural otolith tags can be used for environmental and life history reconstructions (Elsdon et al., 2008). For example, Ba and Sr incorporation into otoliths has been shown to be correlated with ambient concentrations (Izzo et al., 2018; Webb et al., 2012). These alkaline metals are incorporated into the mineral component of the otolith (Izzo et al., 2016; Loewen et al., 2016), and thus appear to be reliable "geographic markers" (Thomas et al., 2017). Although both elements have been related to salinity (e.g. Elsdon and Gillanders, 2005; McDonald and Crook, 2010), the fact that Ba:Ca varied along the transect whereas Sr:Ca not, might suggests that observed Ba variation did not reflect changes in salinity. Indeed, no noticeable seasonal variation of sea surface salinity (SSS) was detected in the western Indian Ocean (Appendix A, Figure A1). Elevated Ba:Ca concentrations in the primordium relative to adjacent parts of the otolith have been previously described in literature (Ruttenberg et al., 2005). However, this does not exclude other external influences of Ba incorporation. For example, as dissolved Ba in seawater possesses a nutrient-like profile (i.e. very low concentration in surface and increased values with deeper water), an increase in Ba:Ca concentration might reflect periods of residence near upwelling zones (Kingsford et al., 2009; Patterson et al., 2004; Wang et al., 2009). During the summer monsoon (period when YOY were born) elevated phytoplankton blooms have been described to extend off the Somalian coast (Appendix A, Figure A2) (Wiggert et al., 2006), which could also be the reason for increased Ba concentration. Equally, throughout the Mozambique Channel classic eddy upwelling occurs, enhancing Chl-a concentrations in the centre of the cyclones (Lamont et al., 2014). Magnesium concentrations decreased linearly with time post-hatch. This pattern matches with

previously described Mg:Ca profiles in literature, with higher levels at early life (near otolith primordium) followed by a transition to lower levels of Mg (Limburg et al., 2018). Uptake rate of Mg into otoliths has been related to somatic growth and otolith precipitation (Limburg and Casini, 2018; Martin and Thorrold, 2005). The incorporation of this element into otoliths seems to be strongly regulated by physiological processes between the otolith and water (Hamer and Jenkins, 2007). Therefore, the concentration of Mg in fish otoliths has been questioned as a reliable environmental indicator (Thomas et al., 2017; Woodcock et al., 2012). Mn:Ca profiles proved to be significantly different between the NW Indian Ocean and Mozambique Channel YOY yellowfin tuna. Manganese is a transitio metal, and as such its incorporation into the otolith can be physiologically regulated, which may caution against its use as an environmental marker (Thomas et al., 2017). Manganese concentrations have also been found to be high near the otolith primordium possibly due to maternal transfer (Ruttenberg et al., 2005). However, no higher Mn concentrations in the first weeks of life were observed for YOY from Mozambique Channel relative to the rest of the transect. Although sensitive to growth effects, environmental influences seem also to affect otolith Mn concentrations (Limburg and Casini, 2018). In particular, otolith Mn:Ca concentrations have been shown to be reliable proxy for fish exposure to hypoxia (Limburg et al., 2011, 2015). During the summer monsoon, dissolved oxygen concentration is lower in NW Indian Ocean compared to the Mozambique Channel (Appendix A, Figure A3). Thermal vents, sediments, rivers and atmospheric dust are also known sources of manganese in seawater (van Hulten et al., 2017). The influence of aeolian deposition of Mn is greater in NW Indian Ocean due to its proximity to the arid Arabian subcontinent (van Hulten et al., 2017). Therefore, changes in wind patterns might be another plausible cause of observed differences in Mn:Ca profiles of the two regions. Life-history otolith chemistry profiles would be valuable for resolving stock structure of the species (e.g. Fowler *et al.*, 2017), but there is still a large need for further empirical studies regarding elemental incorporation processes into otoliths for a comprehensive interpretation of the results.

4.2 Natal origin microchemistry of YOY

The otolith near-core portion showed greater variability in trace elements among the two regions than did the core. Higher levels of Zn and Cu were found in core portions in comparison with the near-core (Appendix A, Figure A7). It is possible that some thermoplastic glue and/or resin residues had entered the pits and crevices occasioned in the primordium of some samples due to polishing (Di Franco et al., 2014). It is also possible that the chemical signature of this zone, which is formed during egg development, could have been affected by maternal inheritance (e.g. Campbell *et al.*, 2002; Ruttenberg *et al.*, 2005; Thorrold *et al.*, 2006). Therefore, this signature can be influenced by the environment that is experienced by the maturing female (Volk et al., 2000), hindering its use as an indicator of fish origin. Given these circumstances, trace element signatures from the primordium may not be appropriate for determining YOY yellowfin tuna origin, and the use of otolith material from a few weeks post-hatch could represent a better alternative for early life history comparisons (see also Macdonald *et al.*, 2008).

Region-specific chemical signatures were detected in the otolith near-core composition, with three elements (Ba, Mg and Mn) showing regional differences in otolith near-core chemistry of YOY yellowfin tuna. As stated above, in the NW Indian Ocean, upwelling events occurring during the south-west (summer) monsoon generate an upward movement of nutrient-rich waters from below the thermocline to shallower depths, which possibly implies the observed higher Ba:Ca concentrations in otolith near-core in comparison with YOY from Mozambique Channel. YOY from NW Indian Ocean also presented higher concentrations of Mn:Ca in otolith near-core when compared to Mozambique Channel, possibly due to their proximity to an arid region or/and oxygen minimum zone (McCreary et al., 2013). Differences in Mg:Ca ratios in otoliths of fish from Mozambique Channel and NW Indian Ocean might also reflect physiological differences rather than environmental differences (Woodcock et al., 2012). Nonetheless, each of the above elements differed significantly between groups and may be useful as tracers of nursery origin regardless of the cause of variation between regions.

Due to the lack of difference in otolith isotopic composition between the two regions in the first 5-6 months of life, $\delta^{13}C$ and $\delta^{18}O$ seem to be of negligible value

for YOY yellowfin tuna origin investigation in the western Indian Ocean. This is likely explained by the lack of variation in oxygen isotopic composition in the seawater of this region (LeGrande and Schmidt, 2006).

4.3 Comparison of classification methods

In our study, RF was the best method to predict the natal origin with both highest accuracy and kappa index. When using otolith microchemistry for fish origin identification, the choice of the optimal classification method is important in order to avoid the misinterpretation of the results. Traditional approaches (LDA and QDA) have been commonly used as classification tools in other tuna otolith chemistry studies (e.g. Rooker *et al.,* 2008, 2016; Wells *et al.,* 2012; Macdonald *et al.*, 2013). However, in recent years, machine-learning techniques have arisen as promising classification tools in otolith related studies (Bouchoucha et al., 2018; Tournois et al., 2017; Zhang et al., 2016). The accuracy of each technique will depend on the nature of the analysed data, and our results agreed with recent studies encouraging the use of machine learning methods when otolith chemical data are not multivariate normal and/or presents skewed distributions (Jones et al., 2017; Mercier et al., 2011). The relatively easy usage of RF, together with the absence of distributional assumptions requirements and its robustness against overfitting (Breiman, 2001), make this technique a useful approach for population structure analyses of yellowfin tuna in the Indian Ocean.

4.4 Natal sources of age-1 fish

Given the highly migratory behaviour and dispersal capacity of yellowfin tuna (Fonteneau and Hallier, 2015), obtaining a sufficiently representative baseline at such a large scale would have been logistically unfeasible in this study. Alternatively, the use of unsupervised learning methods to cluster larval elemental signatures, was well suited for studies where no representative baseline samples are available (Gibb et al., 2017). This RF clustering approach used on the near-core otolith portion inferred the presence of a cluster for age-1 yellowfin tuna of unknown origin. This implies either sample share a common origin, with a common larval source contributing to the samples, or a lack of difference in elemental composition between different source locations. Although the approach does not

directly provide information on the location of this potential common larval source, canonical covariates plot revealed higher similarity with NW Indian Ocean YOY signatures, than did with Mozambique Channel YOY. The sizes of age-1 comprised in this study (i.e. 52-64 cm FL) were of a similar range as those from the Regional Tuna Tagging Program of the Indian Ocean (RTTP-IO), 56-75 cm FL, which reported large movements and low average rate of homing fidelity in yellowfin tuna of the Indian Ocean (Fonteneau and Hallier, 2015). Therefore, the presence of different larval sources would have not been surprising in the age-1 sample composition. However, it has also been shown that distances travelled by yellowfin tuna captured around Seychelles Islands (NW Indian Ocean) were lower compared to other areas (Hallier and Million, 2012). This could possibly explain the origin and retention of age-1 samples in the region. This would highlight the importance of local production of yellowfin tuna recruits in the NW Indian Ocean fishery. A high degree of local production and retention of yellowfin tuna has also been reported in other oceans (Rooker *et al.*, 2008, 2016; Wells *et al.*, 2012).

5. Conclusions and implications

This study supports the utility of otolith chemical analyses to provide valuable information about the stock structure of yellowfin tuna in the western Indian Ocean and suggests a more complex stock structure in the area than previously assumed. However, future work should delve into analysis at a whole ocean scale, preferably sampling distinct regions at the same period. Moreover, further development and application of this approach is now needed, in particular by quantifying spatial and temporal variation in oceanic water chemistry at appropriate scales so that this information can help the interpretation of otolith chemistry data. Otolith chemistry analysis is one of a suite of techniques that can be used to study stock structure in marine fishes. Integrating the information gained from otolith chemistry analysis with complementary techniques, such as genetics, tagging and morphometrics (e.g. Abaunza *et al.*, 2008; Taillebois *et al.*, 2017), will provide a powerful means to define appropriate management units for the sustainable exploitation and conservation objectives of yellowfin tuna in the Indian Ocean.

“And when they fail,

Their failure should be,

a challenge for others”

Amelia Earhart

CHAPTER 3

Baseline of otolith chemical signatures for skipjack tuna

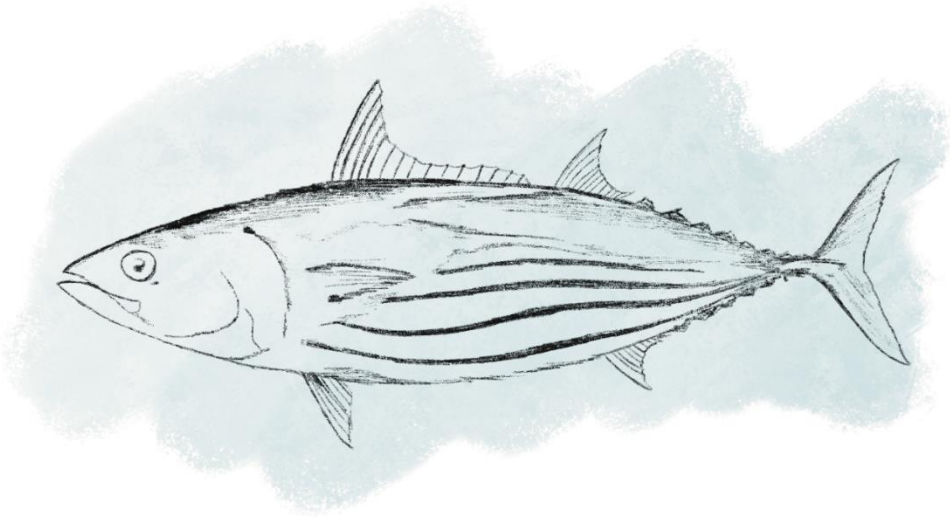

Abstract

The chemical composition of otoliths (earbones) can provide valuable information about stock structure and connectivity patterns among marine fish. For that, chemical signatures must be sufficiently distinct to allow accurate classification of an unknown fish to their area of origin. Here we have examined the suitability of otolith microchemistry as a tool to better understand the spatial dynamics of skipjack tuna (*Katsuwonus pelamis*), a highly valuable commercial species for which uncertainties remain regarding its stock structure in the Indian Ocean. For this aim, we have compared the early life otolith chemical composition of young-of-the-year (<6 months) skipjack tuna captured from the three main nursery areas of the equatorial Indian Ocean (West, Central and East). Elemental (Li:Ca, Sr:Ca, Ba:Ca, Mg:Ca and Mn:Ca) and stable isotopic ($\delta^{13}C$, $\delta^{18}O$) signatures were used, from individuals captured in 2018 and 2019. Otolith Sr:Ca, Ba:Ca, Mg:Ca and $\delta^{18}O$ significantly differed among fish from different nurseries, but, in general, the chemical signatures of the three nursery areas largely overlapped. Multivariate analyses of otolith chemical signatures revealed low geographic separation among Central and Eastern nurseries, achieving a maximum overall random forest cross validated classification success of 51%. Cohort effect on otolith trace element signatures was also detected, indicating that variations in chemical signatures associated with seasonal changes in oceanographic conditions must be well understood, particularly for species with several reproductive peaks throughout the year. Otolith microchemistry in conjunction with other techniques (e.g., genetics, particle tracking) should be further investigated to resolve skipjack stock structure, which will ultimately contribute to the sustainable management of this stock in the Indian Ocean.

Published as:

Artetxe-Arrate, I., Fraile, I., Farley, J., Darnaude, A.M., Clear, N., Rodríguez-Ezpeleta, N., Dettman, D.L., Pécheyran, C., Krug, I., Médieu, A., Ahusan, M., Proctor, C., Priatna, A., Lestari, P., Davies, C., Marsac, F., and Murua, H. (2021). Otolith chemical fingerprints of skipjack tuna (*Katsuwonus pelamis*) in the Indian Ocean: first insights into stock structure delineation. *PLOS ONE*, 16(3), e0249327, doi: 10.1371/journal.pone.0249327.

1. Introduction

Skipjack tuna (*Katsuwonus pelamis*) is a cosmopolitan species inhabiting tropical and subtropical waters of the Indian, Pacific and Atlantic Oceans (Collette and Nauen, 1983). This species is, by far, the most commonly caught tuna worldwide (Galland et al., 2016; ISSF, 2020b). Currently, skipjack tuna stocks are considered to be in a healthy status in all oceans, both in terms of stock abundance and fishing mortality (ISSF, 2020b). Five stocks of skipjack tuna are considered globally for management, two in the Atlantic Ocean, two in the Pacific Ocean and one in the Indian Ocean. Regional studies indicate a more complex stock structure than currently assumed for assessment and management purposes of skipjack tuna in the Indian Ocean (Dammannagoda et al., 2011; Menezes et al., 2012); however, lack of understanding of population dynamics and connectivity at oceanic scale do not allow separation of stocks (IOTC, 2017a).

Stock structure understanding is essential to determine a suitable spatial scale for management, as the way a stock will respond to management decisions cannot be accurately predicted if the boundaries that characterize a stock are not correctly defined (Kerr et al., 2017). Skipjack tuna spawns throughout the year in large warm water tropical areas, but as those areas are often poor feeding grounds, they move towards adjacent colder and more productive subtropical areas to feed (Fonteneau and Pallares-Soubrier, 1995; Grande et al., 2014; Hilborn and Sibert, 1988). However, not all skipjack tuna seem to perform these long-distance movements, but rather, some remain around the tropical spawning area (Fonteneau and Hallier, 2015; Hilborn and Sibert, 1988). As a result, the spatial dynamics of skipjack tuna and, hence, its implications on the stock structure of the species needs to be evaluated. Besides, skipjack tuna are fast growing, early maturing species, and have high reproductive potential, which makes this species more resilient to fishing pressure than many other tuna species (Grande et al., 2016, 2012; Murua et al., 2017). However, fishing pressure may vary spatially due to factors such as fleet operational constrains, variations in population densities, and differences in the value of fish caught, among others (Hoyle and Langley, 2020). Thus, excessive local fishing effort and catches, may lead to situations of local overfishing and depletion when skipjack movements between areas are limited (Fonteneau, 2003). The

understanding of exchange rates and connectivity among recruits from different regions is therefore, essential to achieve a sustainable and effective management of this species (Bosley et al., 2019).

There are several methods that can be used to study fish stock structure, which can provide information at different spatial and/or temporal scales (S. X. Cadrin et al., 2014). Among them, analyses of otolith (i.e., calcified structures found in the inner ear of the fish) chemical composition is widely used to explore movements and habitat use of fish (Tanner et al., 2016). This method relies on the premise that ambient water chemistry and environmental conditions (but also other intrinsic factors such as physiology, diet or genetics) affect the elemental incorporation (at minor and trace quantities) into the concentric growth of the otolith during daily increment formation (Campana, 1999; Elsdon et al., 2008). Since otoliths are both acellular and metabolically inert, material accreted during otolith formation is preserved as fish grows (Campana and Neilson, 1985). As such, the chemical composition of the material accreted during early life stages, serves as a natural marker to identify fish that have inhabited environments with distinct physicochemical characteristics (Kerr and Campana, 2014). Otolith microchemistry proved to be a powerful tool to discriminate among nursery fish groups for other tropical tuna species (Kitchens et al., 2018; Rooker et al., 2016; Wells et al., 2012), and also to depict different movements and life history patters of skipjack tuna in the Pacific Ocean (Arai et al., 2005).

Here, we examined otoliths of young-of-the-year (YOY) skipjack tuna collected across the equatorial strip of the Indian Ocean, where high larvae concentrations and spawning activity of this species have been observed; off Seychelles, Somalia and Mozambique Channel in the western Indian Ocean, off Maldives in the central Indian Ocean, and off Sumatra in the eastern Indian Ocean (Grande et al., 2014; Stéquert et al., 2001b; Stéquert and Marsac, 1989). Besides, those areas are also important fishery grounds of skipjack tuna in the Indian Ocean (IOTC, 2017a). Our aim was to determine whether YOY skipjack tuna captured within these three regions could be spatially discriminated based on their early life otolith microchemistry composition. If so, the characterized nursery origin signature can then be used as a baseline sample to predict older skipjack tuna origin,

by analysing the same early life portion of the otolith (Kitchens, 2017; Thorrold et al., 2001). This in turn, will contribute to improve our understanding of the connectivity and mixing rates and, ultimately, the stock structure of this species in the Indian Ocean.

2. Material and methods

2.1 Fish sampling

Skipjack tuna were collected from three distinct nursery areas in the Indian Ocean: West (10°S-10°N, 40°E-60°E), Central (0°-10°N, 65°E-75°E), and East (5°S-10°N, 85°E-95°E) (**Figure 3.1**).

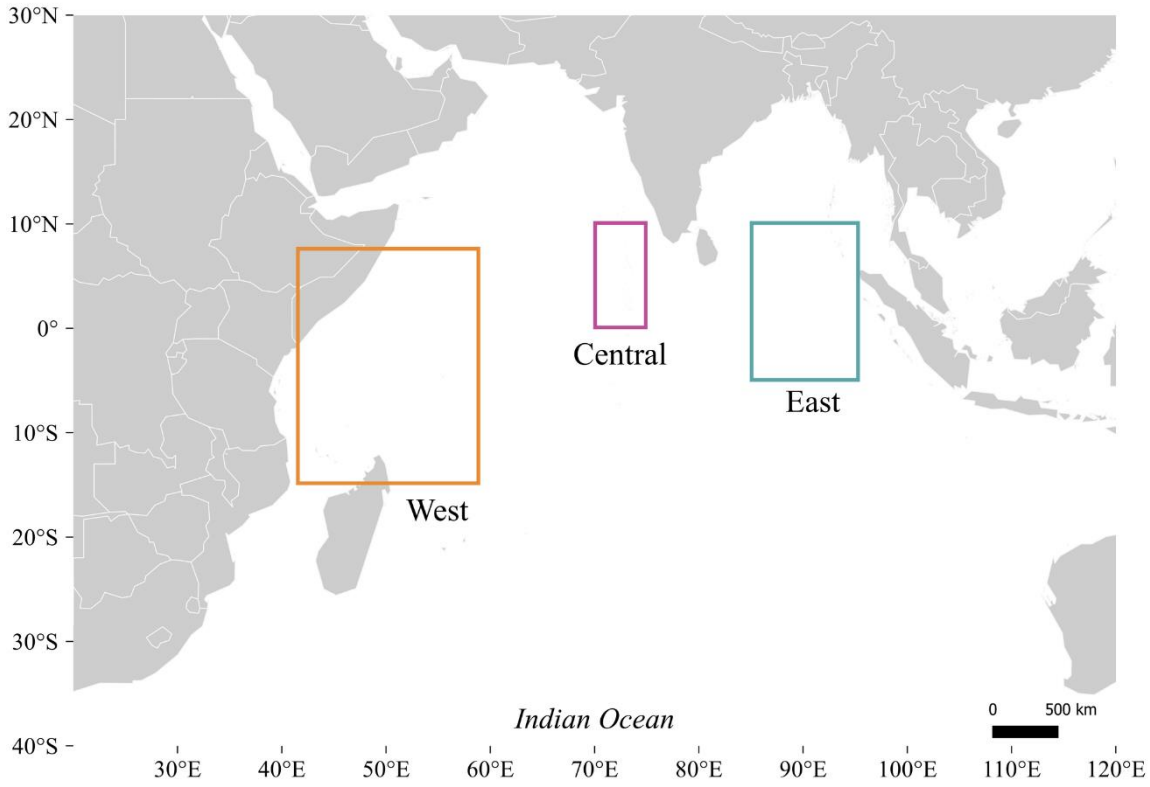

Figure 3.1. Skipjack tuna (*Katsuwonus pelamis*) sampling locations across the equatorial Indian Ocean. Squares represent nursery areas where YOY skipjack tuna were captured from, referred to as West (orange), Central (purple) and East (green).

Samples were obtained directly by scientist or scientific observers on-board purse seine vessels or at port during two consecutive years (2018 and 2019), as part of a collaborative research project on Population Structure of Tuna, Billfish and Sharks of the Indian Ocean (Davies et al., 2020). Fish size ranged between 24.5 and

35.0 cm fork length (FL) (**Tables 3.1 and 3.2**), and were estimated to be about 4-6 months old following the age-length relationship described by Eveson et al. (Eveson et al., 2015). Thus, we assumed that capture locations represent nursery areas where fish reside during the early juvenile stage. Note that fish were sampled at different years/time periods, which implies that the otolith collection available for this study comprised fish from different cohorts (Appendix B, Figure B1). Those spawned from mid (August) 2017 to early (April) 2018 were assigned to the 2017 cohort, hereafter "2017". Those spawned from mid (May) 2018 to early (January) 2019 were assigned to the 2018 cohort, hereafter "2018".

Table 3.1. Number, size, sampling period and mean values of element:Ca ratios measured in otoliths of skipjack tuna (Katsuwonus pelamis) at each of the three nursery areas sampled. Size is fork length (FL) in cm. N, number of fish analyzed.

Nursery	Cohort	N	FL range	Sampling period	Li:Ca (x10-6)	Sr:Ca (x10-3)	Ba:Ca (x10-6)	Mg:Ca (x10-4)	Mn:Ca (x10-6)
West	2017	30	29.0-35.0	Mar 2018	1.18±0.03	3.92±0.06	3.11±0.21	1.16±0.06	6.03±0.42
West	2018	21	29.0-33.0	Apr 2019	1.16±0.05	4.23±0.10	4.19±0.51	1.41±0.06	5.70±0.44
Central	2017	18	28.0-34.0	Aug 2018	1.15±0.05	4.24±0.10	4.03±0.56	1.32±0.06	6.59±0.48
Central	2018	18	28.5-33.0	Feb 2019	1.18±0.05	4.55±0.14	7.00±1.44	1.21±0.06	7.58±0.92
East	2017	20	25.0-33.5	Apr 2018	1.17±0.04	4.28±0.09	6.53±1.01	1.45±0.09	5.17±0.48
East	2018	21	24.5-35.0	Nov 2018	1.13±0.05	4.26±0.16	4.69±0.56	1.34±0.09	8.12±0.87

Table 3.2. Number, size, sampling period and of carbon and oxygen stable isotope ratios mean values measured in otoliths of skipjack tuna (*Katsuwonus pelamis*) at each of the three nursery areas sampled. Size is fork length (FL) in cm. N, number of fish analyzed.

Nursery	Cohort	N	FL range	Sampling period	$\delta^{13}C$	$\delta^{18}O$
West	2017 and 2018	20	29.0-35.0	Mar 2018 and Apr 2019	-8.74±0.09	-1.35±0.06
Central	2017 and 2018	18	29.0-33.0	Aug 2018 and Feb 2019	-8.72±0.13	-1.61±0.06
East	2017 and 2018	18	24.5-35.0	Apr and Nov 2018	-8.80±0.10	-1.78±0.05

2.2 Otolith preparation and analysis

Sagittal otoliths were extracted, cleaned of adhering organic tissue, rinsed with ultrapure water (Milli-Q), and stored dry in plastic vials. In the laboratory, one otolith of each specimen was embedded in two-part epoxy resin (Araldite 2020, Huntsman Advanced Materials, Switzerland). Blocks were polished using 3M® silicon carbide sandpaper (particle size= 220 µm) and a lapping wheel with a series of decreasing grain diameter (30, 15, 9, 3 and 1 µm) 3M® silicon carbide lapping discs, moistened with ultrapure water, to obtain a transverse section where the core was exposed. Sections were ultrasonically cleaned using ultrapure (Milli-Q) water for 10 minutes. Following sonication, otolith sections were left to air dry in loosely capped vials for 24 h before being glued in a sample plate using Crystalbond thermoplastic glue (Crystalbond 509; Buehler). When a single otolith was available only trace element analyses were conducted. When both pairs of otoliths were available, the second one was used for carbon and oxygen stable isotope analyses.

2.3 Trace element analyses

Otoliths (n=128) were analysed for trace element chemistry using a high resolution inductively coupled plasma mass spectrometer (HR-ICP-MS, Element Element XR, Thermo Scientific, Bremen, Germany), coupled to a high repetition rate 1030 nm femtosecond laser (fs-LA) system (Alfamet, Neseya, Canejan, France) available at the Institut des Sciences Analytiques et de Physico-Chimie pour l'Environnement et les Matériaux, Université de Pau et des Pays de l'Adour/CNRS (Pau, France). Each otolith was ablated 200 µm apart from the primordium along the ventral arm (Appendix B, Figure B2). This spot was considered to be representative of the chemical signature corresponding to the first 13-15 days of life of the fish according to direct daily microincrement counts, and thus to exclude the potential maternal effects the primordium (i.e., the initial structure of an otolith) may incorporate (Hegg et al., 2018). Laser ablation conditions were 200 Hz, a laser beam size of 15 µm and 30 µJ per pulse energy corresponding to a fluence of 14 J/cm2, until the depth limit of ablation (< 30 µm). During ablation the small laser beam was continuously and rapidly moved (500 µm s-1) at the surface of the sample due to a 2D galvanometric scanner in order to create a trajectory made of 6 concentric circles (Claverie et al., 2009). This resulted in the ablation of a crater 30

µm in diameter and 30 µm deep. The ablation cell was flushed with argon to transport laser-induced particles to the HR-ICP-MS. The fsLA-HR-ICP-MS was tuned daily to reach optimal particle atomization conditions and minimal elemental fractionation. This was obtained for a U/Th signal ratio of 1 ± 0,05 using NIST 612. The mass spectrometer was used in the medium-resolution mode (R=4000) to ensure a complete polyatomic interference removal for the isotopes of interest. Relative abundances of five isotopes (^{7}Li, ^{88}Sr, ^{138}Ba, ^{24}Mg and ^{55}Mn) were estimated, as well as ^{43}Ca, which was used as the internal standard. The concentration of ^{43}Ca in the otolith was assumed to be constant at 38.3% (Sturgeon et al., 2005). Data reduction including background subtraction, conversion to ppm and standardization to calcium (element:Ca µmol mol-1) was done using an in-lab developed software FOCAL 2.27. National Institute Standards and Technology (NIST) 610 and 612 glass standards with known chemical composition were used for calibration. Measurement accuracy was determined based on an otolith certified reference material for trace elements (FEBS-1, NRC-CNRC, Canada). To correct for short-term instrumental drift, standards and reference material were measured threefold two times a day; at the beginning and the end of each session. Trace element measurements of the blank sample gases were recorded for 20-30s before each sample ablation of ~40s. Mean relative standard deviation (RSD) for NIST 612 and 610 were (n=9): 2.9% and 8.5% (Li), 2.1% and 8.9% (Sr), 1.8% and 4.8% (Ba), 2.5% and 9.4% (Mg), 2.3% and 3.7% (Mn), respectively. The elemental ratios of Li:Ca, Sr:Ca, Ba:Ca, Mg:Ca and Mn:Ca exceeded the detection limits of the fs-LA-ICP-MS for all samples.

2.4 Stable isotopes analyses

For stable isotope analyses (n=56), microsampling of otolith powder for carbon (δ^{13}C) and oxygen (δ^{18}O) stable isotope analysis was performed using a high-resolution computerised micromill (New Wave MicroMill System, NewWave Research G. C. Co., Ltd, Cambs, UK). The area of analysis on the smallest skipjack tuna otolith (24.5 cm FL) was used to create a standard template that was then applied to the remaining otoliths, to ensure that the same portion of the otolith was analyzed in every fish (Appendix B, Figure B2). Therefore, the drill path covered the area of the otolith corresponding to the first ~4 months of life (according to Eveson et al.

(Eveson et al., 2015) age-length relationship), with a larger time period of the otolith sampled for stable isotopes than trace elements due to differences in sample material requirements. Ten drill passes were run at a depth of 50 µm per pass over a preprogrammed drill path using a 300-µm diameter carbide bit (Komet dental; Gebr. Basseler, Lemgo, Germany). Powdered material was then analysed for $\delta^{13}C$ and $\delta^{18}O$ on an automated carbonate preparation device (KIEL-III, Thermo- Fisher Scientific, Waltham, MA, USA) coupled to a gas-ratio mass spectrometer (Finnigan MAT 252, ThermoFisher Scientific) at the Environmental Isotope Laboratory of the University of Arizona. All isotope values were reported according to standards of the International Atomic Energy Agency in Vienna. The isotope ratio measurement was calibrated based on repeated measurements of NBS-19 and NBS-18 (International Atomic Energy Agency standards). Measurement precision was ± 0.10 ‰ for $\delta^{18}O$ and ±0.08‰ for $\delta^{13}C$ (1 sigma).

2.5 Statistical analyses

All statistical analyses were performed using open access R software (R Core Team, 2019). Prior to all multivariate analyses, otolith chemistry data was standardized (i.e., for each element, the data was centered by subtracting the mean and scaled by dividing by the standard deviation) to give the same weight to all elements and stable isotopes.

Elements were first analyzed individually. Parametric assumptions were violated by Ba:Ca, Mg:Ca and Mn:Ca. Therefore, non-parametric tests were used for trace element analyses, to apply a consistent approach for all elements. To determine whether the otolith chemistry of YOY skipjack tuna varied spatially and/or temporally, a permutational multivariate analysis of variance (PERMANOVA) was used to test for differences in element:Ca ratios between nurseries and cohorts (Anderson, 2001; Rogers et al., 2019). Nursery and cohort were fixed factors in the full factorial model. The resemblance matrix was based on euclidean distance dissimilarities and the number of unrestricted permutations was set to 999 random repeats using *adonis* {vegan}. Statistical significance was determined based on adjusted p-values after the Benjamini-Hochberg correction (Benjamini and Hochberg, 1995), and post hoc pairwise comparisons were applied to identify the source of differentiation between group means using *lincon* {WRS2}.

Parametric assumptions of normality and homoscedasticity were met for $\delta^{13}C$ and $\delta^{18}O$ data, and therefore one-way ANOVA test was used for comparisons among nurseries, *aov* {stats}. When significant differences were detected, post hoc comparison were performed to the source of differences between means, using *TukeyHSD* {stats}.

Both trace elements and stable isotopes were them combined for multivariate analyses. The resultant dataset was limited by the number of individuals for which both types of data were available (n=56). A multilevel pairwise comparison was performed using *pairwise.adonis* {pairwiseAdonis} to test for differences in the multielemental signature between nursery areas. The resemblance matrix was based on euclidean distance dissimilarities and the number of unrestricted permutations was set to 999 random repeats. Statistical significance was determined based on adjusted p-values after the Benjamini-Hochberg correction (Benjamini and Hochberg, 1995). Then, multivariate data were reduced to two-dimensions and visualized by a canonical analysis of principal coordinates (CAP) using *CAPdiscrim* {BiodiversityR} function (Anderson and Willis, 2003). Random forest (RF) classification algorithm (number of trees=500, mtry=2) was implemented to test the ability of trace elements and stable isotope signatures to discriminate among fish belonging to different nursery areas (Breiman, 2001). Data was split into a training dataset (70%) and a testing dataset (30%), and this procedure was randomly repeated 1000 times. At each time, the rate of classification success (i.e., rate of correct predicted membership to nursery areas in which the fish were collected) was calculated, and mean values were extracted. Cohen´s Kappa (κ) statistic was also calculated, which is a method that accounts chance-corrected percentage of agreement between actual and predicted group memberships. Values of κ range from 0 to 1, where 0 indicates that the RF resulted in no improvement over chance, and 1 indicates perfect agreement (Titus et al., 1984). Random forest was performed for each cohort, as well as for pooled data from both cohorts in the case of trace element data. For stable isotope data, and combined trace element and stable isotope data, pooled data from both cohorts was only used.

3. Results

3.1 Individual elements

Significant differences were detected in the chemical signatures of skipjack tuna collected from different nurseries, but also between cohorts in the case of trace element data (**Table 3.3**). The concentrations of Sr and Mn differed significantly between years, concentrations being higher in 2018 (**Figure 3.2**). Significant interactions between nursery and cohort were also detected for Ba, Mg and Mn, meaning that the pattern of variation was different among nurseries at each cohort (**Table 3.3, Figure 3.2**). Concentrations of Sr, Ba and Mg differed among nurseries in 2017, being lower for skipjack tuna collected from the West nursery (**Figure 3.2**). For fish belonging to the 2018 cohort no significant differences across regions were detected for any of the trace elements analyzed.

Table 3.3. Summary of two-factor PERMANOVA for the effect of nursery and cohort on individual and combined trace element data of skipjack tuna (Katsuwonus pelamis) otoliths. Nursery area and cohort were fixed factors within the full factorial design. Significant effects are highlighted as follows; *P<0.05, **P<0.01.

Element	Source	df	F	P-value
Li	Nursery	2	0.13	0.879
	Cohort	1	0.11	0.746
	Nursery x Cohort	2	0.01	0.693
Sr	Nursery	2	5.06	0.011*
	Cohort	1	5.11	0.023*
	Nursery x Cohort	2	1.45	0.260
Ba	Nursery	2	5.35	0.007**
	Cohort	1	1.26	0.272
	Nursery x Cohort	2	4.99	0.011*
Mg	Nursery	2	1.97	0.122
	Cohort	1	0.37	0.541
	Nursery x Cohort	2	4.10	0.014*
Mn	Nursery	2	2.04	0.128
	Cohort	1	4.90	0.025*
	Nursery x Cohort	2	3.79	0.038*

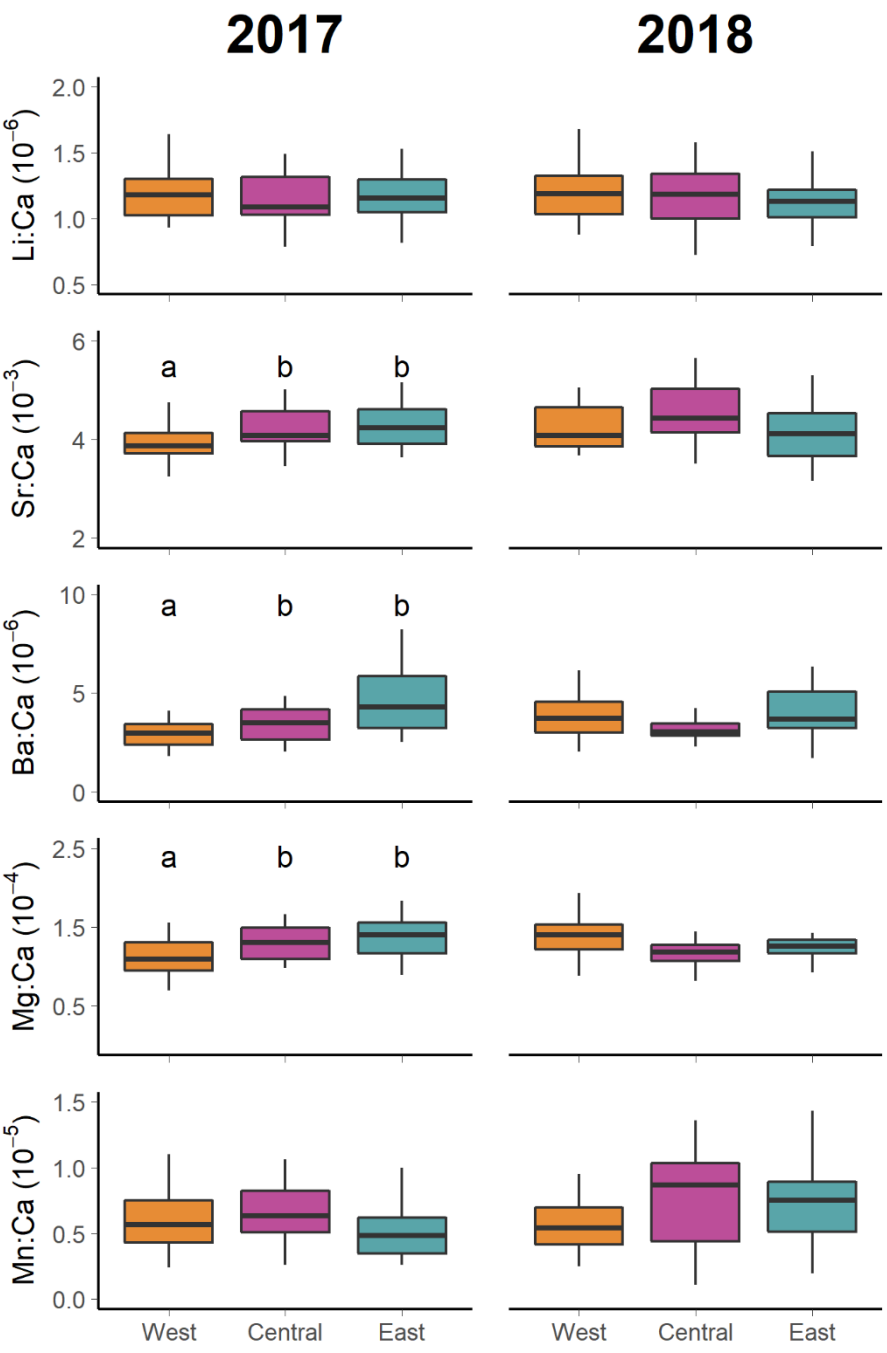

Figure 3.2. Trace element otolith composition of young-of-the-year (YOY) skipjack tuna (*Katsuwonus pelamis*) in the Indian Ocean. Boxplots compare otolith Li:Ca, Sr:Ca, Ba:Ca, Mg:Ca and Mn:Ca composition between nursery areas in the Indian Ocean in 2017 cohort (left panel), 2018 cohort (rigth panel). Letters identify significant differences (heteroscesadic anova, $p<0.05$) between group means. Inter quartile range (25th and 75th percentile) is shown by extent of boxes and error bars represent 10th and 90th percentiles.

Otolith $\delta^{18}O$ values also varied among nurseries (anova, $p<0.001$), with significantly higher values found in the West nursery with respect to the central and

eastern nurseries (**Figure 3.3**). No significant differences were detected in otolith $\delta^{13}C$ composition between nursery areas.

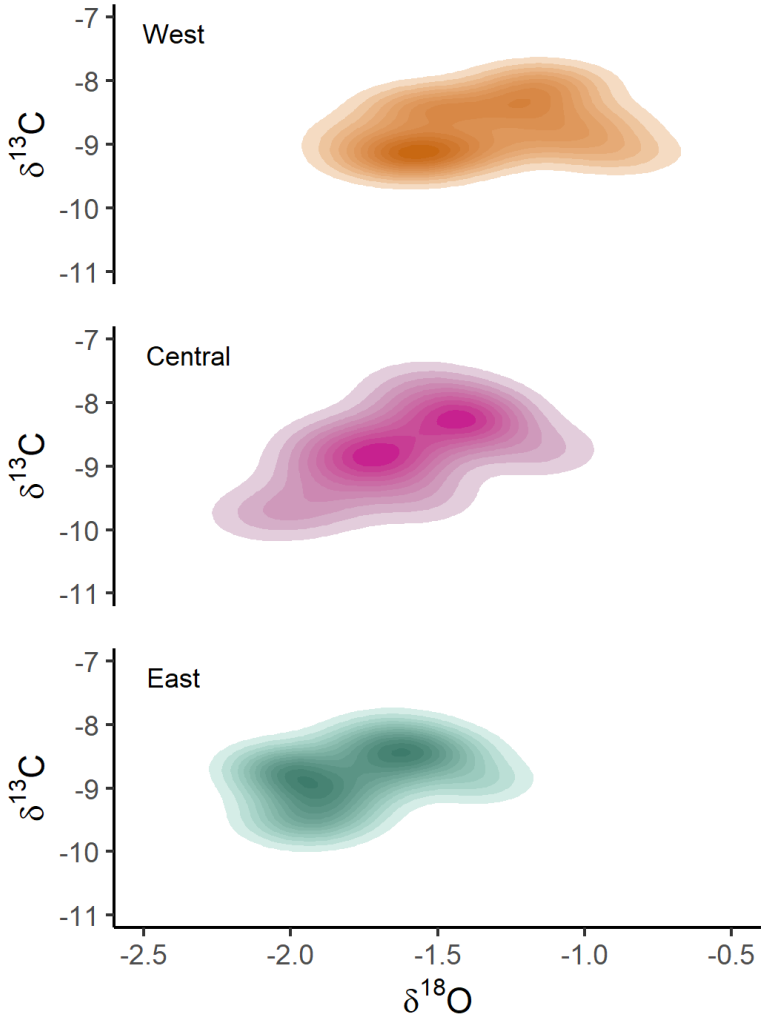

Figure 3.3. Contour plots of $\delta^{13}C$ and $\delta^{18}O$ values in otoliths of young-of-the-year (YOY) skipjack tuna (*Katsuwonus pelamis*) in the Indian Ocean. The composition of each nursery area is shown: West (orange), Central (purple) and East (green). Bivariate kernel density estimated at ten levels (10%, 20%, 30%, 40%, 50%, 60%, 70%, 80%, 90% and 100%).

3.2 Multielemental signatures

When individual trace elements and carbon and oxygen stable isotopes were combined, significant regional differences were found among nursery areas (PERMANOVA, p=0.005). Specifically, multielemental signatures from YOY skipjack tuna from the western nursery were differentiated from the central and eastern nurseries, as supported by posterior pairwise comparisons (**Table 3.4, and Figure 3.4**).

Table 3.4. Results of pairwise comparisons of multielemental (Li:Ca,Sr:Ca, Ba:Ca, Mg:Ca, Mn:Ca, $\delta^{13}C$ and $\delta^{18}O$) signatures among three nursery areas in the Indian Ocean.

Nursery pair	Df	Sum of squares	F-statistic	R squared	P value	Adjusted p value	Significance[1]
West vs Central	1	22.77	3.88	0.10	0.002	0.003	**
West vs East	1	27.77	4.55	0.11	0.001	0.003	**
Central vs East	1	8.60	1.13	0.03	0.335	0.335	

[1]In the significance column, a star (*) means significant differentiation at <0.05 level and two stars (**) at <0.01 after adjusted p-value calculation with Benjamini and Hochenberg (BH) correction.

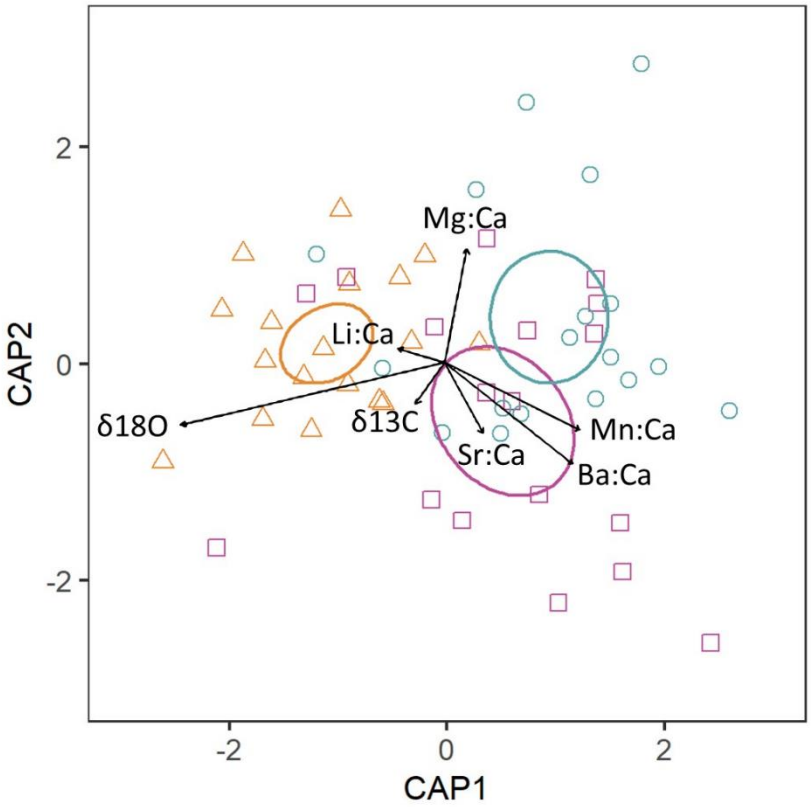

Figure 3.4. Canonical analysis of principal coordinates (CAP) variate plot of the multielemental chemistry of skipjack tuna (*Katsuwonus pelamis*) otoliths. Ellipses show 95% confidence around nursery means, shown as West (triangles, orange), Central (squares, purple) and East (circles, green).

Classification accuracy was generally low regardless of the elemental combination used. Classification success using cohort pooled cohort trace element

data was of 44% and κ=0.16 (**Table 3.5**). Overall classification success of fish back to their nursery area was higher in 2017 (50%, κ=0.33) than in 2018 (44%, κ=0.15). Nursery specific signatures also varied considerably between cohorts. For YOY skipjack tuna from the West nursery classification accuracy decreased from 71% in 2017 to 49% in 2018, while for the Central nursery increased from 23% in 2017 to 40% in 2018. Cohort pooled classification accuracy of YOY skipjack tuna from East nursery remained similar (45% and 42% in 2017 and 2018, respectively).

Carbon and oxygen stable isotopes provided higher classification success than trace elements alone (51%, κ=0.44, **Table 3.5**). The combination of trace elements and stable isotopes did not improve the overall classification accuracy with respect to the use of carbon and stable isotopes alone (51%, κ=0.40). However, nursery specific classification did vary, YOY from the West nursery were better classified with stable isotopes alone, while for YOY from the Central nursery greater classification accuracy was obtained when stable isotope data was combined with trace element data (**Table 3.5, Fig 3.4**). Nevertheless, samples from the Central and East nurseries were often misclassified (<50%), regardless on the elemental combination used.

Table 3.5. Random forest discriminant function analysis classification success (%) assigning young-of-the-year (YOY) skipjack tuna (*Katsuwonus pelamis*) to their nursery area in the Indian Ocean. Results are shown for random forest using data from (1) trace elements (Li:Ca, Sr:Ca, Ba:Ca, Mg:Ca, Mn:Ca), (2) stable isotopes ($\delta^{13}C$ and $\delta^{18}O$), and (3) trace elements and stable isotopes combined, for both cohorts pooled.

Element combination	Nursery	Both cohorts
Li:Ca, Sr:Ca, Ba:Ca, Mg:Ca, Mn:Ca	West	59
	Central	27
	East	39
	Overall	44
	κ	*0.16*
$\delta^{13}C$, $\delta^{18}O$	West	66
	Central	31
	East	47
	Overall	51
	κ	*0.44*
Li:Ca, Sr:Ca, Ba:Ca, Mg:Ca, Mn:Ca $\delta^{13}C$, $\delta^{18}O$	West	65
	Central	41
	East	46
	Overall	51
	κ	*0.40*

4. Discussion

Otolith chemical fingerprints are powerful discriminators of groups as long as differences exist, but of negligible value when differences cannot be detected, as the absence of difference does not necessarily imply that groups own a common origin (Campana, 1999). The high overlap in the otolith chemical signatures of YOY from the central and eastern nurseries, may be at least partly explained by the homogeneity in the physicochemical properties of ambient water fish were exposed to during their early life. Depending on the period, the regions of Maldives (Central) and eastern Indian Ocean are quite homogeneous in terms of sea surface temperature (SST), salinity (SSS), and dissolved oxygen (DO) (Schott et al., 2009; Tomczak and Godfrey, 2003a). Another potential reason to the observed overlap of the chemical signatures, is that important transoceanic mixing may have occurred prior to capture. However, it is unlikely that transoceanic migrations occur before 4 to 6 months of life. To our knowledge, transoceanic movements of skipjack tuna within the first 6 months have not been documented, since tagging studies are generally not available for these size ranges (Fonteneau and Hallier, 2015). Moreover, skipjack tuna predominantly shows diffusion type movements rather than long longitudinal migrations, as they move towards colder and richer subtropical areas adjacent to their spawning areas, where they can temporarily found higher productivity and prey availability than in warm equatorial waters (Fonteneau and Pallares-Soubrier, 1995; Hilborn and Sibert, 1988). Besides, the sub-mesoscale activity present in the nursery areas can minimize long-distance dispersal, by retaining the larvae near their spawning area (Bakun, 2006; Reglero et al., 2014). For all the above, we think that the observed results in the chemical signatures of YOY skipjack tuna are more likely attributed to the fact that biochemical properties of the water masses were relatively homogeneous during the early life of the fish, leading to a low discrimination capacity among fish captured in different nursery areas.

Strong interannual effect was detected in the otolith trace element signatures of fish belonging to two different cohorts. While significant differences were detected among nurseries in Sr, Ba and Mg concentrations in 2017, differences were not significant in 2018. Barium and strontium are incorporated into the otolith via

Ca substitution, and may be appropriate markers of environmental history (Hüssy et al., 2020; Izzo et al., 2016; Thomas et al., 2017). Mg incorporation into the otolith by contrast, has been related with metabolic activity (Limburg et al., 2018; Thomas et al., 2020). Due to sampling constrains, YOY skipjack tuna were hatched during different year periods (Appendix B, Figure B2). North of 10°S the Indian Ocean is characterized by two seasons with distinct wind regimes, the monsoon system, which drives the ocean circulation and climate in the tropics and northern subtropic region of the Indian Ocean (Schott and McCreary, 2001; Shankar et al., 2002). The southwest monsoon, also known as summer monsoon, takes place from June to October with a maximum of intensity during the months of July, August, and September. During this season there is little difference in rainfall intensity within the equatorial region, while temperatures are colder west of 60°E due to the coastal upwelling that takes place off Somalia and Oman Coasts (Keshtgar et al., 2020; Schott et al., 2009; Tomczak and Godfrey, 2003a). The northeast Monsoon, or the winter monsoon, takes place between December and April with a maximum of intensity in the months of January, February, and March. Upwelling events take place off northwest Australian shelf and in open ocean at 5-10°S region (Schott and McCreary, 2001). During the winter monsoon waters off Somalia are colder (26.5°C), whereas SSTs are above 28°C over the rest of the equatorial region (Tomczak and Godfrey, 2003a). Besides, during this season rainfall intensity is stronger in the west south (4.5°S) of the equator off Madagascar and off Sumatra (Keshtgar et al., 2020). During the transition periods between the monsoons (i.e., May and November), a strong equatorial downwelling occurs. For skipjack tuna belonging to the 2017 cohort, those collected from the West nursery were estimated to be hatched during the summer monsoon, while those from Central and East nurseries were considered to be hatched during the winter monsoon and the autumn intermonsoon periods. All skipjack tuna belonging to the 2018 cohort were estimated to be hatched within the summer monsoon period and the two intermonsoons. As seasonal climatology strongly influences the biochemical variability throughout the northern Indian Ocean, it may be possible that observed regional differences in Sr, Ba and Mg in 2017 are due to the seasonal changes in water physicochemical properties that could have masked regional differences (Bao et al., 2020a; Wiggert et al., 2006).

Otolith $\delta^{18}O$ signatures were significantly higher from individuals of the West nursery than the Central and the East nurseries. The isotopic composition of ambient seawater is dependent on evaporation, and largely controlled by salinity (LeGrande and Schmidt, 2006). As otolith $\delta^{18}O$ is incorporated into otolith aragonite close to equilibrium with seawater, the isotopic composition of otolith reflects seawater $\delta^{18}O$ values, being inversely correlated with ambient seawater temperature (Kitagawa et al., 2013; Trueman and MacKenzie, 2012). Otolith composition of YOY skipjack tuna from the Indian Ocean followed the expected trend for $\delta^{18}O$ signatures, presenting higher values in the West (expected due to lower water temperatures, under the influence of the seasonal Somali upwelling) and decreasing towards the east (expected due to higher water temperatures, as confirmed by the overall sea surface temperature pattern in the Indian Ocean). Similar trends have been found in a preliminary study for yellowfin tuna from the Indian Ocean (Artetxe-Arrate et al., 2020a). No differences were detected in otolith $\delta^{13}C$ signatures between fish captured in the three different nursery areas. Otolith $\delta^{13}C$ can be a proxy for metabolic rate in fish, and is influenced by the environment (dissolved inorganic carbon in water, DIC) and diet (Chung et al., 2019; Martino et al., 2019). The observed absence of difference in $\delta^{13}C$ signatures followed the expected trend for surface water carbon isotope composition, which is relatively homogenous within the equatorial Indian Ocean (Magozzi et al., 2017), and therefore providing little value for stock discrimination.

The overall low regional variability in chemical signatures from skipjack tuna resulted in a low classification of YOY individuals to the three nursery areas analyzed in the Indian Ocean. To date, there are no studies aiming to retrospectively determine skipjack tuna to their nursery origin based on otolith chemical signatures. However, studies done with other tuna species inhabiting tropical environments (e.g. yellowfin and bigeye) reported higher classification accuracies of fish back to their nursery area than those reported in this study (Artetxe-Arrate et al., 2019; Kitchens et al., 2018; Rooker et al., 2016; Wells et al., 2012). The use of stable isotopes alone was sufficient for nursery discrimination of yellowfin tuna in the Pacific Ocean, whereas trace elements proved to be more efficient for discriminating among yellowfin nursery areas in the Atlantic and Pacific and Indian Oceans (Artetxe-Arrate et al., 2019; Kitchens et al., 2018; Wells et al., 2012). Here,

the use of carbon and oxygen stable isotope values alone, proved to be effective to differentiate skipjack tuna from the western nursery, but the high overlap in the chemical signature of skipjack tuna from the Central and East nurseries resulted in an overall low classification. The use of trace element data or the combination of stable isotope and trace element data did not improve the overall classification success. It is also possible that differences in classification success between trace elemental ratios and stable isotopes is due to the different the time period of the otolith represented by each tracer (i.e. ~day 13 to 15 for trace elements vs. 4-6 months for stable isotopes) (Kitchens et al., 2018). One possible solution would be to analyze with LA-ICPMS the integrated signal of an ablation square that corresponds to the same otolith portion milled for stable isotopes analyses (i.e., ~4-6 months of life). However, this data should be interpreted with caution as it has been proved that ontogeny strongly influences trace element uptake into the otolith (Macdonald et al., 2020; Thomas et al., 2020).

5. Conclusions

Overall, the differences in the chemical signature of YOY skipjack tuna from the three nursery areas in the Indian Ocean were not strong enough to describe a reference baseline for each nursery that allows the assignment of older individuals to their origin nursery. Temporal differences in the physicochemical characteristics of the Indian Ocean seem to strongly influence otolith trace element composition. Considering also that classification success for models based on otolith trace element data compared to those using only otolith stable isotopes was lower, the effort and cost to incorporate elemental ratios into Indian Ocean skipjack tuna otolith chemistry baseline delineation may not be worthwhile (Rooker et al., 2016). Until there is a proper understanding of the stock structure of skipjack tuna, the uncertainty in relation to the response of this stock to management decisions adopted considering a single stock will be maintained. Further research on skipjack population structure using otolith microchemistry should rely on younger (<4 months) individuals to reduce the possibility of movements between nursery areas and consider temporal stratification of sampling so that seasonal differences in oceanography can be disentangled from potential regional differences. Finally, an holistic approach may provide a more accurate overview to properly define

management units, as single technical approaches may not be sufficient to delineate complex stock structures (Leis et al., 2011; Pita et al., 2016). Recent studies combining different stock delineation techniques (e.g. otolith microchemistry, genetics, biophysical models…), proved to be more effective to fully understand the spatial ecology of highly migratory fish species, and, hence increased the resolving power of stock discrimination (Brophy et al., 2020; P. Reis-Santos et al., 2018; Taillebois et al., 2017). For instance, including passive drift trajectory simulations may also be helpful to understand potential patterns of skipjack larval dispersal in the Indian Ocean (Nikolic et al., 2020). The combination of otolith chemistry data coupled with genetic analyses can increased details on connectivity patterns, as both techniques provide information on complementary timescales (individual for otolith chemistry, and evolutionary for genetics), unravelling otherwise hidden patterns (Hoey et al., 2020). Ultimately, a better understanding of the stock structure and spatial connectivity of skipjack tuna in the Indian Ocean will be essential to implement and enforce management strategies that ensure long-term sustainable fisheries of this important species.

“It matters not what someone is born,

but what they grow to be.”

Joanne Rowling

CHAPTER 4

Baseline of otolith chemical signatures for yellowfin tuna

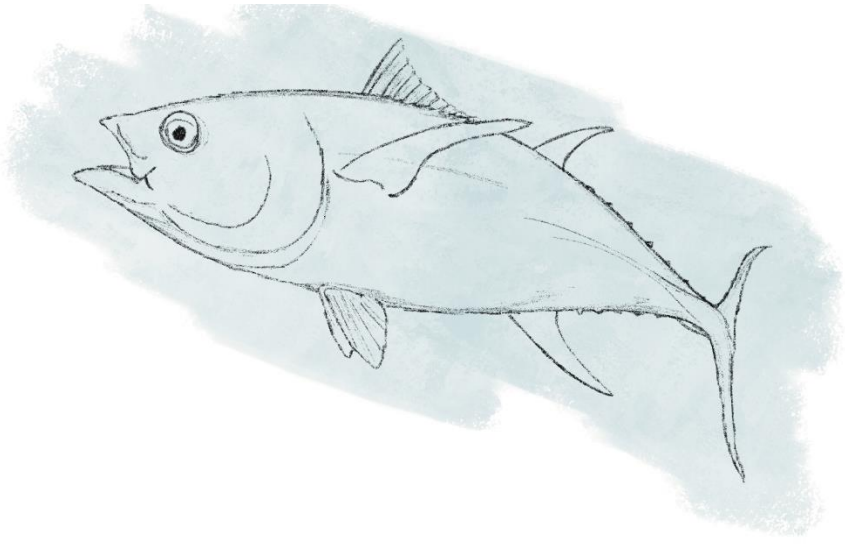

Abstract

Yellowfin tuna (*Thunnus albacares*) is a highly exploited species in the Indian Ocean, yet their stock structure is still not well understood, which may prevent to assess the stock at a suitable spatial scale for management. Here, young-of-the-year (<4 months) yellowfin tuna otoliths were collected in 2018 and 2019, from four different nursery areas in the Indian Ocean: Madagascar, Seychelles-Somalia, Maldives, and Sumatra. First, we examined the age-length relationship based on otolith microstructure and identified the portion of the otolith corresponding to the larval stage. Then, we developed two dimensional maps of trace element concentrations to examine spatial distribution of elements across otolith transverse sections. Different distribution patterns were observed among the elements analysed; Li, Sr and Ba were enriched in the portion of the otolith representing early life, whereas Mn and Mg concentrations were heterogeneous across growth bands. Last, we analysed inter-annual and regional variation in larval stage otolith chemical composition using both trace elements (Li, Mg, Sr, Ba and Mn) and stable isotopes ($\delta^{13}C$ and $\delta^{18}O$). Significant regional variation in otolith chemical signatures was detected among nurseries, except for between Madagascar and Seychelles-Somalia. Otolith $\delta^{13}C$ and $\delta^{18}O$ were important drivers of differentiation between western (Madagascar and Seychelles-Somalia), Maldives and Sumatra nurseries, whereas the elemental signatures were cohort specific. Overall nursery assignment accuracies were 69-71%. The present study demonstrates that baseline chemical signatures in the otoliths of yellowfin tuna are distinct and can, therefore, be used as a natural tag to investigate the nursery origin of older individuals, but temporal stability of the signal is an important factor to account for.

Under review as:

Artetxe-Arrate, I., Fraile, I., Clear, N., Darnaude, A.M., Dettman,D.L., Pécheyran, C., Farley, J., and Murua, H. (2021). Discrimination of yellowfin tuna (*Thunnus albacares*) from nursery areas in the Indian Ocean using otolith chemistry. *Marine Ecology Progress Series.*

1. Introduction

Yellowfin tuna (*Thunnus albacares*) is an important source of food, employment and livelihood for numerous nations, and an important commercial species in the global fisheries market (FAO, 2016; Guillotreau et al., 2017). As such, this species experiences significant fishing pressure, with global catches reaching about 1.45 million tonnes in 2018 (FAO, 2020b). Of the four yellowfin tuna stocks managed in world oceans, the Indian Ocean stock is currently considered overfished and subject to overfishing (IOTC, 2018b; ISSF, 2020b). The Indian Ocean Tuna Commission (IOTC) assessment assumes that yellowfin tuna constitutes a single stock in the Indian Ocean owing to the rapid and large-scale movements observed in the Indian Ocean Regional Tuna Tagging Program (RTTP-IO) (IOTC, 2017c). However, the single stock paradigm has been questioned as findings derived from regional genetic and parasite studies suggested a more fragmented structure than the one currently considered for the assessment of this species (Dammannagoda et al., 2008; Kunal et al., 2013; Moore et al., 2019).

Although adult yellowfin tuna are distributed over the entire Indian Ocean as far south as 45°S (Sharp, 2001), their spawning activity is restricted to particular environments with warmer temperatures and with mesoscale oceanographic activity, such as fronts or eddies (Muhling et al., 2017; Reglero et al., 2014; Schaefer, 2001). Bottom topography is also an important factor to form spawning grounds, with greater abundance of larvae near lands masses, particularly islands, compared to offshore waters (Boehlert and Mundy, 1994). Early larval surveys confirmed a patchy larval distribution of yellowfin tuna along the Indian Ocean (Conand and Richards, 1982; Nishikawa et al., 1985; Ueyanagi, 1969). The main spawning grounds of yellowfin tuna in the Indian Ocean are located in the equatorial (0-10°S) area and west of 75°E (IOTC, 2017c). Spawning has been documented for yellowfin tuna in waters around Seychelles, off Somalia and off Madagascar in the western Indian Ocean (Zudaire et al., 2013a), the Maldives and Chagos Archipelagos in the west central Indian Ocean (Zhu et al., 2008), and off Sri Lanka and west of Sumatra in the north eastern Indian Ocean (Nootmorn et al., 2005).

However, the relative importance of different spawning and nursery areas to the total catches, and the degree of connectivity and mixing rates of yellowfin tuna

in the Indian Ocean are still unknown. Ignoring complex stock structure and connectivity can lead to a misperception of fish productivity and wrong predictions of future stock abundance (Kerr et al., 2017). When the stock structure is more complex than recognized, local overexploitation and possible collapse of less productive stocks may occur and, hence, ignoring the stock structure of a species can lead to a suboptimal utilization of the resource (Ying et al., 2011). Therefore, the understanding of the stock structure of any species, and particularly of highly exploited species such as yellowfin tuna, is essential to develop a suitable spatial scale for management (Bosley et al., 2019; Kerr et al., 2017).

The chemical composition of fish otoliths (i.e. earbones) can be an effective tool to identify nursery areas and thus provide information on stock structure, which is important for determining the appropriate spatial scale that a species should be managed (Campana, 1999; Kerr et al., 2020). This technique has proved to be useful to study the origin and connectivity of yellowfin tuna in other oceans (Kitchens et al., 2018; Rooker et al., 2016; Wells et al., 2012). Otoliths are composed of a calcium carbonate ($CaCO_3$) structure in the form of aragonite (98%), on a non-collagenous organic matrix (2%) (Campana, 1999). Otoliths are acellular and metabolically inert and, as such, material accreted during otolith formation is preserved as a fish grows (Campana and Neilson, 1985). Counts of daily increments in otoliths can be used to select the portion of the otolith to be assayed that corresponds to the age of interest, such as the larval phase of the fish (Campana and Thorrold, 2001). During the biomineralization process, chemical elements are incorporated into the otolith at minor and major concentrations, by either direct Ca substitution, random trapping in the interstitial spaces of the crystal lattice, or interaction with otolith proteins (Campana, 1999; Izzo et al., 2016; Thomas et al., 2017). Most otolith chemistry studies have focussed on elements that are dominant in the salt fraction of the otolith (e.g. Li, Mg, Sr, Ba, Mn, $\delta^{13}C$ and $\delta^{18}O$), while other elements strongly associated with the proteinaceous fraction (e.g. Zn and Cu) have also been used in trace element fingerprinting (Thomas et al., 2020; Thorrold et al., 1997). The uptake of the elements is regulated by a range of intrinsic and extrinsic factors, and thus, the otolith chemical composition reflects a combination of physico-chemical factors of the environment inhabited by the fish, and other intrinsic factors such as physiology, diet, ontogeny, and genetics (Hüssy et al., 2020;

Macdonald et al., 2020). The chemical composition of the otolith material accreted during early life stages, therefore, serves as a "chemical fingerprint" that may differ among groups of fish belonging to different nursery areas (Campana, 1999).

The present study aims to determine whether young-of-the-year (YOY) yellowfin tuna from different nursery areas in the Indian Ocean have distinct chemical signatures in their otoliths. If so, the chemical signatures can be used to develop baseline signatures that allow to retrace the origin of older fish and determine the degree of connectivity and mixing of different yellowfin tuna spawning and feeding zones. This information is important to inform fishery managers on yellowfin stock structure in the Indian Ocean and to determine whether the species should be managed as several discrete stocks. A combination of trace elements and carbon and oxygen stable isotopes ($\delta^{13}C$ and $\delta^{18}O$) in otoliths of YOY yellowfin tuna captured in four nursery regions were analysed. Specifically, (1) we estimated age at early life to assist the interpretation of otolith microchemistry, (2) we analysed the distribution of trace elements throughout the otolith to better understand elemental uptake variability within the otolith, and (3) we assessed the temporal and spatial variation of the chemical signatures both within and between individuals caught in different nursery areas and at different collection dates.

2. Material and methods

2.1 Sample Collection

Samples were obtained by scientific observers on-board purse seine vessels or in port landings, as part of a collaborative research project on Population Structure of Tuna, Billfish and Sharks of the Indian Ocean (Davies et al., 2020). A standard operating procedure was followed to ensure a standardized sample collection. YOY yellowfin tuna (n = 113) were collected from 4 geographically distinct nursery areas in the Indian Ocean: Madagascar, Seychelles-Somalia, Maldives, and Sumatra (**Figure 4.1**). In this study, we define nursery areas as primary regions inhabited by YOY yellowfin tuna in the Indian Ocean, which are therefore considered as important habitat during the first year of life (Wells et al., 2012). Sampling was conducted over short periods during two consecutive years, 2018 and 2019 (**Table 4.1**). Fish were measured (fork length (FL); to the nearest

centimetre), and sagittal otoliths were extracted with stainless steel tweezers, cleaned of adhering organic tissue, rinsed with ultrapure water (Milli-Q), and stored dry in plastic vials. An effort was made to limit the size range (<38 cm FL), to ensure that the fingerprint of the YOY tuna reflected the chemical signature of the nursery ground where fish were captured. The rationale for the latter is that YOY are characterised by a limited swimming ability and are less likely to have moved far from their larval nursery grounds than larger, older individuals (Kitchens et al., 2018; Pecoraro et al., 2018).

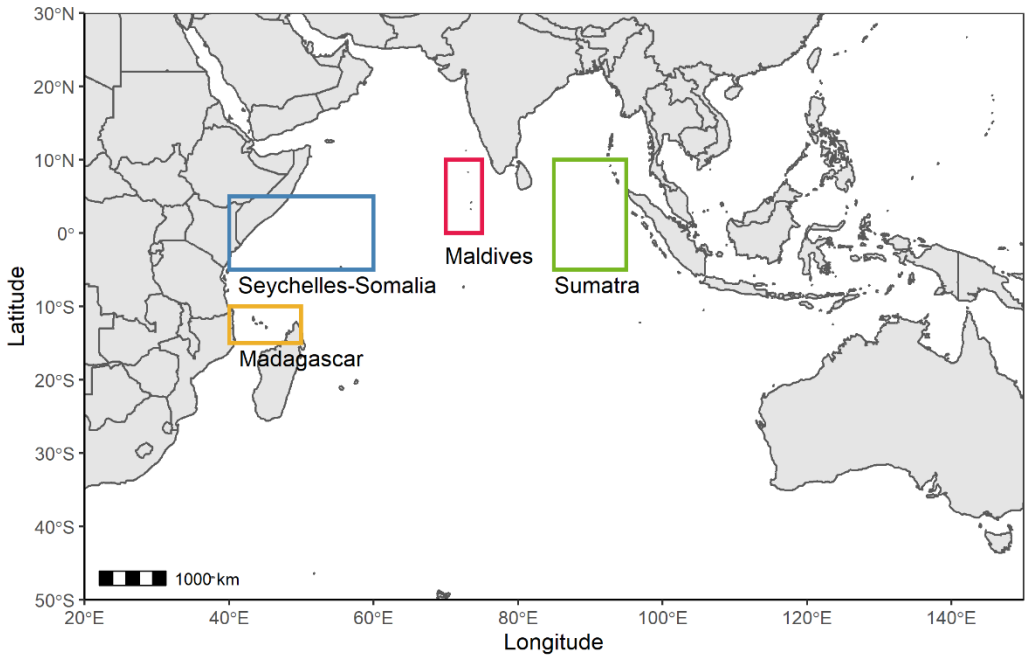

Figure 4.1. Location of the four nursery areas for young-of-the-year (YOY) yellowfin tuna (*Thunnus albacares*) in the Indian Ocean, referred to as: Madagascar (yellow), Seychelles-Somalia (blue), Maldives (pink), and Sumatra (green).

Table 4.1. Summary of young-of-the-year (YOY) yellowfin tuna (*Thunnus albacares*) collected from 4 nursery regions of the Indian Ocean: Madagascar, Seychelles-Somalia, Maldives, and Sumatra. Size is fork length (FL) in cm. Cohort was back-calculated using the age-length curve described in this study.

Region	Cohort	Sampling period	n	Mean FL (sd)
Madagascar	2017	Mar 2018	19	30.6 (3.2)
	2018	Apr 2019	-	-
Somalia-Seychelles	2017	Mar-Apr 2018	18	33.2 (2.2)
	2018	Mar-Apr 2019	14	30.4 (1.8)
Maldives	2017	Aug 2018	15	34.8 (0.9)
	2018	Feb 2019	16	30.9 (1.5)
Sumatra	2017	Apr 2018	16	27.0 (3.6)
	2018	Nov 2018	15	30.6 (2.9)

2.2 YOY age estimates

To be able to estimate the approximate age of the fish examined for otolith microchemistry, an age-length relationship curve was developed. For that, otolith sections (n = 5, from the Western Indian Ocean) were prepared following a 4-step process described by Proctor et al. (2019); (1) otoliths were fixed on the narrower edge of a crystal slide using thermoplastic glue (Crystalbond 509; Buehler) with the anterior side of the otolith hanging over the edge (with the primordium just on the inside of the glass edge), (2) the otolith was then grounded down to the edge using 1200 and 600 grit sandpaper moistened with distilled water, and, when the edge of the slide was reached, (3) the slide was reheated and the otolith was removed and placed (grounded side down) on another slide using thermoplastic glue, (4) once cooled, the otolith section was grounded horizontally to the grinding surface until the primordium was exposed, using a series of 3M® silicon carbide lapping discs (9, 3 and 1 µm) moistened with ultrapure water on a lapping wheel, and were further polished with a micro cloth and 0.3 µm aluminium powder to ensure a smooth surface. Age interpretation was based on digital photographs taken under a transmitted light microscope at different magnifications (x10, x20 and x40). Images were analysed using GNU Image Manipulation Program GIMP version 2.10.12. Age was determined by counting microincrements along the ventral (longer) arm of the section on a path from the primordium to the edge margin (Appendix C, Figure C1). These counts were combined with direct increment counts on otoliths from Proctor et al. (2019) (n = 9, from the Eastern Indian Ocean), and *in situ* development observations from Kobayashi et al., 2015 (n = 3, tank reared) (Appendix C, Table C1). In addition, the count (age in days) was noted at two other points along the counting path of the five otoliths directly examined: at 65 microns from the primordium towards the ventral arm of the otolith, and at the first inflection point of the growth axis, where the direction of growth changes.

2.3 Otolith preparation for microchemical analyses

When both otoliths were available one was used for trace element analyses and the second for $\delta^{13}C$ and $\delta^{18}O$ analyses. When a single otolith was available, all chemical analyses were sequentially conducted on the same otolith. Otoliths from each fish were embedded in two-part epoxy resin (Araldite 2020, Huntsman

Advanced Materials, Switzerland). Resin blocks were polished using 3M® silicon carbide sandpaper (particle size = 220 µm) and a lapping wheel with a series of decreasing grain diameter (30, 15, 9, 3 and 1 µm) 3M® silicon carbide lapping discs, moistened with ultrapure (Milli-Q) water, to obtain a transverse section where the primordium was exposed. Sections were ultrasonically cleaned using ultrapure (Milli-Q) water for 10 minutes. Following sonication, otolith sections were left to air dry in loosely capped vials for 24 h before being glued in a sample plate using Crystalbond thermoplastic glue (Crystalbond 509; Buehler).

2.4 Multielemental 2D imaging

Otoliths of three individuals were selected to perform two-dimensional mapping of multiple elements. These fish were collected in Seychelles-Somalia, Maldives, and Sumatra, during May, August, and April 2018, and were 37, 35, and 32 cm FL respectively. Elemental concentration was measured using a high resolution inductively coupled plasma mass spectrometer fitted with a jet interface using a N2 flow rate of 10 ml/min (HR-ICPMS, Element XR, Thermo Scientific, Bremen, Germany), coupled to a high repetition rate 1030 nm femtosecond laser (fs-LA) system (Alfamet, Neseya, Canejan, France) available at the Institut des Sciences Analytiques et de Physico-Chimie pour l'Environnement et les Matériaux, Université de Pau et des Pays de l'Adour/CNRS (Pau, France). Imaging by fs-LA-HR-ICP-MS was performed to analyse the elemental distribution of ^{7}Li, ^{24}Mg, ^{88}Sr, ^{138}Ba ^{55}Mn, ^{63}Cu, ^{66}Zn to calcium ratios along the ventral arm of otolith transverse sections, which represents the growth axis of the fish (**Figure 4.2A**). The laser was operated at a repetition rate of 200 Hz, energy of 30 µJ per pulse and a beam size of 15 µm. The scanner was used in a fast and continuous back and forth movement of 15 µm at a speed of 1 mm/s in order to simulate an elongated laser beam (15 x 30 µm). Images were built from the fs-LA-HR-ICPMS signal resulting from the samples ablation according to a series of horizontal lines vertically distributed with 30 µm spacing (center to center). Considering that the washout time of the laser cell (based on the 99% criterion) was about 1 s and the ICPMS was set to acquire 0.67 point per second, the sample translation was set to 20 µm s^{-1}. This resulted in image resolution of 30 µm (square pixels of 30 µm). In these conditions the signal corresponding to an image of 2.4 x 1.4 mm was acquired 96 min. Data reduction including background

subtraction, conversion to ppm and standardization to calcium (element:Ca µmol mol^{-1}) was done using an in-lab developed software FOCAL 2.27. The image matrix was then exported to the free ImageJ software (W. Rasband, National Institute of Health, USA) for better visualisation and color processing.

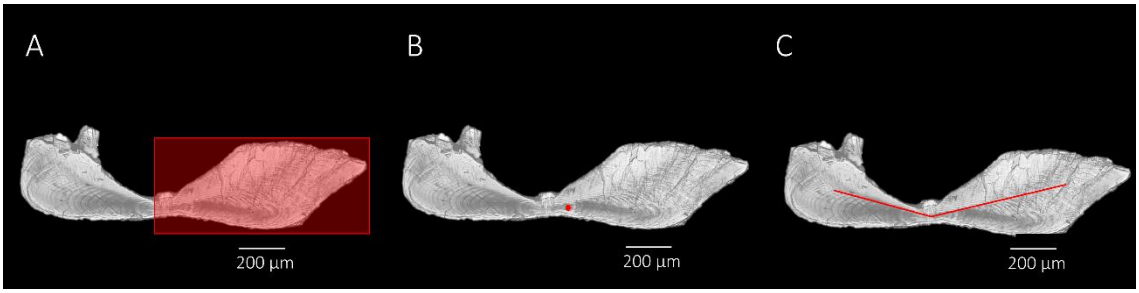

Figure 4.2. Saggital otolith transverse section from a young-of-the-year (YOY) yellowfin tuna (*Thunnus albacares*) showing (A) portion used for 2D chemical mapping, (B) the approximate location of laser ablation spot for trace element analyses, and (C) the MicroMill drilling path used for stable isotope analyses.

2.5 Trace element analyses

Otoliths were analysed for early life trace element composition with a fs-LA-HR-ICPMS. Laser ablation conditions were 200 Hz, a laser beam diameter of 15 µm and 30 µJ per pulse energy corresponding to a fluence of 14 J/cm^2, until the depth limit of ablation (<30 µm). The laser was fitted with a 2D galvanometric scanning beam device, allowing the fast movements of the laser beam (up to 500 µm s^{-1}) ablating the surface of the sample in a series of six concentric circles trajectories (Claverie et al., 2009). This resulted in the ablation of a crater 30 µm in diameter and 30 µm deep. This spot was ablated 65 µm from the primordium along the ventral arm (**Figure 4.2B**), covering a signal of approximately 2-3 days acording to Proctor et al. (2019). This spot was considered to be representative of the larval phase (see Results) and excluded the potential maternal effects the primordium may incorporate (Hegg et al., 2018). The ablation cell was flushed with argon to transport laser-induced particles to the HR-ICPMS. The fs-LA-HR-ICPMS was tuned daily to reach optimal particle atomization conditions and minimal elemental fractionation. This was obtained for a U/Th signal ratio of 1 ± 0.05 using NIST 612. The mass spectrometer was used in the medium-resolution mode (R = 4000) to ensure a complete polyatomic interference removal for the isotopes of interest. Relative abundances of 7 isotopes (^{7}Li, ^{24}Mg, ^{88}Sr, ^{138}Ba ^{55}Mn, ^{63}Cu, ^{66}Zn) were estimated, as well as ^{43}Ca, which was used as the internal standard. The concentration of ^{43}Ca in

the otolith was assumed to be constant at 38.3% (Sturgeon et al., 2005). Data reduction including background subtraction, conversion to ppm and standardization to calcium (element:Ca μmol mol^{-1}) was done using an in-lab developed software FOCAL 2.27. National Institute Standards and Technology (NIST) 610 and 612 glass standards with known chemical composition were used for calibration. Measurement precisions were determined based on an otolith certified reference material for trace elements (FEBS-1, NRC-CNRC, Canada). To correct for short-term instrumental drift, standards and reference material were measured threefold at the beginning, the middle and the end of each session (i.e. every 3-5 hours). Trace element measurements of the blank sample gases were recorded for 20-30s before each sample ablation of ~40s. Mean relative standard deviation (RSD) for NIST 612 and 610 were (n = 10): 5.8% and 4.6 % (Li), 4.7% and 7.1% (Mg), 4.3% and 2.8% (Sr), 2.6% and 4.1% (Ba), 2.8% and 2.3% (Mn), 6.5% and 4.5% (Cu) and 6.8% and 4.16% (Zn), respectively. All elemental ratios exceeded the detection limits of the fs-LA-HR-ICPMS for all samples.

2.6 Stable isotope analyses

Microsampling of otolith powder $\delta^{13}C$ and $\delta^{18}O$ stable isotope analysis was performed using a high-resolution computerised micromill (New Wave MicroMill System, NewWave Research G. C. Co., Ltd, Cambs, UK). The length of the smallest yellowfin tuna (19.5 cm FL) otolith section was used to create a template that was then used for the remaining otoliths to ensure that the same portion of the otolith was analysed in every fish. This drill path covered an area of the otolith that was estimated to represent the material accreted during the first ~2 months of life, based on direct age estimates (**Figure 4.2C**). A larger time period of the otolith was sampled for stable isotopes than for trace elements due to differences in sample material requirements. Ten drill passes were run at a depth of 50 μm per pass over a preprogramed drill path using a 300-μm diameter carbide bit (Komet dental; Gebr. Basseler, Lemgo, Germany). Powdered material was then analysed for $\delta^{13}C$ and $\delta^{18}O$ on an automated carbonate preparation device (KIEL-III, Thermo- Fisher Scientific, Waltham, MA, USA) coupled to a gas-ratio mass spectrometer (Finnigan MAT 252, ThermoFisher Scientific) at the Environmental Isotope Laboratory of the University of Arizona. All isotope values were reported according to standards of the

International Atomic Energy Agency in Vienna. The isotope ratio measurement was calibrated based on repeated measurements of NBS-19 and NBS-18 (International Atomic Energy Agency standards). Measurement precision was ±0.08‰ for $\delta^{13}C$ and ±0.10 ‰ for $\delta^{18}O$ (1 sigma).

2.7 Statistical analyses

All statistical analyses were performed using open access R software version 3.6.1 (R Core Team, 2019). Prior to all multivariate analyses, otolith microchemistry data was scaled (i.e., for each element, the data was centred by subtracting the mean and scaled by dividing by the standard deviation) to give the same weight to all elements and stable isotopes.

Normality and homoscedasticity of the data were tested using Shapiro-Wilks and Fligner-Killen tests, respectively. Not all elements and stable isotopes met the parametric assumptions (Appendix C, Table C2 and C3). Consequently, to enable the combination of all elements for multivariate analyses, non-parametric tests were used. Interaction effects between nurseries and years in otolith microchemistry data was analysed using a two-factor Permutational Multivariate Analysis of Variance (PERMANOVA) design for each element/isotope individually and all elements combined using the function *adonis* {vegan} (Anderson, 2001). Nursery and cohort were fixed factors in the full factorial model, and resemblance matrix was based on Euclidean distance dissimilarities. The number of unrestricted permutations was set to 999 random repeats. Statistical significance was determined based on adjusted P values after the Benjamini-Hochberg correction (Benjamini and Hochberg, 1995). When significant differences were found, post-hoc pairwise comparisons were applied to identify the source of differences between nursery means using *pairwise.adonis* {pairwiseAdonis} in the case of multivariate data, and *lincon* {WRS2} function (trimmed level of the mean = 0.1) in the case of individual elementsand stable isotopes. These analyses were performed separately for each cohort. In addition, we compared the similarity on the multielemental chemical signature of the otolith for all pairs of individuals within each nursery and between pairs of nurseries, by calculating the elemental fingerprinting index (EFI) as described by Moll et al. (2019). The EFI is a measure of similarity between 2 given fish that ranges between 0 and 1, where a value of 0 indicates maximum

dissimilarity and 1 highest similarity. Multivariate data were reduced to two-dimension and visualized with a canonical Analysis of Principal Coordinates (CAP) using *CAPdiscrim* {BiodiveristyR} function (Anderson and Willis, 2003). We then assessed the degree of importance of each element for correctly assigning YOY yellowfin tuna to their nursery area. For that, random forest (RF) classifications were developed (Breiman, 2001), which perform best in the presence of skewness (Jones et al., 2017). Data was split into a training dataset (75%) and a testing dataset (25%). We implemented the classification algorithm with the *randomForest* {randomForest} function (number of trees = 500, mtry = 2) and assessed the degree of importance of each element for correctly assigning YOY yellowfin tuna to their nursery area with *importance* {randomForest} function. Variable importance was determined for each element as the mean decrease in accuracy (MDA), when that element was permuted across all trees, and all other elements were left unchanged (Liaw and Wiener, 2002). This procedure was randomly repeated 1000 times and average MDA values for each element were extracted. Elements contributing to a cumulative importance >90% were kept for subsequent classification analyses which aimed to test the ability of the selected elements to discriminate among nursery areas. For that, data containing only selected elements was split again intro a training dataset (75%) and a testing dataset (25%), and this procedure was randomly repeated 1000 times. At each time, the rate of classification success (i.e. rate of correct predicted membership to nurseries in which the fish were collected) was calculated, and mean values were extracted. The overall performance of RF to discriminate between groups was also evaluated using weighted Cohen´s Kappa (κ) statistic, a method that accounts for the agreement occurring just by chance (Titus et al., 1984). RF was performed separately for each cohort.

3. Results

3.1 YOY age estimates

The YOY yellowfin tuna used for otolith analyses ranged from 19.5 to 37.5 cm FL, which according to the age-length relationship described in this study (**Figure 4.3**), were estimated between 52 and 107 days, or 1.7-3.6 months. Mean hatch dates differed between nurseries and years (Appendix C, Figure C2). Samples collected in 2018 hatched from November 2017 to May 2018 and were assigned to the 2017 cohort (hereafter "2017"). Samples collected in 2019 were hatched from August 2018 to January 2019 were assigned to the 2018 cohort (hereafter "2018"). Mean age at 65 microns from the primordium was estimated to be 10.2±1.3 days, and to the inflection point was 29.8±3.0 days; these were considered representative of the larval and early juvenile phases respectively (**Table 4.2**).

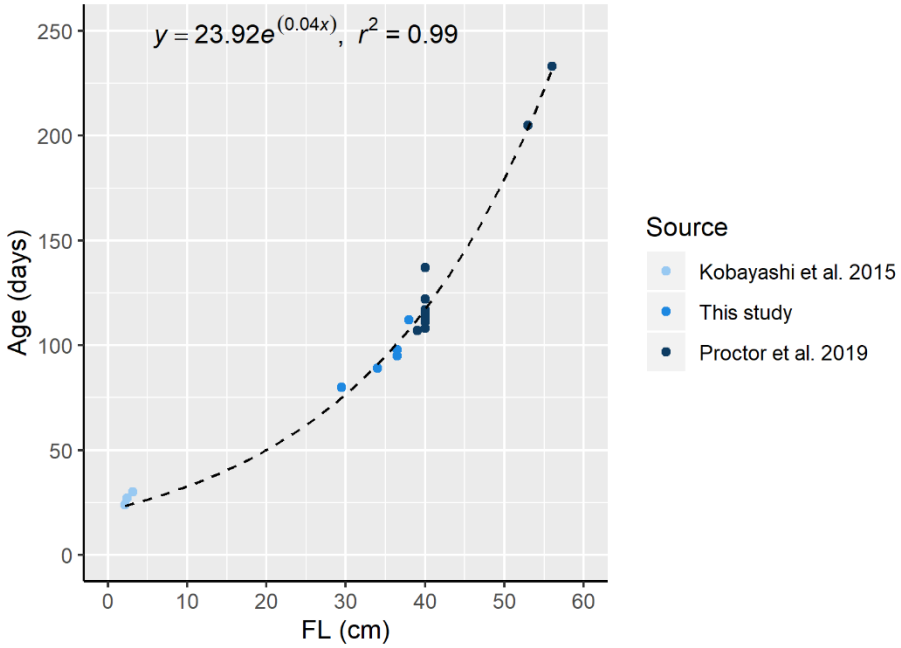

Figure 4.3. Age-length relationship for young-of-the-year (YOY) yellowfin tuna (*Thunnus albacares*) based on *in situ* measures calculated from Kobayashi et al. 2015 cultured yellowfin tuna larvae, and daily age estimates derived from otolith micro-increment counts made by Proctor et al. 2019 and this study.

Table 4.2. Daily increment counts at 65 µm from the primordium and at the inflection point (IP) on otolith transverse sections of young of the year (YOY) yellowfin tuna (*Thunnus albacares*). Size is fork length (FL) in cm. Mean and standard deviation (sd) are also shown at the end of the table.

FL	Days at 65 µm	Days at IP
29.5	12	30
34	11	26
36.5	10	34
36.5	9	31
38	9	28
34.9 (3.0)	*10.2 (1.3)*	*29.8 (3.0)*

3.2 Elemental distribution across otoliths

Two-dimensional mapping of trace elements with fs-HR-LA-ICPMS revealed temporal and/or spatial heterogeneity of elemental distributions across otolith sections for the three individuals analysed (**Figure 4.4**). In all three fish, concentrations of Li were higher during the first month of life (**Figure 4.4Li**), while Sr and Ba concentrations were higher in the otolith portion associated with early larval life stage, with a decrease after ~10 days post hatch (**Figure 4.4Sr and Ba**). Concentrations of these elements were low around the first month of life, but Sr increased again otolith edge in two of the individuals analysed (**Figure 4.4SrB and SrC**) and an increase in concentrations was detected for Ba after fish transitioned into the juvenile stage, increasing thereafter to the otolith edge (**Figure 4.4Ba**). Concentrations of Mg and Mn showed distinct distribution patterns on two different planes (**Figure 4.4Mg and Mn**). A gradient of concentration that was perpendicular to the growth axis was evident, from low values on the proximal side of the otolith, to larger values on the distal side of the otolith. On the distal side, temporal variations of Mg and Mn were visible. Concentrations of Mg were highest in the otolith portion corresponding to the early larval stage, whereas maximum values of Mn were detected after it. Concentrations of Cu and Zn were consistently low across the whole section (**Figure 4.4Cu and Zn**). Overall, high trace element concentrations were detected at the otolith margins, but in most cases these high values were likely to be an artefact related to a decrease of calcium carbonate concentration (Appendix C, Figure C4).

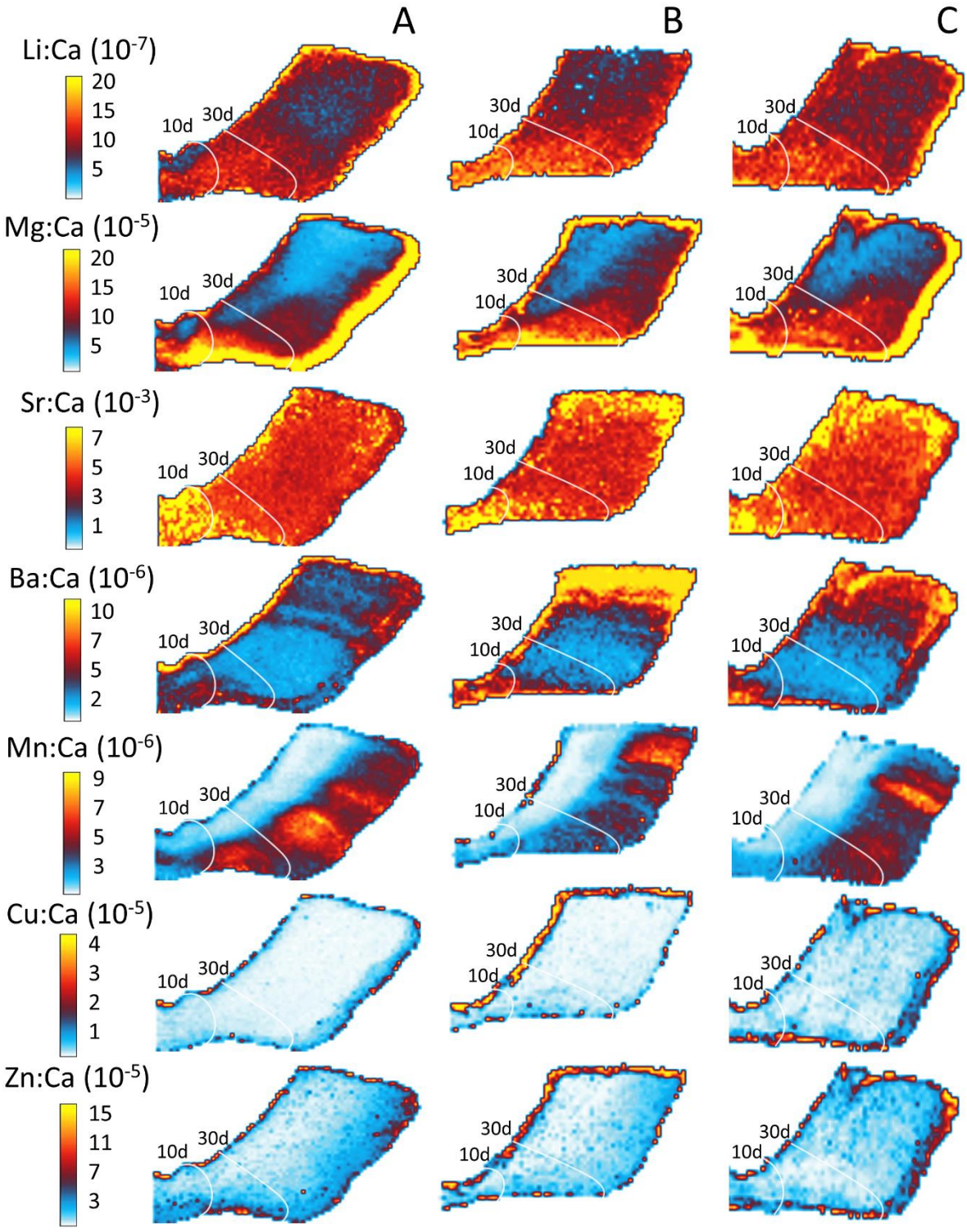

Figure 4.4. Trace element 2D maps of ^{7}Li, ^{24}Mg, ^{88}Sr ,^{138}Ba, ^{55}Mn, ^{63}Cu and ^{66}Zn ratios to ^{43}Ca, of three young-of-the-year (YOY) yellowfin tuna (*Thunnus albacares*) caught in Seychelles-Somalia (A), Maldives (B) and Sumatra (C). Fish were collected during May, August, and April and with a size of 37, 35 and 32 cm fork length, respectively. Image shows the ventral arm of sagittal otolith transverse sections. Colour indicates element concentration (ppm), ranging from low (white) to high (yellow). Approximate position of 10- and 30-days growing bands is noted.

3.3 Variation in nursery signatures

Significant differences were detected between nurseries and/or cohorts for some of the elements and stable isotopes analysed (PERMANOVA, $p<0.05$, **Table 4.3**). Concentrations of Li varied differently at each cohort (PERMANOVA, df=2, p=0.023, **Figure 4.5**). There were significant differences in Mg and Sr concentrations between nurseries (PERMANOVA, df=3, p=0.030 and p=0.002 respectively). Concentrations of Mg were higher in Sumatra than in Maldives (**Figure 4.5**, while Sr was higher in Maldives than in Seychelles-Somalia (**Figure 4.5**), but both differences were only significant in 2018 (heteroscedastic one-way anova post-hoc, p=0.027 and p=0.039 respectively). Sr concentrations differed significantly between cohorts (PERMANOVA, df=1, p=0.018), concentrations being higher in 2018 (**Figure 4.5**). No differences in Ba concentrations were detected; concentrations were similar in all nurseries and between cohorts (**Figure 4.5**, **Table 4.3**). Concentrations of Mn differed between nurseries (PERMANOVA, df=3, p=0.001), but significant interaction between nursery and cohort was also detected (PERMANOVA, df=2, p=0.001). In 2017, Mn concentrations were higher in Sumatra than in any other nursery, while in 2018 concentrations were higher in Maldives than in Seychelles-Somalia (**Figure 4.5**). Carbon and oxygen stable isotopes values differed significantly between nurseries (PERMANOVA, df=3, p=0.001, and p=0.001, respectiely), with higher values in the western nurseries (Madagascar and Seychelles-Somalia) and decreasing towards the east (**Figure 4.5**). Observed temporal variations were mainly derived by differences in fish belonging to the Maldives nursery, with Li, Mg, Sr, and Mn concentrations differing among fish from different cohorts (Appendix C, Table C4).

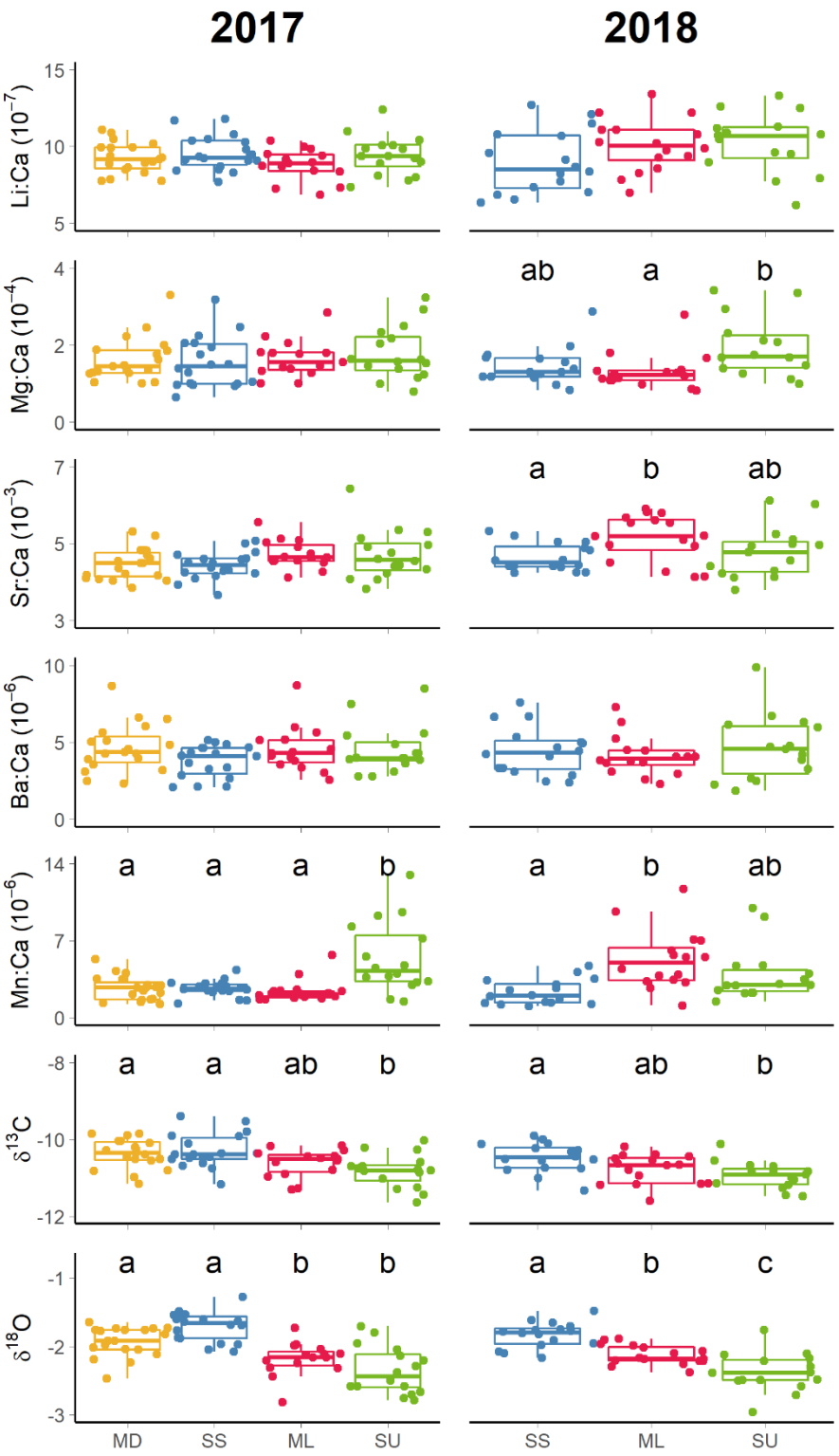

Figure 4.5. Regional comparisons of otolith element:Ca ratios and stable isotope (‰) composition for young-of-the-year (YOY) yellowfin tuna (*Thunnus albacares*) collected in four nursery areas, Madagascar (MD, yellow), Seychelles-Somalia (SS, blue), Maldives (ML, pink) and Sumatra (SU, green), of the Indian Ocean. 2017 cohort (left panel) and 2018 cohort (right panel). Letters identify significant differences ($P < 0.05$) between regions. Inter quartile range (25th and 75th percentile) is shown by extent of boxes and error bars represent 10th and 90th percentiles. Median (50th percentile) is also shown. Dots represent individuals.

Table 4.3. Summary of two-factor PERMANOVA for the effect of nursery and cohort on individual and combined trace element and stable isotopes of yellowfin tuna (*Thunnus albacares*) otoliths. Nursery region and cohort were fixed factors within the full factorial design. Significant effects are highlighted as follows; *P < 0.05, **P < 0.01

Element	Source	df	F	P-value
Li	Nursery	3	0.87	0.470
	Cohort	1	2.38	0.119
	Nursery x Cohort	2	3.50	0.023*
Mg	Nursery	3	2.79	0.030*
	Cohort	1	0.12	0.730
	Nursery x Cohort	2	1.98	0.141
Sr	Nursery	3	5.20	0.002**
	Cohort	1	5.22	0.018*
	Nursery x Cohort	2	0.95	0.397
Ba	Nursery	3	0.80	0.517
	Cohort	1	0.19	0.686
	Nursery x Cohort	2	1.07	0.358
Mn	Nursery	3	8.27	0.001**
	Cohort	1	0.63	0.418
	Nursery x Cohort	2	10.07	0.001*
$\delta^{13}C$	Nursery	3	11.45	0.001**
	Cohort	1	3.65	0.069
	Nursery x Cohort	2	0.06	0.942
$\delta^{18}O$	Nursery	3	36.76	0.001**
	Cohort	1	0.45	0.495
	Nursery x Cohort	2	1.13	0.336
All	Nursery	3	7.37	0.001**
	Cohort	1	1.83	0.113
	Nursery x Cohort	2	2.62	0.006**

When all individual trace elements and stable isotopes were combined into a single matrix, multielement otolith composition varied significantly between regions (PERMANOVA, df=3, p=0.001). The interaction between nursery and cohort was also significant (PERMANOVA, df=2, p=0.006). Posterior pairwise comparisons showed that in both cohorts, fish from Seychelles-Somalia, Maldives, and Sumatra nurseries were significantly different in their multielemental composition (**Table 4.4**). Madagascar, from which only one cohort was sampled, was not differentiated from Seychelles-Somalia (pairwise PERMANOVA, p=0.144), but was different from Maldives and Sumatra (**Table 4.4**). Multielemental composition of individuals within the same nursery varied mostly in Sumatra, which was also characterised by having the most distinct individuals (lower EFI values) when comparing individual fingerprints between nurseries (**Figure 4.6**). This differentiation of fish from Sumatra nursery was mainly driven by Mn in 2017 and Mg in 2018 (**Figure 4.7**). Individuals fingerprints were more similar among and within fish from Madagascar and Seychelles-Somalia nurseries (**Figure 4.6**), that were mainly differentiated from fish from the other nurseries by their $\delta^{13}C$ and $\delta^{18}O$ values (**Figure 4.7**). Concentrations of Mn and Sr were the main drivers of differentiation of fish from Maldives in 2018 (**Figure 4.7**).

Table 4.4. Summary of pairwise PERMANOVA for multielemental signature comparison of yellowfin tuna (*Thunnus albacares*) otoliths collected in four distinct nursery areas. Significant differences are highlighted as follows; *P < 0.05, **P < 0.01

	F. Model	P value	Adjusted P-value	Significance
2017				
Madagascar vs Seychelles-Somalia	1.66	0.144	0.144	
Madagascar vs Maldives	2.30	0.034	0.041	*
Madagascar vs Sumatra	5.42	0.001	0.002	**
Seychelles-Somalia vs Maldives	6.14	0.001	0.002	**
Seychelles-Somalia vs Sumatra	8.44	0.001	0.002	**
Maldives vs Sumatra	2.93	0.028	0.041	*
2018				
Seychelles-Somalia vs Maldives	6.75	0.001	0.002	**
Seychelles-Somalia vs Sumatra	6.96	0.001	0.002	**
Maldives vs Sumatra	3.04	0.001	0.011	*

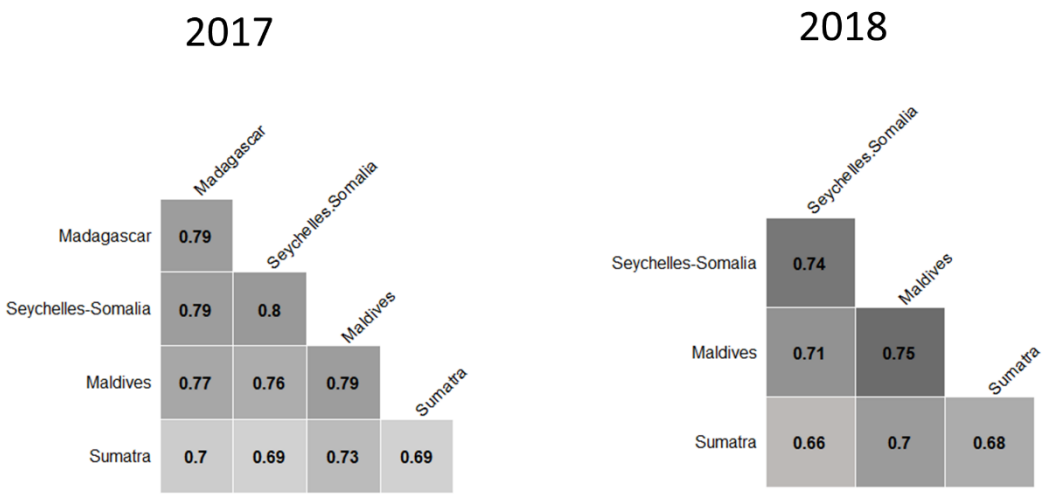

Figure 4.6. Mean values of elemental fingerprinting indices (EFI) calculated within each nursery and among nurseries. The EFI ranges from 0 to 1, where a value of 0 indicates that two compared individuals are most different in otolith elemental composition, whereas a value of 1 indicates highest similarity in elemental composition of two comparing individuals.

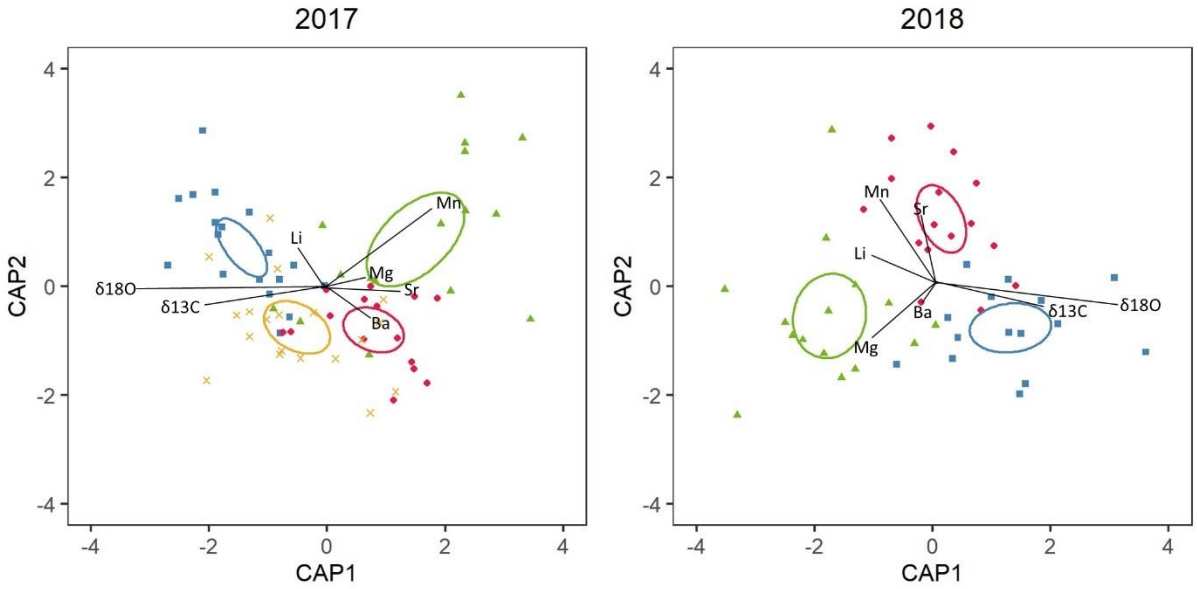

Figure 4.7. Canonical analysis of principal coordinates (CAP, constrained ordination) plots showing multi-elemental (Li, Mg, Sr, Ba, Mn, $\delta^{13}C$, and $\delta^{18}O$) chemistry composition of young-of-the-year (YOY) yellowfin tuna (*Thunnus albacares*) otoliths from four nursey areas in the Indian Ocean; Madagascar (yellow cross), Seychelles-Somalia (blue squares), Maldives (pink circles) and Sumatra (green triangles) for 2017 (left) and 2018 (right) cohorts. Ellipses represent 95% confidence limits around each multivariate mean, and biplot vectors show the relative influence of each element to nursery discrimination.

Due to the absence of difference in the multielemental signature from fish from Madagascar and Seychelles-Somalia nurseries, the latter were combined and treated as a single group, hereafter "West Indian Ocean", for classification purposes. Oxygen was shown to be the most important variable in predicting nursery origin based on calculated mean decrease in accuracy score, regardless of the cohort. Mn and Sr were also also selected in both classification models (**Table 4.5**). High classification success (i.e., ≥80) was observed for samples from the Western Indian Ocean regardless of the cohort, while nursery specific classification accuracy was moderate for samples from Maldives in both cohorts (**Table 4.5**). Classification accuracy greatly varied by cohort for YOY from Sumatra nursery, 58% in 2017 and 70% in 2018. Overall classification success was higher in 2018 (71%, $\kappa = 0.56$) than in 2017 (69% and $\kappa = 0.51$).

Table 4.5. Random forest classification success in assigning young-of-the-year (YOY) yellowfin tuna (*Thunnus albacares*) collected in the Indian Ocean to their nursery of origin based on otolith chemical composition. Results are shown for each sampling cohort and both cohorts combined. The element combination that resulted in a Mean Decrease in Accuracy (MDA) cumulative value >90%, by order of importance, is shown. Data represent the percentage (%) of correctly assigned individuals to their nursery area; West Indian Ocean (Madagascar + Seychelles-Somalia), Maldives, and Sumatra. Overall accuracy and kappa index (κ) are also shown.

Cohort	Element combination	West Indian Ocean	Maldives	Sumatra	Overall	κ
2017	$\delta^{18}O$, Mn:Ca, Sr:Ca	80	55	58	69	*0.51*
2018	$\delta^{18}O$ Mn:Ca, Mg:Ca, Sr:Ca	80	62	70	71	*0.56*

4. Discussion

The aim of this study was to describe chemical signatures in YOY yellowfin tuna otoliths captured in main nursery areas of the Indian Ocean so that they can be used as a baseline to retrace the nursery origin of older fish. Firstly, we obtained daily age information on otoliths to provide an approximate scale to assist the interpretation of otolith microchemistry. We then considered the elemental distribution across otolith sections, to better select the elements and the portion of

the otolith on which to perform spot analyses. We finally assessed the potential of chemical signatures to discriminate among different YOY yellowfin tuna nursery areas in the Indian Ocean.

4.1 YOY age estimates

Yellowfin tuna growth related information has been very limited in the Indian Ocean until the data obtained from the Indian Ocean Tuna Tagging Program (IOTTP) became available (Eveson et al., 2015; Sardenne et al., 2015). However, the aim of these studies was to provide relevant information for stock assessment models, and, as such small size categories have often received less attention. The preliminary age-length curve described in the current study for YOY indicate that yellowfin tuna between 19.5 and 37 cm FL were 52 to 107 days old. Our results are similar to those obtained for small yellowfin from the western Pacific Ocean (Yamanaka, 1990). The portion of the otolith that was 65 μm from the primordium was estimated to represent the signature corresponding to the first ~10 days after hatching. Our results are similar those described by Proctor et al., 2019 (i.e., 9 days). The shift from yolk-sac phase to preflexion larvae is described to occur at 4 days post hatching in yellowfin tuna (Kaji et al., 1999). By placing the spot for microchemical analyses at a location ~10 days from the primordium we reduced the potential effect of maternal investment (via the yolk sack), which may diminish the ability to delineate natal origins (Hegg et al., 2018; Ruttenberg et al., 2005). The position on the transverse section where a shift in growth direction can be observed (i.e., the inflection point) was estimated to correspond to ~30 days of life of YOY yellowfin tuna. This point represents the metamorphosis from larval to early juvenile, which has been described also to occur around one month after hatching in laboratory reared yellowfin tuna (Kaji et al., 1999).

4.2 Elemental distribution across otoliths

The use of transversal sections is a well-established practice in tuna otolith microchemistry studies (Fraile et al., 2016; Kitchens et al., 2018; Macdonald et al., 2013; Rooker et al., 2016). However, to our knowledge, elemental distribution patterns throughout these sections in tuna otolith transverse sections had not been described to date. Concentrations of Li, Sr and Ba proved to be relatively

homogeneously incorporated within growth increments. These elements are primarily bounded into the salt fraction of the otolith, Li likely incorporated by random trapping in interstitial spaces, and Sr and Ba by random replacement of Ca (Doubleday et al., 2014; Hüssy et al., 2020; Izzo et al., 2016). We showed that otolith Li concentrations were higher during the first month of life in all three fish, with a decrease thereafter. Otolith growth rates may influence Li incorporation, the latter decreasing with age (Macdonald et al., 2020). Concentrations of Sr and Ba were high during the first 10 days of life, lowest in the adjacent portion and then increased again after the first month of life toward the edge of the otolith. Localized core enrichment of Ba relative to adjacent regions of the otolith has been described (Ruttenberg et al., 2005). Otolith cores have also been recorded to be enriched in Mn (Brophy et al., 2004; Limburg et al., 2011; Ruttenberg et al., 2005), and as such, this element has been used as a marker for otolith primordium detection (J. I. Macdonald et al., 2008; Rogers et al., 2019). However, we did not observe this pattern in any of the three YOY yellowfin tuna Mn distribution maps, but the maximum values of Mn were shown in parts of the otolith other than the core. Most of the otolith microchemistry studies that describe otolith core Mn enrichment, however, belong to benthic or demersal fish species with very different life strategies compared to yellowfin tuna. Indeed, studies on tuna species show elevated Mn concentrations not just in the primordium, but some weeks after (Artetxe-Arrate et al., 2019; Macdonald et al., 2013; Wang et al., 2009). The distribution of Mg and Mn in the otolith showed a gradient of concentration within the growth bands, with lower concentrations closer to the proximal side of the transverse section. Otolith chemical heterogeneity has also been described in other species, although the ultimate cause of these variations is still unknown (Di Franco et al., 2014; Limburg and Elfman, 2017). Both Mg and Mn are important co-factors required for the enzymatic activity involved in the biomineralization process and, as such, influenced by physiological control on uptake mechanisms and can be incorporated into the proteinaceous fraction of the otolith (Hüssy et al., 2020; Loewen et al., 2016; Thomas and Swearer, 2019). It has been suggested that the preferential binding of the elements into either the protein or mineral component can result in heterogeneous distribution of elements throughout the otolith structure (Izzo et al., 2016). Finally, Cu and Zn concentrations were generally low within the whole otolith section. Elsdon et al.

(2008) described that Cu and Zn may leach out from the otolith during storage. Moreover, these elements are bound to soluble otolith proteins, and are important co-factors in many enzymes (Hüssy et al., 2020; Miller et al., 2006). Thus, it has been suggested that the inclusion of these elements into natal delineation studies may add noise and obscure spatial variation in chemical signatures (Thomas et al., 2020). Given this, Cu and Zn were discarded for posterior analyses aiming to describe the natal signatures of YOY yellowfin tuna from the Indian Ocean. The concentration of most of the elements was especially high in the margins of the otolith section.

Following recent progress on instrumentation and mapping softwares, two dimensional spatial images of elemental distributions are increasingly being used to provide valuable visualizations of chemical heterogeneity across the otolith (McGowan et al., 2014; Walther, 2019). The observed variations in YOY yellowfin tuna otolith sections may be useful to select the portion of otoliths for spot ablations or transects analyses that maximizes discrimination among groups, at the same time as minimizing the noise introduced by the intrinsic factors of individual fish.

4.3 Variation in nursery signatures

Regional differences in otolith chemistry were detected for YOY yellowfin tuna collected from four nursery areas in the Indian Ocean. The multielemental chemical signatures of YOY yellowfin tuna from Seychelles-Somalia, Maldives and Sumatra were significantly different for both cohorts analysed, while fish from Madagascar were not differentiated from those from Seychelles-Somalia, contrary to what was shown in a previous study (Artetxe-Arrate et al., 2019). In that study, however, YOY yellowfin tuna from both nursery areas were from different cohorts, and results from the present study highlight that cohort effect may strongly influence otolith trace element data composition. In any case, the absence of difference does not necessarily imply that fish shared a common origin, but that the technique is of negligible value to discriminate among these two nurseries at this time (Campana et al., 2000). Likewise, the variability in the chemical signature within individuals from Sumatra was almost as high as the difference with samples from any other nursery. It is possible that factors other than ambient water chemistry, such as metabolic sources, variation in genotype, growth rates and/or physiological processes, have influenced the observed among-individual variability

in fish from Sumatra nursery (Clarke et al., 2011; Jed I. Macdonald et al., 2008; Sturrock et al., 2015). Indeed, high Mn and Mg concentrations were the main drivers of differentiation of YOY yellowfin tuna from Sumatra nursery for the 2017 and 2018 cohorts respectively, noting uptake mechanisms for these elements into the otoliths are under considerable physiological control (Hüssy et al., 2020). High concentrations of Mn were also detected for 2018 cohort YOY from Maldives relative to other nurseries. Manganese availability increases in the presence of hypoxia and other redox environments (Limburg and Casini, 2018), and therefore otolith Mn concentrations have been identified as a potentially reliable proxy of fish exposure to hypoxia (Limburg et al., 2011, 2015). Nevertheless, it is unlikely that differences in exposure to hypoxia is driving the observed Mn pattern in YOY yellowfin tuna from different nurseries. We specifically sampled otoliths at a life stage corresponding the first 10 days of life, when yellowfin tuna are still at a preflexion larval stage and inhabit the first 20 m of the water column, where low oxygen levels do not normally occur (Boehlert and Mundy, 1994; Kaji et al., 1999; Wexler et al., 2011). Thus, we concluded that observed differences in Mn concentrations between nurseries at each year may relate to physiological processes occurred during biomineralization of the otolith (Hüssy et al., 2020). Increased Sr concentrations were also detected in the 2018 cohort of YOY yellowfin tuna from Maldives. Sr is a trace element that is positively related to its ambient concentration, and the interaction between temperature and salinity affects otolith Sr concentrations (Bath et al., 2000; Elsdon and Gillanders, 2002; Walther and Thorrold, 2006). The area west of Maldives is characterized by having an annual cycle and ecological regime distinct from the surrounding regions, with an strong zonal advection (Bao et al., 2020b; Huot et al., 2019). These environmental peculiarities of Maldives may have led to the observed differences in otolith Sr concentrations with respect to Seychelles-Somalia nursery.

Carbon and oxygen stable isotopes were an important source of differentiation between nurseries. Otolith $\delta^{13}C$ has been recently described as a proxy for metabolic rate in fish (Chung et al., 2019). Otolith $\delta^{13}C$ is influenced by the environment (dissolved inorganic carbon in water, DIC) and diet, and significantly affected by temperature (Martino et al., 2019). The observed carbon isotope trend in YOY yellowfin tuna otoliths, decreasing west to east, followed the expected trend

according to Indian Ocean water temperature distribution (Fingas, 2019). Ambient temperature is also an accurate proxy of otolith $\delta^{18}O$ (Macdonald et al., 2020). Although other intrinsic factors, such as growth and physiology, may influence otolith $\delta^{18}O$ incorporation, variations in otolith $\delta^{18}O$ closely reflect the ambient temperature experienced by the fish, being inversely correlated with ambient seawater temperature (Darnaude and Hunter, 2018; Kitagawa et al., 2013; Macdonald et al., 2020). Otolith oxygen isotope ratios of YOY yellowfin tuna from the Indian Ocean followed the expected trend, presenting higher values in the western nurseries (expected lower water temperatures, under the influence of the seasonal Somali upwelling) and decreasing towards the east (expected higher water temperatures, from the Indonesian throughflow) (Schott et al., 2002).

Temporal differences were also evident within nursery chemical composition, particularly in Maldives nursery. The Indian Ocean is characterized by a seasonal reversal of surface winds, with two seasons of distinct wind regimes (i.e. monsoons) that strongly influence the oceanography north of 10°S (Ramage, 1969; Schott and McCreary, 2001). Due to sampling constraints, 2017 cohort individuals from Maldives were hatched at the beginning of the boreal summer monsoon, whereas individuals from 2018 cohort were hatched at the beginning of the boreal winter monsoon. The observed among-cohort differences within YOY yellowfin tuna from Maldives nursery are probably derived from the physical and biological variations of the region between the two monsoonal seasons (Huot et al., 2019). A substantial proportion of YOY yellowfin tuna (69-71%) were correctly assigned to their origin when analysed separately for each cohort, but nursery specific classification success was higher in 2018 for Maldives and Sumatra. Interannual differences in region-specific classification have also been reported in other yellowfin tuna nurseries of the Atlantic and Pacific Oceans based on otolith microchemistry (Kitchens et al., 2018; Rooker et al., 2016; Wells et al., 2012), which highlights the importance of constructing year-by-year reference baseline signatures.

The inclusion of trace element data to the baseline of $\delta^{13}C$ and $\delta^{18}O$ stable isotope signatures did not significantly improve classification success in yellowfin tuna from the Pacific Ocean nurseries (Rooker et al., 2016), while trace elements

proved to be more effective to discriminate among yellowfin tuna nurseries in the Atlantic Ocean (Kitchens et al., 2018). Here the most important predictor signatures for models tested included $\delta^{18}O$ and Mn:Ca and Sr:Ca. Oxygen values were the main driver of differentiation between nurseries in the west (Madagascar and Seychelles-Somalia), and those in central-east (Maldives and Sumatra), but the addition of trace elements allowed for finer scale nursery discrimination. Thus, the effort to incorporate trace element ratios into otolith chemistry baselines for yellowfin tuna in the Indian Ocean may benefit from higher power of discrimination but will require age-class matching when adults are assigned to these combined baseline of nursery signatures. Another way to better integrate the results obtained from both approaches, would have been to analyse with fs-HR-LA-ICPMS the integrated signal of an ablation square that corresponds to the same otolith portion milled for stable isotopes analyses (i.e., ~2 months of life). However, by increasing the time frame analysed for trace element analyses, the obtained signal would have reflected a mixture of extrinsic and intrinsic (e.g. ontogenic) influences (Macdonald et al., 2020; Thomas et al., 2020).

5. Conclusions and future directions

Described age estimates provided an accurate temporal scale to assist the interpretation of otolith microchemistry of YOY yellowfin tuna data and to link assay locations with early life history stages. Two-dimensional visualization was useful to gain insights of elemental distribution patterns. The present study shows that some elements exhibit a disjunct accumulation in yellowfin tuna otoliths (i.e., difference in elemental concentration among parts of an otolith corresponding to the same fish age). This is an important issue to consider when, for example, selecting elemental assay locations. Arbitrarily laid transects or spots can differ in element composition among samples just because of their placement. Thus, we strongly recommend sampling the same otolith axis within (and ideally across) studies to avoid misinterpretations of the results and/or to investigate the homogeneity of element composition within the otolith prior to any otolith microchemistry study. As the elemental signatures of YOY yellowfin tuna varied among nurseries, the baseline signature described in this study may be used as an effective tool to assign juvenile and adult individuals to their nursery origin. However, temporal variability of

element concentrations is one important aspect to be considered, and future classifications of older individuals to nursery areas will require that the individuals being characterised belong to the same year classes as the baseline used as a reference. These cohort-matched reference baselines will provide insights into the connectivity and mixing rates of older individuals within the Indian Ocean, as well as the contribution of each nursery area to the overall population. This information will have major implications for fisheries management, as the understanding of stock structure helps determine the appropriate unit for stock assessment and suitable spatial scales for management.

“Utzidazu kontatzen behin ume zirela

Amestu zutela itsaroaren beste aldeaz”

Izaro

CHAPTER 5

Origin and connectivity of yellowfin tuna from fishery grounds in the Indian Ocean

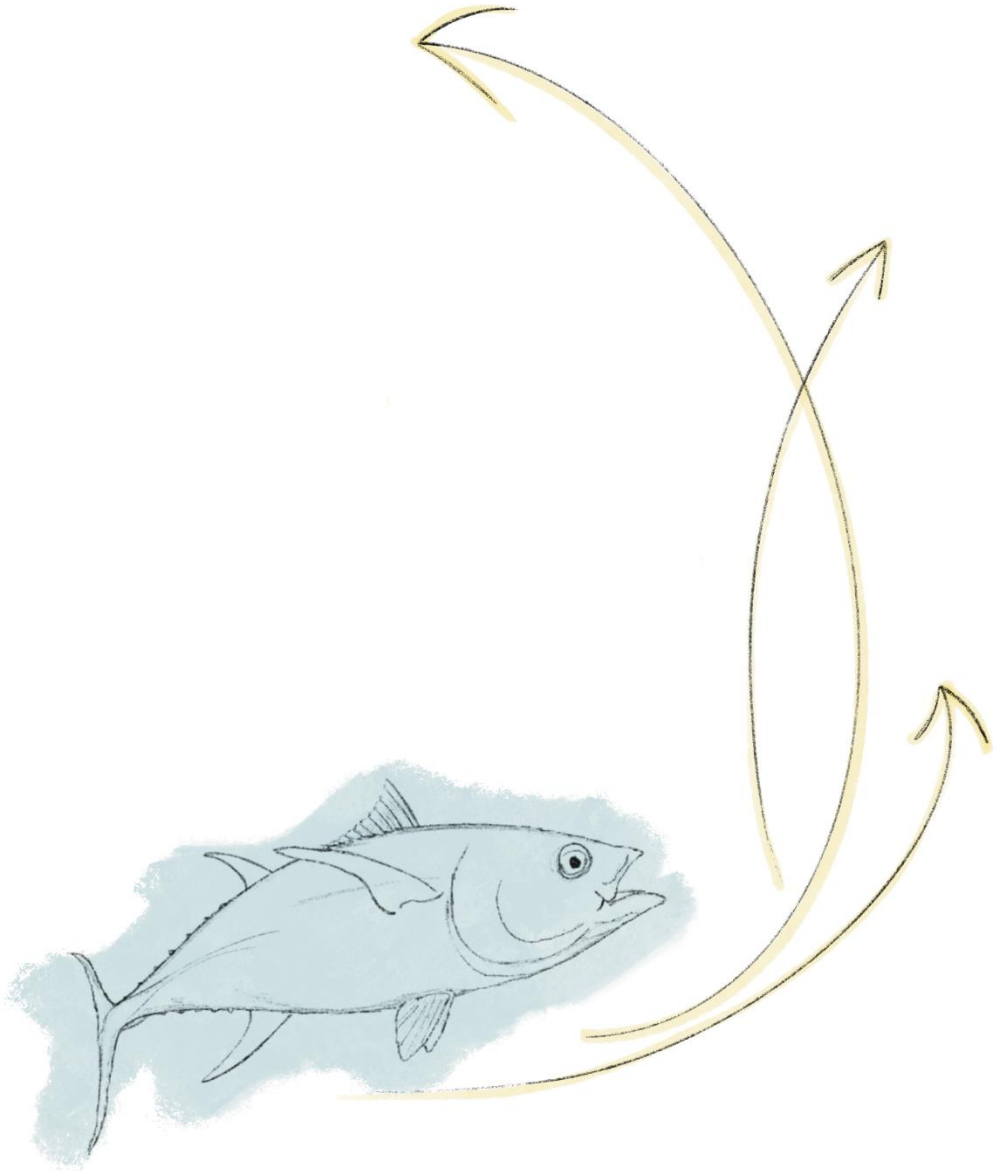

Abstract

Yellowfin tuna of the Indian Ocean is overfished, and a better understanding of the stock structure is needed to enable a sustainable management. Here, otolith $\delta^{18}O$ values of young-of-the-year fish from known nursery areas of the equatorial Indian Ocean (West, Central and East) were used to establish a reference isotopic signature to predict the origin of sub-adult and adult individuals. Sub-adult tuna otolith $\delta^{18}O$ values from the Reunion Island were similar to the western nursery signature, but otolith $\delta^{18}O$ values of sub-adults from Pakistan were unlike any of the nurseries sampled. Therefore, $\delta^{18}O$ values from the Pakistan area samples were considered an additional nursery source for the origin assignment of adult tuna, that was predicted from a multinomial logistic regression classification method. The western equatorial area was the most productive nursery for three fishing grounds sampled, with a minor contribution of Pakistan-like origin fish. Contribution of central or eastern nurseries to the adult population was negligible. One adult otolith was analysed by secondary ion mass spectrometry along the otolith growth transect and results were compared with an isoscape approach to infer lifetime movements. This study is an important first step towards understanding the spatial structure and connectivity of the species.

Under review as:

Artetxe-Arrate, I., Fraile, I., Farley, J., Darnaude, A.M., Clear, N., Dettman, D.L, Davies, C., Marsac, F., and Murua, H. (2021). Otolith $\delta^{18}O$ composition as a tracer of yellowfin tuna (*Thunnus albacares*) origin in the Indian Ocean. *Oceans*.

1. Introduction

An effective management of highly migratory marine species (i.e., species that can migrate long distances between international waters), such as billfishes and tunas, is a great challenge due to their widespread distributions that often straddle domestic and international jurisdictional boundaries (Aranda et al., 2006; Kritzer and Liu, 2014). Yellowfin tuna (*Thunnus albacares*) is one of the species listed as highly migratory in Annex 1 of the United Nations Convention on the Law of the Sea (UNCLOS), and inhabits the pelagic ecosystem of the tropical and subtropical regions of the Atlantic, Indian and Pacific Oceans (Collette and Nauen, 1983). This species has been subject to high fishing pressure over the last three decades (ISSF, 2020b), particularly in the Indian Ocean. Here, recent increases in catches has led to biomass and fishing mortality exceeding those corresponding to the Maximum Sustainable Yield (IOTC, 2019c; ISSF, 2020b). The Indian Ocean yellowfin tuna stock is, therefore, considered overfished and subject to overfishing (IOTC, 2020a). The stock assessment model of yellowfin tuna in the Indian Ocean runs under the single stock assumption, due to the rapid and large-scale movements indicated by the Indian Ocean Regional Tuna Tagging Program (RTTP-IO) (IOTC, 2017c). However, some regional studies suggest that the stock structure and spatial dynamics of yellowfin tuna could be more complex than previously thought (Dammannagoda et al., 2008; Kunal et al., 2013; Moore et al., 2019).

Yellowfin tuna can be found throughout the Indian Ocean, as far south as 45°S (Sharp, 2001), yet their spawning activity is restricted to lower latitudes with higher water temperatures (Reglero et al., 2014; Schaefer, 2001). The main spawning grounds in the Indian Ocean have been described along the equatorial region (Nootmorn et al., 2005; Stéquert and Marsac, 1989; Zhu et al., 2008; Zudaire et al., 2013a). As adults, yellowfin tuna perform extensive migrations between these spawning areas and feeding grounds in southern and northern latitudes (Fonteneau and Pallares-Soubrier, 1995). However, the relative importance of different spawning areas to the total catches, and the degree of connectivity and mixing rates of yellowfin tuna in the Indian Ocean, are still unknown, even though this information is essential to the development of effective and sustainable management strategies (Bosley et al., 2019; Kerr et al., 2017).

Chemical analysis of fish otoliths has proved to be a useful method to study the origin and movement of yellowfin tuna in the Pacific and Atlantic oceans (Kitchens et al., 2018; Rooker et al., 2016; Wells et al., 2012). The approach relies on two assumptions: (1) during otolith formation material is accreted and preserved as fish grows, and (2) the chemical composition of the otolith is related to the physicochemical environment inhabited by the fish at time of deposition (Campana, 1999). As such, the chemical composition of the otolith material deposited during the early life stage of the fish, is often linked to the ambient seawater physicochemical properties at the source (i.e., spawning area) (Thorrold et al., 2001). Particularly, otolith oxygen isotopic composition ($\delta^{18}O$) has proved to be a reliable marker of the individual's origin and an effective tool for stock identification and mixing estimation purposes (Kerr et al., 2020; Rooker and Secor, 2004; Secor, 2015). Oxygen isotope composition in otolith aragonite is influenced by both the isotopic composition and the temperature of the ambient water, being inversely related with the latter (Kitagawa et al., 2013; Thorrold et al., 1997). Thus, variations in otolith $\delta^{18}O$ can be used as natural geolocators for deciphering lifetime movements of teleost fish, albeit individual differences in incorporation rates may exist (Darnaude et al., 2014; Darnaude and Hunter, 2018).

Traditionally, otolith $\delta^{18}O$ composition had been measured by isotope ratio mass spectrometry (IRMS). One of the limitations of the IRMS is that relies on obtaining a minimum amount of powder from otolith milling. As a result, the technique does not allow for fine temporal scale resolution (i.e., the signal corresponding to several months must be integrated) or fine scale life history reconstructions (i.e., core to edge transects) (Hane et al., 2020). Thanks to recent analytical advances, it is now possible to measure stable isotopes with higher spatial/temporal resolution using secondary ion mass spectrometry (SIMS). This technique requires further preparation of the samples to be analysed (Hane et al., 2020), but in return offers a promising tool to unravel migration patterns and life history characteristics at much shorter timescales (Matta et al., 2013; Shiao et al., 2014; Shirai et al., 2018; Willmes et al., 2019). When water temperature and oxygen isotopic composition are known, it is possible to delineate isoscapes (i.e., spatial maps of predicted isotopic variation) that can be used to track potential movements

across water mases with distinct isotopic signatures (Trueman and St John Glew, 2019).

The aim of the present study was to assess the origin and the connectivity of sub-adult (age 1-2) and adult (age >2+) yellowfin tuna from the main fishery grounds in the Indian Ocean. For that, the otolith $\delta^{18}O$ composition of the otolith portion corresponding to the early life was analysed using IRMS. These signatures were then compared to a baseline of nursery signatures developed from young-of-the-year (YOY, age 0) yellowfin tuna from known nursery areas in the Indian Ocean. In addition, SIMS analysis was applied, for the first time to yellowfin tuna, to measure the $\delta^{18}O$ values along the otolith growth axis and assess the potential of this technique to provide detailed insights into the movements and life history of yellowfin tuna in the Indian Ocean. Finally, an isoscape of potential gradients in otolith $\delta^{18}O$ values was predicted to discuss the potential movements of this adult yellowfin tuna.

2. Material and methods

2.1 Fish sampling

Otoliths of yellowfin tuna were collected from 3 major nursery areas (West, Central and East) and from 4 fishery grounds (South Africa, Pakistan, Reunion, and West Australia) in the Indian Ocean (**Figure 5.1**). Samples were collected by scientists or scientific observers directly on-board purse seine and longline vessels, or at port during two consecutive years (2018 and 2019), as part of a collaborative research project on Population Structure of Tuna, Billfish and Sharks of the Indian Ocean (Davies et al., 2020). Fork length (FL, to the nearest cm), sampling date, and sampling location were recorded for all samples collected (**Table 5.1**). Samples were classified as YOY (<38 cm FL), sub-adults (40-75 cm FL) and adults (>102 cm FL) according to the age-length relationship described in Eveson et al. (2015) and the 102 cm maturity threshold in Zudaire et al. (2013). Sagittal otoliths were extracted, cleaned of adhering organic tissue, rinsed with ultrapure water, and stored dry in plastic vials. The otolith collection available for this study comprised fish from different cohorts and hatched at different periods of the year. The baseline samples used to characterise yellowfin tuna nursery areas were first reported in

Artetxe-Arrate et al. (submitted) and were shown to be temporally stable for $\delta^{18}O$. Therefore, YOY otoliths of different year classes, but belonging to the same nursery area, were pooled for this study.

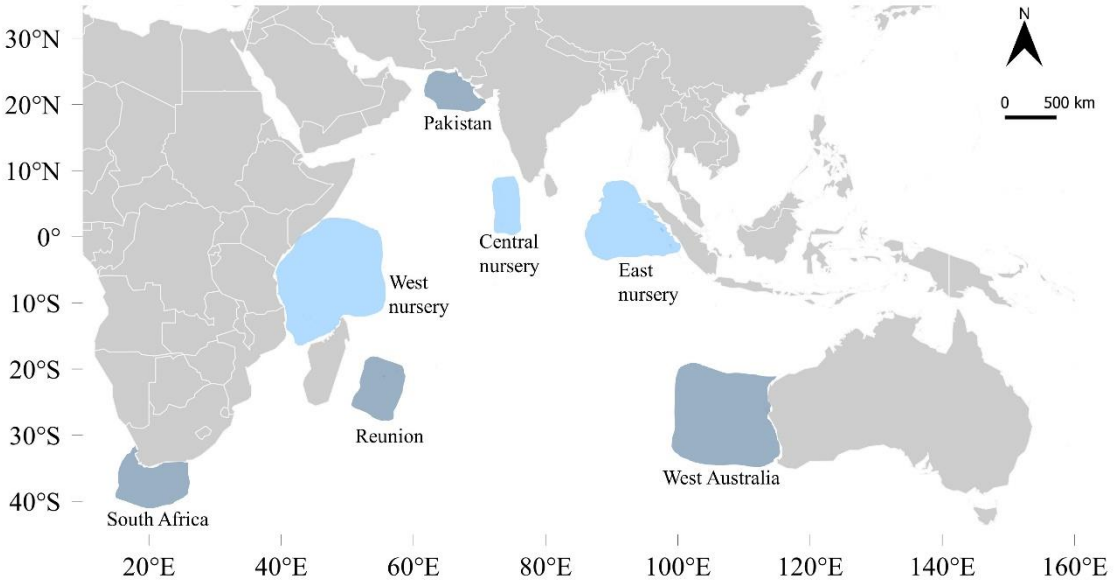

Figure 5.1. Sampling distribution of yellowfin tuna (*Thunnus albacares*) in the Indian Ocean. Otolith collections included young of the year from nursery areas used as baseline (light blue) and sub-adults and/or adults from fishery grounds (dark blue).

Table 5.1. Number, sampling period, size, and estimated ages of yellowfin tuna (*Thunnus albacares*) at each sampling area. Size is fork length (FL) in cm.

Location	N	Sampling dates	FL range (cm)	Estimated age (years)	Life stage classification[1]
West nursery	51	Mar-Apr 2018 and 2019	26-37	<1	YOY
Central nursery	31	Aug 2018 and Feb 2019	28-36	<1	YOY
East nursery	31	Apr and Nov 2018	19-34	<1	YOY
Pakistan	12	Sep 2018	64-75	1-2	Sub-adult
Reunion	15	Dec 2017	47-51	1	Sub-adult
Reunion	12	Feb-Mar 2018 Feb 2019	124-169	>4	Adult
South Africa	19	Mar-May 2018	133-138	>4	Adult
Western Australia	8	May 2019	143-174	>5	Adult

[1] *Life stage classifications according to the age-length key relationship described in Eveson et al. (2015) and 102 cm FL maturity threshold in Zudaire et al. (2013).*

2.2 Otolith $\delta^{18}O$ analysis by IRMS

Otoliths were embedded in two-part epoxy resin (Araldite 2020, Huntsman Advanced Materials, Switzerland). Each rectangular block was polished from the otolith rostrum using 3M® silicon carbide sandpaper (particle size= 220 µm) and a series of decreasing grain diameter lapping discs (30, 15, 9, 3 and 1 µm) with a lapping wheel, moistened with ultrapure water, until the primordium was exposed. The resin blocks were sonicated for 10 minutes in ultrapure water (Milli-Q) and left to air for 24 h before being glued in a sample plate using Crystalbond thermoplastic glue (Crystalbond 509; Buehler). Microsampling of otolith powder for oxygen stable isotope ($\delta^{18}O$) was performed using a high-resolution computerised micromill (New Wave MicroMill System, NewWave Research G. C. Co., Ltd, Cambs, UK). The length of the smallest yellowfin tuna in the baseline (19.5 cm FL) otolith section was used to create a template that was then used for the remaining otoliths, to ensure that the same portion of the otolith was analysed in every fish (approximately two months of life according to (Artetxe-Arrate et al., n.d.). Ten drill passes were run at a depth of 50 µm per pass over a preprogrammed drill path using a 300-µm diameter carbide bit (Komet dental; Gebr. Basseler, Lemgo, Germany). Powdered material was then analysed for $\delta^{18}O$ on an automated carbonate preparation device (KIEL-III, Thermo- Fisher Scientific, Waltham, MA, USA) coupled to an isotope ratio mass spectrometer (IRMS, Finnigan MAT 252, ThermoFisher Scientific) at the Environmental Isotope Laboratory of the University of Arizona. Oxygen isotope values were reported according to standards of the International Atomic Energy Agency in Vienna and represent ratios of $^{18}O/^{16}O$ in the sample relative to the Vienna Pee Dee Belemnite (VPDB) scale. The isotope ratio measurements were calibrated against repeated measurements of National Bureau of Standards (NBS-19 and NBS-18) and analytical precision was ± 0.10 ‰ (1 sigma).

°2.3 Otolith $\delta^{18}O$ analysis by SIMS

One otolith of an adult yellowfin tuna (134 cm FL) captured in South Africa on May 2018 was selected for high precision $\delta^{18}O$ analyses using secondary ion mass spectrometry (SIMS). The individual's age was estimated to be 4.5+ years according to the age-length curve of Eveson et al. (2015). As SIMS is a surface analytical method, any irregularity in the sample surface (e.g. cracks, bubbles, reliefs,

inclinations…) needs to be avoided (Hane et al., 2020; Kita et al., 2009). The otolith was first embedded in a rectangular box following the same methodology as described above. The resin block was then embedded again with the rostrum upwards in a 25 mm diameter silicon cylindric mould with two-part epoxy resin until the surface of the section was covered. It was then kept at a room temperature for 48 h to cure the resin. The obtained cylinder containing the otolith positioned vertically was then polished with a series 3M® silicon carbide lapping discs (9, 3 and 1 μm), moistened with ultrapure water, until the primordium was clearly exposed. Then a velvet polishing pad moistened with ultrapure water and sprinkled with aluminium powder (0.5 μm) was used to expose the core on a flat mirror-finished surface. The oxygen isotope data were acquired at the NERC Ion Microprobe Facility (SIMS) from the University of Edinburgh with a Cameca IMS 1270, using a ~5 nA primary $^{133}Cs^{+}$ beam. Secondary ions were extracted at 10 kV, and $^{16}O^{-}$ (~3.0 x10^{9}cps) and $^{18}O^{-}$ (~4.0 x10^{6} cps) were monitored simultaneously on dual Faraday cups (L'2 and H'2). Each analysis involved a pre-sputtering time of 60 seconds, followed by automatic secondary beam and entrance slit centring and finally data collection in two blocks of ten cycles, amounting to a total count time of 80 seconds. The internal precision of each analysis is < 0.2 per mil. To correct for changes in the instrumental mass fractionation, all data were normalised to a UWC-1 ($\delta^{18}O$ = 23.3 Vienna Standard Mean Ocean Water, VSMOW) calcite standard (Graham et al., 1998) which was mounted together with the samples and measured throughout the analytical sessions. The external precision is estimated from the repeat analysis of the standard to be (0.17 – 0.26) per mil. Measurements were made along the growth axis of the otolith, from the primordium to the edge with a series of 40 spots of ~15 μm each (Appendix D, Figure D1). Temporal resolution covered by each spot increased with increasing distance from the core, from days to weeks (Proctor et al., 2019). To compare $\delta^{18}O$ values measured by the two analytical methods (SIMS and IRMS), $\delta^{18}O$ data were converted from VSMOW to VPDB using the following equation (Brand et al., 2014):

$$\delta^{18}O_{VPDB} = 0.97001 \times \delta^{18}O_{VSMOW} - 29.99‰ \quad (1)$$

To correct for deviations between IRMS and SIMS, a regression equation relating these two types of measurements in cod otoliths was applied (Helser et al., 2018):

$$\delta^{18}O_{IRMS} = 0.4773 \times \delta^{18}O_{SIMS} + 0.483 \quad (2)$$

Raw SIMS $\delta^{18}O$ measurements are presented in Appendix D, Table D1.

2.4 Isoscape computation

A simplistic model was applied to predict the spatial variations in the isotopic composition of oxygen in otoliths ($\delta^{18}O_{OTO}$) in order to infer the probable location of the analysed individual at a given point in time in the horizontal plane. A linear equation, which relates the isotopic composition of water ($\delta^{18}O_{WATER}$) and the seawater temperature (T, in °C) was applied (Trueman and MacKenzie, 2012):

$$T = \gamma (\delta^{18}O_{OTO} - \delta^{18}O_{WATER}) + \beta \quad (3)$$

where $\delta^{18}O_{OTO}$ is relative to the VPDB standard and $\delta^{18}O_{WATER}$ is relative to the VSMOW standard. Global gridded data set of $\delta^{18}O_{WATER}$ was obtained from LeGrande and Schmidt (2006) and averaged for three depth ranges: (1) 0-20m, (2) 20-50m and (3) 50-100m, as these are the depths yellowfin tuna tend to remain primarily in (Schaefer et al., 2007). Parameters γ =-0.27 and β = 5.19, described for Pacific Ocean bluefin tuna (*Thunnus orientalis*), were used for the computation (Kitagawa et al., 2013). Temperature was derived from the reanalyses produced by the European Copernicus Marine Environment Monitoring Service (CMEMS, http://marine.copernicus.eu/), "CORIOLIS-GLOBAL-CORA-OBS_FULL_TIME_SERIE" product. Monthly data from January 2013 to May 2018 was averaged for each 1×1° grid for the three depth ranges described above. Maps were generated using QGis© software (3.8.3-Zanzibar version). Note that this simplistic model assumes constant parameters for the otolith fractionation equation, and that locally, seasonal fluctuations in seawater temperature may result in an increased variability of $\delta^{18}O$ otolith values than considered here.

2.5 Statistical analyses

Early life $\delta^{18}O$ values measured by IRMS were examined for normality and homogeneity of variances using Shapiro-Wilks normality test and Fligner-Killeen test of homogeneity of variances, respectively. All locations met the parametric assumptions. Differences between $\delta^{18}O$ signatures of sub-adult yellowfin tuna from Pakistan and Reunion were compared using a Student´s t-test. Sub-adult signatures were also compared with $\delta^{18}O$ values of YOY yellowfin tuna from the 3 main nursery

regions conforming the baseline, using 1-way ANOVA and Tukey's HSD test. Projections of nursery origin composition of adult yellowfin tuna from each fishery ground were estimated using a multinomial logistic regression (MLR) classification method as described by Rooker et al. (2019). Four probability thresholds were used to predict nursery origin (0.5, 0.6, 0.7 and 0.8). As the probability threshold increases above 0.5, some individuals may not have sufficient predicted probabilities to be assigned to any nursery present in the baseline, and thus will be classified as an undetermined source. As such, the fraction of individuals failing to meet the probability threshold of any nursery will increase as the probability threshold increases (Rooker et al., 2019). The $\delta^{18}O$ SIMS otolith profile was estimated by computing the moving means of two adjacent values at a given distance from the core to the edge. All analyses were performed using R software (R Core Team, 2019).

3. Results

3.1 Nursery origin of sub-adult and adult yellowfin tuna

Sub-adult yellowfin tuna from Pakistan and Reunion showed distinct early life $\delta^{18}O$ composition (t-test, $p<0.001$). The $\delta^{18}O$ otolith measurements ranged from -0.94 to -1.47 for yellowfin tuna captured in Pakistan, while they ranged from -1.58 to -2.35 for fish captured in Reunion (**Figure 5.2**). While the $\delta^{18}O$ values of fish captured in Reunion were not significantly different to the nearest nursery, the West nursery (Tukey HSD, $p=0.998$), $\delta^{18}O$ composition of fish captured in Pakistan was distinct from any of the nurseries present in the baseline (**Figure 5.3**). Therefore, the early life $\delta^{18}O$ signature of Pakistan was considered as an additional nursery signature to be included with the reference samples, although the exact

geographical location of the nursery area represented cannot be determined (hereafter called Pakistan-like origin).

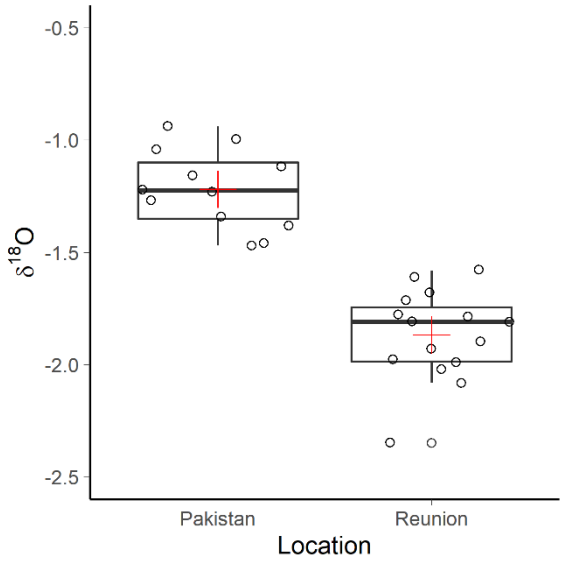

Figure 5.2. Comparison of early life otolith $\delta^{18}O$ signatures of sub-adult yellowfin tuna from Pakistan and Reunion. Inter quartile range (25th and 75th percentile) is shown by extent of boxes and error bars represent 10th and 90th percentiles, and median (50th percentile) is also shown. Red crosses are locations means. Dots represent individuals.

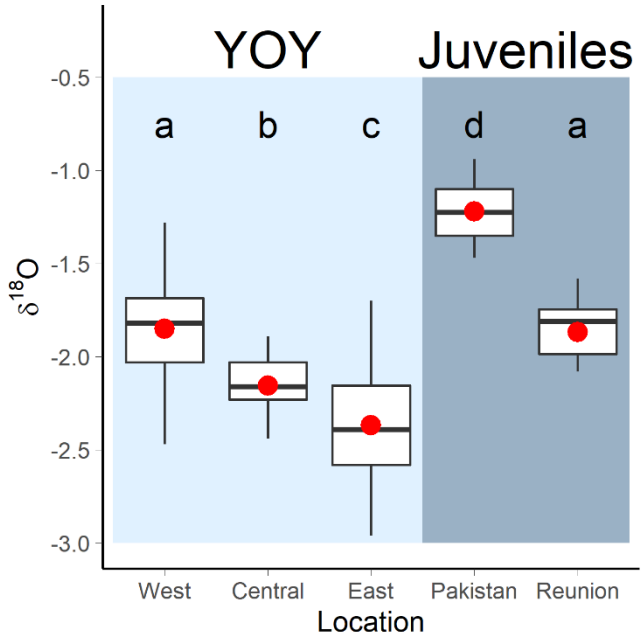

Figure 5.3. Boxplots showing otolith early life $\delta^{18}O$ composition of YOY (light blue) and sub-adult (dark blue) yellowfin tuna (*Thunnus albacares*) from the Indian Ocean. Letters identify significant differences (Tukey HSD, P<0.05) between means. Inter quartile range (25th and 75th percentile) is shown by extent of boxes and error bars represent 10th and 90th percentiles. Median (50th percentile) and mean values are shown in boxes as black lines and red dots, respectively.

Most of the adult yellowfin tuna captured in South Africa, Reunion and West Australia were assigned to the western nursery using the MLR approach. None of the adult yellowfin tuna was assigned to Central or East nurseries, but some adults with Pakistan-like $\delta^{18}O$ signature were detected in the three fishery grounds sampled (**Figure 5.4**). The number of unclassified individuals was highest for adult yellowfin tuna captured in South Africa. When the probability threshold was set at 0.5 and 0.6, one adult yellowfin tuna was classified as undetermined. When the probability threshold was set at 0.7 and 0.8, 5 and 10 out of the 19 adult yellowfin tuna captured in South Africa were classified as undetermined respectively. The other individuals were classified to the West or to the Pakistan-like nursery of origin (**Figure 5.4**). For adult fish captured in Reunion, most of the individuals (9 out of 12) were classified to the West nursery origin with a probability threshold of ≤0.6, while the three remaining fish were classified to the Pakistan-like origin. The number of unclassified fish was 2 and 4 for a probability threshold of 0.7 and 0.8, respectively. For adult fish captured in Western Australia one fish was assigned to the Pakistan-like origin for all probability thresholds, while the rest of the fish were classified to the West nursery of origin (**Figure 5.4**). The number of unclassified individuals increased from 0 to 3 with increasing probability thresholds (0.5-0.8).

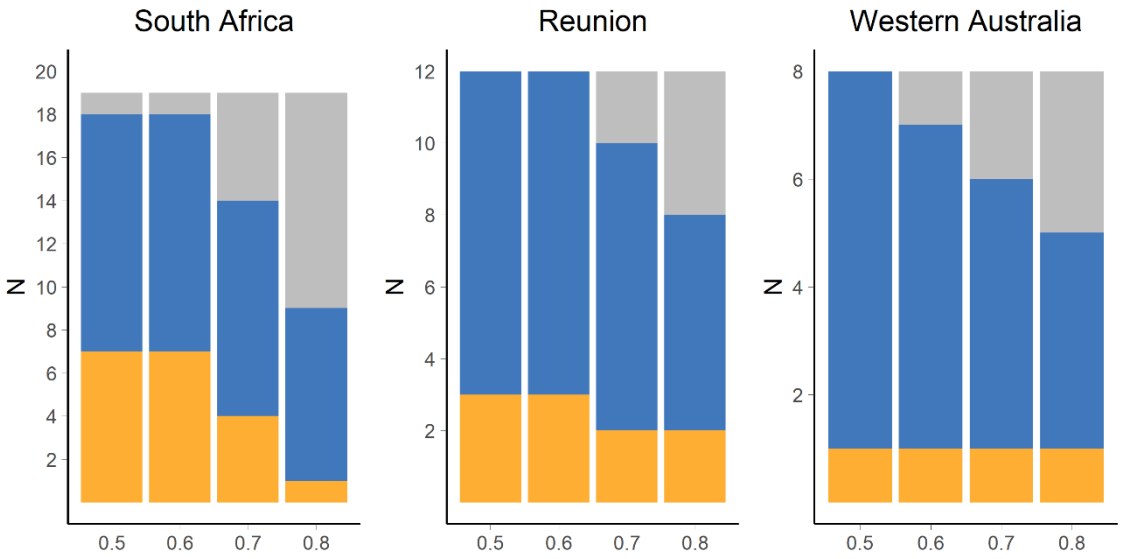

Figure 5.4. Estimated number of Pakistan (yellow), West nursery (blue) and undetermined (grey) origin yellowfin tuna samples captured in three different fishing grounds of the Indian Ocean. Results are based on multinomial logistic regression (MLR) framework. Four probability thresholds (0.5-0.8) are shown.

3.2 Oxygen isotopic distribution along the otolith and isoscape predictions

Otolith $\delta^{18}O$ values measured by SIMS ranged from -2.13 to -0.65 along the growth transect. In total, 40 spots were analysed along the otolith growth axis from core to edge, spanning fish' life history from birth to death. There was an increasing trend in mean $\delta^{18}O$ values from the otolith core to the edge, corresponding with an increasing in fish age (**Figure 5.5**). For spot numbers 0-18, $\delta^{18}O$ values were low and little variability was observed. Indeed, the average value of the signature corresponding to the integrated signal of the first month of life (-1.78),was similar to that obtained by IRMS in the second otolith pair (-1.72) for the integrated signal corresponding to ~2 months of life of the same individual. After spot number 19, $\delta^{18}O$ values started to increase sharply until spot number 23 reaching $\delta^{18}O$ values of the order of -1.50 (**Figure 5.5**). As of spot number 23 until spot number 34, $\delta^{18}O$ values stabilised again, sharply increasing thereafter. Highest $\delta^{18}O$ values (around -1) along the whole transect were observed in spot numbers 35 to 37, after which values decrease again to previous levels (spot numbers 38 to 40). Unfortunately, the last spot in the transect was not set at the otolith edge so that no information related to the isotopic composition of the catch location (South Africa) was available.

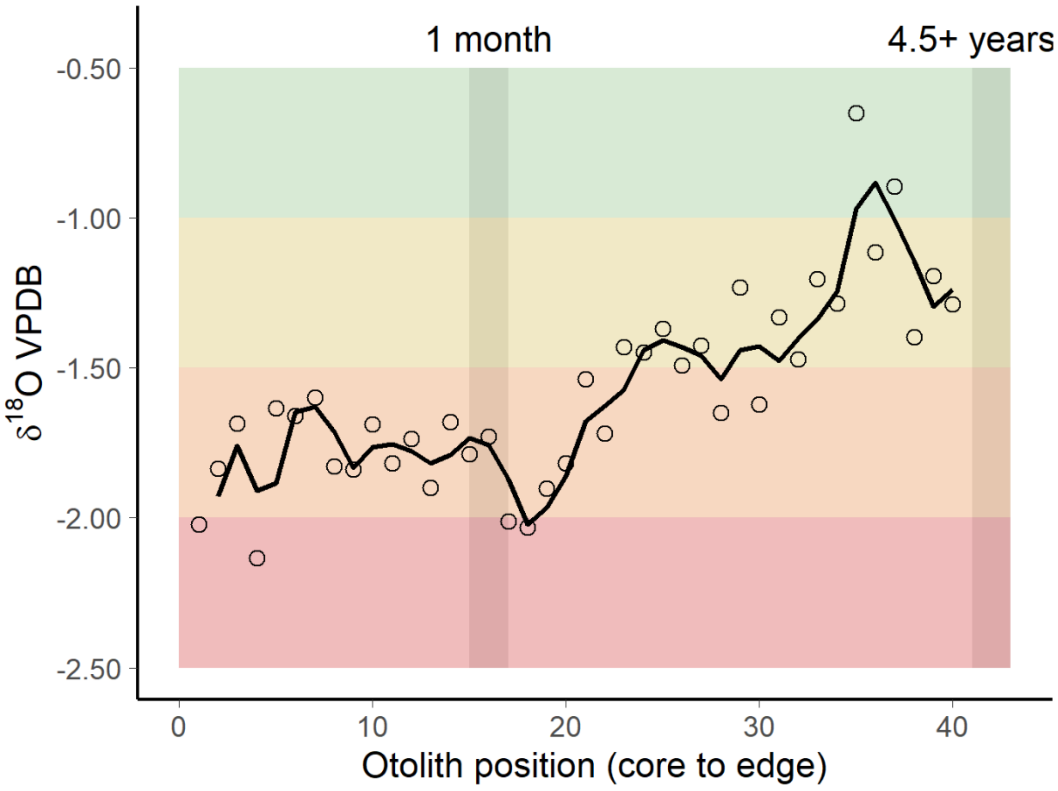

Figure 5.5. Core to edge profile of otolith $\delta^{18}O$ values measured by SIMS in an adult yellowfin tuna (*Thunnus albacares*). The individual was captured in South Africa on May 2018, with a size of 134 FL. Dots are values measured at each spot, and solid line represents the mobile mean. The approximate location of the first month of life and 4.5+ years are indicated.

Predicted spatial variations in the isotopic composition of oxygen in otoliths ranged from 3.0 to -3.0 and overall, expected values were higher in the Atlantic Ocean (**Figure 5.6**). In the Indian Ocean, north of 20°S predicted $\delta^{18}O$ values for 0-20m depth range were higher in the western region, with maximum values found in the Arabian Sea. Predicted $\delta^{18}O$ values decreased eastward, with minimum values found off Sumatra and eastern Bay of Bengal basin (**Figure 5.6A**). A similar pattern of $\delta^{18}O$ values was detected for the 20-50m depth range, although higher $\delta^{18}O$ were found in south of the equator (0-10°S west of 90°E, and around Madagascar Island (**Figure 5.6B**). At this depth, $\delta^{18}O$ values off Sumatra were in the range of those of the rest eastern Indian Ocean. For the 50-100m depth range, $\delta^{18}O$ values were maintained off Sumatra, but increased in the rest of the Indian Ocean (**Figure 5.6C**). South of 20°S, $\delta^{18}O$ values followed a nearly perfect horizontal zonation, with predicted values increasing with increasing southward latitude.

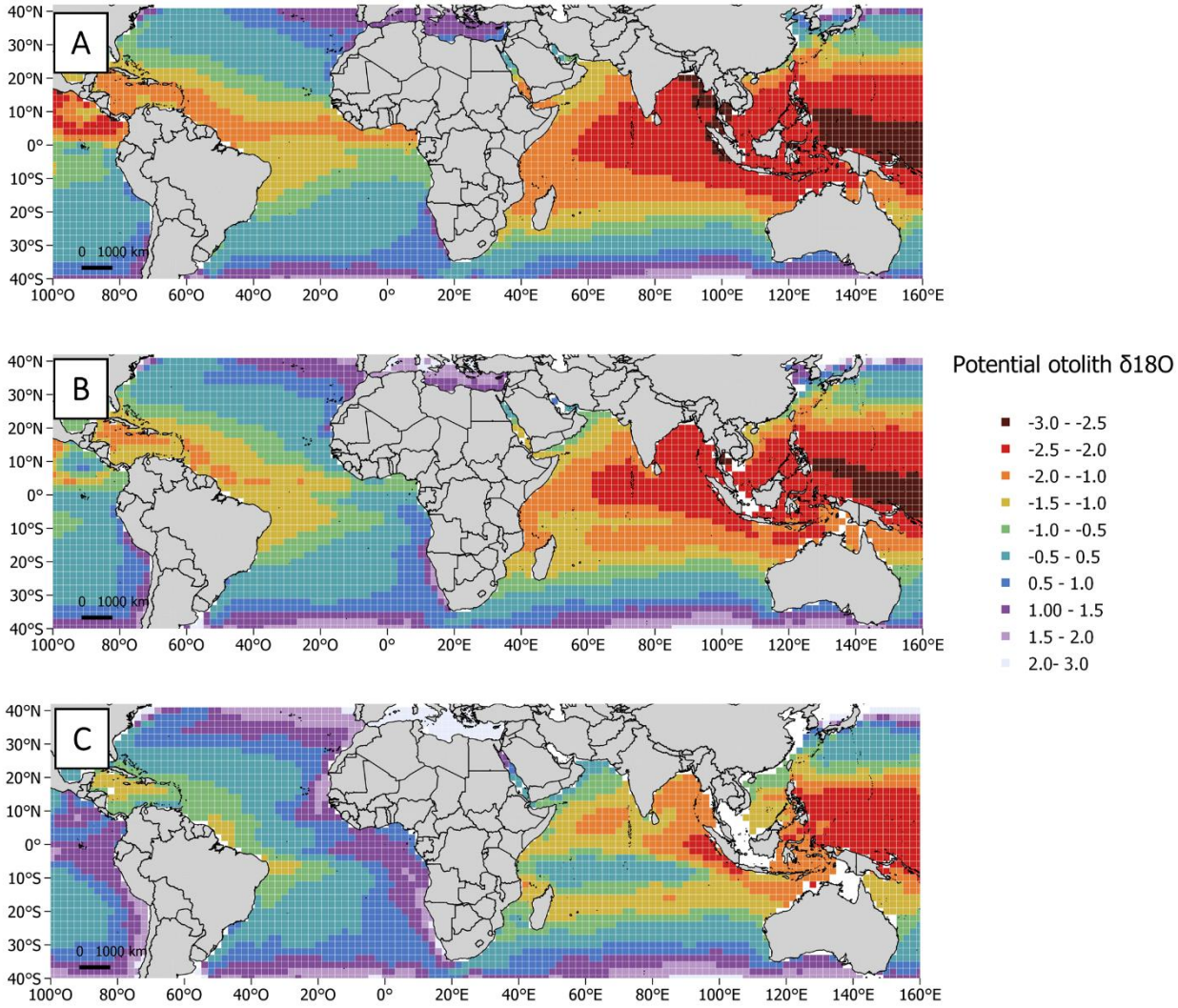

Figure 5.6. Isoscape of predicted $\delta^{18}O$ composition in otoliths based on global surface water measured $\delta^{18}O$ values (LeGrande and Schmidt, 2006) at 0-20m (A), 20-50m (B) and 50-100m (C), using the equation $T = \gamma(\delta^{18}O_{OTO} - \delta^{18}O_{WATER}) + \beta$ (Trueman and MacKenzie, 2012) and parameters γ and β from (Kitagawa et al., 2013). Data was averaged at each 1×1° grid.

4. Discussion

4.1 Nursery origin of sub-adult and adult yellowfin tuna

The current study analyses the $\delta^{18}O$ content in otoliths, to expand our understanding on the movement and mixing of yellowfin tuna in the Indian Ocean. The sizes of sub-adults analysed in this study ranged from 47 to 75 cm FL and although they are not in spawning condition (Zudaire et al., 2013a), yellowfin tuna of this length are capable of large migrations in search of foraging grounds (Fonteneau and Hallier, 2015). Given this, we expected the early life $\delta^{18}O$

composition for both the sub-adults from Pakistan and Reunion to reflect a mix of overlapping signals of fish arrived from different nursery origins. However, juveniles from Pakistan and Reunion showed very different isotopic signatures, suggesting that these fish have originated from distinct nursery areas. The otolith $\delta^{18}O$ composition of sub-adults from Reunion resembled that from the closest known nursery, the West nursery, suggesting some retention of sub-adult fish near this area. High retention of yellowfin tuna from these lengths near to their closest nursery area has also been reported in the Pacific Ocean (Rooker et al., 2016; Wells et al., 2012). Interestingly, the nursery signature of juvenile fish from Pakistan was very different from any other nursery signature available in the baseline. Although it is not possible to directly determine where the nursery area of these fish is located, observed results could indicate the possible existence of a nursery area in the Arabian Basin region. Higher $\delta^{18}O$ content is expected in this area compared to other regions in the Indian Ocean, because of the colder waters that can be found in this area (Keshtgar et al., 2020; Kumari et al., 2005; LeGrande and Schmidt, 2006). We are not aware of any spawning grounds of yellowfin tuna described in this area, although the possibility of a diverged group of yellowfin tuna in the Arabian Sea has been reported (Barth et al., 2017; Grewe et al., 2020).

Otolith $\delta^{18}O$ values proved useful to allocate the origin of adult fish captured in three different fishing grounds of the south Indian Ocean (South Africa, Reunion, and Western Australia). Estimates of nursery origin of adult fish predicted that most of the individuals analysed in the three fishing grounds were derived from the West nursery, regardless of the modelling probability threshold used. This issue highlights the importance of the western Indian Ocean as a major production area for yellowfin tuna in the Indian Ocean. As with sub-adults, a high proportion of adult fish captured in Reunion were detected from the western nursery area. Fish of West nursery origin were also found in the Western Australian fishing ground. This large dispersal capacity was also shown by the Regional Tuna Tagging Program of the Indian Ocean (RTTP-IO), where tagged fish from Tanzania migrated eastward following the 28–29°C isotherm (Langley and Million, 2012), although fish from the west Indian Ocean had not been recaptured as far east as Western Australia (Fonteneau and Hallier, 2015). Fish with West nursery origin were also found among adult fish collected in South Africa. Few yellowfin tuna tagged off Tanzania

were also recovered in the Agulhas current, along the South African coast in the RTTP-IO (Fonteneau and Hallier, 2015). A substantial number of fish were left unclassified in South Africa, and to a lesser extent in Reunion and Western Australia. While this might be a result of the $\delta^{18}O$ overlap among the estimated baselines, it is also possible that individuals from other more local nursery areas not sampled in this study are present in the adult mixed sample. In addition, a few adults with Pakistan-like signature were predicted from each of the three adult locations sampled, suggesting that, as adults, some movements out from the potential Arabian Sea nursery area may occur. This movements from fish outside the Arabian Sea area to has been corroborated by RTTP-IO data analysing the trajectories of yellowfin tuna tagged of Oman (Appendix D, Figure D2). We did not find fish from the Central or East nurseries in the adult mixed samples from the three fishing grounds sampled in this study. This may be explained by the retention of sub-adult and adult yellowfin tuna near these two nursery areas, or because yellowfin tuna from the central and eastern nurseries tend to migrate towards feeding grounds not sampled in this study (e.g. Bay of Bengal). Limited movement of adult yellowfin tuna outside the Maldives region, where the Central nursery is, were described in tagging studies (Kolody and Hoyle, 2013). It is also possible that eastern and central nurseries are less productive than the western equatorial area, and therefore the occurrence of individuals from these origins is lower.

4.2 Oxygen isotopic distribution along the otolith and isoscape predictions

The SIMS analysis provided a good resolution of $\delta^{18}O$ estimates along the otolith growth transect. This is the first time that such type of analysis has been done for a tropical tuna species, and the observed results highlight the potential of SIMS analyses to significantly expand our understanding of the movements and life history of these species. Electronic tagging devices can provide geolocation estimates for a fish on a daily basis, but data for an entire life are not always available, either because very small fish are not able to carry the devices, the devices cannot store such large amount of data, battery exhaustion, or the tags are not retain by the fish over that time (Brownscombe et al., 2019; Musyl et al., 2011). Measuring variations in $\delta^{18}O$ across an otolith growth axis using the SIMS approach provides

fine scale information of the thermal experience of a fish over its lifetime, which may be particularly useful for comparing relative patterns of $\delta^{18}O$ composition among contingents, that is, fish with divergent migrations within stocks (Secor, 1999). In the case of the yellowfin tuna analysed, the results indicate that the fish may have spent parts of its life in different water masses. At the beginning of the transect, relatively little variability in otolith $\delta^{18}O$ was found, which may indicate retention within a homogeneous area in the first months of growth. At this part of the transect observed $\delta^{18}O$ values were lower, and as fish grew, detected $\delta^{18}O$ values increased. According to the inverse relationship between otolith $\delta^{18}O$ and water temperature (Thorrold et al., 1997; Trueman and MacKenzie, 2012), this suggests an overall decrease in experienced ambient waters temperatures. This trend may reflect a migration from equatorial waters to lower latitudes, a shift in the depth niche inhabited, or more likely, a combination of both. It is known that yellowfin tuna perform extensive migrations between spawning and feeding grounds, but also that depth preference changes according to body size (Fonteneau and Pallares-Soubrier, 1995; Graham and Dickson, 2004). By combining available maps of oxygen $\delta^{18}O$ and temperature at three different depth ranges, it was possible to infer the probable location of the analysed individual at a given point in time in the horizontal plane. Although adult yellowfin tuna are capable of diving into depths in excess of 1000m, these deep dives may not have sufficient duration to have been recorded in the otolith (Dagorn et al., 2006; Schaefer et al., 2007).

For the juvenile phase, the $\delta^{18}O$ values were in the range of those predicted for the west equatorial Indian Ocean at 0-20m and 20-50m depth ranges (**Figure 5.6A and 5.6B**). As fish grew, the observed $\delta^{18}O$ values were in the range of those predicted for the south sub-equatorial Indian Ocean or the Arabian Basin for these same depth ranges. Alternatively, the analysed individual may also have moved to deeper waters (50-100m) in west equatorial Indian Ocean or in subtropical waters south of the equator (**Figure 5.6C**). Some values also coincided with the range of $\delta^{18}O$ predicted values for 25-30°S band in the Indian Ocean (all depth ranges), and therefore it is more likely that the fish was moving into south-tropical waters than into the north Arabian Sea. Due to the lack of a representative spot just at the otolith edge, it was not possible to check whether observed $\delta^{18}O$ coincided for that predicted for South Africa (where the fish was caught). It seems clear that this

yellowfin tuna captured in South Africa was originated in the Indian Ocean rather than from the Atlantic Ocean, since higher otolith $\delta^{18}O$ values for the juvenile phase would have been detected in the latter case (**Figure 5.6**). This result is consistent with the findings from Mullins et al., (2018) which did not find Atlantic origin fish among yellowfin tuna captured in South Africa.

However, there are several issues that decrease the accuracy with which environmental histories of yellowfin tuna in the Indian Ocean can be reconstructed using otolith $\delta^{18}O$ composition. First, estimates were made based of the parameters estimated for Pacific Ocean bluefin tuna, a species belonging to the same sub-genus, but with different habitat preferences, which may influence the observed results, since experimentally determined values of γ and β appear to significantly vary among species (Kitagawa et al., 2013). The most robust approach for deriving a field-based fractionation equation parameter for yellowfin tuna, would be to analyse $\delta^{18}O$ data from otoliths formed under stable water temperature and $\delta^{18}O_{water}$ conditions of individuals reared in captivity (Nakamura et al., 2020). In addition, otolith $\delta^{18}O$ transect composition could be analysed on fish for which electronic tag information is available. That would provide a means for evaluating the accuracy of the estimates (Tanner et al., 2016). Second, the need of more precise estimates of water $\delta^{18}O$ values is a current limitation for more precise geolocation using otolith $\delta^{18}O$ composition (Trueman and St John Glew, 2019). Finally, individual variation in the physiological response to temperature needs to be better understood (Darnaude et al., 2014). Working towards solving all these issues will increase the added value of the SIMS technique for understanding yellowfin tuna life history. Another drawback of the present study is that the available samples used as a calibration set (YOYs) did not match the cohort of our sub-adult and adult samples. For otolith chemical analyses, the existence of such temporal variability can diminish the integrity of the observed results and confound spatial interpretations (Gillanders, 2002). However, otolith $\delta^{18}O$ decadal stability has been described by other authors (J. Rooker et al., 2008; Schloesser et al., 2009).

5. Conclusions

Although results obtained from this study come from a limited number of samples, the results suggest that connectivity and mixing rates of yellowfin tuna

within the Indian Ocean might be more complex than previously assumed. This preliminary study points towards an asymmetric connectivity of yellowfin tuna within the Indian Ocean. As such, West nursery seems to be a major source of contribution of yellowfin tuna to south equatorial fisheries of the Indian Ocean, with little apparent contributions from Central and East nurseries. In 2019, 75% of the total catches of yellowfin tuna in the Indian Ocean were derived from the Western region (IOTC, 2020b). The intense fishing of yellowfin tuna in this area, together with a lack of replenishment from the central and eastern components, may result in a differential local or regional stock dynamics. In addition, ignoring such pattern of connectivity can result in inaccurate estimates of stock productivity and misinterpretation of abundance trends in the stock assessment process (Kerr et al., 2015). Analysing YOY from known spawning areas over several years would set up a baseline for matching to otolith early life stage signatures from older fish. Besides, locating and sampling other potential spawning areas in the Indian Ocean will be important too (Artetxe-Arrate et al., 2020b). Further research on the origin of adult yellowfin tuna using otolith microchemistry should be undertaken to investigate the contribution of different nursery regions to fishery catches. Moreover, targeted analysis of otoliths from adult fish in spawning condition at the different nursery areas should be investigated to elucidate the degree of spawning area fidelity and exchange between nurseries. The SIMS approach proved to be a useful tool to infer the lifetime movements of an adult yellowfin tuna. The comparison of relative patterns of $\delta^{18}O$ composition along the growth axis of the otolith among individuals could contribute to a better understand of the contingent structure and metapopulation dynamics of this species (Cadrin and Secor, 2009). Although $\delta^{18}O$ is a promising geolocator for yellowfin tuna in the Indian Ocean, more accurate estimates of water $\delta^{18}O$ and the relationship between water $\delta^{18}O$ and temperature are required. Therefore, additional research must be guaranteed, as the complex connectivity patterns and individual-scale movements of yellowfin tuna within the Indian Ocean will have important implications for the management of this species. Ultimately, this information will be essential to inform sustainable management decisions that ensure the future of the resource and, hence, the fishery.

“Reserve your right to think,

for even to think wrongly is better than not to think at all”

Hypatia of Alexandria

GENERAL DISCUSSION

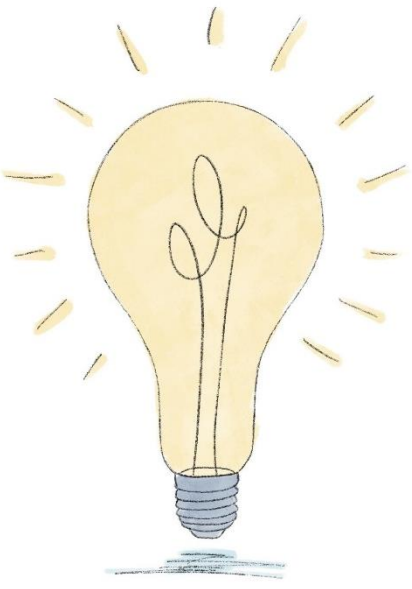

In a human altered marine ecosystem, saving our oceans must remain a priority (UNESCO, 2019). With the beginning of fisheries industrialization in the 1950s, large fleets started to venture out into international waters to harvest the open ocean around the world (Rousseau et al., 2018). Ever since, open ocean large predator species populations such as tunas and their relatives, have declined on average by 60% (Juan-Jordá et al., 2011). Given the reality that global food demand in rising, the world is gearing up to grow ever more reliant on the ocean for nourishment than ever before (Costello et al., 2020). Tropical areas have experience a continuous rising trend in capture production, with catches of tuna particularly increasing in the last decade (FAO, 2020a). The future sustainability of these fisheries will rely on the balance between the amount of biomass harvested and the resilience of these stocks to fishing pressure, which levels are estimated throughout stock assessment models (Merino et al., 2020). There is a compiling evidence showing that under intensive management procedures positive outcomes can be reported from fisheries (Hilborn et al., 2020). A sound understanding of stock structure of fish species can improve the reliability of models used to assess their status and the effects of fishing (Cadrin and Secor, 2009; Kerr et al., 2017). As such, planning sustainable strategies for development requires the identification of coherent units of individuals that have complete to partial discreteness from their congeners, in space and/or time. However, integrating our knowledge of spatial connectivity for a wide range of species is still a major a challenge for conservation science (Dunn et al., 2019).

This thesis focused on improving the understanding on stock structure of tropical tuna in the Indian Ocean, through the use natural chemical markers in otoliths (**Figure D.1**). First, a comprehensive multidisciplinary synthesis of the related literature was conducted (Chapter 1). For the otolith microchemistry perspective, the feasibility of using this technique to better understand the stock structure of tropical tuna was evaluated (Chapter 2) and utility and stability of elemental fingerprints unique to each nursery ground of skipjack (Chapter 3) and yellowfin (Chapter 4) tunas were investigated. Finally, nursery origin of adult yellowfin tuna was elucidated, and connectivity of given fishery grounds and exchange rates among major nursery areas were reported (Chapter 5).

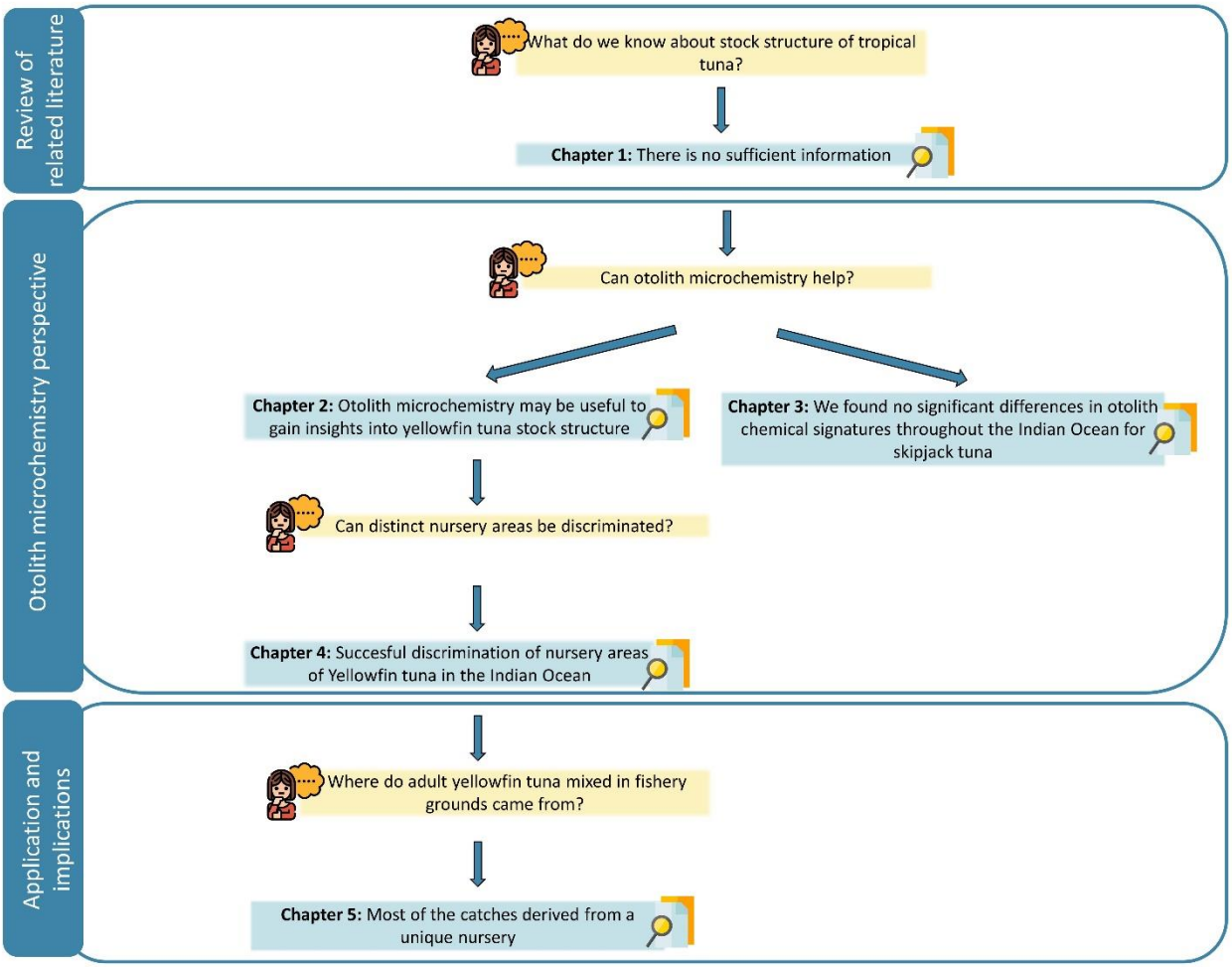

Figure D.1. Major research outcomes addressed in the present dissertation.

1. Available literature on tropical tuna life history parameters and stock structure

We found limited information regarding tropical tuna fundamental life history characteristics and stock structure in the Indian Ocean, composed of dispersed information that did not provide a clear picture of its biology and ecology. Different parameters have been reported for growth and reproduction of tropical tuna species in Indian Ocean. The lack of oceanic scale studies together with the fact that available studies are based on fish from different size/age classes and/or using different methods, make difficult to know whether observed differences stem from regional differences in growth and reproductive traits, or if they are just derived from different sampling/reporting strategies (Murua et al., 2017). This matter requires further clarification, as age, growth and mortality are an integral part of

fisheries stock assessment models (Maunder et al., 2015). Besides, uncertainties remain regarding tropical tuna reproductive behaviour, and there is still not a clear consensus on spawning time and location for these species. This knowledge is essential in order to understand the population productivity (Jakobsen et al., 2016). Expanding the knowledge on habitat utilization, is also needed to inform how tropical tuna might responds to human induced pressures. For example, a better understanding on the behaviour associated with vertical movements and feeding habits, can inform about species-specific or/and age-class vulnerability to different fishing gears (e.g., purse-seine and longline) or evaluate the impact of FADs in the Indian Ocean (Jaquemet et al., 2011; Leroy et al., 2009).

The bibliographic review also evidenced that the spatial structure of tropical tuna may be more complex than the currently assumed for management. This gap in our understanding on the connectivity of tropical tuna species in the Indian Ocean, may be hampering the delineation of proper stock boundaries. This, in turn, may affect the population dynamic models used to assess their status and inform management decisions (Begg et al., 1999; Cadrin, 2020). Chapter 1 review showed that results obtained from a single approach must be interpreted with caution. Determining the most appropriate spatial structure of a species involves a large and often complex process, and should include a comprehensive multidisciplinary synthesis of all available information sources (Cadrin, 2020; Pita et al., 2016). This is because an holistic approach from complementary disciplines (e.g. otolith microchemistry and genetic analysis), at both spatial and temporal scales, will enhance the chances of unravelling the "true" underlying structure of a population (Brophy et al., 2020; Randon and Réveillac, 2021; D. J. Welch et al., 2015). The combination of different stock delineation techniques is therefore needed to clarify the potential existing inconsistencies between the spatial dynamics and the fishery management units considered for tropical tuna in the Indian Ocean. If population are indeed distinct, or if mixing rates are very low within a panmictic population, there is a risk that the management strategies may not achieve conservation objectives and optimal economic use of the resource (Davies et al., 2020; Kitchens, 2017).

Considering all the above, there is an urgent need of improving our understanding of the resource and the fisheries to ensure a sustainable management of these species. Gaining a comprehensive knowledge on life history characteristics (e.g., growth, reproduction, habitat utilization) will contribute to reduce the uncertainty of the assessment models and provide better understanding of tropical tuna population dynamics and their resilience to fishing pressure. Improving our understanding on the stock structure, connectivity and mixing rates among geographically separated tropical tuna groups is paramount to identify the degree of population replenishment and persistence (Cowen et al., 2007). This in turn will improve the scientific advice and help to refine management and conservation strategies as needed. All this information will contribute to ensure the sustainability of these resources, and, hence, the fishery.

2. An otolith microchemistry perspective

Otolith chemical analyses have shown the potential to provide valuable information about natal origin (Wells et al., 2012, 2015), movements (Fraile et al., 2016; Macdonald et al., 2013) and connectivity (J. Rooker et al., 2008; Rooker et al., 2014) in tuna species of the Atlantic and the Pacific Oceans. However, its utility was not yet been proved for tropical tuna in the Indian Ocean. We used this approach to test whether skipjack and yellowfin tunas from different major nursery areas in the Indian Ocean could be discriminated based on their otolith chemical signature. We found that multi-elemental chemical signatures among putative nurseries are distinct enough to discriminate yellowfin tuna, but not for skipjack tuna. This was primarily due to the high overlap in the chemical signatures observed among skipjack tuna from different nursery areas. Apart from species-specific differential patterns of elemental incorporation into otoliths (Hamer and Jenkins, 2007), there were some particularities in the samples available for each species that may have influenced why discrimination was possible for yellowfin tuna, while not for skipjack. The smallest samples obtained for YOY skipjack tuna, were estimated to be older, in the range of 4-6 months (following the age-length relationship of Eveson et al., 2015), than YOY yellowfin tuna, which were less than 4 months (according to Proctor et al. 2019 age-length relationship). Thus, it is possible that skipjack tuna had already been mixing among nursery areas at the sampling age, and therefore

were not captured in their nursery of origin. Unfortunately, there is no tagging data showing distances travelled for skipjack tuna of these size ranges that can help to confirm or refute this hypothesis (Fonteneau and Hallier, 2015). Another potential reason is that the number of available samples with oxygen and carbon stable isotope data was more limited for skipjack (n=61) than for yellowfin (n=113) tuna, so that the sample size has limited the statistical power. This was due to the difficulty in preparing skipjack tuna otolith samples, as this species have smaller otoliths that were easily broken during preparation and micromilling process. Besides, the amount of otolith powder collected was often not sufficient to perform the measurements correctly. Thus, a challenge for future skipjack tuna otolith microchemistry studies will be, among others, to collect more samples, refine the methodological procedures to ensure more samples remain intact and that enough powder is collected from a single otolith. Lastly, skipjack and yellowfin tunas available for this dissertation were hatched at different periods. Whereas most of yellowfin tuna were estimated to hatch during the winter monsoon (Dec-Mar), skipjack tuna were estimated to hatch under distinct monsoon (Dec-Mar and Jun-Sep) and intermonsoon regimes (April-May and October-November). As we will further discuss in this section, temporal variability of the system is an important factor that may be influencing observed results of otolith chemical composition.

There is substantial uncertainty on how intrinsic (i.e. within individual) and extrinsic (i.e. environmental) processes affect elemental incorporation into the otolith (Hüssy et al., 2020; Sturrock et al., 2015). The complexity of the mechanisms behind elemental uptake and deposition in the otolith, do not still allow to fully apply the potential of otolith microchemistry, and available information found in the literature is often contradictory. The reason why the progress on this issue is slow is twofold; (1) physiological responses behind the element incorporation seem to be species specific and (2) controlled experiments are often difficult to perform. In the particular case of tuna species, for example, they are difficult to be reared in tanks (Farwell, 2001). Although there is a widespread agreement that the mere recognition of chemical differences in the otolith composition is enough for stock discrimination, the truth is that a better understanding of the processes governing otolith elemental incorporation could prove valuable to, for example, facilitate the selection of elements to be analysed or to unravel the life history of fishes (Izzo et

al., 2018; Tanner et al., 2016). Recent improvements in technology and software available to date, have started providing unprecedent information from otolith chemical composition that may increase the understanding on the interaction between extrinsic and intrinsic factors in uptake dynamics of elements, opening up a promising field of study (Walther, 2019). For instance, if we are able to confidently identify and relate the elements that are indicative of endogenous events, the reconstruction of physiological events and factors such as maternal investment, growth, condition and sexual maturation could be investigated through this perspective (Hüssy et al., 2020). Similarly, advances in computer algorithms are increasing the accuracy at which locational assignments can be made. Machine learning techniques for instance, have emerged as precise classifier models for otolith chemistry related studies. Traditional approaches (LDA and QDA) have been commonly used as the preferred classification methods in other tuna otolith chemistry studies (e.g. Rooker et al. 2008b, 2016; Wells et al. 2012; Macdonald et al. 2013), but we showed that the classification accuracy improved when using a machine learning technique such as Random Forest (RF). Our results are in accordance with those that encourage the use of machine learning methods when otolith chemical data lack multivariate normality or exhibit skewed distributions (Mercier et al. 2011; Jones et al. 2017). Likewise, a common limitation in otolith microchemistry studies aiming to infer adult origin, is that modelling approaches generally assume that all the potential sources of origin are characterised. For highly migratory species such as tropical tuna, samples composing the baseline are often opportunistically and/or intermittently obtained, and it is not always possible to meet this assumption. Therefore, if individuals of an unknown origin not sampled in the baseline are present in the adult mixed sample, these may not be accurately assigned. To this aim, non-parametric Bayesian mixture models and RF cluster analyses have been developed as promising methods that are able to handle unknown sources within a sample (Gibb et al., 2017; Neubauer et al., 2013; Régnier et al., 2017). As an alternative, classification methods that predict the probability of each individual in the mixed sample to belong to each of the nurseries present in the baseline and that allow to establish probability thresholds that assign individuals with lower predicted probabilities to an undetermined source of origin, can be used (Rooker et al., 2019). Another significant development in otolith microchemistry

field, are mapping approaches that have led to better analyse chemical patterns across otolith structures (Walther, 2019). In this dissertation, the use of two-dimensional spatial mapping of elements, proved useful to gain insights of elemental distribution patterns in yellowfin tuna otoliths. The disjunct accumulation shown for some of the elements analysed (i.e. differences in concentration among parts of the otolith corresponding to the same fish age), has not been previously considered in tuna related otolith microchemistry studies. This means that arbitrarily laid transects or spots can differ in element composition among samples just because of their placement in the otolith, entailing wrong interpretation of the results. Moreover, caution should also be taken when interpreting the results derived from transect analyses in otoliths. Changes in elemental concentrations along the transect have often been associated with changes in the environment experienced by the fish at different stages of their live (e.g. Arai et al., 2005; Macdonald et al., 2013). However, recent studies suggest that ontological changes may strongly influence otolith composition, as they show that fish occupying the same environment differ in their elemental composition according to their sizes (Macdonald et al., 2020; P Reis-Santos et al., 2018).

On the other hand, in the present dissertation we have acknowledged that elemental composition of yellowfin and skipjack tunas collected in the Indian Ocean may vary both inter and intra-annually. Given the fact that tropical tuna have several reproductive peaks during the year (Grande et al., 2010; Zudaire et al., 2013a), and considering the varying oceanographic regime of the Indian Ocean, reliable determination of nursery origin can be seriously undermined if temporal variability of otolith chemical signals is not assessed and accounted. The existence of such temporal variability can diminish the integrity of the observed results and confound spatial interpretations (Gillanders, 2002). Therefore, it is important that adults to be assigned to their nursery area of origin belong to the same cohort and season as those YOY forming the reference baseline. This issue was one of the greatest limitations of the present dissertation. Due to sampling constrains, our calibration set of YOY forming the baseline did not match the cohorts of our adults, which belonged to several year-classes. Nevertheless, not all the trace elements and stable isotopes showed temporal variability. We show that, unlike trace elements, carbon and oxygen stable isotopes did not show inter- nor intra- annual variability in the

period of study. Besides, otolith $\delta^{18}O$ decadal stability was described by other authors (J. Rooker et al., 2008; Schloesser et al., 2009). This issue justified the pooling of years for establishing a baseline of $\delta^{18}O$ signatures for YOY from major nursery areas in the Indian Ocean, that was then used to identify the most likely origin of sub-adult and adult yellowfin tuna collected from regional fisheries in the Indian Ocean.

3. Application and implication for tropical tuna management

When comparing sub-adult and adult yellowfin tuna otolith $\delta^{18}O$ composition corresponding to the early life period (~2 months) with that of the YOYs composing the baseline, the most likely origin of these older fish was predicted. Sub-adult fish (40-75 cm FL) have not reached sexual maturity yet (Zudaire et al., 2013a), but large scale movements can be expected for fish of these lengths according to tag-recapture data observations (Fonteneau and Hallier, 2015). However, from our findings it seems that sub-adult fish captured in the north (Pakistan) and south (Reunion) western Indian Ocean did not mix, otherwise a mix of overlapping nursery origin signals would had been detected. Instead, we found that sub-adult yellowfin tuna captured in both regions own unique oxygen stable isotope fingerprints, suggesting that these fish are derived from distinct nurseries. Furthermore, the otolith $\delta^{18}O$ composition of sub-adult yellowfin tuna from north western Indian Ocean did not resemble to any of the nursery areas present in the baseline. This implies either that (1) there is a nursery area of yellowfin tuna in the Arabian Sea area or (2) they are derived from a distinct nursery area not present in the baseline. Comparing the $\delta^{18}O$ signal found in the sub-adult fish otoliths to that from the calculated isoscapes of potential $\delta^{18}O$, it seems plausible that this fish was originated in the Arabian Sea area. To date no nursery areas of yellowfin tuna have been described in this environment. It would be interesting to sample adult yellowfin tuna and to perform a macroscopic identification of their gonads and/or larval surveys, so that it can be confirmed whether the Arabian Sea is an spawning area or not (Zudaire et al., 2013b). If this is confirmed, the presence of an spawning area of yellowfin tuna in this area would have important implications for

management and conservation, as the Arabian Sea represents the second major area in terms of yellowfin tuna catches of the Indian Ocean (IOTC, 2017c). The Arabian Sea experiences unique features that make this area very different to other worlds marine ecosystems (Kumari et al., 2005; Wafar et al., 2011). Many authors highlighted that other migratory species, such as oceanic sharks and whales, from this area are likely to be isolated (Jabado et al., 2018; Pomilla et al., 2014). Similarly, yellowfin tuna from the Arabian Sea showed to be genetically isolated from other Indo-Pacific yellowfin tuna populations (Barth et al., 2017). All together, these findings indicate that the Arabian Sea may be an area of high research and conservation priority for yellowfin tuna and other flagship species.

Additionally, we also found that the west Indian Ocean is a critical nursery area and production zone for yellowfin tuna, as this region appears to be the major contributor of yellowfin tuna recruits to three south-tropical fishery grounds sampled in the Indian Ocean. Although the number of available samples was limited, if the latter is confirmed, it can have significant implications for the management of yellowfin tuna in the region. Currently, 75% of the total catches of yellowfin tuna in the Indian Ocean are derived from the Western region (IOTC, 2020b). Therefore, continued high exploitation rates of this potential crucial nursery, may lead to ocean wide biomass declines as recruitment replenishment into other regional fisheries that depend on the western individuals may be impaired (**Figure D.2B**). Another potential consequence could be the local depletion and possible collapse of less productive stocks (e.g., central and eastern origin fish), if they keep exposed to the high fishing mortality levels (**Figure D.2C**).

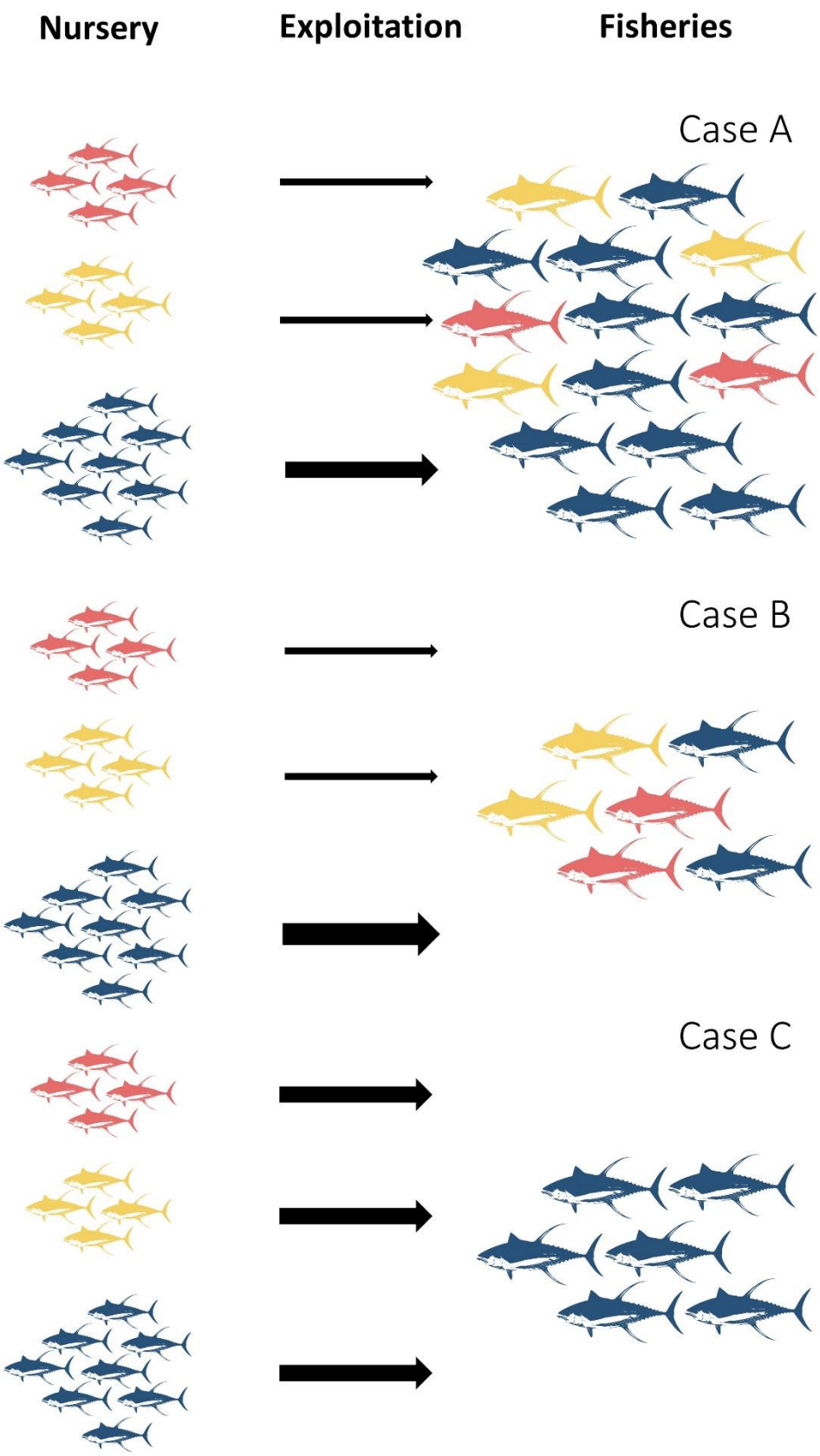

Figure D.2. Potential consequences of intense exploitation rates on discrete stock components to overall fisheries; exploitation rates in accordance with production and connectivity knowledge (A); high exploitation rates of the most productive nursery (B) and high exploitation rates of less productive nurseries (C).

4. Concluding remarks

Overall, observations from this study encourage further use of otolith chemical fingerprints to enhance our understanding of the stock structure and connectivity of yellowfin tuna in the Indian Ocean, while alternative methods or sampling strategies should be explored for skipjack tuna. Although tropical tuna spawn in warm tropical waters, temperature differences among nursery regions in the Indian Ocean were sufficiently distinct to allow otolith $\delta^{18}O$ values to provide regional discrimination among yellowfin tuna putative nursery areas. However, the effort and cost of including trace element data must be also considered as it can help to discriminate among nursery areas more effectively. Future work should create a library of chemical signatures from YOYs captured over several years and hatched under the same monsoon regime. This will provide an empirical procedure to determine the nursery origin of older individuals, that allow to estimate the relative contribution of each nursery area to the overall population. Ultimately, understanding the source of recruitment for the different fishery grounds will be essential to inform stock assessment and, hence, ensure sustainable fishery management. The closer management units reflect the stock structure, the better for achieving sustainable management goals. Meanwhile, the absence of adequate stock structure information shall not prevent the application of conservation and management measures that ensure the sustainability of tuna fisheries in the Indian Ocean. Establishing fishery management actions, for example limiting the increase in fishing capacity, establishing biological reference points or the designation of recovery plans among others, should continue to respond to the uncertainties in relation to more complex stock structure.

“Science makes people reach selflessly for truth and objectivity; it teaches people to accept reality, with wonder and admiration, not to mention the deep awe and joy that the natural order of things brings to the true scientist.”

Lise Meitner

CONCLUSIONS AND THESIS

The overarching aim of this thesis was to improve our understanding on the stock structure of skipjack and yellowfin tunas in the Indian Ocean. The overall aim was divided into four operational objectives that were addressed through the five chapters of the present dissertation.

From the first objective "*Undertake a review of the fisheries, life history and stock structure of tropical tuna in the Indian Ocean*" the main conclusions are:

1. There is general limited information regarding tropical tuna fundamental life history characteristics in the Indian Ocean. Most studies are regionally limited, which impedes a global overview of the complex interaction between the environment and these species. This, in turn, makes it difficult to incorporate life-history parameters at an appropriate scale into stock assessment models (**Chapter 1**).

2. The current stock assumption of single stock for skipjack, yellowfin and bigeye tunas has not been proved, and the information derived from different stock delineation methods highlights that the stock structure of skipjack and yellowfin tunas in the Indian Ocean could be more complex than expected. Due to the lack of oceanic scale analyses, the true nature and extent of the stock structure remains undefined (**Chapter 1**).

From the second objective "*To explore different methodological frameworks and factors to be considered in order to study the stock structure of skipjack and yellowfin species using otolith chemical signatures*" the main conclusions are:

3. Chemical concentrations of certain trace elements highly vary during the first weeks of life of the fish, probably due to factors other than ambient physicochemical properties. The use of otolith material from few weeks after hatch may represent a better alternative for early life history comparisons than the first material accreted in the primordial area (**Chapter 2**).

4. The choice of the optimal classification method is important when using otolith chemistry for fish origin identification purposes, as different classification methods lead to different results. If otolith chemical data is not normal and/or presents skewed distributions Random Forest classification should be the preferred method (**Chapter 2**).

5. Incorporation pathways and bounding preferences of each trace element may strongly influence their distribution within the otolith, as shown with two-dimensional mapping. This issue should be accounted when selecting assay locations for otolith chemical analyses, as element composition may strongly vary among samples even if the samples are positioned on the same growth increment of the otolith (**Chapter 4**).

6. Trace element composition of the otolith can highly vary both inter- and intra-annually. The seasonal variation in oceanographic conditions of the Indian Ocean seem to preclude the temporal stability of the regional differences in chemical signatures of the otolith of YOY from different nursery areas. It is therefore recommended that fish to be compared belong to the same cohort and are sampled at the same season. Likewise, when these signatures are been used as a baseline to determine the origin of older individuals, it may be more appropriate if adult age class match the cohort of the individuals used to describe the baseline (**Chapter 3 and Chapter 4**).

7. The high temporal resolution provided by continued core to edge measurements of the otolith using secondary ion mass spectrometry (SIMS) was useful to infer the lifetime movements of adult yellowfin tuna. The combination of otolith $\delta^{18}O$ chronologies together with the development of isoscapes of potential $\delta^{18}O$ in otoliths, can be used to track potential movements across water mases with distinct isotopic signatures. Besides, the comparison of $\delta^{18}O$ chronologies among individuals could allow better understanding of contingent structure and metapopulation dynamics of this species (**Chapter 5**).

From the third objective "*Develop a baseline of chemical signatures (stable isotopes and trace elements) in otoliths of young-of-the-year (YOY) skipjack and yellowfin tunas collected from nursery areas in the Indian Ocean*" the main conclusions are:

8. Chemical signatures of YOY skipjack tuna from three major nurseries in the Indian Ocean largely overlap for the years studied, hindering a robust discrimination among nursery areas. This suggests that the use of these otolith signatures alone is not sufficient to develop a reference baseline for each nursery area analysed for skipjack tuna (**Chapter 3**).

9. Significant regional differences exist in the chemical signature of YOY yellowfin tuna otoliths from major nursery areas in the Indian Ocean. Although nursery discrimination was mainly driven by $\delta^{18}O$ values, the inclusion of trace elements improved the assignment accuracy of each fish to their nursery of origin. The baseline signatures described in this study can serve as an effective tool for assigning older individuals to their nursery of origin (**Chapter 4**).

From the fourth objective "*Predict the nursery of origin of sub-adult and adult yellowfin tuna collected from regional fisheries in the Indian Ocean to evaluate their connectivity and the contribution of each nursery area to each fishery*" the main conclusions are:

10. There seems to be high level of local retention of sub-adult yellowfin tuna close to the western Indian Ocean nursery area (**Chapter 2 and Chapter 5**).

11. The distinct chemical composition of sub-adult yellowfin tuna captured in waters off Pakistan indicates these fish have a different origin to any of the fish forming the baseline sample. Comparison with isoscapes maps of potential $\delta^{18}O$ composition at each region suggests that there might be a nursery area of yellowfin tuna in the Arabian Sea. Alternatively, sub-adult

yellowfin tuna captured in Pakistan are derived from a nursery area not included in the baseline sample (**Chapter 5**).

12. Results from this study suggest an asymmetric connectivity of yellowfin tuna in the Indian Ocean. Most of the adult yellowfin tuna captured in fishery grounds south of the equator were derived from the western nursery, while no fish was classified to the central or eastern nurseries origins. This asymmetry in production can lead to biomass declines in other regional fisheries that depend on these western recruits, or/and induce local depletion of less productive units if these are overexploited (**Chapter 5**).

The specific results obtained on this thesis dissertation allowed working towards the stated hypothesis, being the thesis that:

"Young of the year yellowfin tuna from different nursery areas own distinct chemical signatures that can ultimately be used to elucidate the nursery origin of adult fish, providing a way to improve our understanding of the stock structure and mixing rates of this species in the Indian Ocean. However, this technique and sample composition were not suitable to discriminate among young of the year skipjack tuna from different nursery areas, and thus, other methods should be explored to better understand the stock structure and connectivity of this species in the Indian Ocean."

“Scientific knowledge belongs to humanity.”

Alexandra Elbakyan

REFERENCES

Abaunza, P., Murta, A.G., Campbell, N., Cimmaruta, R., Comesaña, A.S., Dahle, G., García Santamaría, M.T., Gordo, L.S., Iversen, S.A., MacKenzie, K., Magoulas, A., Mattiucci, S., Molloy, J., Nascetti, G., Pinto, A.L., Quinta, R., Ramos, P., Sanjuan, A., Santos, A.T., Stransky, C., Zimmermann, C., 2008. Stock identity of horse mackerel (Trachurus trachurus) in the Northeast Atlantic and Mediterranean Sea: Integrating the results from different stock identification approaches. Fish. Res. 89, 196–209. https://doi.org/10.1016/J.FISHRES.2007.09.022

Adam, S., Sibert, J.R., 2002. Population dynamics and movements of skipjack tuna (Katsuwonus pelamis) in the Maldivian fishery: analysis of tagging data from an advection-diffusion-reaction model. Aquat. Living Resour. 15, 13–23. https://doi.org/10.1016/S0990-7440(02)01155-5

Agnew, D.J., Pearce, J., Pramod, G., Peatman, T., Watson, R., Beddington, J.R., Pitcher, T.J., 2009. Estimating the worldwide extent of illegal fishing. PLoS One 4. https://doi.org/10.1371/journal.pone.0004570

Ahusan, M., Nadheeh, I., Adam, S., 2016. Length Distribution of Yellowfin Tuna from the Maldives Pole-and-line and Handline Tuna Fisheries.

Allemand, D., Mayer-Gostan, N., De Pontual, H., Boeuf, G., Payan, P., 2007. Fish Otolith Calcification in Relation to Endolymph Chemistry, in: Handbook of Biomineralization. Wiley-VCH Verlag GmbH, Weinheim, Germany, pp. 291–308. https://doi.org/10.1002/9783527619443.ch17

Alvarado-Bremer, J.R., Stéquert, B., Robertson, N.W., Ely, B., 1998. Genetic evidence for inter-oceanic subdivision of bigeye tuna (Thunnus obesus) populations. Mar. Biol. 132, 547–557. https://doi.org/10.1007/s002270050420

Anderson, M., Willis, T., 2003. Canonical analysis of principal coordinates: a useful method of constrained ordination for ecology. Ecology 84, 511–525. https://doi.org/10.1890/0012-9658

Anderson, M.J., 2001. A new method for non-parametric multivariate analysis of variance. Austral Ecol. 26, 32–46. https://doi.org/10.1002/9781118445112.stat07841

Andrews, A.H., Pacicco, A., Allman, R., Falterman, B.J., Lang, E.T., Golet, W., 2020. Age validation of yellowfin (Thunnus albacares) and bigeye (Thunnus obesus) tuna of the northwestern Atlantic Ocean. Can. J. Fish. Aquat. Sci. 77, 637–643. https://doi.org/637-643

Anganuzzi, A., 2004. Gathering data on unreported activities in Indian Ocean fishery, in: OECD (Ed.), Fish Piracy Combating Illegal, Unreported and Unregulated Fishing. pp. 147–155.

Appleyard, S.A., Ward, R.D., Grewe, P.M., 2002. Genetic stock structure of bigeye tuna in the Indian Ocean using mitochondrial DNA and microsatellites. J. Fish Biol. 60, 667–670. https://doi.org/0.1006/jfbi.2002.1866

Arai, T., Kotake, A., Kayama, S., 2005. Movements and life history patterns of the skipjack tuna Katsuwonus pelamis in the western Pacific, as revealed by otolith Sr: Ca ratios. J. Mar. Biol. Assoc. United Kingdom 85, 1211–1216. https://doi.org/10.1017/s0025315405012336

Aranda, M., Murillas, A., Motos, L., 2006. International management of shared stocks, in: Motos, L., Wilson, D, C. (Eds.), Developments in Aquaculture and Fisheries Science. pp. 29–54. https://doi.org/10.1016/S0167-9309(06)80005-0

Arrizabalaga, H., 2003. Estructura poblacional del atún blanco (Thunnus alalunga Bonn. 1788): una aproximación multidisciplinar. Universidad de Vigo.

Arrizabalaga, H., Dufour, F., Kell, L., Merino, G., Ibaibarriaga, L., Chustd, G., Irigoien, X., Santiago, J., Murua, H., Fraile, I., Chifflet, M., Goikoetxea, N., Sagarminaga, Y., Aumont, O., Bopp, L., Herrera, M., Fromentin, J.M., Bonhomeau, S., 2015. Global habitat preferences of commercially valuable tuna. Deep Sea Res. Part II Top. Stud. Oceanogr. 113, 102–112. https://doi.org/10.1016/j.dsr2.2014.07.001

Artetxe-Arrate, I., Fraile, I., Clear, N., Darnaude, A.M., Dettman, D., Pécheyran, C., Farley, J., Murua, H., n.d. Discrimination of yellowfin tuna (Thunnus albacares) from nursery areas in the Indian Ocean using otolith chemistry. Mar. Ecol. Prog. Ser. Under review.

Artetxe-Arrate, I., Fraile, I., Crook, D., Zudaire, I., Arrizabalaga, H., Greig, A., Murua, H., 2019. Otolith microchemistry: a useful tool for investigating stock structure of yellowfin tuna (Thunnus albacares) in the Indian Ocean. Mar. Freshw. Res. 70, 1708–1721. https://doi.org/10.1071/MF19067

Artetxe-Arrate, I., Fraile, I., Farley, J., Clear, N., Darnaude, A.M., Dettman, D., Eveson, P., Krug, I., Nikolic, N., Médieu, A., Ahusan, M., Landsdell, M., Proctor, C., Priatna, A., Lestari, P., Taufik, M., Parker, D., Usmani, H., Zehbra, K., MW, K., Shahid, U., Kazmi, S., Islam, S., Tarique, M., Zafar, S., Zaidi, J., Davies, C., Marscac, F., Murua, H., 2020a. Otolith δ18O as a tracer of yellowfin tuna (Thunnus albacares) nursery origin in the Indian Ocean (No. IOTC-2020-WPTT22(AS)-06_Rev1).

Artetxe-Arrate, I., Fraile, I., Marsac, F., Farley, J.H., Rodriguez-Ezpeleta, N., Davies, C., Clear, N., Grewe, P., Murua, H., 2020b. A review of the fisheries, life history and stock structure of tropical tuna (skipjack Katsuwonus pelamis, yellowfin Thunnus albacares and bigeye Thunnus obesus) in the Indian Ocean. Adv. Mar. Biol. 88, In press.

Asche, F., Garlock, T., Anderson, J., Bush, S., Smith, M., Anderson, C., Chu, J., Garrett, K.., Lem, A., Lorenzen, K., Oglend, A., Tveteras, S., Vannuccini, S., 2018. Three pillars of sustainability in fisheries. PNAS 115, 11221–11225. https://doi.org/10.1073/pnas.1807677115

Báez, J.C., Ramos, M.L., Herrera, M., Murua, H., Cort, J.C., Déniz, S., Rojo, V., Ruiz, J., Pascual-Añayón, P.J., Muniategi, A., Pérez-San Juan, A., Ariz, J., Fernández, F., Abascal, F., 2020. Monitoring of Spanish flagged purse seine fishery targeting tropical tuna in the Indian ocean: Timeline and history. Mar. Policy 119. https://doi.org/10.1016/j.marpol.2020.104094

Bailey, M., Ishimura, G., Paisley, R., Sumaila, U.R., 2013. Moving beyond catch in allocation approaches for internationally shared fish stocks. Mar. Policy 40, 124–136. https://doi.org/10.1016/j.marpol.2012.12.014

Bailey, R.M., Smith, G.R., 1981. Origin and Geography of the Fish Fauna of the Laurentian Great Lakes Basin. Can. J. Fish. Aquat. Sci. 38, 1539–1561. https://doi.org/10.1139/f81-206

Bakun, A., 2006. Fronts and eddies as key structures in the habitat of marine fish larvae: opportunity, adaptive response and competitive advantage. Sci. Mar. 105–122.

Bao, S., Wang, H., Zhang, R., Yan, H., Chen, J., 2020a. Spatial and temporal scales of sea surface salinity in the tropical Indian Ocean from SMOS, Aquarius and SMAP. J. Oceanogr. https://doi.org/10.1007/s10872-020-00552-8

Bao, S., Wang, H., Zhang, R., Yan, H., Chen, J., 2020b. Spatial and temporal scales of sea surface salinity in the tropical Indian Ocean from SMOS, Aquarius and SMAP. J. Oceanogr. 1–12. https://doi.org/10.1007/s10872-020-00552-8

Bard, F., Kouamé, B., Hervé, A., 2002. Schools of large yellowfin (Thunnus albacares) concentrated by foraging on a monospecific layer of Cubiceps pauciradiatus, observed in the eastern tropical Atlantic. ICCAT Coll Vol Sci Pap 54, 33–41.

Bard, F.X., 1984. Croissance de l'albacore (Thunnus albacares) Atlantique d'après les données de marquage. Rec. Doc. Sci. ICCAT 20, 104–116.

Barkley, R., Neill, W., Gooding, R., 1978. Skipjack tuna, Katsuwonus pelamis, habitat based on temperature and oxygen requirements. Fish. Bull. 76, 653–662.

Barnes, T.C., Gillanders, B.M., 2013. Combined effects of extrinsic and intrinsic factors on otolith chemistry: implications for environmental reconstructions. Can. J. Fish. Aquat. Sci. 70, 1159–1166. https://doi.org/10.1139/cjfas-2012-0442

Barth, J., Damerau, M., Matschiner, M., Jentoft, S., Hanel, R., 2017. Genomic differentiation and demographic histories of Atlantic and Indo-Pacific yellowfin tuna (Thunnus albacares) populations.

Genome Biol. Evol. 9, 1084–1098. https://doi.org/10.1093/gbe/evx067

Bath, G., Thorrold, S., Jones, C., Campana, S., 2000. Strontium and barium uptake in aragonitic otoliths of marine fish. Geochim. Cosmochim. Acta 64, 1705–1714. https://doi.org/10.1016/S0016-7037(99)00419-6

Begg, G., Friedland, K., Pearce, J., 1999. Stock identification and its role in stock assessment and fisheries management: an overview. Fish. Res. 43, 1–8. https://doi.org/10.1016/S0165-7836(99)00062-4

Begg, G., Waldman, J., 1999. An holistic approach to fish stock identification. Fish. Res. 43, 35–44. https://doi.org/10.1016/S0165-7836(99)00065-X

Belton, B., Reardon, T., Zilberman, D., 2020. Sustainable commoditization of seafood. Nat. Sustain. 3, 677–684. https://doi.org/10.1038/s41893-020-0540-7

Benjamini, Y., Hochberg, Y., 1995. Controlling the False Discovery Rate: A Practical and Powerful Approach to Multiple Testing. J. R. Stat. Soc. Ser. B 57, 289–300. https://doi.org/10.1111/j.2517-6161.1995.tb02031.x

Berger, A., McKechnie, S., Abascal, F., Kumasi, B., Usu, T., 2014. Analysis of tagging data for the 2014 tropical tuna assessments: data quality rules, tagger effects, and reporting rates. WCPFC-SC10-2014/SA-IP-06. Majuro, Republic of the Marshall Islands.

Berst, A.H., Simon, R.C., 1981. Introduction to the Proceedings of the 1980 Stock Concept International Symposium (STOCS). Can. J. Fish. Aquat. Sci. 38, 1457–1458. https://doi.org/10.1139/f81-194

Block, B., Teo, S., Walli, A., Boustany, A., Stokesbury, M., Farwell, C., Weng, K., Dewar, H., Williams, T., 2005. Electronic tagging and population structure of Atlantic bluefin tuna. Nature 434, 1121–1127. https://doi.org/10.1038/nature03463

Boehlert, G.W., Mundy, B.C., 1994. Vertical and onshore-offshore distributional patterns of tuna larvae in relation to physical habitat features. Mar. Ecol. Prog. Ser. 107, 1–13.

Booke, H., 1981. The conundrum of the stock concept—are nature and nurture definable in fishery science? Can. J. Fish. Aquat. Sci. 38, 1479–1480. https://doi.org/10.1139/f81-200

Bosley, K., Goethel, D., Berger, A., Deroba, J., Fenske, K., Hanselman, D., Langseth, B., Schueller, A., 2019. Overcoming challenges of harvest quota allocation in spatially structured populations. Fish. Res. 220, 105344. https://doi.org/10.1016/j.fishres.2019.105344

Bouchoucha, M., Pécheyran, C., Gonzalez, J., Lenfant, P., Darnaude, A.M., 2018. Otolith fingerprints as natural tags to identify juvenile fish life in ports. Estuar. Coast. Shelf Sci. 212, 210–218. https://doi.org/10.1016/j.ecss.2018.07.008

Brand, W.A., Coplen, T.B., Vogl, J., Rosner, M., Prohaska, T., 2014. Assessment of international reference materials for isotope-ratio analysis. IUPAC Tech. Rep. 86, 425–467. https://doi.org/10.1515/pac-2013-1023

Breiman, L., 2001. Random Forests. Mach. Learn. 45, 5–32.

Brophy, D., Jeffries, T.E., Danilowicz, B.S., 2004. Elevated manganese concentrations at the cores of clupeid otoliths: Possible environmental, physiological, or structural origins. Mar. Biol. 144, 779–786. https://doi.org/10.1007/s00227-003-1240-3

Brophy, D., Rodríguez-Ezpeleta, N., Fraile, I., Arrizabalaga, H., 2020. Combining genetic markers with stable isotopes in otoliths reveals complexity in the stock structure of Atlantic bluefin tuna (Thunnus thynnus). Nat. Sci. Reports 10, 1–17. https://doi.org/10.1038/s41598-020-71355-6

Brownscombe, J.W., Lédée, E.J., Raby, G.D., Struthers, D.P., Gutowsky, L.F., Young, N., Stokesbury, M.J.W., Holbrook, C.M., Brende, T.O., Vandergoot, C.S., Murchie, K.J., Whoriskey, K., Flemming, K.M., Kessel, S.T., Krueger, C.C., Cooke, S.J., 2019. Conducting and interpreting fish telemetry studies: considerations for researchers and resource managers. Rev. Fish Biol. Fish. 29, 396–400. https://doi.org/10.1007/s11160-019-09560-4

Buckel, J.A., Sharack, B.L., Zdanowicz, V.S., 2004. Effect of diet on otolith composition in Pomatomus saltatrix, an estuarine piscivore. J. Fish Biol. 64, 1469–1484. https://doi.org/10.1111/j.0022-1112.2004.00393.x

Cadrin, S., Secor, D., 2009. Accounting for Spatial Population Structure in Stock Assessment: Past, Present, and Future, in: Beamish, R., Rothschild, B. (Eds.), The Future of Fisheries Science in North America. Springer Netherlands. https://doi.org/10.1007/978-1-4020-9210-7_22

Cadrin, S.X., 2020. Defining spatial structure for fishery stock assessment. Fish. Res. 221, 105397. https://doi.org/0.1016/j.fishres.2019.105397

Cadrin, S.X., Kerr, L.A., Mariani, S., 2014. Stock identification methods: an overview, in: Cadrin, S.X., Kerr, L.A., Mariani, S. (Eds.), Stock Identification Methods. Academic Press, pp. 1–5. https://doi.org/10.1016/B978-0-12-397003-9.00001-1

Cadrin, S. X., Kerr, L.A., Mariani, S., 2014. Stock identification methods: applications in fishery science, Second. ed. Academic Press, San Diego, California. https://doi.org/10.1016/B978-0-12-397003-9.01001-8

Campana, S., 1999. Chemistry and composition of fish otoliths: pathways, mechanisms and applications. Mar. Ecol. Prog. Ser. 188, 263–297. https://doi.org/10.3354/meps188263

Campana, S., Chouinard, G., Hanson, J., Frechet, A., 2000. Otolith elemental fingerprints as biological tracers of fish stocks. Fish. Res. 46, 343–357. https://doi.org/10.1016/S0165-7836(00)00158-2

Campana, S., Neilson, J., 1985. Microstructure of fish otoliths. Can. J. Fish. Aquat. Sci. 42, 1014–1032. https://doi.org/10.1139/f85-127

Campana, S.E., 2005. Otolith Elemental Composition as a Natural Marker of Fish Stocks, in: Cadrin, S.X., Friedland, K.D., Waldman, J. (Eds.), Stock Identification Methods . Applications in Fishery Science. Elsevier Academic Press, pp. 227–245. https://doi.org/10.1016/B978-012154351-8/50013-7

Campana, S.E., Thorrold, S.R., 2001. Otoliths, increments, and elements: keys to a comprehensive understanding of fish populations? Can. J. Fish. Aquat. Sci. 58, 30–38. https://doi.org/10.1139/f00-177

Campbell, J.L., Babaluk, J.A., Cooper, M., Grime, G.W., Halden, N.M., Nejedly, Z., Rajta, I., Reist, J.D., 2002. Strontium distribution in young-of-the-year Dolly Varden otoliths: Potential for stock discrimination. Nucl. Instruments Methods Phys. Res. Sect. B Beam Interact. with Mater. Atoms 189, 185–189. https://doi.org/10.1016/S0168-583X(01)01039-4

Cardinale, M., Svedäng, H., Bartolino, V., Maiorano, L., Casini, M., Linderholm, H., 2012. Spatial and temporal depletion of haddock and pollack during the last century in the Kattegat-Skagerrak. J. Appl. Ichthyol. 28, 200–208. https://doi.org/10.1111/j.1439-0426.2012.01937.x

Carey, F., Teal, J., Kanwisher, J., Lawson, K.D., Beckett, J.S., 1971. Warm-bodied fish. Am. Zool. 11, 137–143. https://doi.org/10.1093/icb/11.1.137

Carvalho, G.R., Hauser, L., 1994. Molecular genetics and the stock concept in fisheries. Rev. Fish Biol. Fish. 4, 326–350. https://doi.org/10.1007/BF00042908

Casselman, J.M., Collins, J.J., Grossman, E.J., Ihssen, P.E., Spangler, G.R., 1981. Lake Whitefish (Coregonus clupeaformis) Stocks of the Ontario Waters of Lake Huron . Can. J. Fish. Aquat. Sci. 38, 1772–1789. https://doi.org/10.1139/f81-225

Catalano, S., Whittington, I., Donnellan, S., 2014. Parasites as biological tags to assess host population structure: guidelines, recent genetic advances and comments on a holistic approach. Int. J. Parasitol. Parasites Wildl. 3, 220–226. https://doi.org/10.1016/j.ijppaw.2013.11.001

Ceo, M., Fagnani, S., Swan, J., Tamada, K., Watanabe, H., 2012. Performance reviews by regional fishery bodies: Introduction, summaries, synthesis and best practices, Volume I: CCAMLR, CCSBT, ICCAT, IOTC, NAFO, NASCO, NEAFC,. Rome, Italy.

Chen, Z., Jones, C.M., 2006. Simultaneous Determination of 33 Major, Minor, and Trace Elements in Juvenile and Larval Fish Otoliths by High Resolution Double Focusing Sector Field Inductively Coupled Plasma Mass Spectrometry *, in: Winter Conference on Plasma Spectrochemistry. Tucson, Arizona, pp. 8–14.

Chiang, H., Hsu, C., Wu, G., Chang, S., Yang, H., 2008. Population structure of bigeye tuna (Thunnus obesus) in the Indian Ocean inferred from mitochondrial DNA. Fish. Res. 90, 305–312. https://doi.org/10.1016/j.fishres.2007.11.006

Chow, S., Hazama, K., Nishida, T., Ikame, S., Kurihara, S., 2000a. A preliminary genetic analysis on yellowfin tuna stock structure in the Indian Ocean using mitochondrial DNA variation, in: IOTC Proceedings. pp. 312–316.

Chow, S., Okamoto, H., Miyabe, N., Hiramatsu, K., 2000b. Genetic divergence between Atlantic and Indo-Pacific stocks of bigeye tuna (Thunnus obesus) and admixture around South Africa. Mol. Ecol. 9, 221–227. https://doi.org/10.1046/j.1365-294x.2000.00851.x

Christ, H.J., White, R., Hood, L., Vianna, G.M.S., Zeller, D., 2020. A Baseline for the Blue Economy: Catch and Effort History in the Republic of Seychelles' Domestic Fisheries. Front. Mar. Sci. 7. https://doi.org/10.3389/fmars.2020.00269

Chung, M., Trueman, C., Godiksen, J., Grønkjær, P., 2019. Otolith δ13C values as a metabolic proxy: approaches and mechanical underpinnings. Mar. Freshw. Res. 70, 1747–1756. https://doi.org/10.1071/MF18317

Clarke, L.M., Thorrold, S.R., Conover, D.O., 2011. Population differences in otolith chemistry have a genetic basis in Menidia menidia. Can. J. Fish. Aquat. Sci. 68, 105–114. https://doi.org/10.1139/F10-147

Claverie, F., Fernández, B., Pécheyran, C., Alexis, J., Donard, O.F.X., 2009. Elemental fractionation effects in high repetition rate IR femtosecond laser ablation ICP-MS analysis of glasses. J. Anal. At. Spectrom. 24, 891–902. https://doi.org/10.1039/b904134f

Collette, B.B., 2017. Bluefin tuna science remains vague. Science (80-.). 358, 879–880. https://doi.org/10.1126/science.aar3928

Collette, B.B., Nauen, C.E., 1983. Scombrids of the World. An Annotated and Illustrated Catalogue of Tunas, Mackerels, Bonitos and Related Species Known to Date, FAO, Rome. ed.

Collette, B.B., Reeb, C., Block, B.A., 2001. Systematics of the tunas and mackerels (Scombridae). Fish Physiol. 19, 1–33. https://doi.org/10.1016/S1546-5098(01)19002-3

Conand, F., Richards, W.J., 1982. Distribution of tuna larvae between Madagascar and the Equator, Indian Ocean. Biol. Oceanogr. 1, 321–336. https://doi.org/10.1080/01965581.1982.10749446

Costello, C., Cao, L., Gelcich, S., Cisneros-Mata, M.A., Free, C.M., Froelich, H.., C.D., G., Ishimura, G., Maier, J., Macadam-Somer, I., Manging, T., Melnychuck, M.C., Miyahara, M., de Moor, C., Naylor, R., Nøstbakken, L., Ojea, E., O´Reilly, E., Parma, A.M., Plantinga, A.J., Thilstead, S.H., Lubchenco, J., 2020. The future of the sea. Nature 588, 95–100. https://doi.org/10.1038/s41586-020-2616-y

Cowen, R., Gawarkiewicz, G., Pineda, J., Thorrold, S., Werner, F., 2007. Population connectivity in marine systems: an overview. Oceanography 20, 14–21.

Craig, C.A., Jarvis, K.E., Clarke, L.J., 2000. An assessment of calibration strategies for the quantitative and semi-quantitative analysis of calcium carbonate matrices by laser ablation-inductively coupled plasma-mass spectrometry (LA-ICP-MS). J. Anal. At. Spectrom. 15, 1001–1008. https://doi.org/10.1039/B002097O

Cullis-Suzuki, S., Pauly, D., 2010. Failing the high seas: a global evaluation of regional fisheries management organizations. Mar. Policy 34, 1036–1042. https://doi.org/10.1016/j.marpol.2010.03.002

Cutler, D.R., Edwards, T.C., Beard, K.H., Cutler, A., Hess, T.K., Gibson, J., Lawler, J.J., 2007. Random forests for classification in ecology. Ecology 88, 2783–2792. https://doi.org/10.1890/07-0539.1

Dagorn, L., Holland, K., Hallier, J., Taquet, M., Moreno, G., Sancho, G., Itano, D.G., Aumeeruddy, R., Girard, C., Million, J., Fonteneau, A., 2006. Deep diving behavior observed in yellowfin tuna (Thunnus albacares). Aquat. Living Resour. 19, 85–88. https://doi.org/10.1051/alr:2006008

Dahl, K., 1909. The problem of sea fish hatching. Special Part B, No. 5., in: Rapport Sur Les Travaux de Commision A, Dans La Période 1902–1907. Conseil Permanent International Pour l'Exploration de La Mer. Rapports et Procès-Verbaux, Vol. X. Special Part B, No. 5.

Dammannagoda, S., Hurwood, D., Mather, P., 2011. Genetic analysis reveals two stocks of skipjack tuna (Katsuwonus pelamis) in the northwestern Indian Ocean. Can. J. Fish. Aquat. Sci. 68, 210–223. https://doi.org/10.1139/F10-136

Dammannagoda, S., Hurwood, D., Mather, P., 2008. Evidence for fine geographical scale heterogeneity in gene frequencies in yellowfin tuna (Thunnus albacares) from the north Indian Ocean around Sri Lanka. Fish. Res. 90, 147–157. https://doi.org/10.1016/j.fishres.2007.10.006

Darnaude, A.M., Hunter, E., 2018. Validation of otolith δ18O values as effective natural tags for shelf-scale geolocation of migrating fish. Mar. Ecol. Prog. Ser. 598, 167–185.

Darnaude, A.M., Sturrock, A., Trueman, C.N., Mouillot, D., Craven, J.A., Campana, S.E., Hunter, E., 2014. Listening in on the past: What can otolith δ18O values really tell us about the environmental history of fishes? PLoS One 9. https://doi.org/10.1371/journal.pone.0108539

Daszykowski, M., Kaczmarek, K., Vander Heyden, Y., Walczak, B., 2007. Robust statistics in data analysis — A review: Basic concepts. Chemom. Intell. Lab. Syst. 85, 203–219. https://doi.org/10.1016/J.CHEMOLAB.2006.06.016

Davies, C., Marsca, F., Murua, H., Fraile, I., Fahmi, Z., Farley, J., Grewe, P., Proctor, C., Clear, N., Landsdell, M., Aulich, J., Feutry, P., Cooper, S., Foster, S., Rodríguez-Ezpeleta, N., Artetxe-Arrate, I., Nikolic, N., Krug, I., Mendibidil, I., Leone, A., Labonne, M., Darnaude, A.M., Arnaud-Haond, S., Devloo-Delva, F., Rougeuc, C., Parker, D., Diaz-Arce, N., Wudianto, Ruchimat, T., Satria, F., Lestari, P., Taufik, M., Priatna, A., Zamroni, A., 2020. Study of population structure of IOTC species and sharks of interest in the Indian Ocean using genetics and microchemistry: 2020 Final Report to IOTC.

Degens, E.T., Deuser, W.G., Haedrich, R.L., 1969. Molecular structure and composition of fish otoliths. Mar. Biol. 2, 105–113. https://doi.org/10.1007/BF00347005

Di Franco, A., Bulleri, F., Pennetta, A., De Benedetto, G., Clarke, K.R., Guidetti, P., 2014. Within-Otolith Variability in Chemical Fingerprints: Implications for Sampling Designs and Possible Environmental Interpretation. PLoS One 9, e101701. https://doi.org/10.1371/journal.pone.0101701

Díaz-Arce, N., Arrizabalaga, H., Murua, H., Irigoien, X., Rodríguez-Ezpeleta, N., 2016. RAD-seq derived genome-wide nuclear markers resolve the phylogeny of tunas. Mol. Phylogenet. Evol. 102, 202–207. https://doi.org/10.1016/j.ympev.2016.06.002

Dickson, K., 1995. Unique adaptations of the metabolic biochemistry of tunas and billfishes for life in the pelagic environment. Environ. Biol. Fishes 2, 65–97. https://doi.org/10.1007/BF00002352

Dizon, A.E., Neill, W.H., Magnuson, J.J., 1977. Rapid temperature compensation of volitional swimming speeds and lethal temperatures in tropical tunas (Scombridae). Environ. Biol. Fishes 2, 83–92. https://doi.org/10.1007/BF00001418

Dortel, E., Sardenne, F., Bousquet, N., Rivot, E., Million, J., 2015. An integrated Bayesian modeling approach for the growth of Indian Ocean yellowfin tuna. Fish. Res. 163, 69–84. https://doi.org/10.1016/j.fishres.2014.07.006

Doubleday, Z.A., Harris, H.H., Izzo, C., Gillanders, B.M., 2014. Strontium Randomly Substituting for Calcium in Fish Otolith Aragonite. Anal. Chem. 86, 865–869. https://doi.org/10.1021/ac4034278

Doubleday, Z.A., Izzo, C., Woodcock, S.H., Gillanders, B.M., 2013. Relative contribution of water and diet to otolith chemistry in freshwater fish. Aquat. Biol. 18, 271–280. https://doi.org/10.3354/ab00511

Druon, J.N., Chassot, E., Murua, H., Lopez, J., 2017. Skipjack Tuna Availability for Purse Seine Fisheries Is Driven by Suitable Feeding Habitat Dynamics in the Atlantic and Indian Oceans. Front. Mar. Sci. 4, 315. https://doi.org/10.3389/fmars.2017.00315

Duffy, L., Kuhnert, P., Pethybridge, H., Young, J., Olson, R., Logan, J., Goñi, N., Romanov, E., Allain, V., Staudinger, M., Abecassis, M., Choy, C., Hobday, A., Simier, M., Galván-Magaña, F., Potier, M., Ménard, F., 2017. Global trophic ecology of yellowfin, bigeye, and albacore tunas: Understanding predation on micronekton communities at ocean-basin scales. Deep Sea Res. Part II Top. Stud. Oceanogr. 140, 55–73. https://doi.org/10.1016/j.dsr2.2017.03.003

Dunn, D.C., Harrison, A.L., Curtice, C., DeLand, S., Donnelly, B., Fujioka, E., Heywood, E., Kot, C.Y., Poulin, S., Whitten, M., Åkesson, S., Alberini, A., Appeltans, W., Arcos, J.M., Bailey, H., Ballance, L.T., Block, B., Blondin, H., Boustany, A.M., Brenner, J., Catry, P., Cejudo, D., Cleary, J., Corkeron, P., Costa, D.P., Coyne, M., Crespo, G.O., Davies, T.E., Dias, M.P., Douvere, F., Ferretti, F., Formia, A., Freestone, D., Friedlaender, A.S., Frisch-Nwakanma, H., Froján, C.B., Gjerde, K.M., Glowka, L., Godley, B.J., Gonzalez-Solis, J., Granadeiro, J.P., Gunn, V., Hashimoto, Y., Hawkes, L.M., Hays, G.C., Hazin, C., Jimenez, J., Johnson, D.E., Luschi, P., Maxwell, S.M., McClellan, C., Modest, M., Di Sciara, G.N., Palacio, A.H., Palacios, D.M., Pauly, A., Rayner, M., Rees, A.F., Salazar, E.R., Secor, D., Sequeira, A.M.M., Spalding, M., Spina, F., Van Parijs, S., Wallace, B., Varo-Cruz, N., Virtue, M., Weimerskirch, H., Wilson, L., Woodward, B., Halpin, P.N., 2019. The importance of migratory connectivity for global ocean policy. Proc. R. Soc. B Biol. Sci. 286. https://doi.org/10.1098/rspb.2019.1472

Durand, J., Collet, A., Chow, S., Guinand, B., Borsa, P., 2005. Nuclear and mitochondrial DNA markers indicate unidirectional gene flow of Indo-Pacific to Atlantic bigeye tuna (Thunnus obesus) populations, and their admixture off southern Africa. Mar. Biol. 147, 313–322. https://doi.org/10.1007/s00227-005-1564-2

Elsdon, T., Gillanders, B., 2005. Alternative life-history patterns of estuarine fish: barium in otoliths elucidates freshwater residency. Can. J. Fish. Aquat. Sci. 62. https://doi.org/10.1139/f05-029

Elsdon, T., Gillanders, B., 2004. Fish otolith chemistry influenced by exposure to multiple environmental variables. J. Exp. Mar. Bio. Ecol. 313, 269–284. https://doi.org/10.1016/j.jembe.2004.08.010

Elsdon, T.S., Gillanders, B.M., 2002. Interactive effects of temperature and salinity on otolith chemistry: challenges for determining environmental histories of fish. Can. J. Fish. Aquat. Sci. 59, 1796–1808. https://doi.org/10.1139/f02-154

Elsdon, T.S., Wells, B.K., Campana, S.E., Gillanders, B.M., Jones, C.M., Limburg, K.E., Walther, B.D., 2008. Otolith chemistry to describe movements and life-history parameters of fishes: hypotheses, assumptions, limitations and inferences. Oceanogr. Mar. Biol. an Annu. Rev. 46, 297–330.

Ely, B., Viñas, J., Alvarado-Bremer, J., Black, D., Lucas, L., Covello, K., Labrie, A., Thelen, E., 2005. Consequences of the historical demography on the global population structure of two highly migratory cosmopolitan marine fishes: the yellowfin tuna (Thunnus albacares) and the skipjack tuna (Katsuwonus pelamis). BMC Evol. Biol. 5, 1–9. https://doi.org/10.1186/1471-2148-5-19

Erceg-Hurn, D.., Mirosevich, V.M., 2008. Modern robust statistical methods: An easy way to maximize the accuracy and power of your research. Am. Psychol. 63, 591–601. https://doi.org/10.1037/0003-066X.63.7.591

Estes, J.A., Heithaus, M., McCauley, D.J., Rasher, D.B., Worm, B., 2016. Megafaunal Impacts on Structure and Function of Ocean Ecosystems. Annu. Rev. Environ. Resour. 41, 83–116. https://doi.org/10.1146/annurev-environ-110615-085622

Evans, K., Langley, A., Clear, N.P., Williams, P., Patterson, T., Sibert, J., Hampton, J., Gunn, J.S., 2008. Behaviour and habitat preferences of bigeye tuna (Thunnus obesus) and their influence on longline fishery catches in the western Coral Sea. Can. J. Fish. Aquat. Sci. 65, 2427–2443. https://doi.org/10.1139/F08-148

Eveson, J., Million, J., Sardenne, F., Croizier, G.L., 2015. Estimating growth of tropical tunas in the Indian Ocean using tag-recapture data and otolith-based age estimates. Fish. Res. 163, 58–68. https://doi.org/10.1016/j.fishres.2014.05.016

Eveson, J., Million, J., Sardenne, F., Le Croizier, G., 2012. Updated growth estimates for Skipjack, Yellowfin and Bigeye tuna in the Indian Ocean using the most recent tag-recapture and otolith data. IOTC-2012-WPTT14-23 1–57.

FAO, 2020a. The State of World Fisheries and Aquaculture 2020. Sustainability in action. Rome. https://doi.org/10.4060/ca9229en

FAO, 2020b. Fishery Statistical Collections [WWW Document]. Glob. Capture Prod. 1950-2018 (online query). URL http://www.fao.org/fishery/statistics/global-capture-production/query/en (accessed 4.1.20).

FAO, 2018. The State of World Fisheries and Aquaculture 2018- Meeting the sustainable development goals. Rome.

FAO, 2016. The State of World Fisheries and Aquaculture 2016. Contributing to food security and nutrition for all., Food and Agriculture Organization of the United Nations. Rome.

Farley, J., Clear, N., Leroy, B., Davis, T., McPherson, G., 2006. Age, growth and preliminary estimates of maturity of bigeye tuna, Thunnus obesus, in theAustralian region. Mar. Freshw. Res. 57, 713–724. https://doi.org/10.1071/MF05255

Farwell, C., 2001. Tunas in captivity, in: Block, B., Stevens, E. (Eds.), Tuna: Physiology, Ecology and Evolution. Academic Press, London, pp. 391–412.

Fielding, A.H., Bell, J.F., 1997. A review of methods for the assessment of prediction errors in conservation presence/absence models. Environ. Conserv. 24, 38–49.

Fingas, M., 2019. Remote Sensing for Marine Management, in: Sheppard, C. (Ed.), World Seas: An Environmental Evaluation. Elsevier Ltd., pp. 103–119. https://doi.org/10.1016/B978-0-12-805052-1.00005-X

Flynn, A., Paxton, J., 2013. Spawning aggregation of the lanternfish Diaphus danae (family Myctophidae) in the north-western Coral Sea and associations with tuna aggregations. Mar. Freshw. Res. 63, 1255–1271.

Fonteneau, A., 2014. On the movements and stock structure of skipjack (Katsuwonus pelamis) in the Indian ocean. IOTC–2014–WPTT16–36, 16 1–16.

Fonteneau, A., 2010. Atlas des pêcheries thonières de l'océan Indien/Atlas of Indian Ocean tuna fisheries. IRD Ed. 191.

Fonteneau, A., 2003. A Comparative overview of skipjack fisheries and stocks worlwide. IOTC Proc. no. 6 WPTT-03-02, 8–21.

Fonteneau, A., 1980. La croissance de l'albacore de l'Atlantique. Est. Rec. Doc. Sci. ICCAT 9, 152–168.

Fonteneau, A., Hallier, J.P., 2015. Fifty years of dart tag recoveries for tropical tuna: A global comparison of results for the western Pacific, eastern Pacific, Atlantic,and Indian Oceans. Fish. Res. 163, 7–22. https://doi.org/10.1016/j.fishres.2014.03.022

Fonteneau, A., Pallares-Soubrier, P., 1995. Interactions between tuna fisheries: A global review with specific examples from the Atlantic Ocean, in: Shomura, R.S.., Majkowski, J., Harman, R.F. (Eds.), Status of Interactions of Pacific Tuna Fisheries. in 1995. Proceedings of the Second FAO Expert Consultation Interactions of Pacific Tuna Fisheries. Shimizu, Japan, 23-31 January 1995. FAO Fisheries Technical Paper. FAO, Rome, Italy.

Fowler, A., Hamer, P., Kemp, J., 2017. Age-related otolith chemistry profiles help resolve demographics and meta-population structure of a widely-dispersed, coastal fishery species. Fish. Res. 189, 77–94. https://doi.org/10.1016/j.fishres.2017.01.010

Fox, W.W.J., Nammack, M.F., 1995. Conservation guidelines on significant population units: responsibilities of the National Marine Fisheries Service, in: American Fisheries Society Symposium 17. pp. 419–422.

Fraile, I., Arrizabalaga, H., Santiago, J., Goñi, N., Arregi, I., Madinabeitia, S., Wells, R.J.D., Rooker, J.R., 2016. Otolith chemistry as an indicator of movements of albacore (Thunnus alalunga) in the North Atlantic Ocean. Mar. Freshw. Res. 67, 1002–1013. https://doi.org/10.1071/MF15097

Fritzsch, B., 2000. Sensory systems- Hearing, in: Ostrander, G.K. (Ed.), The Laboratory Fish. Elsevier Academic Press, Johns Hopkins University Baltimore, USA, pp. 250–259. https://doi.org/978-0-12-529650-2

Froese, R., Pauly, D.., 1999. Thunnus albacares [WWW Document]. FishBaseConsortium. URL www.fishbase.org (accessed 2.3.16).

Fu, D., 2019. Preliminary Indian Ocean bigeye tuna stock assessment 1950–2018 (stock synthesis). IOTC–2019–WPTT21–61.

Fu, D., Merino, G., Langley, A., Ijurco, A., 2018. Preliminary Indian Ocean yellowfin tuna stock assessment 1950–2017 (stock synthesis). IOTC–2018–WPTT20–33. IOTC–2018–WPTT20–33.

Fujino, K., Sassaki, K., Okumura, S., 1981. Genetic diversity of skipjack tuna in the Atlantic, Indian and Pacific Oceans. Bull. Japanese Soc. Sci. Fish 47, 215–222.

Galland, G., Rogers, A., Nickson, A., 2016. Netting Billions: A Global Valuation of Tuna.

Gauldie, R.W., 1991. Taking stock of genetic concepts in fisheries management. Can. J. Fish. Aquat. Sci. 48, 722–731. https://doi.org/10.1139/f91-087

Gauldie, R.W., 1988. Tagging and genetically isolated stocks of fish: a test of one stock hypothesis and the development of another. J. Appl. Ichthyol. 4, 168–173. https://doi.org/10.1111/j.1439-0426.1988.tb00557.x

Gibb, F., Régnier, T., Donald, K., Wright, P., 2017. Connectivity in the early life history of sandeel inferred from otolith microchemistry. J. Sea Res. 119, 8–16. https://doi.org/10.1016/j.seares.2016.10.003

Gillanders, B.M., 2002. Temporal and spatial variability in elemental composition of otoliths: implications for determining stock identity and connectivity of populations. Can. J. Fish. Aquat. Sci. 59, 669–679. https://doi.org/10.1139/F02-040

Glaser, S.M., Roberts, P.M., Hurlburt, K.J., 2019. Foreign Illegal, Unreported, and Unregulated Fishing in Somali Waters Perpetuates Conflict. Front. Mar. Sci. 6. https://doi.org/10.3389/fmars.2019.00704

Golden, C., Allison, E. H. Cheung, W.W., Dey, M.M., Halpern, B. S. McCauley, D.J., Smith, M., Vaitla, B., Zelle, D., Myers, S.., 2016. Nutrition: Fall in fish catch threatens human health. Nature 534. https://doi.org/10.1038/534317a

Gonzalez, E., Beerli, P., Zardoya, R., 2008. Genetic structuring and migration patterns of Atlantic bigeye tuna, Thunnus obesus (Lowe, 1839). BMC Evol. Biol. 8. https://doi.org/10.1186/1471-2148-8-252

Goujon, M., Majkowski, C., 2010. Biological characteristics of tuna [WWW Document]. FAO Fish. Aquac. Dep. URL http://www.fao.org/fishery/ (accessed 3.7.18).

Govindraj, M.E., Premchand, J., Unnikrishnan, N., Thomas, J., Somvanshi, V.., 2000. Oceanic tuna resources in the north west region of Indian EEZ. Bull. Fish. Surv. India 27, 20.

Graham, B., Grubbs, D., Holland, K., Popp, B., 2007. A rapid ontogenetic shift in the diet of juvenile yellowfin tuna from Hawaii. Mar. Biol. 150, 647–658. https://doi.org/10.1007/s00227-006-0360-y

Graham, C.M., Valley, J.W., Eiler, J.M., Wada, H., 1998. Timescales and mechanisms of fluid infiltration in a marble: an ion microprobe study. Contrib. to Mineral. Petrol. 132, 371–389.

Graham, J., 1975. Heat exchange in the yellowfin tuna, Thunnus albacares, and skipjack tuna, Katsuwonus

pelamis, and the adaptive significance of elevated body temperatures in scombrid fishes. Fish. Bull. 73, 219–229.

Graham, J.B., Dickson, K.A., 2004. Tuna comparative physiology. J. Exp. Biol. 207, 4015–4024. https://doi.org/10.1242/jeb.01267

Grammer, G.L., Morrongiello, J.R., Izzo, C., Hawthorne, P.J., Middleton, J.F., Gillanders, B.M., 2017. Coupling biogeochemical tracers with fish growth reveals physiological and environmental controls on otolith chemistry. Ecol. Monogr. 87, 487–507. https://doi.org/10.1002/ecm.1264

Grande, M., 2013. The reproductive biology, condition and feeding ecology of the skipjack, Katsuwonus pelamis, in the Western Indian Ocean. University of the Basque Country (UPV-EHU).

Grande, M., Murua, H., Zudaire, I., Arsenault-Pernet, E.J., Pernet, F., Bodin, N., 2016. Energy allocation strategy of skipjack tuna Katsuwonus pelamis during their reproductive cycle. J. Fish Biol. 89, 2434–2448. https://doi.org/10.1111/jfb.13125

Grande, M., Murua, H., Zudaire, I., Goni, N., Bodin, N., 2014. Reproductive timing and reproductive capacity of the Skipjack Tuna (Katsuwonus pelamis) in the western Indian Ocean. Fish. Res. 156, 14–22. https://doi.org/10.1016/j.fishres.2014.04.011

Grande, M., Murua, H., Zudaire, I., Korta, M., 2012. Oocyte development and fecundity type of the skipjack, Katsuwonus pelamis, in the Western Indian Ocean. J. Sea Res. 73, 117–125. https://doi.org/10.1016/j.seares.2012.06.008

Grande, M., Murua, H., Zudaire, I., Korta, M., 2010. Spawning activity and batch fecundity of skipjack, Katsuwonus pelamis, in the Western Indian Ocean. IOTC-2010- WPTT-47.

Graves, J.E., Ferris, S.D., Dizon, A.E., 1984. Close genetic similarity of Atlantic and Pacific skipjack tuna (Katsuwonus pelamis) demonstrated with restriction endonuclease analysis of mitochondrial DNA. Mar. Biol. 79, 315–319. https://doi.org/10.1007/BF00393264

Grewe, P., Feutry, P., Foster, S., Aulich, J., Landsdell, M., Cooper, S., Clear, N., Farley, J., Nikolic, N., Krug, I., Mendibil, I., Ahusan, M., Parker, D., Wudianto, Ruchimat, T., Satria, F., Lestari, P., Taufik, M., Fernando, D., Priatna, A., Zamroni, A., Rodríguez-Ezpeleta, N., Artetxe-Arrate, I., Fahmi, Z., Murua, H., Marsac, F., Davies, C., 2020. Genetic population connectivity of yellowfin tuna in the Indian Ocean from the PSTBS-IO Project (No. IOTC-2020-WPTT22(AS)12_REV1).

Grewe, P., Feutry, P., Hill, P., Gunasekera, R., Schaefer, K., Itano, D.G., Fuller, D., Foster, S., Davies, C., 2015. Evidence of discrete yellowfin tuna (Thunnus albacares) populations demands rethink of management for this globally important resource. Nat. Sci. Reports 5, 16916. https://doi.org/10.1038/srep16916

Guillotreau, P., Squires, D., Sun, J., Compeán, G.A., 2017. Local, regional and global markets: what drives the tuna fisheries? Rev. Fish Biol. Fish. 27, 909–929. https://doi.org/10.1007/s11160-016-9456-8

Hallier, J., Fonteneau, A., 2015. Tuna aggregation and movement from tagging data: A tuna “hub” in the Indian Ocean. Fish. Res. 163, 34–43. https://doi.org/10.1016/j.fishres.2014.06.003

Hallier, J., Gaertner, D., 2008. Drifting fish aggregation devices could act as an ecological trap for tropical tuna species. Mar. Ecol. Prog. Ser. 353, 255–264. https://doi.org/10.3354/meps07180

Hallier, J., Million, J., 2012. The Indian Ocean Tuna Tagging Programme, in: Indian Ocean Tuna Tagging Symposium. Mauritius, pp. 1–36.

Hamer, P., Jenkins, G.P., 2007. Comparison of spatial variation in otolith chemistry of two fish species and relationships with water chemistry and otolith growth. J. Fish Biol. 71, 1035–1055. https://doi.org/10.1111/j.1095-8649.2007.01570.x

Hamer, P.A., Jenkins, G.P., Gillanders, B.M., 2005. Chemical tags in otoliths indicate the importance of local and distant settlement areas to populations of a temperate sparid, Pagrus auratus. Can. J. Fish. Aquat. Sci. 62, 623–630. https://doi.org/10.1139/f04-221

Han, W., McCreary, P.J., 2001. Modeling salinity distributions in the Indian Ocean. J. Geophys. Res. Ocean. 106, 859–877. https://doi.org/10.1029/2000JC000316

Han, W., Vialard, J., McPhaden, M.J., Lee, T., Masumoto, Y., Feng, M., de Ruijter, W.P.M., 2014. Indian Ocean Decadal Variability: A Review. Bull. Am. Meteorol. Soc. 95, 1679–1703. https://doi.org/10.1175/BAMS-D-13-00028.1

Hane, Y., Kimura, S., Yokoyama, Y., Miyairi, Y., Ushikubo, T., Ishimura, T., Ogawa, N., Aono, T., Nishida, K., 2020. Reconstruction of temperature experienced by Pacific bluefin tuna Thunnus orientalis larvae using SIMS and microvolume CF-IRMS otolith oxygen isotope analyses. Mar. Ecol. Prog. Ser. 175–188. https://doi.org/10.3354/meps13451

Hassani, S., Stéquert, B., 1991. Sexual maturity spawning and fecundity of the yellowfin tuna (Thunnus albacares) of the Western Indian Ocean. Indo-Pacific Tuna Manag. Prog. Coll. Work. Doc. 4, 1–107.

Hegg, J.C., Kennedy, B.P., Chittaro, P., 2018. What did you say about my mother? The complexities of maternally derived chemical signatures in otoliths. Can. J. Fish. Aquat. Sci. 76, 81–94. https://doi.org/10.1139/cjfas-2017-0341

Heithaus, M.R., Frid, A., Wirsing, A.J., Worm, B., 2008. Predicting ecological consequences of marine top predator declines. Trends Ecol. Evol. 23, 202–210. https://doi.org/10.1016/j.tree.2008.01.003

Helser, T.E., Kastelle, C.R., McKay, J.L., Orland, I.J., Kozdon, R., Valley, J.W., 2018. Evaluation of micromilling/conventional isotope ratio mass spectrometry and secondary ion mass spectrometry of δ18O values in fish otoliths for sclerochronology. Rapid Commun. Mass Spectrom. 32, 1781–1790. https://doi.org/10.1002/rcm.8231

Hijmans, R.J., 2018. raster: Geographic Data Analysis and Modeling.

Hijmans, R.J., Phillips, S., Leathwick, J., Elith, J., 2017. dismo: Species Distribution Modeling.

Hilborn, R., Amoroso, R.O., Anderson, C.M., Baum, J.K., Branch, T.A., Costello, C., Moor, C.L., Faraj, A., Hively, D., Jensewn, O.P., Kurota, H., Litle, L.R., Mace, P., McClanahan, T., Melnychuk, C.M., Minto, C., Osio, G.C., Parma, A.M., Pons, M., Segurado, S., Szuwalski, C.S., Wilson, J.R., Ye, Y., 2020. Effective fisheries management instrumental in improving fish stock status. PNAS 117, 2218–2224. https://doi.org/10.1073/pnas.1909726116

Hilborn, R., Sibert, J., 1988. Is international management of tuna necessary? Mar. Policy 12, 31–39.

Hilborn, R., Walters, C., 1992. Quantitative Fisheries Stock Assessment. Choice, Dynamics and Uncertainty. Rev. Fish Biol. Fish. 2, 177–178. https://doi.org/10.1007/BF00042883

Hoey, J.A., Fodrie, F.J., Walker, Q.A., Hilton, E.J., Kellison, G.T., Targett, T.E., Taylor, J.C., Able, K.W., Pinsky, M.L., 2020. Using multiple natural tags provides evidence for extensive larval dispersal across space and through time in summer flounder. Mol. Ecol. 29, 1421–1435. https://doi.org/10.1111/mec.15414

Hout, M.C., Papesh, M.H., Goldinger, S.D., 2013. Multidimensional scaling. Wiley Interdiscip. Rev. Cogn. Sci. 4, 93–103.

Hoyle, S.D., 2018. Indian Ocean tropical tuna regional scaling factors that allow for seasonality and cell areas. IOTC-2018-WPM09-13.

Hoyle, S.D., Langley, A., 2020. Scaling factors for multi-region stock assessments, with an application to Indian Ocean tropical tunas. Fish. Res. 228, 105586. https://doi.org/10.1016/j.fishres.2020.105586

Hunter, J.R., Macewicz, B.J., Sibert, J.R., 1986. The spawning frequency of skipjack tuna, Katsuwonus pelamis, from the south Pacific. Fish. Bull. 84, 895–903.

Huot, Y., Antoine, D., Daudon, C., 2019. Partitioning the Indian Ocean based on surface fields of physical and biological properties. Deep. Res. Part II 166, 75–89. https://doi.org/10.1016/j.dsr2.2019.04.002

Hüssy, K., Limburg, K., Pontual, H., Thomas, O., Cook, P., Heimbrand, Y., Blass, M., Sturrock, A.M., 2020.

Trace Element Patterns in Otoliths: The Role of Biomineralization. Rev. Fish. Sci. Aquac. 10.1080/23308249.2020.1760204. https://doi.org/10.1080/23308249.2020.1760204

Hutchings, J., 2000. Collapse and recovery of marine fishes. Nature 406, 882–885. https://doi.org/10.1038/35022565

Ihssen, P., Booke, H., Casselman, J., 1981. Stock identification: materials and methods. Can. J. Fish. Aquat. Sci. 38, 1838–1855. https://doi.org/10.1139/f81-230

IOTC, 2020a. Status of yellowfin tuna (Thunnus albacares) in the Indian Ocean. Exec. Summ. Appendix 11.

IOTC, 2020b. Nominal Catches by fleet, year, gear,IOTC area and species [WWW Document]. IOTC-2020-WPTT22(AS)-DATA03. URL https://www.iotc.org/WPTT/22AS/Data/03-NC (accessed 12.4.21).

IOTC, 2019a. Report on IOTC data collection and statistics [WWW Document]. IOTC–2019–WPDCS15–07. URL https://iotc.org/documents/report-15th-session-iotc-working-party-data-collection-and-statistics-0

IOTC, 2019b. Report of the 22nd session of the IOTC scientific committee [WWW Document]. IOTC-2019-SC22-R. URL https://iotc.org/documents/SC/22/RE

IOTC, 2019c. Nominal catch by species and gear, by vessel flag reporting country [WWW Document]. IOTC-2019-DATASETS-NCDB. URL https://www.iotc.org/data/datasets/latest/NC (accessed 1.17.20).

IOTC, 2018a. Nominal catch by species and gear, by vessel flag reporting country [WWW Document]. URL http://www.iotc.org/documents/nominal-catch-species-and-gear-vessel-flag-reporting-country (accessed 11.1.18).

IOTC, 2018b. Status of the Indian Ocean yellowfin tuna (YFT: Thunnus albacares) resource. Executive Summary.

IOTC, 2017a. Skipjack Tuna Supporting Information [WWW Document]. Status Summ. Species Tuna Tuna-Like Species Under IOTC Mandate, as well as Other Species Impacted by IOTC Fish. URL http://www.iotc.org/science/status-summary-species-tuna-and-tuna-species-under-iotc-mandate-well-other-species-impacted-iotc (accessed 5.15.17).

IOTC, 2017b. Bigeye Tuna Supporting Information [WWW Document]. Status Summ. Species Tuna Tuna-Like Species Under IOTC Mandate, as well as Other Species Impacted by IOTC Fish. URL http://www.iotc.org/science/status-summary-species-tuna-and-tuna-species-under-iotc-mandate-well-other-species-impacted-iotc (accessed 2.3.17).

IOTC, 2017c. Yellowfin Tuna Supporting Information [WWW Document]. Status Summ. Species Tuna Tuna-Like Species Under IOTC Mandate, as well as Other Species Impacted by IOTC Fish. URL http://www.iotc.org/documents/status-indian-ocean-yellowfin-tuna-yft-thunnus-albacares-resource (accessed 2.3.17).

IOTC, 2017d. Status of the Indian Ocean yellowfin tuna (YFT: Thunnus albacares) resource.

ISSF, 2020a. Status of the world fisheries for tuna: November 2020. ISSF Technical Report 2020-16. Washington, D.C., USA.

ISSF, 2020b. Status of the world fisheries for tuna. Mar. 2020. ISSF Technical Report 2020-12. Washington, D.C., USA.

ISSF, 2017. Status of the world fisheries for tuna: November 2017.ISSF Technical Report 2017-02A. Washington, D.C., USA.

Itano, D.G., 2005. A handbook for the identification of yellowfin and bigeye tuna in fresh condition, 2nd ed. Pelagic Fisheries Research Program University of Hawaii, JIMAR Honolulu, Hawaii USA.

Izzo, C., Doubleday, Z., Gillanders, B., 2016. Where do elements bind within the otoliths of fish? Mar. Freshw. Res. 67, 1072–1076. https://doi.org/10.1071/MF15064

Izzo, C., Reis-Santos, P., Gillanders, B.M., 2018. Otolith chemistry does not just reflect environmental conditions: A meta-analytic evaluation. Fish Fish. 19, 441–454. https://doi.org/10.1111/faf.12264

Izzo, C., Ward, T., Ivey, A., Suthers, I., Stewart, J., 2017. Integrated approach to determining stock structure: implications for fisheries management of sardine, Sardinops sagax, in Australian waters. Rev. Fish Biol. Fish. 27, 267–284. https://doi.org/10.1007/s11160-017-9468-z

Jabado, R.W., Kyne, P.M., Pollom, R.A., Ebert, D. A. Simpfendorfer, C. A. Ralph, G.M., (...) & Dulvy, N.K., 2018. Troubled waters: Threats and extinction risk of the sharks, rays and chimaeras of the Arabian Sea and adjacent waters. Fish Fish. 19, 1043–1062. https://doi.org/10.1111/faf.12311

Jakobsen, T., Fogarty, M.J., Megrey, B.A., Moksness, E., (Eds.), 2016. Fish reproductive biology: implications for assessment and management., Second. ed. John Wiley & Sons, Ltd.

Jamieson, A., 1974. Genetic tags for marine fish stocks, in: Hardin, J.F.R. (Ed.), Sea Fisheries Research. Elek Science, London, pp. 91–99.

Jaquemet, S., Potier, M., Ménard, F., 2011. Do drifting and anchored Fish Aggregating Devices (FADs) similarly influence tuna feeding habits? A case study from the western Indian Ocean. Fish. Res. 107, 283–290. https://doi.org/10.1016/j.fishres.2010.11.011

Jatmiko, I., Zedta, R.R., Agustina, M., Setyadji, B., 2019. Genetic Diversity and Demography of Skipjack Tuna (Katsuwonus pelamis) In Southern and Western Part of Indonesian Waters. ILMU Kelaut. Indones. J. Mar. Sci. 24, ILMU KELAUTAN: Indonesian Journal of Marine Scienc. https://doi.org/10.14710/ik.ijms.24.2.61-68

Jennings, S., Reynolds, J.D., Mills, S.C., 1998. Life history correlates of responses to fisheries exploitation. R. Soc. London B Biol. Sci. 265, 333–339. https://doi.org/10.1098/rspb.1998.0300

Joanes, D.N., Gill, C.A., 1998. Comparing measures of sample skewness and kurtosis. The statician 183–189.

John, M.E., 1995. Studies on Yellowfin tuna, Thunnus albacares (Bonnaterre, 1788) in the Indian Seas. Dr. Diss. Univ. Mumbai 258.

John, M.E., Neelakandan, M., Sivaji, V., Premchand, Parasuraman, P.S. Sanjeevan, M.., Sivaraj, P., 1998. Some aspects on the reproductive biology of Yellowfin tuna (Thunnus albacres) in the Bay of Bengal. Bull. Fish. Surv. India 26, 42–50.

John, M.E., Sudarsan, D., 1993. Fishery biology of yellowfin tuna occurring in oceanic fishing in Indian Seas, in: Sudarsan, D., John M. E. (Eds.), Tuna Research in India. Bombay, India, pp. 39–61.

Jones, C.M., Palmer, M., Schaffler, J.J., 2017. Beyond Zar: the use and abuse of classification statistics for otolith chemistry. J. Fish Biol. 90, 492–504. https://doi.org/10.1111/jfb.13051

Joseph, J., 1963. Fecundity of yellowfin tuna (Thunnus albacares) and skipjack (Katsuwonus pelamis) from the Pacific Ocean. Inter-Am. Trop. Tuna Comm. Bull. 7, 257–292.

Juan-Jordá, M.J., Mosqueira, I., Cooper, A.B., Freire, J., Dulvy, N.K., 2011. Global population trajectories of tunas and their relatives. PNAS 108, 20650–20655. https://doi.org/10.1073/pnas.1107743108

Juan-Jordá, M.J., Mosqueira, I., Freire, J., Dulvy, N.K., 2013. Life in 3-D: life history strategies in tunas, mackerels and bonitos. Rev. Fish Biol. Fish. 23, 135–155. https://doi.org/10.1007/s11160-012-9284-4

Juan-Jordá, M.J., Murua, H., Arrizabalaga, H., Dulvy, N.K., Restrepo, V., 2017. Report card on ecosystem-based fisheries management in tuna regional fisheries management organizations. Fish Fish. 19, 321–339. https://doi.org/10.1111/faf.12256

Jury, M., McClanahan, T., Maina, J., 2010. West Indian Ocean variability and East African fish catch. Mar. Environ. Res. 70, 162–170. https://doi.org/10.1016/j.marenvres.2010.04.006

Kaji, T., Tanaka, M., Oka, M., Takeuchi, H., Ohsumi, S., Teruya, K., Hirokawa, J., 1999. Growth and

Morphological Development of Laboratory-Reared Yellowfin Tuna Thunnus albacares Larvae and Early Juveniles, with Special Emphasis on the Digestive System. Fish. Sci. 65, 700–707.

Kaplan, D., Chassot, E., Amandé, J., Dueri, S., Herve, D., Dagorn, L., Fonteneau, A., 2014. Spatial management of Indian Ocean tropical tuna fisheries: potential and perspectives. ICES J. Mar. Sci. 71, 1728–1749. https://doi.org/10.1093/icesjms/fst233

Kayama, S., Tanabe, T., Ogura, M., Okamoto, H., Watanabe, Y., 2004. Daily age of skipjack tuna, Katsuwonus pelamis (Linnaeus), in the eastern Indian Ocean. IOTC-2004-WPTT-03.

Kerr, L., Campana, S., 2014. Chemical Composition of Fish Hard Parts as a Natural Marker of Fish Stocks, in: Cadrin, S., Kerr, L., Mariani, S. (Eds.), Stock Identification Methods: Applications in Fishery Science. Academic Press, pp. 205–234. https://doi.org/10.1016/B978-0-12-397003-9.00011-4

Kerr, L., Hintzen, N., Cadrin, S., 2017. Lessons learned from practical approaches to reconcile mismatches between biological population structure and stock units of marine fish. ICES J. Mar. Sci. 74, 1708–1722. https://doi.org/10.1093/icesjms/fsw188

Kerr, L., Whitener, Z., Cadrin, S., Morse, M., Secor, D., Golet, W., 2020. Mixed stock origin of Atlantic bluefin tuna in the US rod and reel fishery (Gulf of Maine) and implications for fisheries management. Fish. Res. 224, 105461. https://doi.org/10.1016/j.fishres.2019.105461

Kerr, L.A., Cadrin, S.X., Secor, D.H., Taylor, N., 2015. Evaluating the effect of Atlantic bluefin tuna movement on the perception of stock units. ICCAT Collect. Vol. Sci. Pap. 74, 1660–1682.

Keshtgar, B., Alizadeh-Choobari, O., Irannejad, P., 2020. Seasonal and interannual variations of the intertropical convergence zone over the Indian Ocean based on an energetic perspective. Clim. Dyn. 54, 3627–3639. https://doi.org/10.1007/s00382-020-05195-5

Kim, Y., Delgado, D.I., Cano, I.A., Sawada, Y., 2015. Effect of temperature and salinity on hatching and larval survival of yellowfin tuna Thunnus albacares. Fish. Sci. 81, 891–897. https://doi.org/10.1007/s12562-015-0901-8

Kimura, S., Nakata, H., Margulies, D., Suter, J., Hunt, S., 2004. Effect of oceanic turbulence on the survival of yellowfin tuna larvae. Bull. Japanese Soc. Sci. Fish. 70, 175–178.

King, J.R., McFarlane, G.A., 2003. Marine fish life history strategies: applications to fishery management. Fish. Manag. Ecol. 10, 249–264. https://doi.org/10.1046/j.1365-2400.2003.00359.x

Kingsford, M.J., Hughes, J.M., Patterson, H.M., 2009. Otolith chemistry of the non-dispersing reef fish Acanthochromis polyacanthus: Cross-shelf patterns from the central Great Barrier Reef. Mar. Ecol. Prog. Ser. 377, 279–288. https://doi.org/10.3354/meps07794

Kita, N.T., Ushikubo, T., Fu, B., Valley, J.W., 2009. High precision SIMS oxygen isotope analysis and the effect of sample topography. Chem. Geol. 264, 43–57. https://doi.org/10.1016/j.chemgeo.2009.02.012

Kitagawa, T., Ishimura, T., Uozato, R., Shirai, K., Amano, Y., Shinoda, A., Otake, T., Tsunogai, U., Kimura, S., 2013. Otolith δ18O of Pacific bluefin tuna Thunnus orientalis as an indicator of ambient water temperature. Mar. Ecol. Prog. Ser. 481, 199–209. https://doi.org/10.3354/meps10202

Kitchens, L., 2017. Origin and Population Connectivity of Yellowfin Tuna (Thunnus albacares) in the Atlantic Ocean. Dr. Diss. Texas A M Univ.

Kitchens, L., Rooker, J., Reynal, L., Falterman, B., Saillant, E., Murua, H., 2018. Discriminating among yellowfin tuna Thunnus albacares nursery areas in the Atlantic Ocean using otolith chemistry. Mar. Ecol. Prog. Ser. 603, 201–213. https://doi.org/10.3354/meps12676

Kittinger, J.N., Teh, L.C., Allison, E.H., Bennett, N.J., Crowder, L.B., Finkbeiner, E.M., Hicks, C., Scarton, C.G., Nakamura, K., Ota, Y., Young, J., Alifano, A., Apel, A., Arbib, A., Bishop, L., Boyle, M., Cisneros-Montemayor, A.M., Hunter, P., Le Cornu, E., Levine, M., Jones, R.S., Koehn, Z., Marschke, M., Mason, J.G., Micheli, F., McClenachan, L., Opal, C., Peacey, J., Peckham, S.H., Schemmel, E., V, S.-R., Swartz,

W., Wilhelm, T., 2017. Committing to socially responsible seafood. Science (80-.). 356, 912–913. https://doi.org/10.1126/science.aam9969

Kobayashi, T., Honryo, T., Agawa, Y., Sawada, Y., Tapia, I., Macías, K.A., Cano, A., Scholey, V.P., Margulies, D., Yagishita, N., 2015. Gonadogenesis and slow proliferation of germ cells in juveniles of cultured yellowfin tuna, Thunnus albacares. Reprod. Biol. 15, 106–112. https://doi.org/10.1016/j.repbio.2015.01.003

Kolody, D., Adam, S., 2011. Maldives Skipjack Pole and Line Fishery Catch Rate Standardization 2004-2010. IOTC-2011-WPDCS08-INF01.

Kolody, D., Hoyle, S., 2013. Evaluation of Tag Mixing Assumptions for Skipjack, Yellowfin and Bigeye Tuna Stock Assessments in the Western Pacific and Indian Oceans. WCPFC-SC9-2013/ SA-IP-11.

Kornilova, G., 1980. Feeding of yellowfin tuna, Thunnus albacares, and bigeye tuna Thunnus obesus, in the equatorial zone of the Indian Ocean. J. Ichthyol. 20, 111–119.

Korsmeyer, K.., Dewar, H., 2001. Tuna metabolism and energetics. Fish Physiol. 19, 35–78. https://doi.org/10.1016/S1546-5098(01)19003-5

Koya, K., Joshi, K., Abdussamad, E., 2012. Fishery, biology and stock structure of skipjack tuna, Katsuwonus pelamis (Linnaeus, 1758) exploited from Indian waters. Indian J. Fish. 59, 39–47.

Kritzer, J.P., Liu, O.R., 2014. Fishery management strategies for addressing complex spatial structure in marine fish stocks, in: Cadrin, S.X., Kerr, L., Mariani, S. (Eds.), Stock Identification Methods: Applications in Fishery Science. Elsevier Academic Press, pp. 29–57. https://doi.org/10.1016/B978-0-12-397003-9.00001-1

Kumar, G., Kocour, M., 2015. Population Genetic Structure of Tunas Inferred from Molecular Markers: A Review. Rev. Fish. Sci. Aquac. 23, 72–89. https://doi.org/10.1080/23308249.2015.1024826

Kumari, B., Mass, H., Panigrahy, R.C., Navalgund, R.R., 2005. A persistent eddy in the Central Arabian Sea: Potential trophic significance. Indian J. Mar. Sci. 34, 449–458.

Kume, S., Morita, Y., Ogi, T., 1971. Stock structure of the Indian bigeye tuna, Thunnus obesus (Lowe), on the basis of distribution, size composition and sexual maturity. Bull. Far Seas Fish. Res. Lab 4, 141–164.

Kunal, S., Kumar, G., Menezes, M., Meena, R., 2013. Mitochondrial DNA analysis reveals three stocks of yellowfin tuna Thunnus albacares (Bonnaterre, 1788) in Indian waters. Conserv. Genet. 14, 205–213. https://doi.org/10.1007/s10592-013-0445-3

Kurogane, K., Hiyama, Y., 1958. Morphometric comparison of the yellowfin tuna from six grounds in the Indian Ocean. Bull. Japanese Soc. Sci. Fish 24.

Lamont, T., Barlow, R., Morris, T., van den Berg, M., 2014. Characterisation of mesoscale features and phytoplankton variability in the Mozambique Channel. Deep Sea Res. Part II Trop. Stud. Oceanogr. 100, 94–105. https://doi.org/10.1016/j.dsr2.2013.10.019

Langley, A., 2016. Stock assessment of bigeye tuna in the Indian Ocean for 2016-model development and evaluation. IOTC-2016-WPTT18-20.

Langley, A., Hampton, J., Herrera, M., Million, J., 2008. Preliminary stock assessment of yellowfin tuna in the Indian Ocean using MULTIFAN-CL. IOTC-2008-WPTT-10.

Langley, A., Million, J., 2012. Determining an appropriate tag mixing period for the Indian Ocean yellowfin tuna stock assessment. IOTC–2012–WPTT14–31, IOTC–2012–WPTT14–31.

Larkin, P.., 1972. The stock concept and management of Pacific salmon, in: ..R. MacMillan, Lectures in Fisheries. Univ. British Columbia, Vancouver. p. 231.

Le Manach, F., Gough, C., Harris, A., Humber, F., Harper, S., Zeller, D., 2016. Madagascar, in: Pauly, D., Zeller, Dirk (Eds.), Global Atlas of Marine Fisheries: A Critical Appraisal of Catches Ad Ecosystem

Impacts. Island Press, Washington, D.C., USA, p. 322.

Lee, K.H., Noh, J., Khim, J.S., 2020. The Blue Economy and the United Nations' sustainable development goals: Challenges and opportunities. Environ. Int. 137. https://doi.org/10.1016/j.envint.2020.105528

Lee, P.-F., Chen, I.-C., Tzeng, W.-N., 2005. Spatial and Temporal Distribution Patterns of Bigeye Tuna (Thunnus obesus) in the Indian Ocean. Zool. Stud. 44, 260–270.

LeGrande, A.N., Schmidt, G.A., 2006. Global gridded data set of the oxygen isotopic composition in seawater. Geophys. Res. Lett. 33. https://doi.org/10.1029/2006GL026011

Leis, J.M., Van Herwerden, L., Patterson, H., 2011. Estimating connectivity in marine fish populations: what works best? Oceanogr. Mar. Biol. an Annu. Rev. 49, 193–234.

Leroy, B., Itano, D.G., Usu, T., Nicol, S.J., Holland, K.N., Hampton, J., 2009. Vertical Behavior and the Observation of FAD Effects on Tropical Tuna in the Warm-Pool of the Western Pacific Ocean, in: Ielsen, J.L., Arrizabalaga, H., Fragoso, N., Hobday, A., Lutcavage, M., Sibert, J. (Eds.), Tagging and Tracking of Marine Animals with Electronic Devices. Springer, Dordrecht, pp. 161–179. https://doi.org/10.1007/978-1-4020-9640-2_10

Lestari, P., Lester, R., Proctor, C., 2017. Parasites as potential stock markers for tuna in Indonesian Waters. Indones. Fish. Res. J. 23, 23–28.

Li, P., Chen, J.T., Zhu, G.P., 2010. Biological characteristics of bigeye tuna (Thunnus obesus) in southern and central Indian Ocean. Mar. Coast. Fish. 32, 283–289.

Liaw, A., Wiener, M., 2002. Classification and Regression by randomForest. R News 2, 18–22.

Limburg, K., Olson, C., Walther, Y., Dale, D., Slomp, C.P., Høie, H., 2011. Tracking Baltic hypoxia and cod migration over millennia with natural tags. PNAS 108, E177–E182. https://doi.org/10.1073/pnas.1100684108

Limburg, K.E., Casini, M., 2018. Effect of Marine Hypoxia on Baltic Sea Cod Gadus morhua: Evidence From Otolith Chemical Proxies. Front. Mar. Sci. 5, 10.3389/fmars.2018.00482. https://doi.org/10.3389/fmars.2018.00482

Limburg, K.E., Elfman, M., 2017. Insights from two-dimensional mapping of otolith chemistry. J. Fish Biol. 90, 480–491. https://doi.org/10.1111/jfb.13048

Limburg, K.E., Walther, B.D., Lu, Z., Jackman, G., Mohan, J., Walther, Y., Nissling, A., Weber, P.K., Schmitt, A.K., 2015. In search of the dead zone: Use of otoliths for tracking fish exposure to hypoxia. J. Mar. Syst. 141, 167–178. https://doi.org/10.1016/j.jmarsys.2014.02.014

Limburg, K.E., Wuenschel, M.J., Hüssy, K., Heimbrand, Y., Samson, M., 2018. Making the Otolith Magnesium Chemical Calendar-Clock Tick: Plausible Mechanism and Empirical Evidence. Rev. Fish. Sci. Aquac. 26, 479–493. https://doi.org/10.1080/23308249.2018.1458817

Loewen, T., Carriere, B., Reist, J., Halden, N., Anderson, W., 2016. Linking physiology and biomineralization processes to ecological inferences on the life history of fishes. Comp. Biochem. Physiol. Part A Mol. Integr. Physiol. 202, 123–140. https://doi.org/10.1016/j.cbpa.2016.06.017

Longhurst, A.R., 2007. The Indian Ocean, in: Ecological Geography of the Sea. Elsevier Academic Press, pp. 275–320.

Ludsin, S., Fryer, B., Gagnon, J., 2006. Comparison of solution-based versus laser ablation inductively coupled plasma mass spectrometry for analysis of larval fish otolith microelemental composition. Trans. Am. Fish. Soc. 135, 218–231. https://doi.org/10.1577/T04-165.1

Macdonald, J.I., Drysdale, R.N., Witt, R., Cságoly, Z., Marteinsdóttir, G., 2020. Isolating the influence of ontogeny helps predict island-wide variability in fish otolith chemistry. Rev. Fish Biol. Fish. 30, 173–202. https://doi.org/10.1007/s11160-019-09591-x

Macdonald, J.I., Farley, J.H., Clear, N.P., Williams, A.J., Carter, T.I., Davies, C.R., Nicol, S.J., 2013. Insights into mixing and movement of South Pacific albacore Thunnus alalunga derived from trace elements in otoliths. Fish. Res. 148, 56–63. https://doi.org/10.1016/j.fishres.2013.08.004

Macdonald, J. I., Shelley, J.M., Crook, D.A., 2008. A Method for Improving the Estimation of Natal Chemical Signatures in Otoliths. Trans. Am. Fish. Soc. 137, 1674–1682. https://doi.org/10.1577/T07-249.1

Macdonald, Jed I., Shelley, J.M.G., Crook, D.A., 2008. A Method for Improving the Estimation of Natal Chemical Signatures in Otoliths. Trans. Am. Fish. Soc. 137, 1674–1682. https://doi.org/10.1577/t07-249.1

Macfadyen, G., 2016. Estimate of the global sales values from tuna fisheries_ Phase 3 Report. Windrush, Warborne Lane, Portmore, Lymington, Hampshire SO41 5RJ, UK.

MacLean, J.A., Evans, D.O., 1981. The Stock Concept, Discreteness of Fish Stocks, and Fisheries Management. Can. J. Fish. Aquat. Sci. 38, 1889–1898. https://doi.org/10.1139/f81-235

Magozzi, S., Yool, A., Vander Zanden, H.B., Wunder, M.B., Trueman, C.N., 2017. Using ocean models to predict spatial and temporal variation in marine carbon isotopes. Ecosphere 8, Article e01763. https://doi.org/10.1002/ecs2.1763

Maguire, J.., Sissenwine, M., Csirke, J., Grainger, R., Garcia, S., 2006. The state of world highly migratory, straddling and other high seas fishery resources and associated species (No. FAO Fisheries Technical Paper. No. 495). Rome.

Majid, A., Ahmed, M., 1991. Status of yellowfin tuna (Thuunus albacares) fishery in Pakistan. IPTP Coll. Vol. Work. Doc. 34.

Majkowski, C., Arrizabalaga, H., Murua, H., 2011. Tuna and tuna-like species, in: Review of the State of World Marine Fishery Resources. Rome, Italy, pp. 227–244.

Maldeniya, R., 1996. Food consumption of yellowfin tuna, Thunnus albacares, in Sri Lankan waters. Environ. Biol. Fishes 47, 101–107. https://doi.org/10.1007/BF00002384

Mann, S., 2001. Biomineralization: Principles and Concepts in Bioinorganic Materials Chemistry., Oxford Uni. ed.

Marohn, L., Prigge, E., Zumholz, K., Klügel, A., Anders, H., Hanel, R., 2009. Dietary effects on multi-element composition of European eel (Anguilla anguilla) otoliths. Mar. Biol. 156, 927–933. https://doi.org/10.1007/s00227-009-1138-9

Marr, J.C., 1957. The problem of defining and recognizing subpopulations of fishes, in: Wildlife Serv. Spec. Sci. Rep. 208. pp. 1–6.

Marsac., F., 2017. The Seychelles Tuna fishery and climate change, in: Perez-Ramirez, M., Phillips, B. (Eds.), Climate Change Impacts on Fisheries and Aquaculture. Wiley Blackwell, pp. 523–568.

Marsac, F., 1991. Growth of Indian Ocean yellowfin tuna estimated from size frequencies data collected on French purse seiners. TWS/91/17, IPTP, Coll. Vol. Work. Doc. 6, 34–39.

Marsac, F., Fonteneau, A., Michaud, P., 2014. L'or bleu des Seychelles. Histoire de la pêche industrielle au thon dans l'océan Indien. IRD Ed. 269.

Marsac, F., Fonteneau, E., Ménard, F., 2000. Drifting FADs used in tuna fisheries: an ecological trap?, in: Le Gall, J., Cayré, P., Taquet, M. (Eds.), Pêche Thonière et Dispositifs de Concentration de Poissons. Ed. Ifremer, Actes Colloq., pp. 537–552.

Marsac, F., Le Blanc, J.L., 1999. Oceanographic changes during the 1997-1998 El Niño in the Indian Ocean and their impact on the purse seine fishery. 1st session of the IOTC working party on tropical tunas, Mahe, Seychelles, 4-8/09/99. WPTT/99/03. IOTC Proc. 2 147–157.

Marsac, F., Le Blanc, J.L., 1998. Interannual and ENSO-associated variability of the coupled ocean-atmosphere system with possible impacts on the yellowfin tuna fisheries of the Indian and Atlantic

oceans, in: Beckett, J.S. (Ed.), ICCAT Tuna Symposium. Coll. Vol. Sci. Pap. p. L(1):345-377.

Martin, G., Thorrold, S., 2005. Temperature and salinity effects on magnesium, manganese, and barium incorporation in otoliths of larval and early juvenile spot Leiostomus xanthurus. Mar. Ecol. Prog. Ser. 293, 223–232.

Martinez, P., Gonzalez, E., Castilho, R., Zardoya, R., 2006. Genetic diversity and historical demography of Atlantic bigeye tuna (Thunnus obesus). Mol. Phylogenet. Evol. 39, 404–416. https://doi.org/10.1016/j.ympev.2005.07.022

Martino, J.C., Doubleday, Z.A., Gillanders, B.M., 2019. Metabolic effects on carbon isotope biomarkers in fish. Ecol. Indic. 97, 10–16. https://doi.org/10.1016/j.ecolind.2018.10.010

Matsumoto, W., Skillman, R., Dizon, A., 1984. Synopsis of biological data on skipjack tuna, Katsuwonus pelamis. FAO Fish. Synopsis 45, 1–92.

Matta, M.E., Orland, I.J., Ushikubo, T., Helser, T.E., Black, B.A., Valley, J.W., 2013. Otolith oxygen isotopes measured by high-precision secondary ion mass spectrometry reflect life history of a yellowfin sole (Limanda aspera). Wiley Online Libr. 27, 691–699. https://doi.org/10.1002/rcm.6502

Maunder, M., Crone, P., Valero, J., Semmens, B., 2015. Growth: theory, estimation, and application in fishery stock assessment models, in: CAPAM Workshop Series Report 2. La Jolla, California.

McCluney, J.K., Anderson, C., Anderson, J., 2019. The fishery performance indicators for global tuna fisheries. Nat. Commun. 10, 1641. https://doi.org/10.1038/s41467-019-09466-6

McCreary, J., Yu, Z., Hood, R., Vinaychandranc, P.N., Furuea, R., Ishido, A., Richards, K., 2013. Dynamics of the Indian-Ocean oxygen minimum zones. Prog. Oceanogr. 112–113, 15–37. https://doi.org/10.1016/j.pocean.2013.03.002

McDonald, J.I., Crook, D., 2010. Variability in Sr:Ca and Ba:Ca ratios in water and fish otoliths across an estuarine salinity gradient. Mar. Ecol. Prog. Ser. 413, 147–161. https://doi.org/10.3354/meps08703

McGowan, N., Fowler, A.M., Parkinson, K., Bishop, D.P., Ganio, K., Doble, P.A., Booth, D.J., Hare, D.J., 2014. Beyond the transect: An alternative microchemical imaging method for fine scale analysis of trace elements in fish otoliths during early life. Sci. Total Environ. 494–495, 177–186. https://doi.org/10.1016/j.scitotenv.2014.05.115

Ménard, F., Labrune, C., Shin, Y.-J., Asine, A.-S., Bard, F., 2006. Opportunistic predation in tuna: a size-based approach. Mar. Ecol. Prog. Ser. 323, 223–231. https://doi.org/10.3354/ meps323223

Ménard, Frédéric, Lorrain, A., Potier, M., Marsac, F., 2007. Isotopic evidence of distinct feeding ecologies and movement patterns in two migratory predators (yellowfin tuna and swordfish) of the western Indian Ocean. Mar. Biol. 153, 141–152. https://doi.org/10.1007/s00227-007-0789-7

Ménard, F., Marsac, F., Bellier, E., Cazelles, B., 2007. Climatic oscillations and tuna catch rates in the Indian Ocean: a wavelet approach to time series analysis. Fish. Oceanogr. 16, 95–104.

Menezes, M., Kumar, G., Kunal, S., 2012. Population genetic structure of skipjack tuna Katsuwonus pelamis from the Indian coast using sequence analysis of the mitochondrial DNA D-loop region. J. Fish Biol. 80, 2198–2212. https://doi.org/10.1111/j.1095-8649.2012.03270.x

Menezes, M.R., Ikeda, M., Taniguchi, N., 2006. Genetic variation in skipjack tuna Katsuwonus pelamis(L.) using PCR-RFLP analysis of the mitochondrial DNA D-loop region. J. Fish Biol. 68, 156–161. https://doi.org/10.1111/j.0022-1112.2006.00993.x

Menezes, M.R., Noguchi, D., Nakajima, M., Taniguchi, N., 2008. Microsatellite development and survey of genetic variation in skipjack tuna Katsuwonus pelamis. J. Fish Biol. 73, 463–473. https://doi.org/10.1111/j.1095-8649.2008.01912.x

Mercier, L., Darnaude, A.M., Bruguier, O., Vasconcelos, R.P., Cabral, H.N., Costa, M.J., Lara, M., Jones, D.L., Mouillot, D., 2011. Selecting statistical models and variable combinations for optimal classification using otolith microchemistry. Ecol. Appl. 21, 1352–1364. https://doi.org/10.1890/09-1887.1

Merino, G., Murua, H., Santiago, J., Arrizabalaga, H., Restrepo, V., 2020. Characterization, Communication, and Management of Uncertainty in Tuna Fisheries. Sustainability 12, 1–22. https://doi.org/10.3390/su12198245

Miller, K.I., Nadheeh, I., Riyaz Jauharee, A., Charles Anderson, R., Shiham Adam, M., 2017. Bycatch in the Maldivian pole-and-line tuna fishery. PLoS One 12. https://doi.org/10.1371/journal.pone.0177391

Miller, M.B., Clough, A.M., Batson, J.N., Vachet, R.W., 2006. Transition metal binding to cod otolith proteins. J. Exp. Mar. Bio. Ecol. 329, 135–143. https://doi.org/10.1016/j.jembe.2005.08.016

Milton, D.A., Shaklee, J.B., 1987. Biochemical Genetics and Population Structure of Blue Grenadier, Macruronus novaezelandiae (Hector) (Pisces : Merluccidae), from Australian Waters, Mar. Freshw. Res.

Miyake, M.P., Miyabe, N., Nakano, H., 2004. Historical trends of tuna catches in the world. Rome, Italy.

Miyama, T., McCreary Jr, J.P., Jensen, T.G., Loschnigg, J., Godfrey, S., Ishida, A., 2003. Structure and dynamics of the Indian-Ocean cross-equatorial cell. Deep Sea Res. Part II Top. Stud. Oceanogr. 50, 2023–2047. https://doi.org/10.1016/S0967-0645(03)00044-4

Moll, D., Kotterba, P., Jochum, K.P., von Nordheim, L., Polte, P., 2019. Elemental Inventory in Fish Otoliths Reflects Natal Origin of Atlantic Herring (Clupea harengus) From Baltic Sea Juvenile Areas. Front. Mar. Sci. 6, 10.3389/fmars.2019.00191. https://doi.org/10.3389/fmars.2019.00191

Moore, B., Bell, J., Evans, K., Hampton, J., Grewe, P., Marie, A., Minte-Vera, C., Nicol, S., Phillips, J., Pilling, G., Tremblay-Boyer, L., Williams, A., Smith, N., 2018. Current knowledge, key uncertainties and future research directions for defining the stock structure of skipjack, yellowfin, bigeye and South Pacific albacore tunas in the Pacific Ocean.

Moore, B., Lestari, P., Cutmore, S., Proctor, C., Lester, R., 2019. Movement of juvenile tuna deduced from parasite data. ICES J. Mar. Sci. 76, 1678–1689. https://doi.org/10.1093/icesjms/fsz022

Morales-Nin, B., 2000. Review of the growth regulation processes of otolith daily increment formation. Fish. Res. 46, 53–67. https://doi.org/Review of the growth regulation processes of otolith daily increment formation

Morgan, M.J., Murua, H., Kraus, G., Lambert, Y., Marteinsdóttir, G., Marshall, C.T., O'Brien, L., Tomkiewicz, J., 2009. The evaluation of reference points and stock productivity in the context of alternative indices of stock reproductive potential. Can. J. Fish. Aquat. Sci. 66, 404–414. https://doi.org/10.1139/F09-009

Morita, Y., Koto, T., 1970. Some consideration on the population structure of yellowfin tuna in the Indian Ocean based on the longline fishery data. Bull. Far. Seas Fish. Res. Lab 4, 125–140.

Muhling, B.A., Lamkin, J.T., Alemany, F., García, A., Farley, J., Ingram, G.W., Berastegui, D.A., Reglero, P., Carrion, R.L., 2017. Reproduction and larval biology in tunas, and the importance of restricted area spawning grounds. Rev. Fish Biol. Fish. 27, 697–732. https://doi.org/10.1007/s11160-017-9471-4

Mullins, R., McKeown, N., Sauer, W., Shaw, P., 2018. Genomic analysis reveals multiple mismatches between biological and management units in yellowfin tuna (Thunnus albacares). ICES J. Mar. Sci. fsy102. https://doi.org/10.1093/icesjms/fsy102

Murua, H., Eveson, J., Marsac, F., 2015. The Indian Ocean Tuna Tagging Programme: Building better science for more sustainability. Fish. Res. 163, 1–6. https://doi.org/10.1016/j.fishres.2014.07.001

Murua, H., Rodriguez-Marin, E., Neilson, J.D., Farley, J.H., Juan-Jordá, M.J., 2017. Fast versus slow growing tuna species: age, growth, and implications for population dynamics and fisheries management. Rev. Fish Biol. Fish. 1–41. https://doi.org/10.1007/s11160-017-9474-1

Musyl, M.K., Domeier, M.L., Nasby-Lucas, N., Brill, R.W., McNaughton, L.M., Swimmer, J.Y., Lutcavage, M.S., Wilson, S.G., Galuardi, B., Liddle, J.B., 2011. Performance of pop-up satellite archival tags. Mar. Ecol. Prog. Ser. 433, 1–28. https://doi.org/10.3354/meps09202

Nakamura, M., Yoneda, M., Ishimura, T., Shirai, K., Tamamura, M., Nishida, K., 2020. Temperature dependency equation for chub mackerel (Scomber japonicus) identified by a laboratory rearing experiment and microscale analysis. Mar. Freshw. Res. 71, 1384–1389. https://doi.org/10.1071/MF19313

Neubauer, P., Shima, J.S., Swearer, S., 2013. Inferring dispersal and migrations from incomplete geochemical baselines: analysis of population structure using Bayesian infinite mixture models. Methods Ecol. Evol. 4, 836–845. https://doi.org/10.1111/2041-210X.12076

Nikolic, N., Montes, I., Lalire, M., Puech, A., Bodin, N., Arnaud-Haond, S., Kerwath, S., Corse, E., Gaspar, P., Hollanda, S., Bourjea, J., West, W., Bonhomeau, S., 2020. Connectivity and population structure of albacore tuna across southeast Atlantic and southwest Indian Oceans inferred from multidisciplinary methodology. Nat. Sci. Reports 10. https://doi.org/10.1038/s41598-020-72369-w

Ningsih, N.S., Rakhmaputeri, N., Harto, A.B., 2013. Upwelling Variability along the Southern Coast of Bali and in Nusa Tenggara Waters. Ocean Sci. J. 48, 49–57. https://doi.org/10.1007/s12601-013-0004-3

Nishida, T., 1992. Considerations of stock structure of yellowfin tuna (Thunnus albacares) in the Indian Ocean based on fishery data. Fish. Oceanogr. 1, 143–152. https://doi.org/10.1111/j.1365-2419.1992.tb00033.x

Nishida, T., Chow, S., Grewe, P., 1998. Review and research plan on the stock structure of yellowfin tuna (Thunnus albacares) and bigeye tuna (Thunnus obesus) in the Indian Ocean. IOTC Proceedings, 7th Expert Consult. Indian Ocean Tunas 230–236.

Nishida, T., Chow, S., Ikame, S., Kurihara, S., 2001. RFLP analysis on single copy nuclear gene loci in yellowfin tuna (Thunnus albacares) to examine the genetic differentiation between the western and eastern. IOTC Proc. 4, 437–441.

Nishikawa, Y., Honma, M., Ueyanagi, S., Kikawa, S., 1985. Average distribution of larvae of oceanic species of scombrid fishes, 1956–1981. Far Seas Fish Res Lab S Ser 12, 1–99.

Nootmorn, P., 2004. Reproductive biology of Bigeye tuna in the eastern Indian Ocean. IOTC Proc., IOTC Proceedings no. 7 7, 1–5.

Nootmorn, P., Yakoh, A., Kawises, K., 2005. Reproductive biology of yellowfin tuna in the Eastern Indian Ocean. IOTC-2005-WPTT-14 379–385.

Nugraha, B., Baskoro, M.S., Pane, A.B., Nugroho, E., 2010. Genetic Diversity of bigeye tuna (Thunnus obesus) based on mtDNA analysis with the PCR-RFLP technique. Indones. Fish. Res. J. 16, 25–32.

Oksanen, J., Blanchet, F.., Friendly, M., Kindt, R., Legendre, P., McGlinn, D., Minchin, P.R., O'Hara, R.B., Simpson, G.L., Solymos, P., Henry, M., Stevens, H., Szoecs, E., Wagner, H., 2017. vegan: Community Ecology Package. R package version 2.4-3.

Olden, J.D., Joy, M.K., Death, R.., 2004. An accurate comparison of methods for quantifying variable importance in artificial neural networks using simulated data. Ecol. Modell. 178, 389–397.

Olivier, L., 2002. Study of the growth of Yellowfin tuna (Thunnus albacares) in the Western Indian Ocean based on length frequency data. IOTC Proc. 5, 316–327.

Olson, R.J., Young, J.W., Ménard, F., Potier, M., Allain, V., Goñi, N., Logan, J., Galván-Magaña, F., 2016. Bioenergetics, trophic ecology, and niche separation of tunas. Adv. Mar. Biol. 74, 199–344. https://doi.org/10.1016/bs.amb.2016.06.002

Ovenden, J.R., 1990. Mitochondrial DNA and marine stock assessment: A review. Aust. J. Mar. Freshw. Res 41, 835–53. https://doi.org/10.1071/MF9900835

Panfili, J., De Pontual, H., Troadec, H., Wright, P.J., 2002. Manual of Fish Sclerochronology. Ifremer-IRD coedition, Brest, France.

Paton, C., Hellstrom, J., Paul, B., Woodhead, J., Hergt, J., 2011. Iolite: freeware for the visualization and processing of mass spectrometric data. J. Anal. At. Spectrom. 26, 2508–2518.

https://doi.org/10.1039/ C1JA10172B

Patterson, H., Kingsford, M., McCulloch, M., 2004. The influence of oceanic and lagoonal plume waters on otolith chemistry. Can. J. Fish. Aquat. Sci. 61, 898–904. https://doi.org/10.1139/f04-036

Paul, B., Paton, C., Norris, A., Woodhead, J., Hellstrom, J., Hergt, J., Greig, A., 2012. CellSpace: a module for creating spatially registered laser ablation images within the Iolite freeware environment. J. Anal. At. Spectrom. 27, 700–706. https://doi.org/10.1039/ C2JA10383D

Pauly, D.., Zeller, D., 2016. Catch reconstructions reveal that global marine fisheries catches are higher than reported and declining. Nat. Commun. 7, 10244. https://doi.org/10.1038/ncomms10244

Pauly, D., Alder, J., Bennet, E., Christensen, V., Tyedmers, P., Watson, R., 2003. The future of fisheries. Science (80-.). 302, 1359–1361. https://doi.org/10.1126/science.1088667

Payan, P., De Pontual, H., Bœuf, G., Mayer-Gostan, N., 2004. Endolymph chemistry and otolith growth in fish. Comptes Rendus Palevol 3, 535–547. https://doi.org/10.1016/j.crpv.2004.07.013

Pecoraro, C., Babbucci, M., Franch, R., Rico, C., Papetti, C., Chassot, E., Bodin, N., Cariani, A., Bargelloni, L., Tinti, F., 2018. The population genomics of yellowfin tuna (Thunnus albacares) at global geographic scale challenges current stock delineation. Sci. Rep. 8, 13890. https://doi.org/10.1038/s41598-018-32331-3

Pecoraro, C., Zudaire, I., Bodin, N., Murua, H., Taconet, P., Díaz-Jaimes, P., Cariani, A., Tinti, F., Chassot, E., 2016. Putting all the pieces together: integrating current knowledge of the biology, ecology, fisheries status, stock structure and management of yellowfin tuna (Thunnus albacares). Rev. Fish Biol. Fish. 27, 811–841. https://doi.org/10.1007/s11160-016-9460-z

Petitgas, P., Secor, D., McQuinn, Huse, G., Lo, N., 2010. Stock collapses and their recovery: mechanisms that establish and maintain life-cycle closure in space and time. ICES J. Mar. Sci. 67, 1841-1848,.

Pillai, P., Silas, E., 1979. Distribution and biology of the Skipjack tuna Katsuwonus pelamis (Linnaeus) taken by the longline fishery in the Indian Ocean. J. Mar. Biol. Assoc. 21, 147–170.

Pita, A., Casey, J., Hawkins, S.J., Villarreal, M.R., Gutiérrez, M.J., Cabral, H., Carocci, F., Abaunza, P., Pascual, S., Presa, P., 2016. Conceptual and practical advances in fish stock delineation. Fish. Res. 173, 185–193. https://doi.org/10.1016/j.fishres.2015.10.029

Pollock, K.H., Pine, W.E., 2007. The design and analysis of field studies to estimate catch-and-release mortality. Fish. Manag. 14, 1–8.

Pomilla, C., Amaral, A.R., Collins, T., Minton, G., Findlay, K., Leslie, M.S., Ponnampalam, L., Baldwin, RRosenbaum, H., 2014. The world's most isolated and distinct whale population? Humpback whales of the Arabian Sea. PLoS One 9, e114162. https://doi.org/10.1371/journal.pone.0114162

Pons, M., Melnychuk, M.C., Hilborn, R., 2017. Management effectiveness of large pelagic fisheries in the high seas. Fish Fish. 00, 1–11. https://doi.org/10.1111/faf.12253

Popper, A.., Lu, Z., 2000. Structure–function relationships in fish otolith organs. Fish. Res. 46, 15–25. https://doi.org/10.1016/S0165-7836(00)00129-6

Potier, M., Lucas, V., Marsac., F., Ménard, F., Sabatié, R., 2002. On-going research activities on trophic ecology of tuna in equatorial ecosystems of Indian Ocean. IOTC Proc. 5 368–374.

Potier, M., Marsac, F., Cherel, Y., Lucas, V., Sabatié, R., 2007. Forage fauna in the diet of three large pelagic fishes (lancetfish, swordfish and yellowfin tuna) in the western equatorial Indian Ocean. Fish. Res. 83, 60–72. https://doi.org/10.1016/j.fishres.2006.08.020

Potier, M., Marsac, F., Lucas, V., Sabatié, R., Hallier, J., Ménard, F., 2004. Feeding Partitioning among Tuna Taken in Surface and Mid-water Layers: The Case of Yellowfin (Thunnus albacares) and Bigeye (T. obesus) in the Western Tropical Indian Ocean. West. Indian Ocean J. Mar. Sci. 3, 51–62.

Potier, M., Romanov, E., Cherel, Y., Sabatié, R., Zamorov, V., Ménard, F., 2008. Spatial distribution of

Cubiceps pauciradiatus (Perciformes: Nomeidae) in the tropical Indian Ocean and its importance in the diet of large pelagic fishes. Aquat. Living Resour. 21, 123–134. https://doi.org/10.1051/alr:2008026

Proctor, C.H., Lester, R.J.G., Clear, N.P., Grewe, P.M., Moore, B.R., Eveson, J.P., Lestari, P., Wujdi, A., Taufik, M., Wudianto, Lansdell, M.J., Hill, P.L., Dietz, C., Thompson, J.M., Cutmore, S.C., Foster, S.D., Gosselin, T., Davies, C.R., 2019. Population structure of yellowfin tuna (Thunnus albacares) and bigeye tuna (T. obesus) in the Indonesian region. Final Report as output of ACIAR Project FIS/2009/059. Camberra.

Qiu, F., Kitchen, A., Beerli, P., Miyamoto, M., 2013. A possible explanation for the population size discrepancy in tuna (genus Thunnus) estimated from mitochondrial DNA and microsatellite data. Mol. Phylogenet. Evol. 66, 463–468. https://doi.org/10.1016/j.ympev.2012.05.002

Quartly, G., Srokosz, M., 2004. Eddies in the southern Mozambique Channel. Deep Sea Res. Part II Top. Stud. Oceanogr. 51, 69–83. https://doi.org/10.1016/j.dsr2.2003.03.001

R Core Team, 2019. R: A language and environment for statistical computing. R Foundation for Statistical Computing, Vienna, Austria. URL https://www.R-project.org/.

Ramage, C.S., 1969. Indian Ocean surface meteorology. Oceanogr. Mar. Biol. An Annu. Rev. 7, 11–33.

Ranaldi, M., Gagnon, M., 2008. Zinc incorporation in the otoliths of juvenile pink snapper (Pagrus auratus Forster): The influence of dietary versus waterborne sources. J. Exp. Mar. Bio. Ecol. 360, 56–62. https://doi.org/10.1016/j.jembe.2008.03.013

Randon, M., Réveillac, E., 2021. A holistic investigation of tracers at population and individual scales reveals population structure for the common sole of the Eastern English Channel. Estuar. Coast. Shelf Sci. 249, 107096. https://doi.org/10.1016/j.ecss.2020.107096

Reglero, P., Tittensor, D., Álvarez-Berastegui, D., Aparicio-González, A., Worm, B., 2014. Worldwide distributions of tuna larvae: revisiting hypotheses on environmental requirements for spawning habitats. Mar. Ecol. Prog. Ser. 501, 207–224. https://doi.org/10.3354/meps10666

Régnier, T., Augley, J., Devalla, S., Robinson, C., Wrigth, P., Neat, F., 2017. Otolith chemistry reveals seamount fidelity in a deepwater fish. Deep Sea Res. Part I Oceanogr. Res. Pap. 121, 183–189.

Reis-Santos, P., Tanner, S.E., Aboim, M. A. Vasconcelos, R. P. Laroche, J., Charrier, G., Perez, M., Presa, P., Gillanders, B.M., Cabral, H.N., 2018. Reconciling differences in natural tags to infer demographic and genetic connectivity in marine fish populations. Sci. Rep. 8, 1–122. https://doi.org/10.1038/s41598-018-28701-6

Reis-Santos, P, Vasconcelos, R.P., Tanner, S., Fonseca, V.F., Cabral, H., Gillanders, B.M., 2018. Extrinsic and intrinsic factors shape the ability of using otolith chemistry to characterize estuarine environmental histories. Mar. Environ. Res. 140, 332–341. https://doi.org/10.1016/j.marenvres.2018.06.002

Reiss, H., Hoarau, G., Dickey-Collas, M., Wolff, W.J., 2009. Genetic population structure of marine fish: mismatch between biological and fisheries management units. Fish Fish. 10, 361–395. https://doi.org/10.1111/j.1467-2979.2008.00324.x

Reygondeau, G., Maury, O., Beaugrand, G., 2012. Biogeography of tuna and billfish communities. J. Biogeogr. 39, 114–129. https://doi.org/10.1111/j.1365-2699.2011.02582.x

Rodríguez-Ezpeleta, N., Díaz-Arce, N., Walter, J.F., Richardson, D.E., Rooker, J.R., Nøttestad, L., Hanke, A.R., Franks, J.S., Deguara, S., Lauretta, M. V., Addis, P., Varela, J.L., Fraile, I., Goñi, N., Abid, N., Alemany, F., Oray, I.K., Quattro, J.M., Sow, F.N., Itoh, T., Karakulak, F.S., Pascual-Alayón, P.J., Santos, M.N., Tsukahara, Y., Lutcavage, M., Fromentin, J.M., Arrizabalaga, H., 2019. Determining natal origin for improved management of Atlantic bluefin tuna. Front. Ecol. Environ. 17, 439–444. https://doi.org/10.1002/fee.2090

Roger, C., 1994. Relationships among yellowfin and skipjack tuna, their prey-fish and plankton in the tropical western Indian Ocean. Fish. Oceanogr. 3, 133–141. https://doi.org/10.1111/j.1365-

2419.1994.tb00055.x

Rogers, T.A., Fowler, A., Steer, M., Gillanders, B.M., 2019. Discriminating Natal Source Populations of a Temperate Marine Fish Using Larval Otolith Chemistry. Front. Mar. Sci. 6, 10.3389/fmars.2019.00711. https://doi.org/10.3389/fmars.2019.00711

Romanov, E., Potier, M., Zamorov, V., Ménard, F., 2009. The swimming crab Charybdis smithii: distribution, biology and trophic role in the pelagic ecosystem of the western Indian Ocean. Mar. Biol. 156, 1089–1107. https://doi.org/10.1007/s00227-009-1151-z

Rooker, J.., Fraile, I., Liu, H., Abid, N., Dance, M.A., Itoh, T., Kimoto, A., Tsukaraha, Y., Rodriguez-Marin, E., Arrizabalaga, H., 2019. Wide-Ranging Temporal Variation in Transoceanic Movement and Population Mixing of Bluefin Tuna in the North Atlantic Ocean. Front. Mar. Sci. 6, 1–13. https://doi.org/10.3389/fmars.2019.00398

Rooker, J., Arrizabalaga, H., Fraile, I., Secor, D., Dettman, D., Abid, N., Addis, P., Deguara, S., Karakulak, F., Kimoto, A., Sakai, O., Macías, D., Santos, M., 2014. Crossing the line: migratory and homing behaviors of Atlantic bluefin tuna. Mar. Ecol. Prog. Ser. 504, 265–276. https://doi.org/10.3354/meps10781

Rooker, J., Secor, D., DeMetrio, G., Schloesser, R., Block, B., Neilson, J., 2008. Natal Homing and Connectivity in Atlantic Bluefin Tuna Populations. Science (80-.). 322, 742–744. https://doi.org/10.1126/science.1161473

Rooker, J.R., David Wells, R.J., Itano, D.G., Thorrold, S.R., Lee, J.M., 2016. Natal origin and population connectivity of bigeye and yellowfin tuna in the Pacific Ocean. Fish. Oceanogr. 25, 277–291. https://doi.org/10.1111/fog.12154

Rooker, J.R., Secor, D.H., 2004. Stock structure and mixing of Atlantic bluefin tuna: Evidence from stable δ13C and δ18O isotopes in otoliths. ICCAT Collect. Vol. Sci. Pap. 56, 1115–1120.

Rooker, J.R., Secor, D.H., DeMetrio, G., Kaufman, A.J., Ríos, A.B., Tičina, V., 2008. Evidence of trans-Atlantic movement and natal homing of bluefin tuna from stable isotopes in otoliths. Mar. Ecol. Prog. Ser. 368, 231–239. https://doi.org/10.3354/meps07602

Rooker, J.R., Secor, D.H., Zdanowicz, V.S., De Metrio, G., Relini, L.O., 2003. Identification of Atlantic bluefin tuna (Thunnus thynnus) stocks from putative nurseries using otolith chemistry. Fish. Oceanogr. 12, 75–84. https://doi.org/10.1046/j.1365-2419.2003.00223.x

Rooker, J.R., Zdanowicz, V., Secor, D., 2001. Chemistry of tuna otoliths: assessment of base composition and postmortem handling effects. Mar. Biol. 139, 35–43. https://doi.org/10.1007/s002270100568

Roul, S.K., Retheesh, B., Prakasan, D., Abdussamad, E.M., 2016. Field identification of yellowfin and bigeye tuna. Mar. Fish. Inf. Serv. Tech. Ext. Ser. 227, 14–16. https://doi.org/10.13140/RG.2.2.27354.03525

Rousseau, Y., Watson, R.., Blanchard, J.., Fulton, E.A., 2018. Evolution of global marine fishing fleets and the response of fished resources. PNAS 116, 12238–12243. https://doi.org/10.1073/pnas.1820344116

Ruttenberg, B., Hamilton, S., Hickford, M., 2005. Elevated levels of trace elements in cores of otoliths and their potential for use as natural tags. Mar. Ecol. Prog. Ser. 297, 273–281.

Saila, S., Jones, C., 1983. Fishery science and the stock concept. Final Report P.O. NA83- B-A-0078 (MS).

Saji, N.H., Goswami, B.N., Vinayachandran, P.N., Yamagata, T., 1999. A dipole mode in the tropical Indian Ocean. Nature 401, 360–363. https://doi.org/10.1038/43854

Sardenne, F., Bodin, N., Chassot, E., Amiel, A., Fouché, E., Degroote, M., Hollanda, S., Pethybridge, H., Lebreton, B., Guillou, G., Ménard, F., 2016. Trophic niches of sympatric tropical tuna in the Western Indian Ocean inferred by stable isotopes and neutral fatty acids. Prog. Oceanogr. 146, 75–88. https://doi.org/10.1016/j.pocean.2016.06.001

Sardenne, F., Dortel, E., Le Croizier, G., Million, J., Labonne, M., Leroy, B., Bodin, N., Chassot, E., 2015.

Determining the age of tropical tunas in the Indian Ocean from otolith microstructures. Fish. Res. 163, 44–57. https://doi.org/10.1016/j.fishres.2014.03.008

Sardenne, F., Kraffe, E., Amiel, A., Fouché, E., Debrauwer, L., Ménard, F., Bodin, N., 2017. Biological and environmental influence on tissue fatty acid compositions in wild tropical tunas. Comp. Biochem. Physiol. Part A Mol. Integr. Physiol. 204, 17–27. https://doi.org/10.1016/j.cbpa.2016.11.007

Schaefer, K., Fuller, D., Block, B., 2007. Movements, behavior, and habitat utilization of yellowfin tuna (Thunnus albacares) in the northeastern Pacific Ocean, ascertained through archival tag data. Mar. Biol. 152, 503–525. https://doi.org/10.1007/s00227-007-0689-x

Schaefer, K.M., 2001. Reproductive biology of tunas, in: Block, B.A., Stevens, E. (Eds.), Tuna: Physiology, Ecology and Evolution. Academic Press, San Diego, California, pp. 225–270. https://doi.org/10.1016/S1546-5098(01)19007-2

Schaefer, K.M., Fuller, D.W., Block, B.A., 2009. Vertical Movements and Habitat Utilization of Skipjack (Katsuwonus pelamis), Yellowfin (Thunnus albacares), and Bigeye (Thunnus obesus) Tunas in the Equatorial Eastern Pacific Ocean, Ascertained Through Archival Tag Data, in: Nielsen J.L., Arrizabalaga H., Fragoso N., Hobday A., Lutcavage M., S.J. (Ed.), Tagging and Tracking of Marine Animals with Electronic Devices. Reviews: Methods and Technologies in Fish Biology and Fisheries. Vol 9. Springer, Dordrecht, pp. 121–144. https://doi.org/10.1007/978-1-4020-9640-2_8

Schloesser, R.W., Rooker, J.., Louchuoran, P., Neilson, J.D., Secor, D., 2009. Interdecadal variation in seawater d13C and d18O recorded in fish otoliths. Limnol. Oceanogr. 54, 1665–1668. https://doi.org/10.4319/lo.2009.54.5.1665

Schoener, T.W., 1968. The Anolis Lizards of Bimini: Resource Partitioning in a Complex Fauna. Ecology 49, 704–726. https://doi.org/10.2307/1935534

Schott, F., Dengler, M., Schoenefeldt, R., 2002. The shallow overturning circulation of the Indian Ocean. Prog. Oceanogr. 53, 57–103. https://doi.org/10.1016/S0079-6611(02)00039-3

Schott, F., McCreary, J., 2001. The monsoon circulation of the Indian Ocean. Prog. Oceanogr. 51, 1–123. https://doi.org/10.1016/S0079-6611(01)00083-0

Schott, F.A., Xie, S.-P., McCreary, J.P., 2009. Indian Ocean circulation and climate variability. Rev. Geophys. 47, RG1002. https://doi.org/10.1029/2007RG000245

Schouten, M.W., de Ruijter, W.P., Van Leeuwen, P.J., Ridderinkhof, H., 2003. Eddies and variability in the Mozambique Channel. Deep Sea Res. Part II Trop. Stud. Oceanogr. 50, 1987–2003. https://doi.org/10.1016/S0967-0645(03)00042-0

Secor, D., 2005. Fish migration and the unit stock: three formative debates., in: Cadrin, S., Friedland, K., Waldman, J. (Eds.), Stock Identification Methods. Elsevier Inc., pp. 17–44.

Secor, D.H., 2015. Synopsis of regional mixing levels for atlantic bluefin tuna estimated from otolith stable isotpe analysis, 2007-2014. Collect. Vol. Sci. Pap. ICCAT 71, 1683–1689.

Secor, D.H., 2014. The Unit Stock Concept: Bounded Fish and Fisheries, in: Cadrin, S.X., Kerr, L., Mariani, S. (Eds.), Stock Identification Methods . Applications in Fishery Science. Academic Press, pp. 7–28.

Secor, D.H., 1999. Specifying divergent migrations in the conceptof stock: the contingent hypothesis. Fish. Res. 43, 13–34.

Seto, K., Galland, G.R., McDonald, A., Abolhassani, A., Azmi, K., Sinan, H., Timmiss, T., Bailey, M., Hanich, Q., 2021. Resource allocation in transboundary tuna fisheries: A global analysis. Ambio 50, 242–259. https://doi.org/10.1007/s13280-020-01371-3

Shankar, D., Vinayachandran, P.N., Unnikrishnan, A.S., 2002. The monsoon currents in the north Indian Ocean. Prog. Oceanogr. 63–120.

Sharp, G.D., 2001. Tuna Oceanography-an applied science, in: Block, B., Stevens, G. (Eds.), Tuna: Physiology, Ecology, and Evolution. Academic Press, San Diego, California, pp. 345–388.

Sharp, G.D., Dizon, A.E., 1978. The physiological ecology of tunas. Academic Press, London. https://doi.org/10.1016/B978-0-12-639180-0.X5001-0

Shi, T., Horvath, S., 2006. Unsupervised Learning With Random Forest Predictors. J. Comput. Graph. Stat. 15, 118–138. https://doi.org/10.1198/106186006X94072

Shiao, J., Itoh, S., Yurimoto, H., Iizuka, Y., Liao, Y.., 2014. Oxygen isotopic distribution along the otolith growth axis by secondary ion mass spectrometry: Applications for studying ontogenetic change in the depth inhabited by deep-sea fishes. Deep Sea Res. Part I Oceanogr. Res. Pap. 84, 50–58. https://doi.org/10.1016/j.dsr.2013.10.006

Shiao, J., Wang, S., Yokawa, K., Ichinokawa, M., Takeuchi, Y., Chen, Y., Shen, C., 2010. Natal origin of Pacific bluefin tuna Thunnus orientalis inferred from otolith oxygen isotope composition. Mar. Ecol. Prog. Ser. 420, 207–219.

Shih, C.L., Hsu, C.C., Chen, C.Y., 2014. First attempt to age yellowfin tuna, Thunnus albacares, in the Indian Ocean, based on sectioned otoliths. Fish. Res. 149, 19–23. https://doi.org/10.1016/j.fishres.2013.09.009

Shirai, K., Otake, T., Amano, Y., Kuroki, M., Ushikubo, T., Kita, T., Murayama, M., Tsukamoto, K., Valley, J.W., 2018. Temperature and depth distribution of Japanese eel eggs estimated using otolith oxygen stable isotopes. Geochemica Cosmochim. Acta 236, 373–383. https://doi.org/10.1016/j.gca.2018.03.006

Shotton, R., 2005. Western Indian Ocean, in: Review of the State of World Marine Fishery Resources. Marine Resources Service Fishery Resources Division FAO Fisheries Department, Rome, pp. 87–93.

Shuford, R.L., Dean, J.M., Stéquert, B., M., L., 2007. Elemental fingerprints in otoliths of juvenile yellowfin tuna from spawning grounds in the Atlantic Ocean. Collect. Vol. Sci. Pap. ICCAT 60, 314–329.

Shung, S.H., 1973. The sexual activity of yellowfin tuna caught by the longline fishery in the Indian Ocean based on the examination of ovaries. Bull. / Far Seas Fish. Res. Lab. 9, 123–142.

Smale, M.J., 1986. The feeding habits of six pelagic and predatory teleosts in eastern Cape coastal waters (South Africa). J. Zool. 1, 357–409.

Smith, A., Dixon, P., Black, M., 1988. Population structure of yellowfin tuna (Thunnus albacares) in Eastern Australian waters University of New South Wales, Centre for Marine S.

Smith, M.D., Roheim, C.A., Crowder, L.B., Halpern, B. S. Turnipseed, M., Anderson, J.L., Asche, F., Bourillon, L., Guttormsen, A.G., Khan, A., Liguori, L.A., McNevin, A., O+Connor, M.I., Squires, D., Tyedmers, P., Brownstein, C., Carden, K., Klinger, D.H., Sagarin, R., Selkoe, K.A., 2010. Sustainability and global seafood. Science (80-.). 327, 784–786. https://doi.org/10.1126/science.1185345

Smith, P.J., 1990. Protein electrophoresis for identification of Australasian fish stocks. Aust. J. mar. Freshwat. Res 41, 823–833.

Solovieff, B.S., 1970. Distribution and biology of bigeye tuna in the Indian Ocean. Rybn. Khoz. 3, 313.

Song, L., Zhou, J., Zhou, Y., Nishida, T., Jiang, W., Wang, J., 2009. Environmental preferences of bigeye tuna, Thunnus obesus, in the Indian Ocean: an application to a longline fishery. Environ. Biol. Fishes 85, 153–171. https://doi.org/10.1007/s10641-009-9474-7

Song, L.M., Zhang, Y., Xu, L.X., Jiang, W.X., Wang, J., 2008. Environmental preferences of longlining for yellowfin tuna (Thunnus albacares) in the tropical high seas of the Indian Ocean. Fish. Oceanogr. 17, 239–253. https://doi.org/10.1111/j.1365-2419.2008.00476.x

Sparre, P., Venema, S., 1998. Introduction to Tropical Fish Stock Assessment. Part1. Manual. FAO Fisheries Technical Paper No 306.1, Rev. 2. Rome.

Stephenson, R.L., 2002. Stock structure and management structure: an ongoing challenge for ICES, ICES Marine Science Symposia.

Stephenson, R.L., 1999. Stock complexity in fisheries management: a perspective of emerging issues related to population sub-units. Fish. Res. 43, 247–249. https://doi.org/10.1016/S0165-7836(99)00076-4

Stepien, C.., 1995. Population genetic divergence and geographic patterns from DNA sequences: examples from marine and freshwater fishes, in: American Fisheries Society Symposium.

Stéquert, B., 1976. Etude de la maturité sexuelle, de la ponte et de la fécondité du listao (Katsuwonus pelamis) de la côte nord-ouest de Madagascar. Cah. ORSTOM. Série Océanographie 14, 227–247.

Stéquert, B., Marsac, F., 1989. Tropical tuna–surface fisheries in the Indian Ocean. FAO Fish. Tech. Pap. 238.

Stéquert, B., Nuñez-Rodriguez, J., Cuisset, B., Le Menn, F., 2001a. Gonadosomatic index and seasonal variations of plasma sex steroids in skipjack tuna (Katsuwonus pelamis) and yellowfin tuna (Thunnus albacares) from the western Indian ocean. Aquat. Living Resour. 14, 313 – 318. https://doi.org/10.1016/S0990-7440(01)01126-3

Stéquert, B., Panfili, J., Dean, J., 1996. Age and growth of yellowfin tuna, Thunnus albacares, from the western Indian Ocean, based on otolith microstructure. Oceanogr. Lit. Rev. 43.

Stéquert, B., Ramcharrun, B., 1995. La fécondité du listao (Katsuwonus pelamis) de l'ouest de l'océan Indien. Aquat. Living Resour. 8, 79–89.

Stéquert, B., Rodriguez, J., Cuisset, B., 2001b. Gonadosomatic index and seasonal variations of plasma sex steroids in skipjack tuna (Katsuwonus pelamis) and yellowfin tuna (Thunnus albacares) from the western Indian Ocean. Aquat. Living Resour. 14, 313–318. https://doi.org/10.1016/S0990-7440(01)01126-3

Stobberup, K.A., Marsac, F., Anganuzzi, A.A., 1998. A review of the biology of bigeye tuna, Thunnus obesus, and fisheries for this species in the Indian Ocean, in: Deriso, R.B., Bayliff, W.H., Webb, N.J. (Eds.), Proceedings Od the First World Meeting on Bigeye Tuna. Inter-American Tropical Tuna Commission, La Jolla, California, pp. 81–128.

Sturgeon, R.E., Willie, S.N., Yang, L., Greenberg, R., Spatz, R.O., Chen, Z., Scriver, C., Clancy, V., Lam, J.W., Thorrold, S., 2005. Certification of a fish otolith reference material in support of quality assurance for trace element analysis. J. Anal. At. Spectrom. 20, 1067–1071. https://doi.org/10.1039/B503655K

Sturrock, A.M., Hunter, E., Milton, J.A., Johnson, R.C., Waring, C.P., Trueman, C.N., 2015. Quantifying physiological influences on otolith microchemistry. Methods Ecol. Evol. 6, 806–816. https://doi.org/10.1111/2041-210X.12381

Sturrock, A.M., Trueman, C.N., Darnaude, A.M., Hunter, E., 2012. Can otolith elemental chemistry retrospectively track migrations in fully marine fishes? J. Fish Biol. 81, 766–795. https://doi.org/10.1111/j.1095-8649.2012.03372.x

Taillebois, L., Barton, D.P., Crook, D.A., Saunders, T., Taylor, J., Hearnden, M., Saunders, R.J., Newman, S.J., Travers, M.J., Welch, D.J., Greig, A., Dudgeon, C., Maher, S., Ovenden, J.R., 2017. Strong population structure deduced from genetics, otolith chemistry and parasite abundances explains vulnerability to localized fishery collapse in a large Sciaenid fish, Protonibea diacanthus. Evol. Appl. 10, 978–993. https://doi.org/10.1111/eva.12499

Tanabe, T., Kayama, S., Ogura, M., 2003. Precise age determination of young to adult skipjack tuna (Katsuwonus pelamis) with validation of otolith daily increment. Fish. Sci 69, 731–737.

Tanner, S., Reis-Santos, P., Cabral, H., 2016. Otolith chemistry in stock delineation: A brief overview, current challenges and future prospects. Fish. Res. 173, 206–213. https://doi.org/10.1016/j.fishres.2015.07.019

Temple, A.J., Kiszka, J.J., Stead, S.M., Wambiji, N., Brito, A., Poonian, C.N.S., Amir, O.A., Jiddawi, N., Fennessy, S.T., Pérez-Jorge, S., Berggren, P., 2018. Marine megafauna interactions with small-scale fisheries in the southwestern Indian Ocean: a review of status and challenges for research and

management. Rev. Fish Biol. Fish. https://doi.org/10.1007/s11160-017-9494-x

Tew Kai, E., Marsac, F., 2010. Influence of mesoscale eddies on spatial structuring of top predators' communities in the Mozambique Channel. Prog. Oceanogr. 86, 214–223. https://doi.org/10.1016/j.pocean.2010.04.010

Thomas, O., Ganio, K., Roberts, B., Swearer, S., 2017. Trace element–protein interactions in endolymph from the inner ear of fish: implications for environmental reconstructions using fish otolith chemistry. Metallomics 9, 239–249. https://doi.org/10.1039/C6MT00189K

Thomas, O., Swearer, S., 2019. Otolith Biochemistry—A Review. Rev. Fish. Sci. Aquac. 27, 458–489. https://doi.org/10.1080/23308249.2019.1627285

Thomas, O.R.B., Thomas, K.V., Jenkins, G.P., Swearer, S., 2020. Spatio-temporal resolution of spawning and larval nursery habitats using otolith microchemistry is element dependent. Mar. Ecol. Prog. Ser. 636, 169–187. https://doi.org/10.3354/meps13229

Thorrold, S., Campana, S., Jones, C., 1997. Factors determining δ 13 C and δ 18 O fractionation in aragonitic otoliths of marine fish. Geochim. Cosmochim. Acta 61, 2909–2919. https://doi.org/10.1016/S0016-7037(97)00141-5

Thorrold, S.R., Jones, C.M., Campana, S.E., McLaren, J.W., Lam, J.W.H., 1998. Trace element signatures in otoliths record natal river of juvenile American shad (Alosa sapidissima). Limnol. Oceanogr. 43, 1826–1835. https://doi.org/10.4319/lo.1998.43.8.1826

Thorrold, S.R., Jones, G.P., Planes, S., Hare, J.A., 2006. Transgenerational marking of embryonic otoliths in marine fishes using barium stable isotopes. Can. J. Fish. Aquat. Sci. 63, 1193–1197. https://doi.org/10.1139/f06-048

Thorrold, S.R., Latkoczy, C., Swart, P.K., Jones, C.M., 2001. Natal Homing in a Marine Fish Metapopulation. Science (80-.). 291, 297–299.

Tibshirani, R., Walther, G., Hastie, T., 2001. Estimating the number of clusters in a data set via the gap statistic. J. R. Stat. Soc. Ser. B (Statistical Methodol. 63, 411–423. https://doi.org/10.1111/1467-9868.00293

Titus, K., Mosher, J.A., Williams, B.K., 1984. Chance-corrected classification for use in discriminant analysis: ecological applications. Am. Midl. Nat. 111, 1–7. https://doi.org/10.2307/2425535

Tomczak, M., Godfrey, J.., 2003a. The Indian Ocean, in: Regional Oceanography: An Introduction. Elsevier, Tasmania, Australia.

Tomczak, M., Godfrey, J.., 2003b. Hydrology of the Indian Ocean, in: Regional Oceanography: An Introduction. Elsevier.

Tournois, J., Darnaude, A.M., Ferraton, F., Aliaume, C., Mercier, L., McKenzie, D.J., 2017. Lagoon nurseries make a major contribution to adult populations of a highly prized coastal fish. Limnol. Oceanogr. 62, 1219–1233. https://doi.org/10.1002/lno.10496

Trueman, C.., St John Glew, K., 2019. Isotopic Tracking of Marine Animal Movement, in: Hobson, K.., Wassenaar, L.I. (Eds.), Tracking Animal Migration with Stable Isotopes. Academic Press, pp. 137–172. https://doi.org/10.1016/B978-0-12-814723-8.00006-4

Trueman, C.N., MacKenzie, K., 2012. Identifying migrations in marine fishes through stable-isotope analysis. J. Fish Biol. 81, 826–847. https://doi.org/10.1111/j.1095-8649.2012.03361.x

Ueyanagi, S., 1969. Observations on the distribution of tuna larvae in the Indo-Pacific Ocean with emphasis on the delineation of the spawning areas of albacore, Thunnus alalunga. Bull.Far Seas Fish.Res.Lab. 177–256.

UNESCO, 2019. United Nations Decade of Ocean Science for Sustainable Development [WWW Document]. URL https://www.oceandecade.org/ (accessed 12.10.20).

United Nations, 2014. Blue Economy Concept paper [WWW Document]. URL https://sustainabledevelopment.un.org/content/documents/2978BEconcept.pdf (accessed 12.10.20).

van Denderen, P.D., Lindegren, M., MacKenzie, B.R., Watson, R.A., Andersen, K.H., 2018. Global patterns in marine predatory fish. Nat. Ecol. Evol. 2, 65–70. https://doi.org/10.1038/s41559-017-0388-z

van der Elst, R., Everett, B., Jiddawi, N., Mwatha, G., Afonso, P.S., Boulle, D., 2005. Fish, fishers and fisheries of the Western Indian Ocean: their diversity and status. A preliminary assessment. Philos. Trans. R. Soc. A Math. Phys. Eng. Sci. 363, 263–284. https://doi.org/10.1098/rsta.2004.1492

van Hulten, M., Middag, R., Dutay, J., De Baar, H., Roy-Barman, M., Gehlen, M., Tagliabue, Sterl, A., 2017. Manganese in the West Atlantic Ocean in context of the first global ocean circulation model of manganese. Biogeosiences 14, 1123–1152. https://doi.org/10.5194/bg-14-1123-2017

Venables, W.N., Ripley, B.D., 2002. Modern Applied Statistics with S.

Volk, E.C., Blakley, A., Schroder, S.L., Kuehner, S.., 2000. Otolith chemistry reflects migratory characteristics of Pacific salmonids:: Using otolith core chemistry to distinguish maternal associations with sea and freshwaters. Fish. Res. 46, 251–266. https://doi.org/10.1016/S0165-7836(00)00150-8

Wafar, M., Venkataraman, K., Ingole, B., Khan, S.., LokaBharathi, P., 2011. State of Knowledge of Coastal and Marine Biodiversity of Indian Ocean Countries. PLoS One 6, e14613. https://doi.org/10.1371/journal.pone.0014613.

Waldman, J., 2005. Definition of Stocks: an Evolving Concept, in: Cadrin, S., Friedland, K., Waldman, J. (Eds.), Stock Identification Methods: Applications in Fishery Science. Academic Press, pp. 7–17.

Walmsley, S., Purvis, J., Ninnes, C., 2006. The role of small-scale fisheries management in the poverty reduction strategies in the Western Indian Ocean region. Ocean Coast. Manag. 49, 812–833. https://doi.org/10.1016/j.ocecoaman.2006.08.006

Walther, B.D., 2019. The art of otolith chemistry: interpreting patterns by integrating perspectives. Mar. Freshw. Res. 70, 1643–1658. https://doi.org/10.1071/MF18270

Walther, B.D., Limburg, K.E., Jones, C.M., Schaffler, J.J., 2017. Frontiers in otolith chemistry: insights, advances and applications. J. Fish Biol. 90, 473–479. https://doi.org/10.1111/jfb.13266

Walther, B.D., Thorrold, S.R., 2006. Water, not food, contributes the majority of strontium and barium deposited in the otoliths of a marine fish. Mar. Ecol. Prog. Ser. 311, 125–130. https://doi.org/10.3354/meps311125

Wang, C.H., Lin, Y.T., Shiao, J.C., You, C.F., Tzeng, W.N., 2009. Spatio-temporal variation in the elemental compositions of otoliths of southern bluefin tuna Thunnus maccoyii in the Indian Ocean and its ecological implication. J. Fish Biol. 75, 1173–1193. https://doi.org/10.1111/j.1095-8649.2009.02336.x

Ward, R., Elliott, N., Innes, B., Smolenski, A., Grewe, P.M., 1997. Global population structure of yellowfin tuna, Thunnus albacares, inferred from allozyme and mitochondrial DNA variation. Fish. Bull. 95, 566–575.

Warren, D., Glor, R., Turelli, M., 2008. Environmental niche equivalency versus conservatism: quantitative approaches to niche evolution. Evolution (N. Y). 62. https://doi.org/10.1111/j.1558-5646.2008.00482.x

Webb, S.D., Woodcock, S.H., Gillanders, B.M., 2012. Sources of otolith barium and strontium in estuarine fish and the influence of salinity and temperature. Mar. Ecol. Prog. Ser. 453, 189–199. https://doi.org/10.3354/meps09653

Welch, D., Newman, S., Buckworth, R., Ovenden, J., 2015. Integrating different approaches in the definition of biological stocks: A northern Australian multi-jurisdictional fisheries example using grey

mackerel, Scomberomorus semifasciatus. Mar. Policy 55, 73–80. https://doi.org/10.1016/j.marpol.2015.01.010

Welch, D.J., Newman, S.J., Buckworth, R.C., Ovenden, J.R., Broderick, D., Lester, R.J., Gribble, N.A., Ballagh, A.C., Charters, R.A., Stapley, J., Street, R., Garrett, R.N., Begg, G.A., 2015. Integrating different approaches in the definition of biological stocks: A northern Australian multi-jurisdictional fisheries example using grey mackerel, Scomberomorus semifasciatus. Mar. Policy 55, 73–80. https://doi.org/10.1016/j.marpol.2015.01.010

Wells, R.D., Rooker, J.R., Itano, D.G., 2012. Nursery origin of yellowfin tuna in the Hawaiian Islands. Mar. Ecol. Prog. Ser. 461, 87–196. https://doi.org/10.3354/meps09833

Wells, R.J.D., Kinney, M., Kohin, S., Dewar, H., Rooker, J.R., Snodgrass, O., 2015. Natural tracers reveal population structure of albacore (Thunnus alalunga) in the eastern North Pacific. ICES J. Mar. Sci. 72, 2118–2127. https://doi.org/10.1093/icesjms/fsv051

Wexler, J.B., Margulies, D., Scholey, V.P., 2011. Temperature and dissolved oxygen requirements for survival of yellowfin tuna, Thunnus albacares, larvae. J. Exp. Mar. Bio. Ecol. 404, 63–72. https://doi.org/10.1016/j.jembe.2011.05.002

Wiggert, J., Murtugudde, R., Christian, J., 2006. Annual ecosystem variability in the tropical Indian Ocean: Results of a coupled bio-physical ocean general circulation model. Deep Sea Res. Part II Top. Stud. Oceanogr. 53, 644–676. https://doi.org/10.1016/j.dsr2.2006.01.027

Wilcox, R., 2012. Introduction to Robust Estimation and Hypothesis Testing, 3rd ed.

Willmes, M., Lewis, L.S., Davis, B.E., Loiselle, L., James, H.F., Denny, C., Baxter, R., Conrad, J.L., Fangue, N.A., Hung, T.C., Armstrong, R.A., Williams, I.S., Holden, P., Hobbs, J.A., 2019. Calibrating temperature reconstructions from fish otolith oxygen isotope analysis for California's critically endangered Delta Smelt. Rapid Commun. Mass Spectrom. 33, 1207–1220. https://doi.org/10.1002/rcm.8464

Wolf, R., Wilson, S., 2007. USGS reference materials program.

Woodcock, S., Munro, A., Crook, D., Gillanders, B., 2012. Incorporation of magnesium into fish otoliths: Determining contribution from water and diet. Geochim. Cosmochim. Acta 94, 12–21. https://doi.org/10.1016/J.GCA.2012.07.003

Worm, B., Tittensor, D., 2011. Range contraction in large pelagic predators. PNAS 108, 11942–11947. https://doi.org/10.1073/pnas.1102353108

Wright, P.J., Régnier, T., Gibb, F.M., Augley, J., Devalla, S., 2018. Assessing the role of ontogenetic movement in maintaining population structure in fish using otolith microchemistry. Ecol. Evol. 8, 7907–7920. https://doi.org/10.1002/ece3.4186

Wu, G., Chiang, H., Chou, Y., Wong, Z., Hsu, C., Chen, Y., Yang, H., 2010. Phylogeography of yellowfin tuna (Thunnus albacares) in the Western Pacific and the Western Indian Oceans inferred from mitochondrial DNA. Fish. Res. 105, 248–253. https://doi.org/10.1016/j.fishres.2010.03.015

Wujdi, A., Setyadji, B., Nugroho, S.C., 2017. Preliminary stock structure study of Skipjack tuna (Katsuwonus pelamis) from south java using otolith shape analysis. IOTC–2017–WPTT19–42.

Yamanaka, K.L., 1990. Age, growth and spawning of yellowfin tuna in the southern Philippines (No. IPTP/90/WP/21). PhD dissertation, University of British Columbia, Vancouver, Canada.

Yano, K., 1991. An interim analysis of the data on tuna tagging collected by R/V Nippon Karu in the Indian Ocean, 1980-1990, in: Southeast Asian Tuna Conference. Bangkok, Thailand.

Ye, Z.J., Wang, Y.J., Gao, T.X., 2003. Study on tuna longline fishery in the Eastern Indian Ocean: The Biology of Thunnus obesus Captured. Ocean Univ. Qingdao 33, 343-348 (In Chinese).

Ying, Y., Chen, Y., Lin, L., Gao, T., 2011. Risks of ignoring fish population spatial structure in fisheries management. Can. J. Fish. Aquat. Sci. 68, 2101–2120. https://doi.org/10.1139/F2011-116

Young, J., Davis, T., 1990. Feeding ecology of larvae of southern bluefin, albacore and skipjack tunas (Pisces: Scombridae) in the eastern Indian Ocean. Mar. Ecol. Prog. Ser. 61, 17–29.

Zeileis, A., Grothendieck, G., 2005. zoo: S3 infrastructure for regular and irregular time series. J. Stat. Softw. 14, 1–27. https://doi.org/1.1837/JSS.V014.I06

Zhang, C., Ye, Z., Li, Z., Wan, R., Ren, Y., Dou, S., 2016. Population structure of Japanese Spanish mackerel Scomberomorus niphonius in the Bohai Sea, the Yellow Sea and the East China Sea: evidence from random forests based on otolith features. Fish. Sci. 82, 251–256 |. https://doi.org/10.1007/s12562-016-0968-x

Zhu, G., Xu, L., Zhou, Y., Song, L., 2008. Reproductive Biology of Yellowfin Tuna T. albacares in the West-Central Indian Ocean. J. Ocean Univ. China 7, 327–332. https://doi.org/10.1007/s11802-008-0327-3

Zhu, G.P., Dai, X.J., Song, L.M., Xu, L.X., 2011. Size at Sexual Maturity of Bigeye Tuna Thunnus obesus (Perciformes: scombridae) in the Tropical Waters: a Comparative Analysis. Turkish J. Fish. Aquat. Sci. 11, 149–156. https://doi.org/10.4194/trjfas.2011.0119

Zudaire, I., Chassot, E., Murua, H., Dhurmeea, Z., Cedras, M., Bodin, N., 2016. Sex-ratio, size at maturity, spawning period and fecundity of bigeye tuna (Thunnus obesus) in the western Indian Ocean. IOTC-2016-WPTT18-37.

Zudaire, I., Murua, H., Grande, M., Bodin, N., 2013a. Reproductive potential of yellowfin tuna (Thunnus albacares) in the western Indian Ocean. Fish. Bull. 11, 252–264. https://doi.org/10. 7755/FB.111.3.4

Zudaire, I., Murua, H., Grande, M., Goñi, N., Potier, M., 2015. Variations in the diet and stable isotope ratios during the ovarian development of female yellowfin tuna (Thunnus albacares) in the Western Indian Ocean. Mar. Biol. 162, 2363–2377. https://doi.org/10.1007/ s00227-015-2763-0

Zudaire, I., Murua, H., Grande, M., Korta, M., 2013b. Fecundity regulation strategy of the yellowfin tuna (Thunnus albacares) in the Western Indian Ocean. Fish. Res. 138, 80–88. https://doi.org/10.1016/j.fishres.2012.07.022

Zudaire, I., Murua, H., Grande, M., Pernet, F., Bodin, N., 2014. Accumulation and mobilization of lipids in relation to reproduction of yellowfin tuna (Thunnus albacares) in the Western Indian Ocean. Fish. Res. 160, 50–59. https://doi.org/10.1016/j.fishres.2013.12.010

“I never am really satisfied that I understand anything; because understand it well as I may, my comprehension can only be an infinitesimal fraction of all I want to understand…”

Ada Lovelace

APPENDICES

Appendix A

Table A1. Summary of element:Ca precision and accuracy for standards analysed in this study; MACS3, NIST610. Measurement precision are shown as percent relative standard deviation (%RSD) and percent Accuracy. The last was calculated by dividing the averages to preferred 2011 values from the GEOREM website (Jochum et al. 2005).

Standard	Measure	^{7}Li	^{25}Mg	^{55}Mn	^{57}Fe	^{59}Co	^{60}Ni	^{63}Cu	^{66}Zn	^{88}Sr	^{138}Ba
MACS3	%RSD	4	4	3	14	5	7	3	6	4	3
	%Accuracy	107	116	106	49	103	117	101	100	105	103
NIST610	%RSD	1	1	1	13	1	1	2	2	1	1
	%Accuracy	103	124	104	54	105	104	98	101	100	101

Jochum, K.P., Nohl, U., Herwig, K., Lammel, E., Stoll, B. and Hofmann, A.W. (2005). GeoReM: A new geochemical database for reference materials and isotopicl standars. *Geostandards Geoanalytical Research*, 29, 333-338. doi: 10.1111/j.1751-908X.2005.tb00904.x

Table A2. In order to ascertain the level of interannual variability in the studied area, spatial structure similarity was examined for the periods of interest; 2008 and 2009 summer monsoons (i.e. May-Oct), estimated period at which YOY fish were born. For that E.U. Copernicus Marine Service Information on sea surface salinity (SSS), sea surface temperature (SST), mixed layer thickness (MLD), mass concentration of chlorophyll a in seawater (CHL) and dissolved molecular oxygen concentration (DO_2) were explored in the 20°N-30°S and 30°E-70°E area at a spatial resolution of 0.25° x 0.25° grid. Daily data of SSS (psu), SST (K) and MLD (m) was obtained from the "*GLOBAL_REANALYSIS_PHY_001_025*" dataset. Daily data of CHL (mg m^{-3}) and DO_2 (mmol m^{-3}) was obtained from "*GLOBAL_REANALYSIS_BIO_001_029*" dataset. The value of each parameter at each grid was then averaged for each corresponding period of interest. Resultant matrixes were converted into a raster object using "rasterFromXYZ" function from "raster" package (Hijmans, 2018). Two measures of spatial similarity Schoener´s D (Schoener, 1968) and Warren´s I (Warren et al., 2008), were calculated using "*nicheOverlap*" function of the "*dismo*" package (Hijmans et al., 2017). In addition, the overall correlation between raster layers was assessed using Pearson´s (r) and Spearman´ (ρ) correlation coefficients.

Parameter	Unit	Schoener´s D	Warren´s I	Pearson r	Spearman ρ
SSS	psu	0.998	1.000	0.957	0.917
SST	K	1.000	1.000	0.987	0.985
MLD	m	0.936	0.996	0.850	0.849
CHL	mg m^{-3}	0.890	0.990	0.930	0.909
DO_2	mmol m^{-3}	1.000	1.000	0.987	0.977

Schoener, T. W. (1968). The Anolis lizards of Bimini: resource partitioning in a complex fauna. Ecology 49, 704–726. doi:10.2307/1935534

Warren, D. L., Glor, R. E., and Turelli, M. (2008). Environmental niche equivalency versus conservatism: quantitative approaches to niche evolution. Evolution 62(11), 2868–2883 doi:10.1111/j.1558-5646.2008.00482.x.

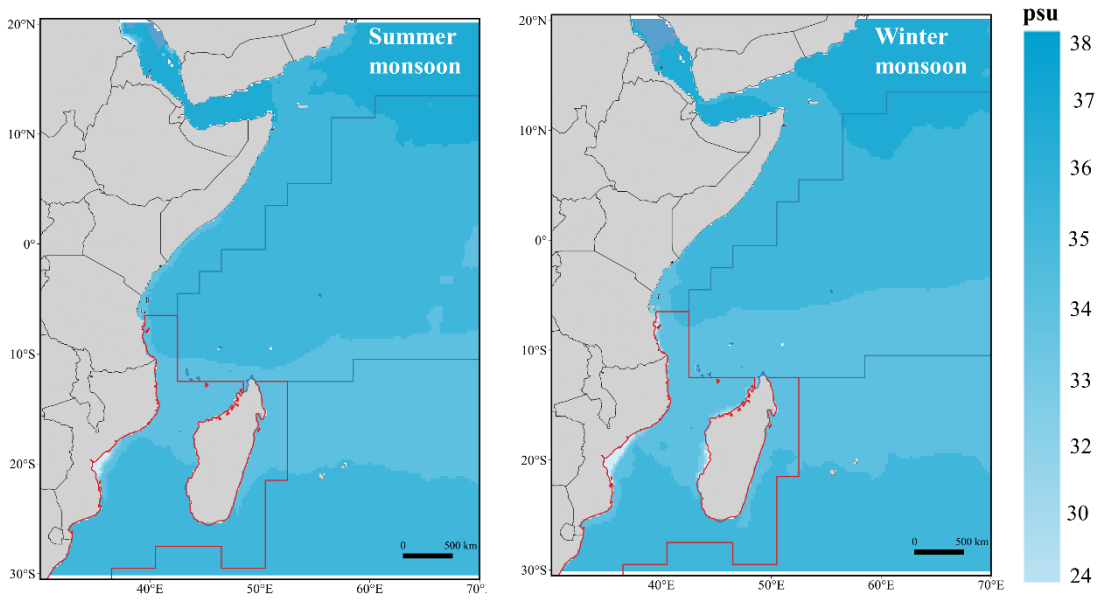

Figure A1. Mean sea surface salinity (SSS) in the western Indian Ocean within the studied period. Maps are differentiated for summer monsoon (May–Oct 2008 and May–Oct 2009) and winter monsoon (Nov–Apr 2008–09 and Nov–Apr 2009–10). Daily data of SSS (PSU) was obtained from the '*GLOBAL_REANALYSIS_PHY_001_025*' dataset available in the EU Copernicus Marine Service Information.

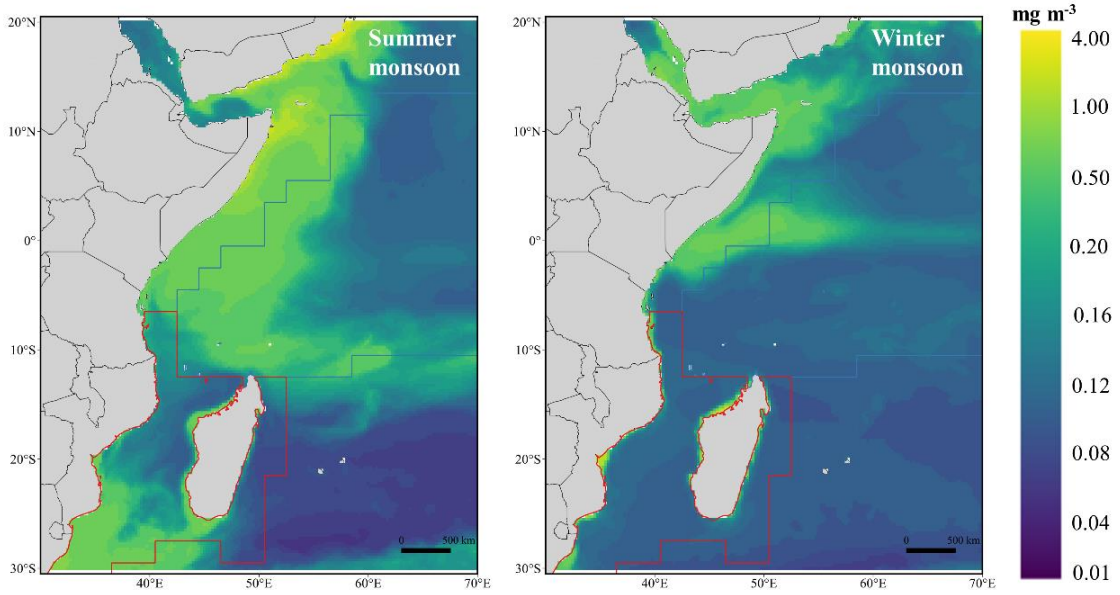

Figure A2. Mean sea surface chlorophyll (Chl-*a*) in the western Indian Ocean within the studied period. Maps are differentiated for summer monsoon (May–Oct 2008 and 2009) and winter monsoon (Nov–Apr 2008–09 and Nov–Apr 2009–10). Daily data of Chl-a (mg m^{-3}) was obtained from the 'GLOBAL_REANALYSIS_BIO_001_029' dataset available in the EU Copernicus Marine Service Information.

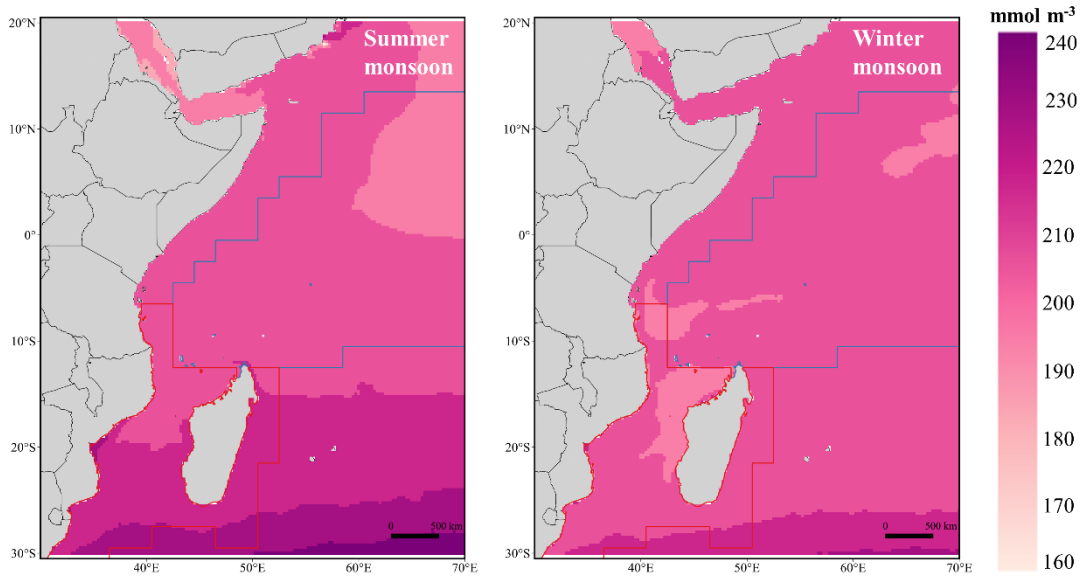

Figure A3. Mean sea surface dissolved molecular oxygen concentration (DO_2) in the western Indian Ocean within the studied period. Maps are differentiated for summer monsoon (May–Oct 2008 and 2009) and winter monsoon (Nov–Apr 2008–09 and Nov–Apr 2009–10). Daily data of DO2 (mmol m^{-3}) was obtained from the '*GLOBAL_REANALYSIS_BIO_001_029*' dataset available in the EU Copernicus Marine Service Information.

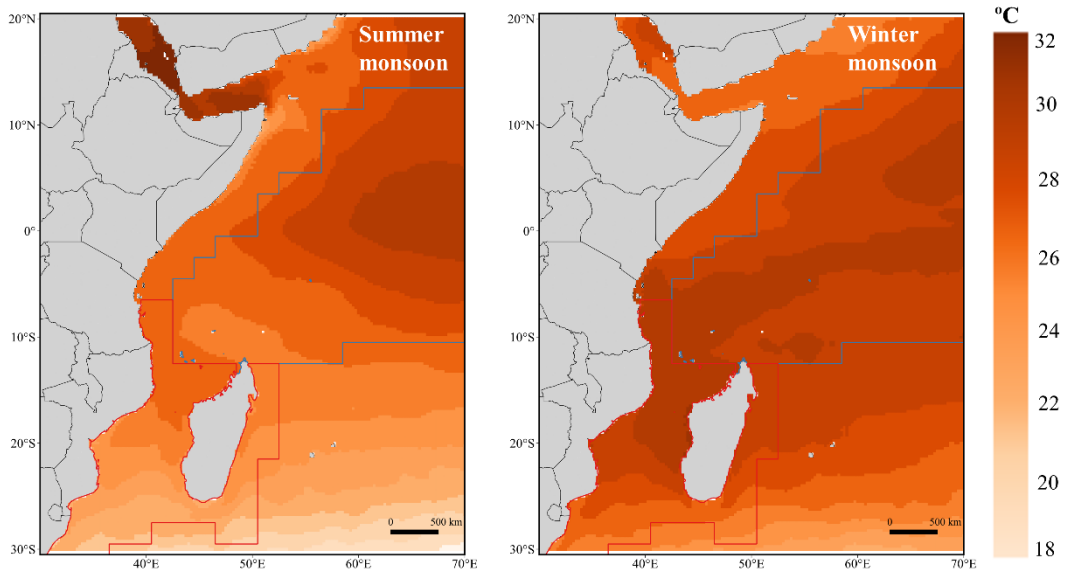

Figure A4. Mean sea surface temperature (SST) in the western Indian Ocean within the studied period. Maps are differentiated for summer monsoon (May–Oct 2008 and 2009) and winter monsoon (Nov–Apr 2008–09 and Nov–Apr 2009–10). Daily data of SST (°C) was obtained from the '*GLOBAL_REANALYSIS_PHY_001_025*' dataset available in the EU Copernicus Marine Service Information.

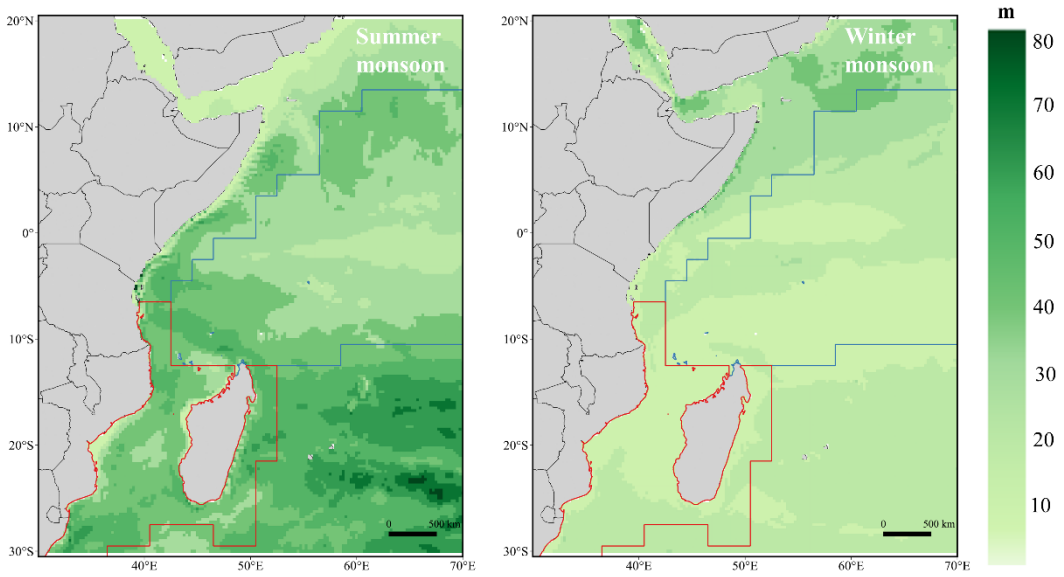

Figure A5. Mean mixed layer depth (MLD) in the western Indian Ocean within the studied period. Maps are differentiated for summer monsoon (May–Oct 2008 and 2009) and winter monsoon (Nov–Apr 2008–09 and Nov–Apr 2009–10). Daily data of MLD (m) was obtained from the 'GLOBAL_REANALYSIS_PHY_001_025' dataset available in the EU Copernicus Marine Service Information.

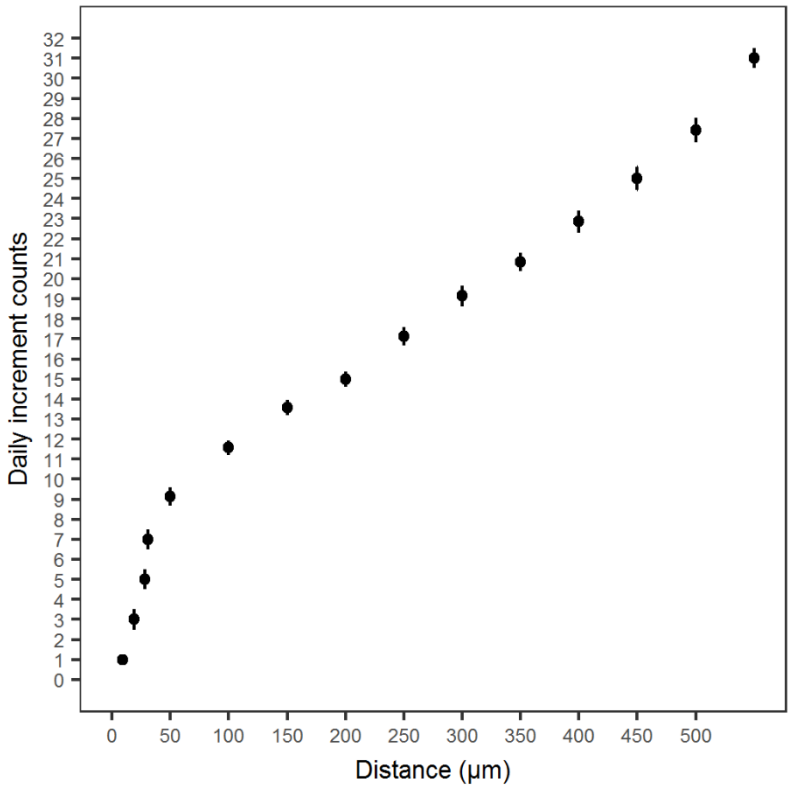

Figure A6. The relationship between the micro-increment counts and the distance from the primordium (µm) measured along the growth axis of the otolith in young-of-the-year (YOY) yellowfin tuna (*Thunnus albacares*, n= 8). Points represent mean count estimates, and bars standard errors.

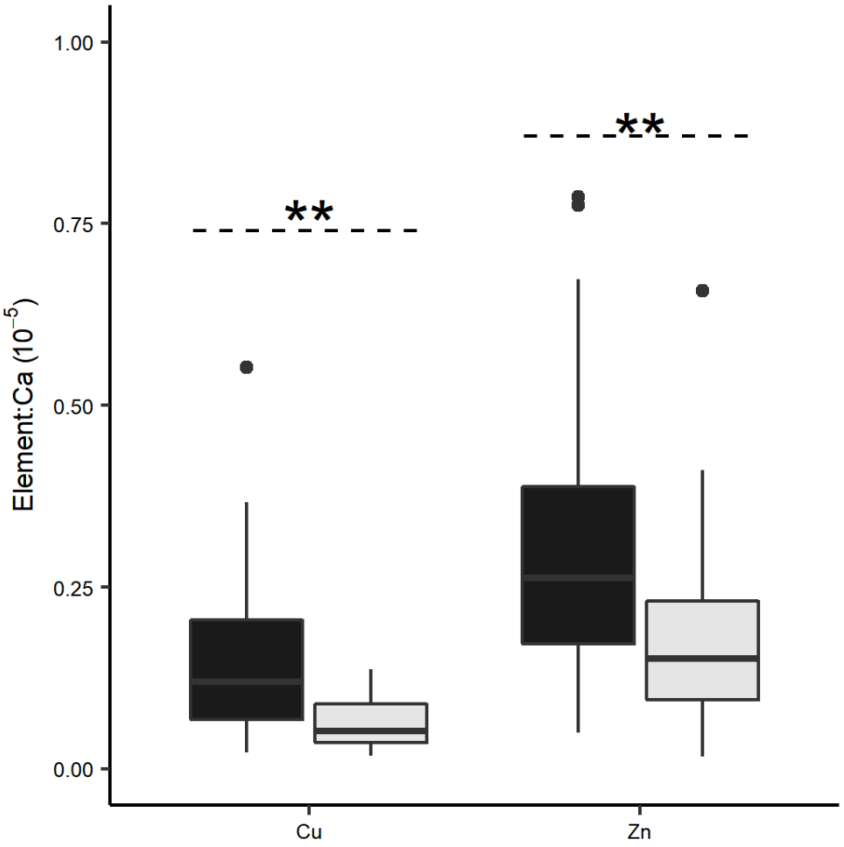

Figure A7. Otolith core (black) and near-core (grey) Cu:Ca and Zn:Ca ratios for young-of-the-year (YOY) yellowfin tuna (Thunnus albacares) collected in the western Indian Ocean. Boxes, interquartile range (25th and 75th percentiles); midline, median; error bars, range (excluding outliers, dots). Asterisks indicate the significance differences between otolith portions according to bootstrapped Yuen t-tests (*, $p < 0.05$; **, $p < 0.01$).

Appendix B

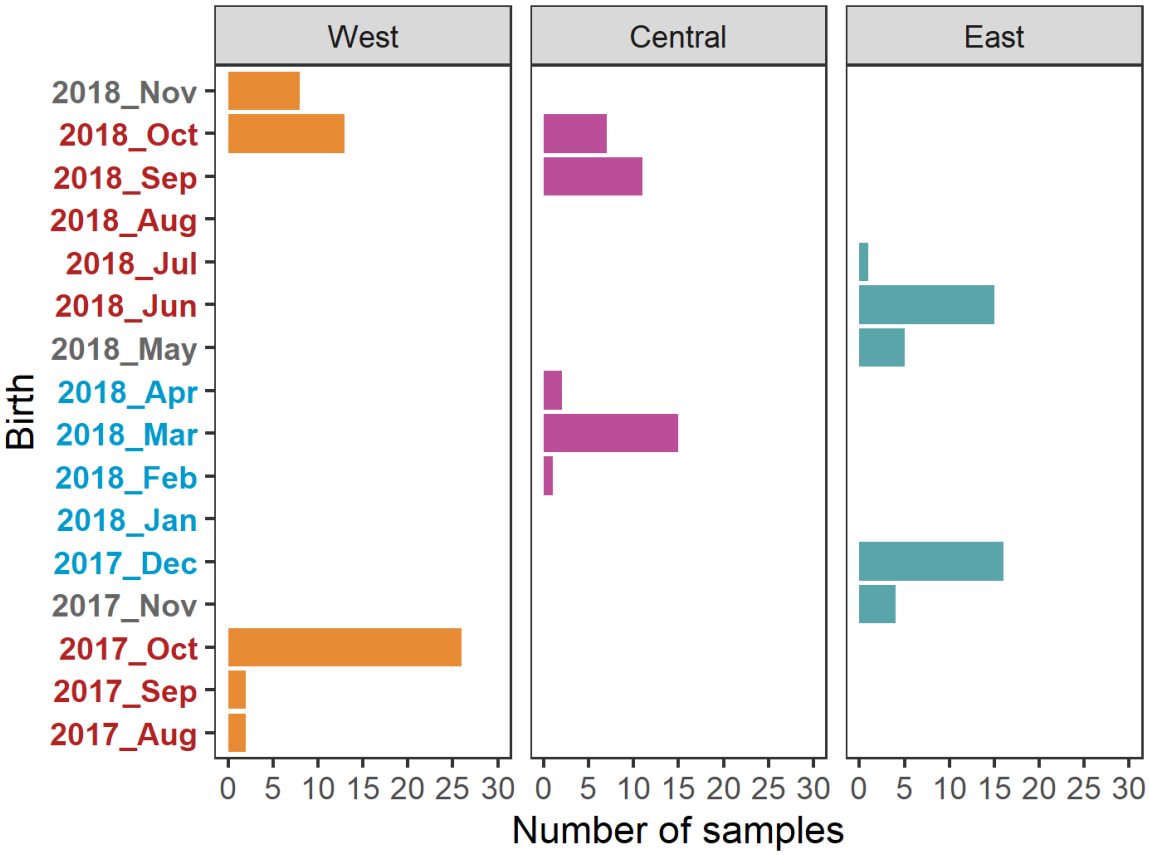

Figure B1. Back-calculated hatch period. Frequency histograms show the distribution of estimated hatching dates (year_month) of young-of-the-year (YOY) skipjack tuna (*Katsuwonus pelamis*) collected in three nursery areas West (orange), central (purple) and East (green) of the Indian Ocean.

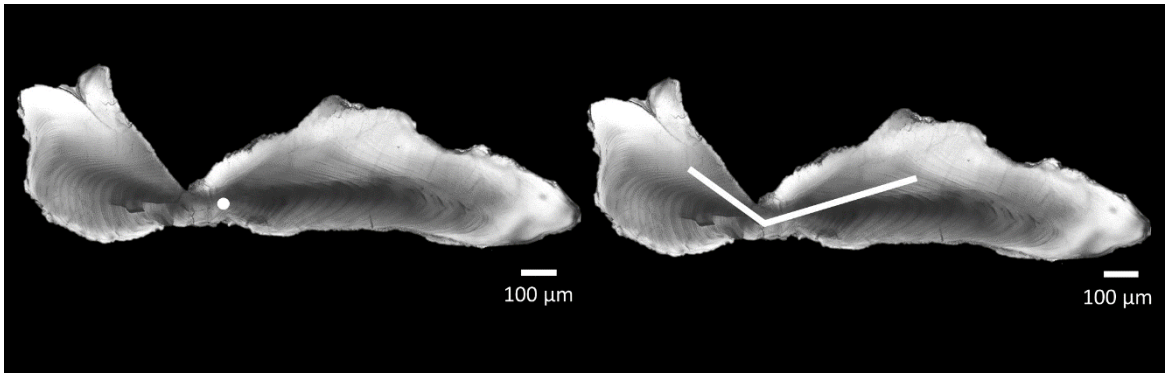

Figure B2. Chemical analyses location in the otolith. Transverse section of a 33 cm FL skipjack tuna (*Katsuwonus pelamis*) otolith. Approximate location of laser ablation spot for trace element analyses (left) and the MicroMill drilling path used for stable isotope analyses (right) are shown.

Appendix C

Table C1. Summary of yellowfin tuna (*Thunnus albacares*) individuals used for young-of-the-year (YOY) age estimation. Size is fork length (FL) in cm.

FL	Age (days)	Sampling date	Sampling location	Approach	Study
39	107	30/04/2013	Eastern Indian Ocean	Otolith microincrement counts	Proctor et al. (2019)
40	108	29/04/2013	Eastern Indian Ocean	Otolith microincrement counts	Proctor et al. (2019)
40	137	30/04/2013	Eastern Indian Ocean	Otolith microincrement counts	Proctor et al. (2019)
40	113	30/04/2013	Eastern Indian Ocean	Otolith microincrement counts	Proctor et al. (2019)
40	116	24/06/2014	Eastern Indian Ocean	Otolith microincrement counts	Proctor et al. (2019)
40	115	25/06/2014	Eastern Indian Ocean	Otolith microincrement counts	Proctor et al. (2019)
40	122	24/06/2014	Eastern Indian Ocean	Otolith microincrement counts	Proctor et al. (2019)
40	117	17/06/2014	Eastern Indian Ocean	Otolith microincrement counts	Proctor et al. (2019)
40	130	17/06/2014	Eastern Indian Ocean	Otolith microincrement counts	Proctor et al. (2019)
29.5	80	06/08/2017	Western Indian Ocean	Otolith microincrement counts	This study
36.5	95	27/06/2017	Western Indian Ocean	Otolith microincrement counts	This study
36.5	98	25/08/2017	Western Indian Ocean	Otolith microincrement counts	This study
38	112	26/08/2017	Western Indian Ocean	Otolith microincrement counts	This study
34	89	26/08/2017	Western Indian Ocean	Otolith microincrement counts	This study
3.12	30	-	-	Direct measures of tank reared fish	Kobayashi et al. (2015)
2.46	27	-	-	Direct measures of tank reared fish	Kobayashi et al. (2015)
2.16	24	-	-	Direct measures of tank reared fish	Kobayashi et al. (2015)

Table C2. Summary of data distribution by nursery region. Normality was obtained performing the Shapiro-Wilk test of normality, *shapiro.test* {stats} function implemented in R. Significant deviations from normality are highlighted as follows *P<0.05, **P<0.01. Skewness was calculated following the formula from (Joanes and Gill, 1998)[1] with the *skewness* {e1071} function implemented in R.

Element	Test measure	Madagascar	Seychelles -Somalia	Maldives	Sumatra	All
Ba	Normality	0.002**	0.132	0.012*	0.038*	<0.001**
	Skewness	1.391	0.512	1.180	0.976	1.622
Li	Normality	0.484	0.755	0.581	0.930	0.511
	Skewness	0.259	0.165	0.459	0.0626	0.273
Mg	Normality	0.003**	<0.001**	0.003**	0.002**	<0.001**
	Skewness	1.453	1.636	1.179	1.393	1.816
Mn	Normality	0.334	0.257	<0.001**	<0.001**	<0.001**
	Skewness	0.624	0.333	1.359	1.172	1.961
Sr	Normality	0.012*	0.616	0.128	0.054	<0.001**
	Skewness	1.273	0.179	0.185	0.818	0.807
Zn	Normality	0.002**	0.002**	<0.001**	<0.001**	<0.001**
	Skewness	0.980	1.139	1.603	1.731	1.515
$\delta^{13}C$	Normality	0.785	0.853	0.095	0.532	0.848
	Skewness	-0.216	0.123	-0.551	0.205	-0.040
$\delta^{18}O$	Normality	0.153	0.791	0.531	0.549	0.212
	Skewness	-0.533	0.010	-0.854	0.375	-0.333

[1]*Joanes DN, Gill CA (1998) Comparing measures of sample skewness and kurtosis. The statician:183–189.*

Table C3. Homogeneity of variances between nursery regions. Homoscedasticity was calculated performing *fligner.test* {stats} function implemented in R. Significant differences in nursery variances are highlighted as follows *P<0.05, **P<0.01.

Ba	Li	Mg	Mn	Sr	Zn	$\delta^{13}C$	$\delta^{18}O$
0.242	0.334	0.101	<0.001**	0.058	0.289	0.976	0.017*

Table C4. Within nursery interannual variability (2017vs 2018) in otolith trace element and stable isotope composition of young-of-the-year (YOY) yellowfin tuna (*Thunnus albacares*) from the Indian Ocean. Yuen test was used for comparisons, *yuen* {WRS2}, which performs independent samples t-tests on robust location measures including effect sizes. Test value (t), degrees of freedom (df) and P values are reported. Significant differences are highlighted as follows *P<0.05, **P<0.01.

Element		**Seychelles-Somalia**	**Maldives**	**Sumatra**
Li	*t*	1.005	2.369	1.815
	df	12.56	13.11	15.35
	P	0.334	0.034*	0.089
Mg	*t*	0.193	3.441	0.696
	df	17.55	11.75	14.03
	P	0.850	0.005**	0.496
Sr	*t*	1.202	2.49	0.272
	df	16.43	12.76	16.5
	P	0.246	0.027*	0.789
Ba	*t*	0.773	1.131	0.343
	df	17.88	15.23	11.45
	P	0.449	0.276	0.738
Mn	*t*	1.483	4.29	1.678
	df	10.86	9.67	13.16
	P	0.167	0.002**	0.117
$\delta^{13}C$	*t*	0.792	1.195	0.879
	df	19.78	16.59	16.82
	P	0.438	0.249	0.392
$\delta^{18}O$	*t*	1.618	0.478	0.129
	df	19.26	16.1	14.65
	P	0.122	0.639	0.899

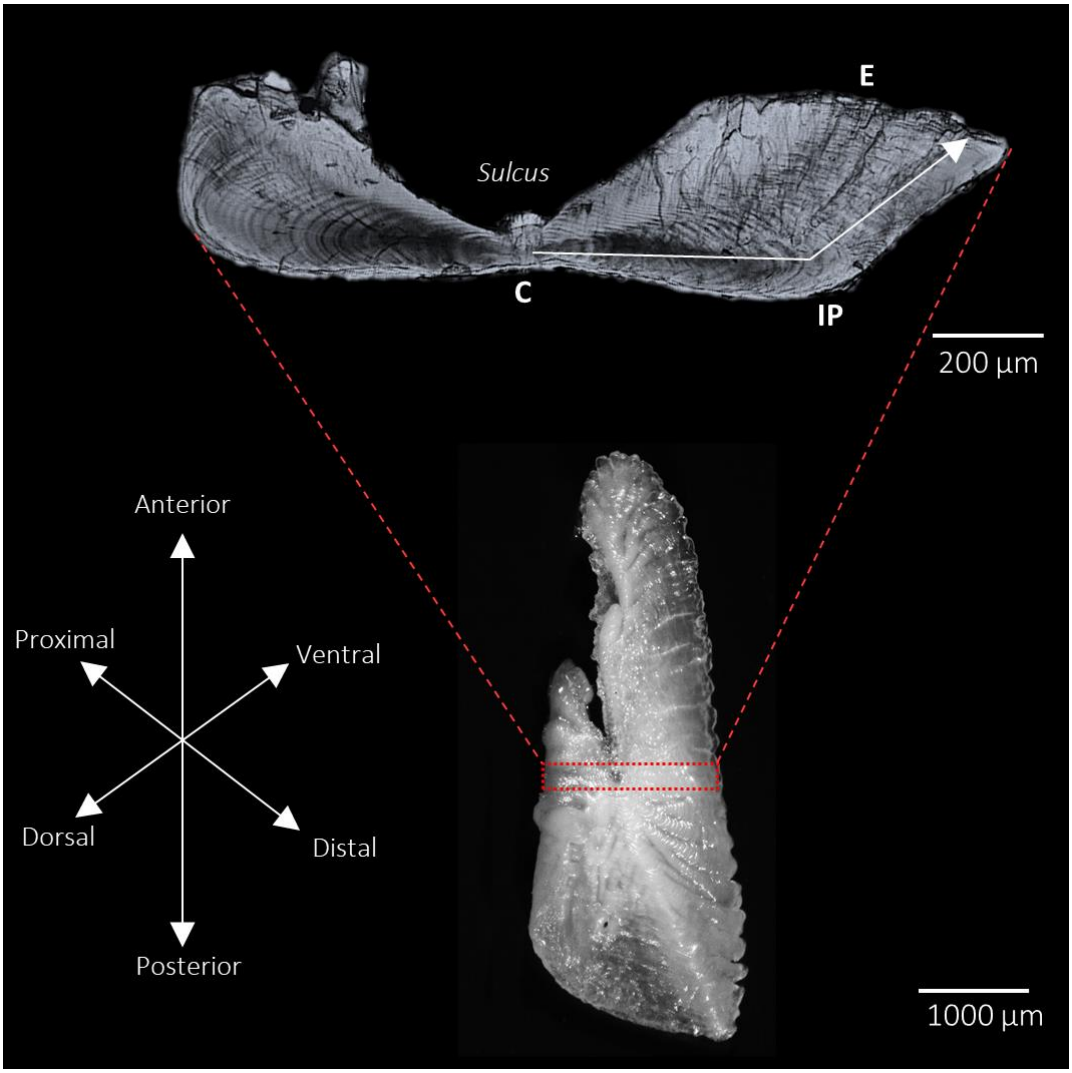

Figure C1. Transverse section (top image) of a 30 cm FL yellowfin tuna (*Thunnus albacares*) otolith (bottom image). Position of the core (C), inflection point (IP) and edge (E) are indicated, while white arrow in the transverse section depicts the otolith growth axis. The approximate dorsal/ventral, anterior/posterior and proximal/distal axes and sulcus position are given for orientation.

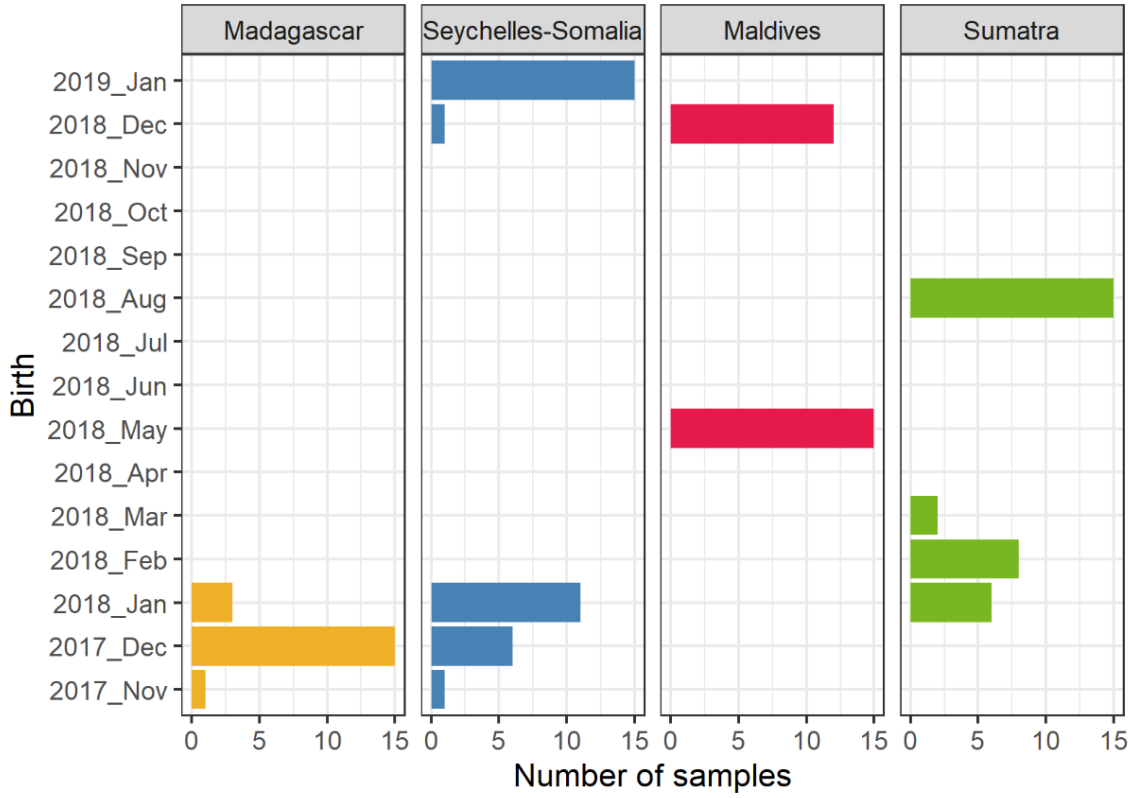

Figure C2. Frequency histograms showing the distribution of estimated spawning dates (year and month) of young-of-the-year (YOY) yellowfin tuna (*Thunnus albacares*) collected in four nursery areas Madagascar (yellow), Seychelles-Somalia (blue), Maldives (pink) and Sumatra (green) of the Indian Ocean.

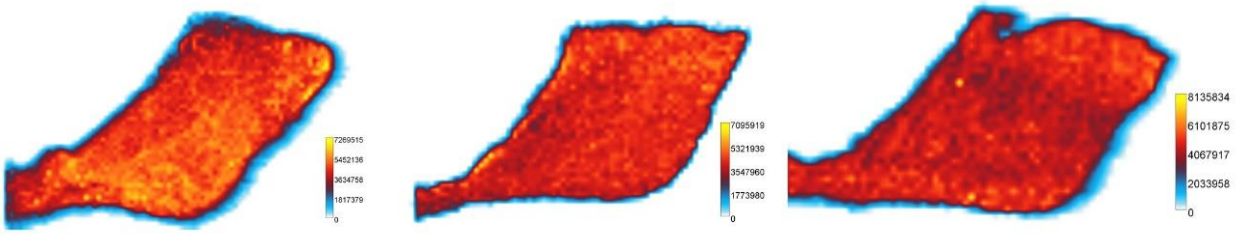

Figure C3. Raw ^{43}Ca composition within otolith transverse sections.

Appendix D

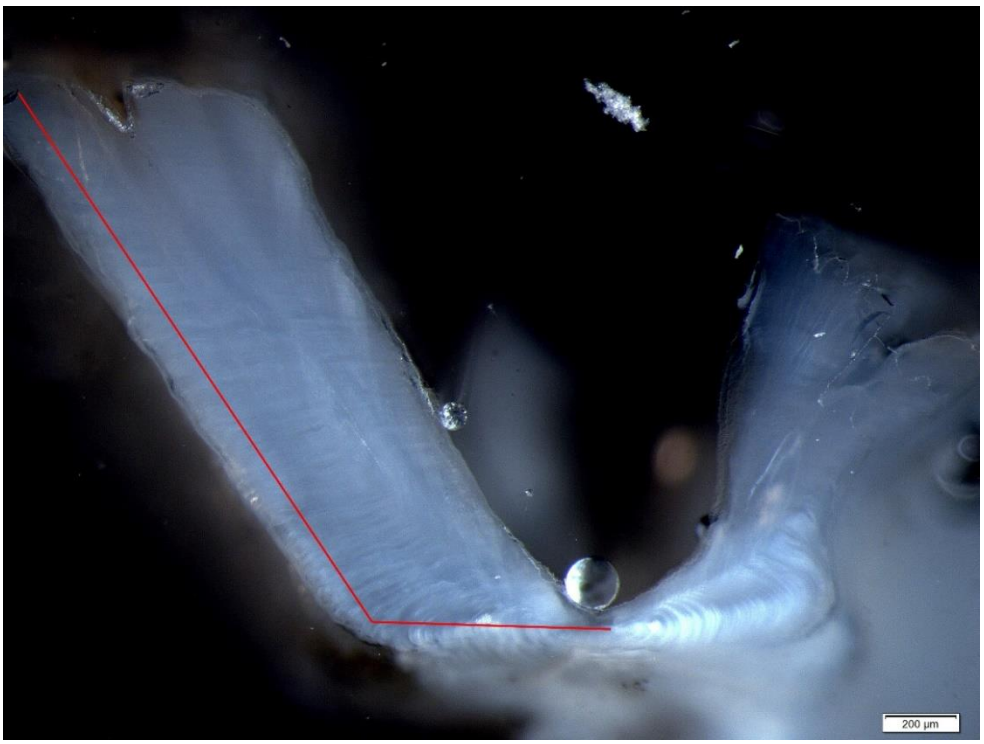

Figure D1. Adult yellowfin tuna (*Thunnus albacares*) otolith transverse section showing the transect followed (red line) for $\delta^{18}O$ SIMS analysis.

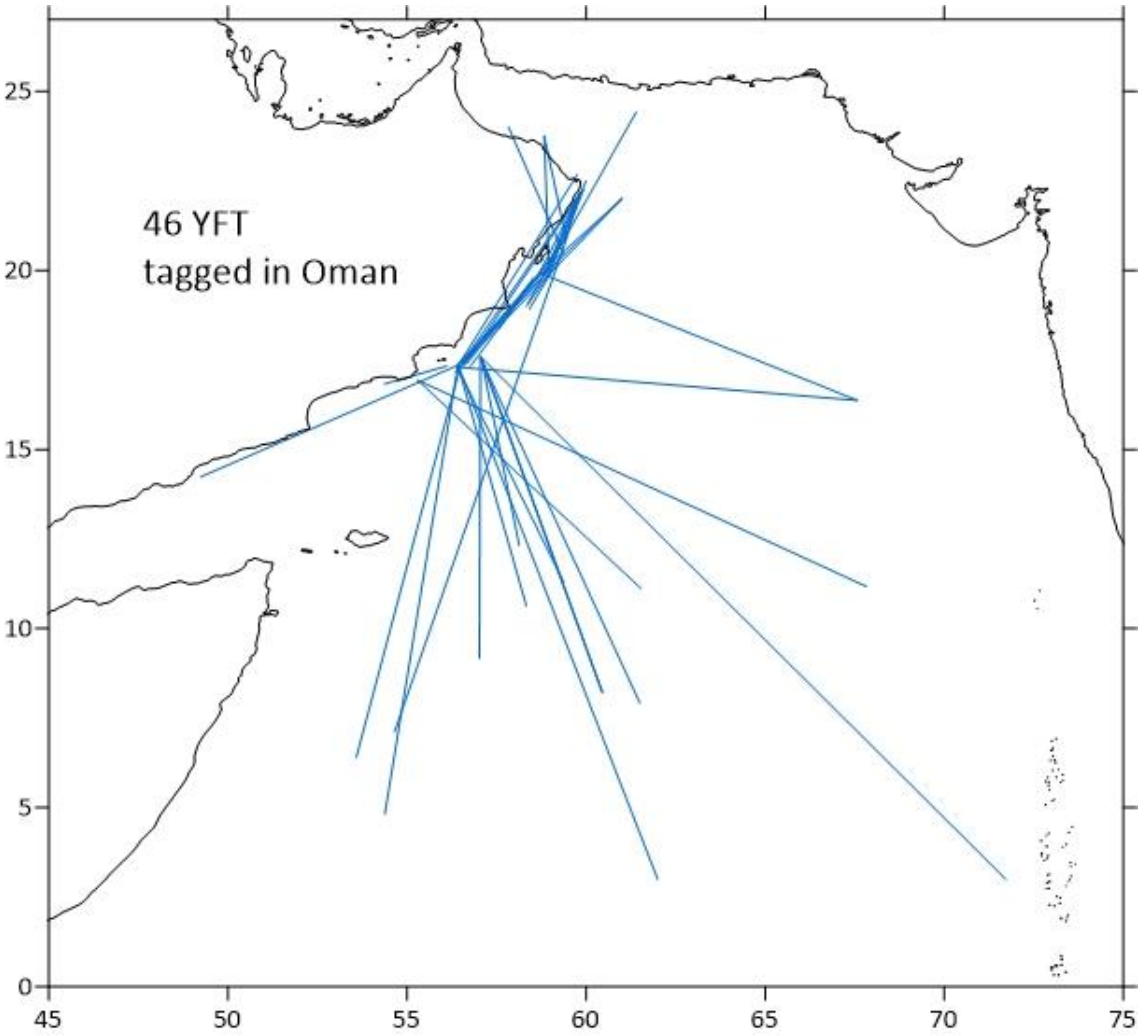

Figure D2. Trajectories of 46 yellowfin tuna (Thunnus albacares) tagged off Oman. Data from the RTTP-IO database [https://www.iotc.org/tagging-data-2014-0].

Table D1. Raw secondary ion mass spectrometry measurements of $\delta^{18}O$ along the otolith growth axis of an otolith of a 134 FL yellowfin tuna (*Thunnus albacares*) captured in South Africa.

Otolith position	Isotope (VSMOW)
1	25.50644967
2	25.90928783
3	26.23297005
4	25.26494845
5	26.34439337
6	26.28943797
7	26.42254094
8	25.92441316
9	25.90424605
10	26.2249032
11	25.94911788
12	26.12406762
13	25.77013472
14	26.24406196
15	26.01365265
16	26.13919295
17	25.52611261
18	25.48477002
19	25.7661013
20	25.94558864
21	26.55413138
22	26.16339349
23	26.78504486
24	26.7431981
25	26.91814783
26	26.649421
27	26.79613678
28	26.30910091
29	27.2110752
30	26.37212315
31	26.99730377
32	26.69630955
33	27.27157655
34	27.09511428
35	28.46799074
36	27.46719758
37	27.94062064
38	26.85613395
39	27.29376038
40	27.09410593

“Stories never really end…

Even if books like to pretend they do.

They dont end on the last page,

Any more than they begin on the first page.”

Cornelia Funke